

SMITHSONIAN
CONTRIBUTIONS

to

ASTROPHYSICS



Volume 10, Number 1

**An Analysis of the
Atmospheric Trajectories
of 413 Precisely Reduced
Photographic Meteors**

By Luigi G. Jacchia,
Franco Verniani, and
Robert E. Briggs

Smithsonian Institution
Astrophysical Observatory

Smithsonian Institution Press

Smithsonian
Contributions to Astrophysics

VOLUME 10, NUMBER 1

AN ANALYSIS OF THE ATMOSPHERIC TRAJECTORIES
OF 413 PRECISELY REDUCED PHOTOGRAPHIC METEORS

by LUIGI G. JACCHIA, FRANCO VERNIANI, *and* ROBERT E. BRIGGS



SMITHSONIAN INSTITUTION PRESS

Washington, D.C.

1967

Publications of the Astrophysical Observatory

This series, *Smithsonian Contributions to Astrophysics*, was inaugurated in 1956 to provide a proper communication for the results of research conducted at the Astrophysical Observatory of the Smithsonian Institution. Its purpose is the "increase and diffusion of knowledge" in the field of astrophysics, with particular emphasis on problems of the sun, the earth, and the solar system. Its pages are open to a limited number of papers by other investigators with whom we have common interests.

Another series, *Annals of the Astrophysical Observatory*, was started in 1900 by the Observatory's first director, Samuel P. Langley, and was published about every 10 years. These quarto volumes, some of which are still available, record the history of the Observatory's researches and activities. The last volume (vol. 7) appeared in 1954.

Many technical papers and volumes emanating from the Astrophysical Observatory have appeared in the *Smithsonian Miscellaneous Collections*. Among these are *Smithsonian Physical Tables*, *Smithsonian Meteorological Tables*, and *World Weather Records*.

Additional information concerning these publications may be secured from the Smithsonian Institution Press, Washington, D.C.

FRED L. WHIPPLE, *Director,*
Astrophysical Observatory,
Smithsonian Institution.

Cambridge, Mass.

Contents

	Page
1. Basic meteor theory	2
2. The observed decelerations; errors, fragmentation	3
3. The tables of basic observational data	5
a. Explanation to table 1.1	5
b. Explanation to table 1.2	7
4. Heights, lengths, and durations	7
a. Description of least-squares analysis; interrelation of variables	7
b. Results of least-squares analysis	10
c. Tables and diagrams	14
d. Small-camera meteors	15
e. Position of maximum light	17
f. Duration	19
5. Decelerations	20
6. Magnitudes and "color index"	24
a. Magnitudes	24
b. "Color index"	28
7. The ablation coefficient σ	28
a. Dependence of the mean σ on the other parameters	28
b. The variation of σ along the trajectory	32
8. The fragmentation index χ	33
9. Wake and blending	38
10. Peculiarities of individual showers; meteors with abrupt beginnings; asteroidal meteors	41
a. Showers	41
b. Meteors with abrupt beginnings	42
c. Search for asteroidal meteors	43
Acknowledgments	44
References	44
Abstract	46
Tables	47

An Analysis of the Atmospheric Trajectories of 413 Precisely Reduced Photographic Meteors

Luigi G. Jacchia,¹ Franco Verniani,² and Robert E. Briggs³

A previous paper (Jacchia and Whipple, 1961) contains a discussion of the orbital characteristics of 413 precision-reduced meteors doubly photographed with the Baker Super-Schmidt cameras in New Mexico. The present paper contains an analysis of the atmospheric trajectories of those same meteors and deals with the physical aspect of the meteor phenomenon.

A description of the observational material has been given in the above-cited paper by Jacchia and Whipple (1961); reduction techniques have been fully described by Whipple and Jacchia (1957) and will not be repeated here except for points that need more detailed explanation. We shall outline here the criteria used in the selection of these 413 meteors out of a total of about 3500 meteors doubly photographed by the Super-Schmidt cameras during the same time interval. The shutters of the Super-Schmidt cameras have two 45° openings and rotate at 1800 rpm; the meteor trail is thus interrupted 60 times a second and presents the aspect of a row of segments separated by wider breaks. In making the selection we deliberately chose only those meteors that were likely to yield excellent decelerations. On this basis we discarded nearly all meteor trails showing less than 20 clearly discernible segments and those whose segments were too closely spaced, as

well as trails appearing against rich star fields or too faint to be measured with accuracy. The selected meteors have an average of 40 well-measured segments on the better of the two films, and 34 on the other, and for all but 17 meteors the instant of appearance was recorded visually. A secondary criterion for selection was that comparable numbers of meteors should be chosen in the low, medium, and high-velocity groups, and for each month of the year. For months particularly rich in meteors, the standards of acceptance were set a little higher so that the month in question should not exert an overwhelming weight in the analysis of seasonal effects on decelerations. On the other hand, we have occasionally included a larger number of meteors belonging to a few selected showers (Quadrantids, for example) because their reductions were deemed useful for orbital purposes.

As a result of this selection, the data presented here do not represent a random sample, a fact that should be kept in mind in evaluating the analysis. In particular, it should be remembered that by excluding meteors with closely spaced trail segments we have eliminated more of the low-velocity than of the high-velocity meteors. The bias introduced by our selection is added, of course, to the bias already inherent in meteor photography.

Basic trajectory data are presented in table 1.1; the individual determinations of velocity and decelerations with other quantities derived from them are collected in table 1.2.

¹ Harvard College Observatory and Smithsonian Astrophysical Observatory.

² Centro Nazionale per la Fisica dell' Atmosfera e la Meteorologia del CNR, Rome, Italy; formerly at Harvard College Observatory and Smithsonian Astrophysical Observatory.

³ Smithsonian Astrophysical Observatory.

1. Basic meteor theory

In this paper meteor theory is considered only as a framework for the reduction of the observational material and is used in its simplest, most unsophisticated form. We expect that the observed deviations from this basic theory might be of some help in future theoretical work. Here is a summary of the basic equations and assumptions.

The acceleration \dot{v} of a body of mass m and frontal area A moving with velocity v through a gas of density ρ can be written as

$$\dot{v} = -\frac{1}{2} C_D \frac{A}{m} \rho v^2, \quad (1)$$

where C_D is the so-called drag coefficient. For supersonic velocities, C_D has a nearly constant value close to two for free-molecule flow, and again a nearly constant value of 0.92 in the case of continuum flow. The meteors photographed with the Super-Schmidt cameras have dimensions that are generally small compared with the mean free path of atmospheric molecules at the heights at which they are observed, so we have assumed that free-molecule flow is valid for them and we have assumed $C_D = \text{constant}$.

The presentation area A can be written as $A = \alpha m^{2/3}$, where α is a proportionality factor, which depends on the density and shape of the body. We have taken $\alpha = \text{constant}$, which is equivalent to assuming that all meteors have the same density and shape factor. Equation (1) can thus be written as

$$\dot{v} = -C m^{-1/3} \rho v^2, \quad (2)$$

where C is a positive constant. This equation is generally referred to as the "drag equation." The value of C can be determined from the observed velocities and decelerations if ρ and m are known.

The mass m can be computed from the observed light curve of the meteor under the basic assumption that the amount of light I_p in the photographic domain emitted by the meteor body at any instant is proportional to the kinetic energy of the atoms in the meteor coma that collide with atmospheric molecules (Öpik, 1933). The number of atoms in the meteor coma is, in turn, proportional to

the rate dm/dt at which the meteor loses its mass, so we can write (Whipple, 1943)

$$I_p = -\frac{\tau_p}{2} \frac{dm}{dt} v^2, \quad (3)$$

where τ_p is a proportionality factor; the subscript p refers to photographic intensities. This equation is generally called the "luminosity equation."

Since the spectra of meteors consist mainly of a discrete number of emission lines whose relative intensities greatly vary with meteor velocity, we must expect τ_p to depend on v .

Let us assume that

$$\tau_p = \tau_{0p} v^n. \quad (4)$$

Whipple (1943), on the basis of Öpik's theoretical results, had assumed $n=1$. Using this value of n , Jacchia (1948) derived from Öpik's data the value $\tau_{0p} = 6.46 \times 10^{-19}$ (c.g.s.), when the photographic intensity I_p is expressed in units of the intensity of a zero-magnitude star. These values of n and τ_{0p} were used by Jacchia (1948, 1949a, 1952) for deriving the masses of meteors of the Harvard-M.I.T. meteor program.

Recently, Verniani (1964a), using the observational material of the present paper, found $n = 1.0 \pm 0.15$ and $\tau_{0p} = 1.0 \times 10^{-19}$; the same values were found to apply also to the brighter meteors photographed with small cameras prior to the use of the Super-Schmidt cameras. Masses ($m_{\infty 2}$) computed using this new value of τ_{0p} are given in table 1.1, after the values computed with the old coefficient ($m_{\infty 1}$). It is these "new" masses (m_2) that have been used in the present analysis; whenever the symbol m appears in the tables without a subscript, it is understood that the mass it represents was computed using $\tau_{0p} = 1.0 \times 10^{-19}$ (c.g.s.).

Meteor masses can be computed from equation (3). Integrating and taking $n=1$, we have

$$m_b - m_a = -\frac{2}{\tau_{0p}} \int_{t_a}^{t_b} \frac{I_p}{v^3} dt, \quad (5)$$

where the subscripts a and b refer to two arbitrary points on the meteor trajectory. Removing t_b to infinity and assuming that the

residual mass of the meteor, after complete deceleration, is zero, we have

$$m = \frac{2}{\tau_{0p}} \int_t^{\infty} \frac{I_p}{v^3} dt = \frac{2E_p}{\tau_{0p}v^3}. \quad (6)$$

Here, \bar{v} stands for the effective mean velocity in the course of the visible trajectory and

$$E_p = \int_t^{\infty} I_p dt \quad (7)$$

is the meteor brightness integrated from the point corresponding to the time t to the end of the trajectory. The mass of the meteor before entering the atmosphere is, then,

$$m_{\infty} = \frac{2}{\tau_{0p}} \int_{-\infty}^{+\infty} \frac{I_p}{v^3} dt = \frac{2E_{p\infty}}{\tau_{0p}v^3}; \quad (8)$$

$E_{p\infty}$ is the total photographic light energy radiated by the meteor. For most meteors v does not change by more than a few percent in the course of the trajectory, so m_{∞} can be easily evaluated from $E_{p\infty}$. The quantity $\log_{10} E_{p\infty}$ is used in the present analysis as an index of brightness and is called ϵ_{∞} .

In a time interval dt the meteor body strikes a mass $A\rho v dt$ of air. This provides a kinetic energy $\frac{1}{2}A\rho v^3 dt$ that is used to heat, melt, vaporize, and fragment the body, causing it to lose a mass dm . We can thus write

$$dm = -\frac{1}{2}\beta A\rho v^3 dt, \quad (9)$$

where β is a proportionality factor that depends on the efficiency of the energy-transfer process and on the physical characteristics of the meteor body.

Dividing (9) by (1) we obtain

$$dm = \sigma m v dv, \quad (10)$$

where $\sigma = \beta/C_D$. This equation is sometimes called the "mass equation." Since C_D should be nearly constant (we take it as being constant) and is known with a greater degree of accuracy than any other parameter of the theory of meteors, we see that equation (10) provides the means of determining the factor β for individual meteors when m , \dot{m} , v , and \dot{v} are known. The factor σ , which is the directly determinable quantity, is sometimes referred to as the "ablation coefficient."

In (10) we can replace m and dm with their expressions from the luminosity equation; solving for σ we have

$$\sigma = \frac{\frac{I_p}{v^3} / \int_t^{+\infty} \frac{I_p}{v^3} dt}{-v\dot{v}} \approx \frac{I_p/E_p}{-v\dot{v}}, \quad (11)$$

an equation that contains only observable quantities.

Integrating (10) between two points of the trajectory characterized by the subscripts a and b , respectively, we have

$$\sigma = 2 \frac{\ln m_a - \ln m_b}{v_a^2 - v_b^2}. \quad (12)$$

Whenever more than one independent determination of the velocity is available in the course of the trajectory it is preferable to determine σ from equation (12), which involves the integrated light curve and not the instantaneous brightness as in equation (11); in this fashion the effect of short-lived flares is smoothed out. Actually, equation (11) is slightly inconsistent from the observational point of view because the instantaneous value of I_p can always be determined, while \dot{v} is computed from smoothed data covering a sizable time interval.

2. The observed decelerations; errors, fragmentation

The process for deriving instantaneous decelerations has been described in detail elsewhere (Whipple and Jacchia, 1957); here we shall repeat only the essentials. Distance D_i from an arbitrary point is computed for the observed centers of all shutter-induced trail segments i on each of the two plates. The constants a , b , c of the equation

$$D_i = a + bt_i + ce^{kt_i} \quad (13)$$

are computed by least squares; k is determined from four equidistant points on a curve of $D_i - v_{\infty}t_i$ as a function of t_i . In the above equation, b is the velocity of the meteor before the onset of deceleration, v_{∞} ; the instantaneous velocity is given by

$$v = b + kce^{kt_i}$$

and the instantaneous acceleration by

$$\dot{v} = k^2 ce^{kt_i}.$$

The aim has been to derive accelerations about 20 times larger than their inner probable error. Trails of longer duration, for which it appeared that a single least-squares solution would have yielded a much larger ratio $\dot{v}/p.e.$, were subdivided into separate sections, for each of which an independent deceleration was computed. In addition to yielding accelerations at different points of the trajectory, this division of long trails into sections has the advantage of ensuring an excellent fit of equation (13), which cannot be expected to hold perfectly from beginning to end of a long trajectory.

The sources of error in the results of meteor reductions have been discussed by Jacchia and Whipple (1961). They include effects deriving from the occasional lack of visual timing or from a small angle of intersection of the two meteor trails. Since meteors were not included in the present material when the geometric solution was not satisfactory, errors from these causes in the heights, velocities, and decelerations can be considered small. We shall, however, repeat here what was said in the paper on orbits concerning the effect of a shutter flutter since this source of error is greatest in the decelerations.

After a number of Super-Schmidt meteors had been completely reduced, there was clear evidence that a "flutter" affected the rotation of all camera shutters. Although this instrumental trouble was later eliminated by the installation of more powerful motors, it was nevertheless present during the entire period of time covered by the meteors included in this paper.

The shutter flutter was semiregular in character and exhibited widely different amplitudes, ranging from zero to 5° , with a fundamental period of $0^{\text{s}}23$, but with occasional lapses into cycles half or twice that length. When two or more cycles of the flutter are covered by the photographic trail, its effect can be eliminated with relative confidence (Whipple and Jacchia, 1957). For shorter trails, however, the process becomes more questionable, and a few meteors had to be rejected for this reason. It should be kept in mind that for short trails the shutter flutter may be the most important source of scatter in the deceleration data.

When the observed accelerations \dot{v} are compared with the theoretical accelerations \dot{v}_T computed from equation (2), a striking feature emerges. While the accelerations in the early part of the trajectories are in general statistical agreement with the theoretical values, they become increasingly too large, compared to theory, as one proceeds toward the end of the trajectories. This systematic effect has been attributed to progressive fragmentation of the meteor body (Jacchia, 1955). It was found that in the course of an individual trajectory the variation of $\log(\dot{v}/\dot{v}_T)$ is roughly proportional to that of the quantity

$$s = \log_{10} \left(\frac{m_\infty}{m} - 1 \right), \quad (14)$$

which was called the "mass-loss parameter." The proportionality coefficient χ , i.e.,

$$\chi = \frac{d}{ds} \log_{10} \frac{\dot{v}}{\dot{v}_T}, \quad (15)$$

was called the "fragmentation index." Levin (1961) rightly thinks that it should more appropriately be referred to as the "progressive fragmentation index." The introduction of the fragmentation index has proved very useful—we could say indispensable—in the analysis of the Super-Schmidt decelerations.

Severe fragmentation is found to affect the factor σ of the mass equations (10) to (12). While it may be reasonable to assume that σ is nearly constant for bodies of similar composition that experience a gradual and regular ablation in the course of their atmospheric trajectories, it is hard to see how it could keep the same value if the body dissolves in a train of fragments. In such a case, the numerator in equation (11) refers to the light emitted by all the fragments, while the deceleration in the denominator is probably that of the larger fragments in front of the train. While the meaning of σ may then become obscure, it still remains a useful parameter since it characterizes the rate at which the meteor is destroyed. If we take two meteors with the same initial mass, velocity, and angle of incidence, but characterized by different values of σ , the one with the larger σ will have a shorter duration and greater maximum brightness.

A question that logically arises is: what is the meaning of the observed deceleration of a fragmenting body? As long as the fragmentation consists of the progressive flaking off of the outer layers of the meteor body, we shall observe the same body at different points of the trajectory, and the deceleration will refer to this body. When, however, we have to deal with a train of fragments of various sizes that keep fragmenting, we may observe different bodies at different times and the measuring of the acceleration becomes more obscure. In such cases we often observe a progressive elongation of the photographic segments ("terminal blending") and, since we measure the center of these segments, a contribution to the acceleration may arise from the progressive shift of the segment center, unless the elongation happens to increase linearly with time. It would be wrong, however, to attribute the anomaly in the observed decelerations ($\chi > 0$) entirely to this effect. Although a statistical correlation exists between χ and the magnitude of terminal blending, it is not infrequent to find relatively large values of χ among meteors with no observable terminal blending, even in the presence of favorable conditions for its detection (long meteor duration, small angle of incidence). This is what we could expect if the spectrum of fragment sizes were to vary greatly from meteor to meteor.

3. The tables of basic observational data

As was mentioned earlier, tables 1.1 and 1.2 list the basic observational data pertaining to the 413 Super-Schmidt meteors involved in the present analysis. An explanation of the headings of the tables is given below.

a. Explanation to table 1.1

Trail No. Serial number of trail photographed at the Doña Ana station.

Date Year (1952, 1953, or 1954; the first two digits are omitted), month and day, with the fraction of the day given to 0^d00001, in U.T.

Shower No. Identification of associated meteor shower, if any, as indicated in table 3 of Jacchia and Whipple (1961); the table is

repeated at the end of these explanations. Only the better-known showers have been included; the letter "Q" after the code number indicates a questionable association.

Apparent Radiant	The right ascension α and the declination δ of the apparent radiant of the meteor trajectory. (The true radiant, after correction for zenith attraction and diurnal aberration, can be found in Jacchia and Whipple, 1961.)
Sin Q	Sine of the angle formed at the apparent radiant by the trails as seen from the two observing stations.
Cos Z_R	Cosine of the zenith distance of the apparent radiant.
v_a	Velocity with respect to the stations, corrected for atmospheric drag, in km/s.
M_{pm}	Photographic absolute (i.e., reduced to a standard distance of 100 km) magnitude reached by the meteor at maximum light.
H	Height above the geoid. The heights listed are as follows:
H_B	Height corresponding to the beginning of the photographic trajectory. The letter "G" after a beginning height indicates that the beginning of the meteor trajectory occurred outside the film limits and that the actual beginning height was greater than the given value.
H_{BD}	Height corresponding to the center of the first measured trail segment (BD =beginning dash).
$H_{2.5}$	Height of the point where the absolute photographic magnitude of the brightening meteor reached the value +2.5.
H_{ML}	Height of the point where the meteor reached its maximum absolute brightness.

H_{ED}	Height corresponding to the center of the last measurable segment (ED =end dash).
H_E	Height corresponding to the end of the photographic trajectory. The letter "L" after an end height indicates that the end of the trajectory was cut off by the edge of the film and that the actual end height was lower than the given value.
L_A, L_B	Length, in degrees, of the trail as photographed at the Doña Ana (A) and at the Soledad (B) stations, respectively. The letter "G" indicates that part of the trajectory was cut off by the edge of the film and that the true length is greater than the given value.
D	Duration of the photographic trail, from H_B to H_E , in seconds. The letter "G" has the same meaning as after L_A and L_B .
n_A, n_B	Number of measurable segments on the trails photographed at Doña Ana (A) and Soledad (B), respectively.
ΔM	Magnitude difference between the maximum light of the meteor and the film limit, on the better of the two photographs.
Vis. A, Vis. B	Visual magnitudes recorded by the observers at Doña Ana (A) and Soledad (B), respectively.
C.I.	"Color Index," i.e., photographic minus visual magnitude, obtained by comparing the maximum of the smoothed photographic light curve with the visual magnitude recorded by the observer. If the visual magnitude was recorded by two observers, the mean of the two values was taken. The photographic emulsion was Kodak X-ray, a blue-sensitive film.
ϵ_∞	A measure of the integrated brightness of the meteor; this quantity is defined as

$$\epsilon_\infty = \log_{10} \int_{-\infty}^{+\infty} I_p dt,$$

where I_p is the absolute photographic brightness of the meteor expressed in units of zero-magnitude stars.

m_∞ Mass of the meteor, computed from the integration of the photographic light curve, according to the formula

$$m_\infty = \frac{2}{\tau_{0p}} \int_{-\infty}^{+\infty} \frac{I_p}{v^3} dt.$$

Two values are given for the mass: $m_{\infty 1}$ is the mass in the Öpik-Jacchia system used in previous listings (Jacchia, 1948, 1949a, 1949b, 1952), computed using for the photographic luminous-efficiency coefficient the value $\tau_{0p} = 6.46 \times 10^{-19}$ (c.g.s.; I_p in zero-magnitude units); $m_{\infty 2}$ is the mass computed using $\tau_{0p} = 1.0 \times 10^{-19}$ (c.g.s.; I_p in zero-magnitude units), a value close to that derived by Verniani (1964a).

$\log \sigma$ Logarithm of the quantity $\sigma = (dm/dv)/mv$. The given value is the one that best fits the whole trajectory. For fuller explanation, see text (p. 28).

χ The "progressive-fragmentation index." For explanation, see text (p. 33).

W, B Wake and blending, respectively, expressed in an arbitrary scale from 0 to 4. For fuller explanation, see text (p. 38). A letter "Q" indicates that the given quantity is questionable.

Rem. The letters in this column describe peculiarities in the trail, as follows:

A: abrupt beginning

F: one or more fragments became detached in the course of the trajectory

S: trajectory of unusually short duration; the film probably recorded only a broad flare.

Code for identifying meteor showers listed in table 1.1

Shower No.	Shower	Shower No.	Shower
None	Sporadic meteors	10	Quadrantids
1	α Capricornids	11	Virginids
2	Southern Taurids	12	κ Cygnids
3	Southern ι Aquarids	13	Leonids
4	Geminids	14	χ Orionids
5	δ Aquarids	15	Ursids
6	Lyrids	16	σ Hydrids
7	Perseids	17	Northern Taurids
8	Orionids	18	Andromedids
9	Draconids	19	η Aquarids
		20	Northern ι Aquarids

b. Explanation to table 1.2

All data refer to the center of the trajectory sections from which velocities and accelerations were derived by least squares. For each meteor the data derived from the photograph taken at Doña Ana are listed first in consecutive order, followed, in the same order, by those derived from the Soledad photograph.

Trail No.	Serial number of trail photographed at the Doña Ana station.
H	Height above the geoid of the point in the trajectory for which v and \dot{v} were determined.
v	Instantaneous velocity of the meteor, in km/s.
\dot{v}	Instantaneous acceleration of the meteor, in km/s ² .
$p.e.$	Probable error of the acceleration, in km/s ² .
n	Number of trail segments used in the least squares.
m_1	The instantaneous mass of the meteor, computed from

$$m = \frac{2}{\tau_{0p}} \int_t^{\infty} \frac{I_p}{v^3} dt,$$

using the old value $\tau_{0p} = 6.46 \times 10^{-19}$ (c.g.s.; I_p in zero-magnitude units).

The mass-loss parameter

$$s = \log_{10} \left(\frac{m_{\infty}}{m} - 1 \right).$$

$\log \sigma$ The logarithm of the quantity $\sigma = (dm/dv)/mv$, determined from the instantaneous values of m , v , and dv/dt .

$\log \rho_{obs}$ The logarithm of the atmospheric density computed from the drag equation

$$\dot{v} = -Cm^{-1/3} \rho v^2.$$

The adopted value of the constant is $\log C = 0.333$ when the masses are expressed in the "old" system (m_1) and $\log C = 0.603$ when the "new" masses (m_2) are used.

$\Delta \log \rho_{obs}$ The difference $\log \rho_{obs} - \log \rho_{st}$, where ρ_{st} is the density tabulated in the U.S. Standard Atmosphere 1962 (1962) for the observed height H .

$\Delta \log \rho_{corr}$ This quantity is defined as

$$\Delta \log \rho_{corr} = \Delta \log \rho_{obs} - \chi(s - s_0),$$

with $s_0 = 0$.

p The weight of $\Delta \log \rho_{corr}$, computed according to the formula

$$p = 10 \psi \left(\frac{\dot{v}}{p.e.} \right) \psi(n-3) \left(\frac{m}{m_{\infty}} \right)^{1/2},$$

where

$$\psi(x) = \frac{1}{2} [1 + \operatorname{erf}(2.5 \log x - 2.1)]$$

(erf is the notation for the probability integral).

4. Heights, lengths, and durations

a. Description of least-squares analysis; interrelation of variables

We have considered four sets of heights: beginning height H_B , corresponding to the first discernible dash on either of the two plates; the height $H_{2.s}$, corresponding to the point where the absolute photographic magnitude of the meteor reaches the value +2.5 (Jacchia, 1960); the maximum light height

H_{ML} ; and the end height H_E , corresponding to the last discernible dash on the two plates. The heights $H_{2.5}$ are generally quite close to the beginnings of the meteors. They have been chosen for the analysis with the purpose of eliminating the scatter due to the variability of the plate limit. Since the increase in light of a meteor in the early part of its trajectory is mostly gradual, even small differences in the plate limit can have a considerable effect on the height of appearance.

From the basic equations of meteor theory it is possible to derive expressions that relate these four sets of heights—or rather the corresponding atmospheric densities ρ —to the parameters that characterize the meteor body and its flight. Combining the drag equation (2), the mass equation (10), and the luminosity equation (3), we obtain (Jacchia, 1949a)

$$I = C \frac{\tau_{0p}}{2} \sigma m^{2/3} \rho v^6, \quad (16)$$

from which we can compute ρ at any given point, provided we know I , m , v , and σ . With the conditions proper to each set of heights, we obtain

$$\rho_B = (2/C\tau_{0p})\sigma^{-1} I_{lim} v_\infty^{-6} m_\infty^{-2/3}, \quad (17)$$

$$\rho_{2.5} = (1/5C\tau_{0p})\sigma^{-1} v_\infty^{-6} m_\infty^{-2/3}, \quad (18)$$

$$\rho_{ML} = (1/CH_p)\sigma^{-1}(v_\infty^2 + 6/\sigma)^{-1} m_\infty^{1/3} \cos Z_R, \quad (19)$$

and, from the integration of equation (9),

$$\rho_E = (3/CH_p)\sigma^{-1} \bar{v}^{-2} m_\infty^{1/3} \cos Z_R. \quad (20)$$

In equation (17), the symbol I_{lim} indicates the limiting magnitude of the film. For a random selection of meteors we can assume that the angular velocity is proportional to the velocity v , so that $I_{lim} \sim v_\infty$, which would result in a change from -6 to -5 in the power of v_∞ in the equation. Our meteors were not randomly selected, but the relation between I_{lim} and v_∞ can be assumed to be still valid in a first approximation.

In equations (19) and (20), the symbol H_p indicates the atmospheric pressure scale height; in the last equation, \bar{v} is a mean velocity, which is defined as

$$\bar{v}^2 = \frac{\int_B^E v^2 \rho dl}{\int_B^E \rho dl},$$

where dl is an element of distance along the trajectory and B and E indicate the beginning and end points, respectively.

In all four equations the first factor, in parentheses, is a combination of quantities that we can regard as constants. We have excluded σ from the parentheses because it is a basic parameter, variable from meteor to meteor, whose value is generally determined. The other basic parameters that we find with various exponents in all four equations are v_∞ , m_∞ , and $\cos Z_R$. It is true that in equation (19) the velocity term is $(v_\infty^2 + 6/\sigma)^{-1}$, but this is equivalent to v_∞^{-n} , with n close to 2 (2.2 for $v_\infty = 20$ km/s, 2.1 for $v_\infty = 30$ km/s; 2.0 for higher velocities). In equation (20) we commit only a tolerable error if we replace \bar{v} with v_∞ . It is these four fundamental parameters (v_∞ , m_∞ , $\cos Z_R$, σ) that we shall use in the analysis of the observed heights; we shall add to them a fifth, the fragmentation index χ , which is also likely to affect the heights. For all sets of heights we shall write the equation of condition in the form

$$\log \rho = c_0 + c_1 \log \cos Z_R + c_2 \log v_\infty + c_3 \log m_\infty + c_4 \log \sigma + c_5 \chi. \quad (21)$$

Since the proper form in which χ enters the equation is not known, we have selected the simplest form, remembering that χ is already a logarithmic quantity. In view of the relatively weak dependence of ρ on χ , a change in the form of the last term would leave the solutions essentially unaltered.

Because of natural selection and other factors, hardly any of the five parameters can be considered to be entirely independent of all the other four. For example, there is an obvious relation between mass and velocity. A less obvious relation exists between Z_R and velocity, and, therefore, also between Z_R and m_∞ , since the field covered by the Super-Schmidt photographs was always close to the zenith. A dependence of σ on velocity is apparent from the analysis of the section devoted to the ablation

coefficient. The degree of interrelation between the various parameters can be appraised by examining tables 2.1, 2.2, 17.1.2, and 19.3. An analysis with all possible combinations of the basic parameters would have led to an enormous, and probably meaningless, number of solutions, so we decided on four sets of solutions for each set of heights, starting with the solution for c_0 , c_1 , and c_2 only, i.e., with only $\cos Z_R$ and v_∞ as variable parameters, and adding the remaining parameters one at a time, until the last solution contains all five of them. The order in which the parameters are added after the first solution was decided on the basis of the prospective importance of the parameter in affecting the heights.

A further proliferation of solutions is dictated by the advisability of separating special categories of meteors from the solutions and of evaluating their effect when they are included. Thus, we have excluded, singly or jointly, meteors of the following categories: 123 meteors in well-established showers (Sh); 26 meteors with an abrupt beginning (A); 12 meteors with short, flarelike trails (S); 22 meteors with highly anomalous deceleration (D).

In addition, separate solutions have been made for meteors with aphelion distances respectively smaller and larger than 6 a.u., for three different groups of $\log \sigma$ (< -11.4 , between -11.4 and -11.0 , and > -11.0), and three groups of χ ($-0.2 \leq \chi \leq 0.2$ and $\chi > 0.2$ and $\chi > 0.4$). Altogether, the following tables of solutions were computed:

- 3.1 All Super-Schmidt (S.S.) meteors
- 3.2 All minus D
- 3.3 Sporadic (Sp) [=all minus Sh]
- 3.4 Sp minus D
- 3.5 Sp minus (A+S)
- 3.6 Sp minus (A+S+D)
- 3.7 Sp minus (A+S+D) with $\log \sigma < -11.4$
- 3.8 Sp minus (A+S+D) with $-11.4 \leq \log \sigma \leq -11.0$
- 3.9 Sp minus (A+S+D) with $\log \sigma > -11.0$
- 3.10 Sp minus (A+S+D) with $-0.2 \leq \chi \leq 0.2$
- 3.11 Sp minus (A+S+D) with $\chi > 0.2$
- 3.12 Sp minus (A+S+D) with $\chi > 0.4$
- 3.13 A only
- 3.14 Sp with $Q \leq 6$ a.u.
- 3.15 Sp with $Q > 6$ a.u.

For the sake of comparison we have also computed two solutions for the small-camera meteor material, for which most of the observational data have been published by Jacchia (1952). The first solution includes all available meteors, while the second solution is limited to sporadic meteors only (tables 3.16 and 3.17, respectively).

The results of all these solutions are given in tables 3.1 to 3.17, in which the coefficients c_0 to c_5 can be found with their respective standard deviations. Table 4 presents what we believe are the most reliable values of all the coefficients from a survey of all solutions for Super-Schmidt meteors.

The coefficient c_0 given in all these tables is not the one defined by equation (21), i.e., the value $\log \rho$ takes when all the five variables are zero. Some of the variables, such as $\log v$ and $\log \sigma$, never come even close to zero; so c_0 , defined in this manner, would represent a tremendous extrapolation and its standard deviation would be entirely meaningless for the user of the tables. To bring c_0 within the range of the observed values of ρ , we have subtracted from each variable in the equation a constant close to its logarithmic mean value. The constants, expressed in the c.g.s. system, are:

$$\left. \begin{array}{l} \log \cos Z_R = -0.2 \\ \log v_\infty = 6.477 \\ \log m_\infty = -0.523 \\ \log \sigma = -11.20 \\ \chi = 0.25 \end{array} \right\} \begin{array}{l} (v_\infty = 30 \text{ km/s}) \\ (m_\infty = 0.3 \text{ g}) \end{array} \quad (22)$$

In computing the theoretical value of c_0 for the beginning heights in table 4 we have assumed, on the basis of figure 3a, that the plate limit for the "standard" meteor, as defined by (22), is magnitude $+2.6(pg)$. The equation for the end points does not contain the plate limit: in equation (20) the end point is defined as the point where the mass of the meteor is reduced to zero. Whenever we compare the observed meteor heights and lengths with those given by theory, we must keep in mind that the latter could be affected by a systematic error owing to the assumptions in the computations of the c_0 's.

For the other constants involved in the computation of the theoretical values of c_0 we

have used $C=4.01$ and $\tau_{0p}=10^{-19}$ (c.g.s.); for H_p we have taken 5.4 km, which, according to the U.S. Standard Atmosphere 1962 (1962), is the scale height prevalent in the height range from 80 to 90 km.

In compiling table 4 we have generally given the greatest weight to the solutions containing only the "cleanest" and most uniform material, i.e., sporadic meteors, from which the most anomalous members—those of classes A, S, and D—had been removed. Concerning the results summarized in table 4, a few cautionary remarks seem to be in order before any discussion. It should be clear that the least-squares process cannot give a correct solution when the parameters are interrelated—and, as we said, nearly all our meteor parameters show some degree of intercorrelation. The saving factor in such a situation is the relative looseness of the correlations. In any case, we must expect that the variables that—owing to a large coefficient, or a wide range, or both—can cause large variations in $\log \rho$ will have the better determined coefficients. Thus we feel that the coefficients of $\log v_\infty$, $\log \cos Z_R$, and $\log m_\infty$ can be trusted to be rather safe, although in decreasing order. On the other hand, it may be questioned whether the coefficients of $\log \sigma$ (which varies with v_∞) and of χ (which varies with m_∞ and $\cos Z_R$) are always significant.

To give an idea of the effect of the interrelations between the variables, we have taken three groups of meteors, each within narrow velocity limits, and have computed for them the value of c_3 in the equations

$$\log \rho = \text{const} + c_3 \log m_\infty \quad (\text{for } \rho_B \text{ and } \rho_{2.5})$$

and

$$\log \rho = \text{const} + \log \cos Z_R + c_3 \log m_\infty \\ (\text{for } \rho_{ML} \text{ and } \rho_E).$$

The results are given below. The last line gives the results for c_3 as obtained from the least-squares solutions for the coefficients c_0 , c_1 , c_2 , and c_3 , covering all Super-Schmidt meteors.

v_∞ (km/s)	H_B	$H_{2.5}$	H_{ML}	H_E	No. obs.
21-24	-0.11 ± 0.18	-0.24 ± 0.18	0.45 ± 0.12	0.48 ± 0.11	41
29-32	-0.23 ± 0.11	-0.34 ± 0.10	0.33 ± 0.10	0.34 ± 0.09	45
60-65	-0.35 ± 0.09	-0.33 ± 0.10	0.29 ± 0.14	0.30 ± 0.13	25
All	-0.25 ± 0.04	-0.30 ± 0.04	0.41 ± 0.03	0.45 ± 0.03	~400

b. Results of least-squares analysis

The observational values of the coefficients c_0 to c_3 are compared in table 4 with their theoretical values. As expected, c_1 , the coefficient of $\log \cos Z_R$, is in essential agreement with theory. In view of the purely geometric nature of this variable, any difference in c_1 from its theoretical value should probably be ascribed to inadequacies in the least-squares process caused by the interrelation of the variables.

The coefficient c_1 is the only coefficient that actually conforms to theory. Even a cursory glance at table 4 will reveal that the discrepancies between theory and observation are quite large, and it may come as a surprise that the largest discrepancies in all coefficients, except c_1 , occur in the beginning heights. In the case of c_0 there might be a partial justification for this discrepancy in the fact that the values of C and σ in equations (17) to (20) come from decelerations at points that are mostly located in the second half of the trajectory. This, however, is definitely no reason why the other coefficients should also be anomalous for the beginning heights.

While the discrepancies in the heights of maximum light and in the end heights can be blamed on the effects of fragmentation, it is more difficult to do the same for the beginning heights and for $H_{2.5}$, where fragmentation should presumably be less important. While it cannot be excluded that even near the beginning of the trajectory, fragmentation might play some role, it appears probable that at least part of the discrepancy can be explained by assuming that in the early parts of the photographic trail a nonnegligible fraction of the heating energy is dissipated as surface radiation. The heating energy available to a spherical meteor of radius r and velocity v is $\frac{1}{2}\Lambda\pi r^2\rho v^3 dt$, where Λ is the heat-transfer coefficient and ρ the atmospheric density. The energy radiated by the meteor surface is $4\pi r^2\epsilon\sigma T^4 dt$, where ϵ is the emissivity, σ the Stefan-Boltzmann constant, and T the temperature of the radiating surface. Thus, the

ratio of the energy radiated by the meteor to the heating energy is

$$R = \frac{8\epsilon\sigma T^4}{\Lambda v^3 \rho}$$

Since we can expect to have $\epsilon/\Lambda \geq 1$ and $T \geq 2000^\circ \text{K}$, we shall obtain a minimum value of R if we put $\epsilon/\Lambda = 1$ and $T = 2000^\circ \text{K}$. For the average Super-Schmidt meteor, the velocity is 35 km/s and the height of appearance is 100 km, where, according to the U.S. Standard Atmosphere 1962 (1962), the density is $5.0 \times 10^{-10} \text{g/cm}^3$. Using the above values, we obtain $R = 0.33$; in other words, at least one-third of the heating energy is radiated from the meteor surface. In view of the interplay of v , ρ , and T in the beginning heights, it is understandable that in the early part of the trajectory R should be velocity-dependent, thus altering the relation between velocity and height of appearance as derived under the assumption that surface radiation is negligible.

Thus, according to observations, for the beginning heights we have $\rho v^{3.5} = \text{const}$, when we consider meteors of equal masses, instead of the theoretical relation $\rho v^{5+} = \text{const}$. For the fixed threshold of magnitude $+2.5$ on the ascending branch of the light curve, we have $\rho v^4 = \text{const}$ instead of $\rho v^5 = \text{const}$. The effect of the meteor mass on the height of appearance is, according to observations, less than one-half of the effect predicted by theory, and the effect of σ is nil—a fact that looks rather puzzling. For the heights of maximum light and end, the dependence on the mass is close to theory, but the coefficients of $\log v$ and $\log \sigma$ are smaller than their theoretical values.

For a standard meteor, whose characteristics are given by equation (22), the observed values of c_0 are -9.23 at the beginning and -8.06 at the end; these values correspond to a height of appearance of 99.0 km and a height of disappearance of 84.5 km. We thus have a height range of 14.5 km, which corresponds to a length of trajectory of 23.0 km. This compares with a theoretical length of 34.1 km. The length of

the observed trajectory is thus only 67 percent of the theoretical length.

Since, according to observations, σ affects the end heights but not the beginning ones, its ultimate effect is that of changing the length of the trajectory. From the values $c_4 = 0$ for the beginning points and $c_4 = -0.4$ for the end points, we deduce that two meteors, identical except for a difference of one unit in $\log \sigma$ ($\log \sigma = -10.7$ and -11.7 , respectively, are well within the observed range) will appear at the same height but will disappear at heights differing by 5 km. The meteor with the larger σ has a shorter trajectory, and the difference (about 35 percent) arises from the greater end height.

This effect can be seen also from the inspection of the c_0 's in the sets of solutions given in tables 3.7, 3.8, and 3.9. Since the meteors within each group have a small range in $\log \sigma$, it is best to take the solutions for the first four coefficients only. Converting densities to heights, we have the results given below for the three groups of meteors. From these data we have $dL/d \log \sigma \approx -8$.

As we can see, the theoretical trajectory length is approached as we go to lower values of σ . From the above data it looks as if a meteor with a value of $\log \sigma$ in the vicinity of -12.0 should have a length close to that predicted by theory. Starting from the length of our standard meteor and extrapolating linearly with $\Delta c_4 = +0.4$ to low values of σ , we must go to $\log \sigma = -12.5$ before we reach agreement with theory. This extrapolation, however, is less justifiable than the first because the relation between $\Delta \log \rho$ and $\log \sigma$ does not appear to be linear and the value $\Delta c_4 = +0.4$ was derived from all meteors whose majority have values of $\log \sigma$ larger than -11.3 .

The coefficient c_5 of χ is generally rather small and close to its standard deviation for the heights of maximum light and end. The beginning heights and $H_{2.5}$, on the other hand, show a more definite dependence on χ . The

Group	Mean $\log \sigma$	$\log \rho_B - \log \rho_E$	$H_B - H_E$	Length
$\log \sigma < -11.4$	-11.55	-1.54	19.2 km	30.5 km
$-11.4 \leq \log \sigma \leq -11.0$	-11.19	-1.19	14.9 km	23.6 km
$-11.0 < \log \sigma$	-10.86	-1.07	13.3 km	21.1 km

difference between the value of c_5 for the beginning heights and that for the end heights is $\Delta c_5 = +0.3$. As in the case of σ , the larger χ is, the shorter the trajectory. With the above value of Δc_5 , we find that a meteor with $\chi=1$ has a trajectory 6 or 7 km shorter than an otherwise identical meteor with $\chi=0$; the shorter trajectory is mainly due to a lower beginning point. The effect can also be seen comparing the values of c_0 in tables 3.10, 3.11, and 3.12, as follows.

Group	Mean χ	$\log \rho_B - \log \rho_E$	$H_B - H_E$	Length
$ \chi < 0.2$	0.04	-1.26	15.7	24.9
$\chi > 0.2$	0.49	-1.06	13.1	20.8
$\chi > 0.4$	0.70	-0.97	11.9	18.8

From these data we derive $dL/d\chi = -9$. For the variation of L with σ we had previously found $dL/d \log \sigma = -8$. If we want to compare the relative effects of the observed scatter in σ and in χ on trajectory lengths, we must multiply these derivatives by the standard deviations for one observation in σ (± 0.235) and in χ (± 0.29), respectively. Thus we find that the observed scatter in χ has an effect 1.4 times greater than the observed scatter in σ .

Comparing the respective effects of σ and χ on the trajectories, we see that σ affects mainly the end heights, while χ has its greatest effect on the beginning heights. The effect of σ is what would be expected if σ controls the rate of ablation: the larger σ , the higher the end of the meteor. The significance of the effect of χ on the beginning heights—a lowering of the beginning height when χ is larger—is not so clear. Verniani (1964a) found that the luminous efficiency τ_{0p} of Super-Schmidt meteors varies with the fragmentation index χ according to the relation

$$d \log \tau_{0p} / d\chi = -0.50$$

with a probable error of ± 0.11 .

A change in τ_{0p} in equation (16) involves a corresponding change in m_∞ , since our masses

are derived from the integrated luminosities according to equation (8). We shall then have

$$d \log \rho_B = -\frac{1}{2} d \log \tau_{0p},$$

and

$$\frac{d \log \rho_B}{d\chi} = \frac{d \log \rho_B}{d \log \tau_{0p}} \frac{d \log \tau_{0p}}{d\chi} = -\frac{1}{3} \cdot \left(-\frac{1}{2}\right) = \frac{1}{6}.$$

This is just about the value of c_5 we found for the beginning heights (table 4). It thus appears possible that the effect of χ on the beginning heights might come about through a variation of the luminous efficiency with χ . In this connection it will be recalled that Millman (1935) and Russell (1960) have noted that the excitation of the iron vapor in meteor spectra is lowered in flares. On the other hand, according to Millman and McKinley (1963), it is quite normal for the ionized elements to appear strong in bursts.

Since fragmentation lowers the height of appearance of meteors, the case of the highly fragmentable Draconids, for which Jacchia, Kopal, and Millman (1950) and Jacchia (1963) found anomalously great heights, remains more puzzling than ever. We can only surmise, on the basis of the unique appearance of some members of this shower (Jacchia, 1956, 1963), that this group of meteors is so different from the ordinary meteors regarding their physical characteristics that in their flight other phenomena overshadow the usual effects.

It may be of interest to compare the values of c_2 and c_3 , the coefficients of $\log v$ and of $\log m$, in the three sets of solutions, tables 3.10, 3.11, and 3.12, which cover different ranges of χ . Taking c_3 from the solutions for c_0 to c_3 we have the beginning heights as shown below.

As we can see, an increase in fragmentation causes the coefficients to stray more from their theoretical values; it is clear, however, that even for $\chi=0$ we are still very far from having agreement with theory. For the heights of maximum light and end, the dependence of the coefficients on χ is considerably less evident.

Group	Mean χ	c_2	c_3	No. obs.
$ \chi < 0.2$	0.04	-3.60 ± 0.21	-0.29 ± 0.06	117
$\chi > 0.2$	0.49	-3.32 ± 0.23	-0.11 ± 0.07	109
$\chi > 0.4$	0.70	-3.07 ± 0.40	-0.03 ± 0.12	50
Theoretical values		(-5 ⁺)	-½.	

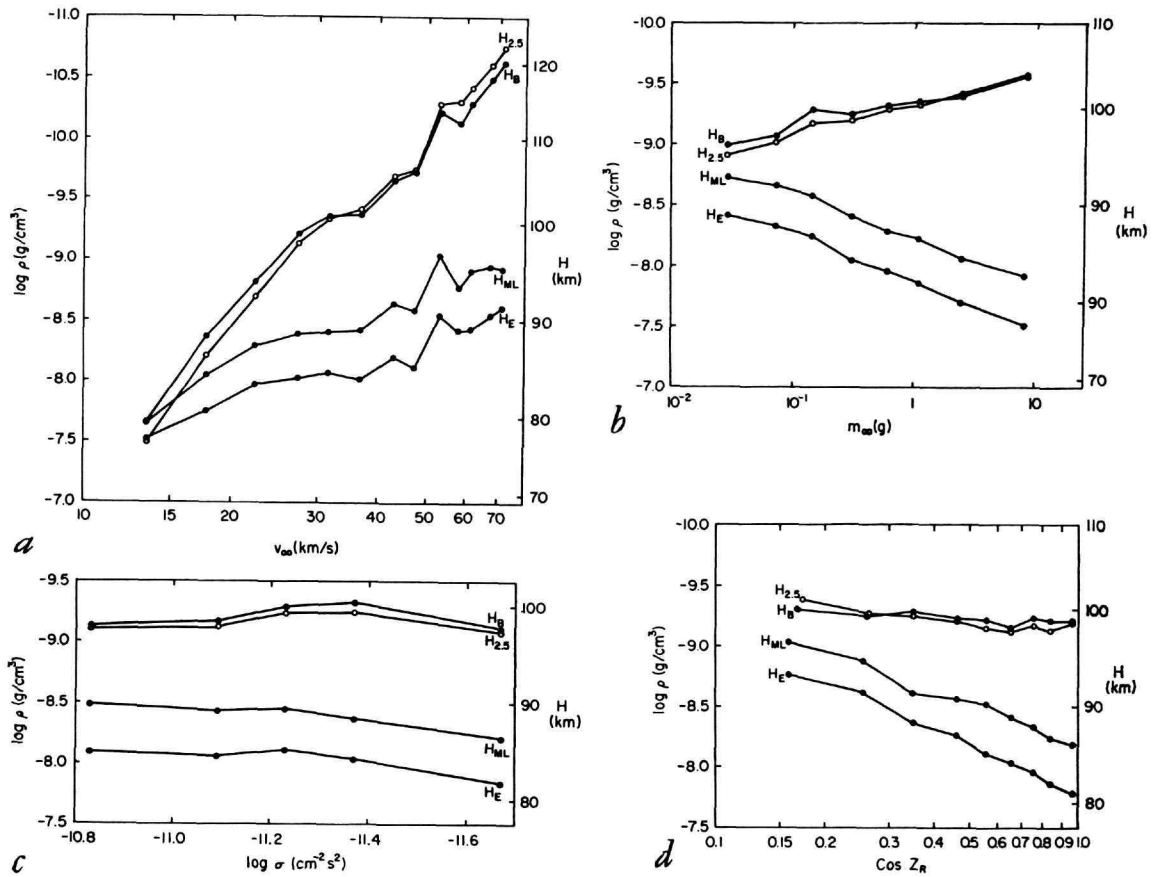


FIGURE 1.—Heights of the standard meteor for all Super-Schmidt meteors: *a*, means for velocity groups when velocity is varied; *b*, means for mass groups when mass is varied; *c*, means for ablation coefficient groups when ablation coefficient is varied; *d*, means for zenith angle groups when zenith angle is varied.

The separate solutions for meteors with aphelion distances greater than 6 a.u. and smaller than 6 a.u., respectively (tables 3.14 and 3.15), confirm the effect found by Jacchia (1958, 1963) for the beginning heights, namely that meteors in long-period orbits appear at greater heights than those in short-period orbits. The difference between the two groups is about 1.8 km (0.12 in $\log \rho$), and with little change it carries through to the heights of maximum light and end. The average values of $\log \sigma$ and χ for the two groups are as follows:

	$\log \sigma$	χ
$Q > 6$ a.u.	-11.27 ± 0.02	0.24 ± 0.03
$Q \leq 6$ a.u.	-11.14 ± 0.02	0.26 ± 0.03

The difference in χ is inconclusive, while the

difference in σ is accounted for by the difference in velocity between the two groups (see sec. 7).

The solutions for the 26 meteors with abrupt rise from beginning to maximum light (table 3.13) show that such meteors become visible, on the average, 4 km lower than the other meteors with the same characteristics of mass, velocity, and angle of incidence, and disappear about 1 km lower than these. (These data have been taken from the solutions for the first four coefficients only, since a larger number of unknowns is bound to make the solutions unreliable with such a scanty sampling; actually the difference becomes a little larger when all six variables are introduced.) By having an abrupt beginning, a meteor trajectory is, therefore, shorter by 20 percent on the average.

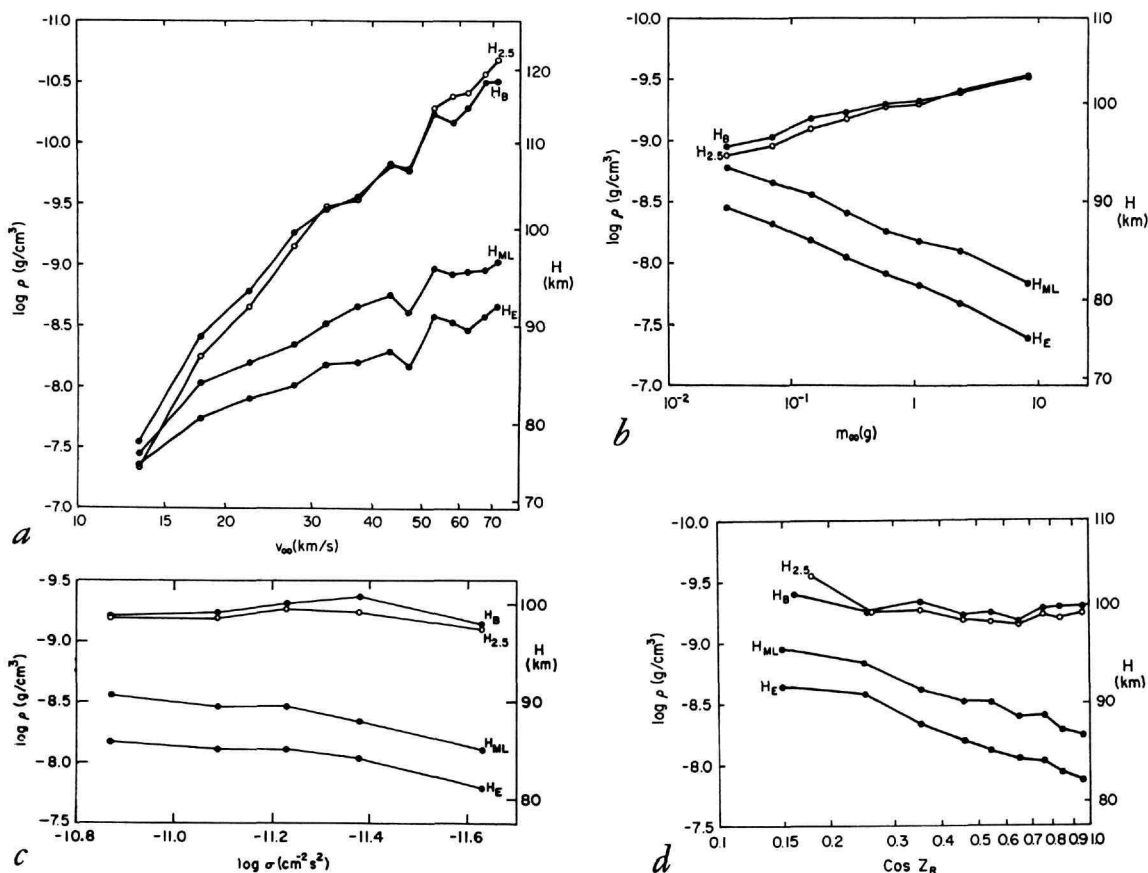


FIGURE 2.—Heights of the standard meteor for sporadic Super-Schmidt meteors only, excluding classes A, S, and D: *a*, means for velocity groups when velocity is varied; *b*, means for mass groups when mass is varied; *c*, means for ablation coefficient groups when ablation coefficient is varied; *d*, means for zenith angle groups when zenith angle is varied.

An abrupt rise to maximum is invariably followed by a gradual blurring of the shutter breaks; clearly the phenomenon is caused by a sudden disintegration of the meteor body. If it had not been for this disintegration, with its concomitant increase of effective presentation area, the meteor probably would not have been visible at all on the photographs, because it was too faint; this explains the lower heights of appearance of such objects.

We shall conclude this account of the least-squares analysis of the heights of Super-Schmidt meteors by giving, for quick reference, the equations for $\log \rho$ at the four usual heights with the observational coefficients from table 4—except for c_0 , which here has the same meaning as in equation (21).

$$\log \rho_B = 13.26 - 3.5 \log v_\infty - 0.25 \log m_\infty + 0.2\chi \quad (23)$$

$$\log \rho_{2.5} = 16.59 - 4.0 \log v_\infty - 0.28 \log m_\infty + 0.1 \log \cos Z_R \quad (24)$$

$$\log \rho_{ML} = -2.61 - 1.7 \log v_\infty + 0.37 \log m_\infty + 1.0 \log \cos Z_R - 0.5 \log \sigma \quad (25)$$

$$\log \rho_E = -3.00 - 1.4 \log v_\infty + 0.40 \log m_\infty + 1.2 \log \cos Z_R - 0.4 \log \sigma - 0.1\chi. \quad (26)$$

c. Tables and diagrams

The correlation between meteor heights and the variables that were used in the least-squares analysis is better visualized when we vary one parameter at a time. To do this we must first

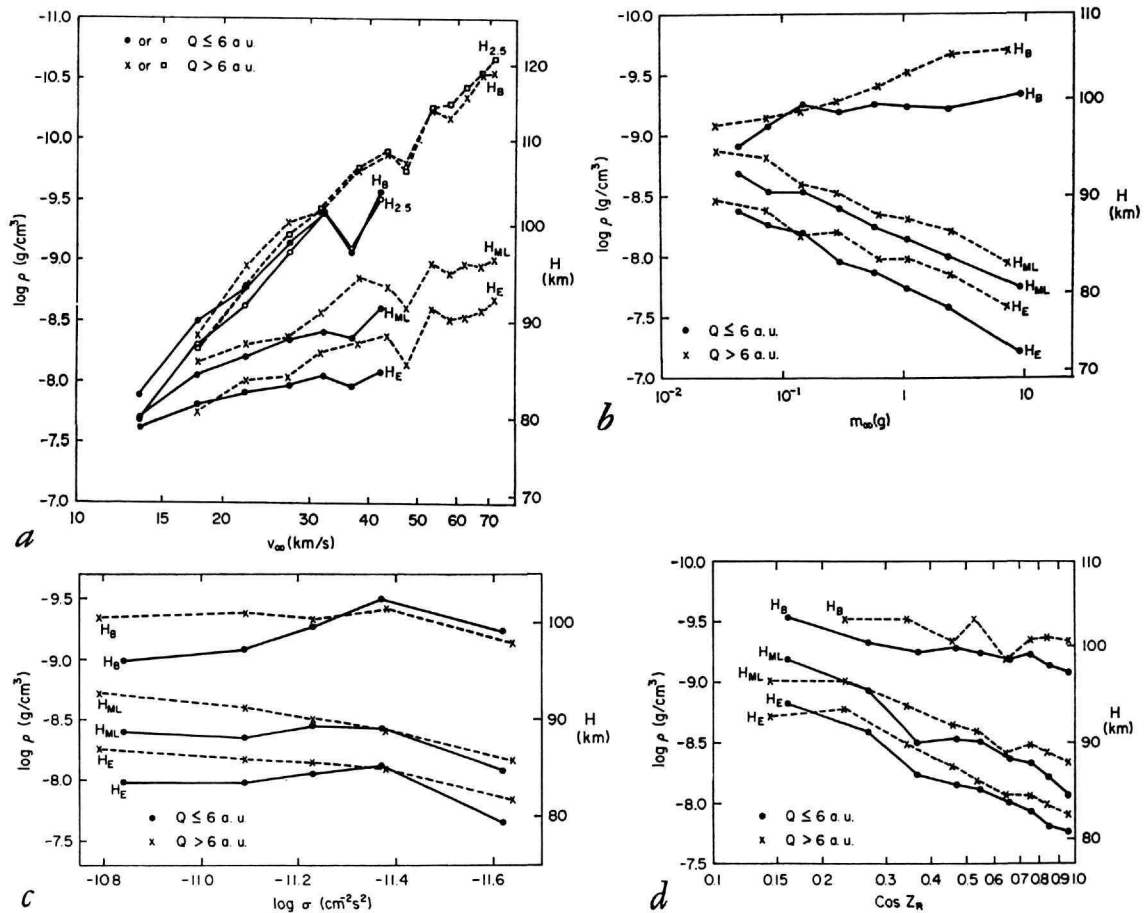


FIGURE 3.—Heights of the standard meteor for all Super-Schmidt meteors, divided into two groups according to aphelion distance Q : a , means for velocity groups when velocity is varied; b , means for mass groups when mass is varied; c , means for ablation coefficient groups when ablation coefficient is varied; d , means for zenith angle groups when zenith angle is varied.

reduce the heights to standard values of all the other parameters, then divide the heights into groups that fall within convenient intervals of the variable in question, and finally take means of the values within each group. The standard values that were selected for the various parameters are the same that were used for the computation of c_0 , equation (22). For the reduction to standard values we used the coefficients obtained from the particular least-squares solution pertaining to the group of meteors analyzed.

The results of these efforts appear in tables 5.1.1 to 5.6.4 and figures 1 to 4. For the sake of completeness we have added in tables 6.1 to 6.2 and figure 5 the unreduced means of the four

types of heights for the usual velocity and mass groups. The latter data may be useful for purely statistical purposes.

The relation between $\log v_\infty$ and $\log \rho$ corresponding to the various heights we consider is not strictly linear. As a result the averages computed for all meteors do not necessarily fall on the curves of $\log \rho$ as a function of v_∞ .

Whenever mean values appear in tables throughout this paper, we have also given their standard deviations. These appear as confidence marks in all diagrams where means are plotted.

d. Small-camera meteors

Basic data for 119 meteors photographed in Massachusetts and in New Mexico with small-

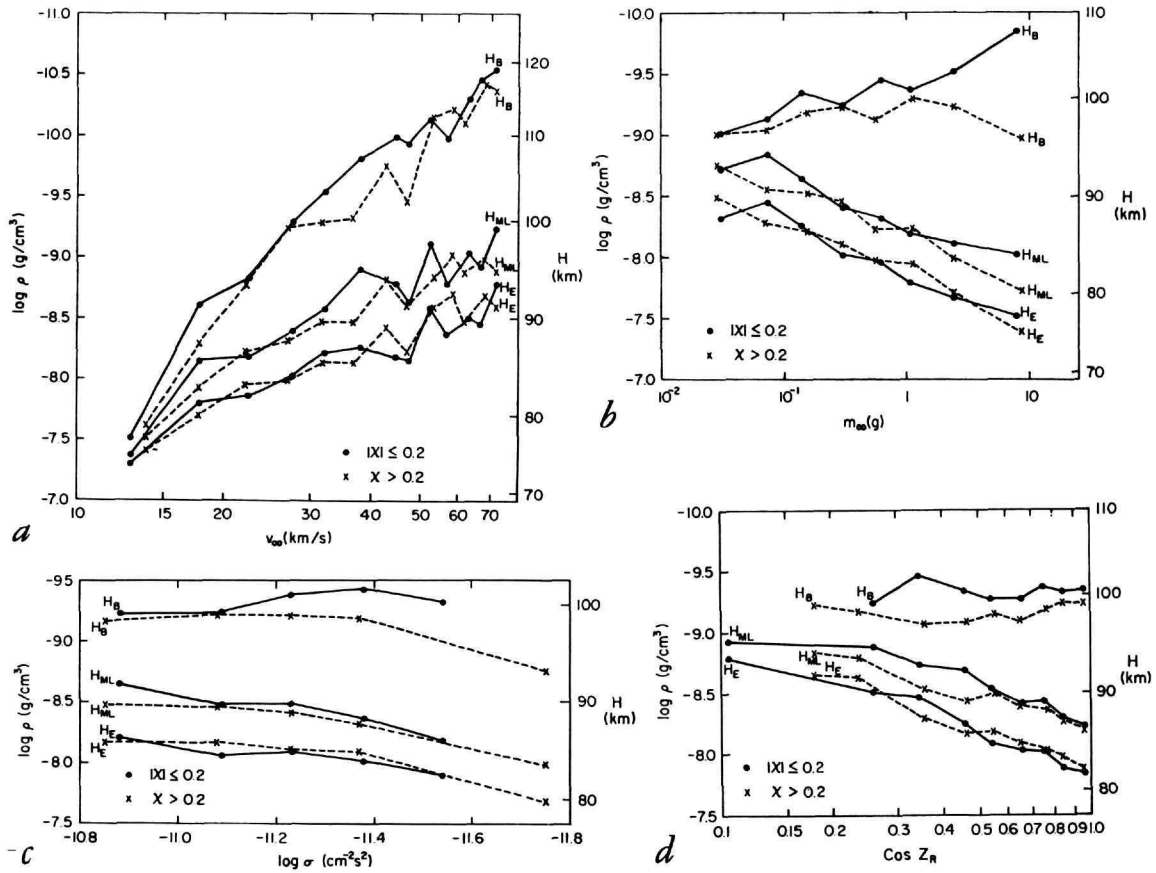


FIGURE 4.—Heights of the standard meteor for sporadic Super-Schmidt meteors minus (A+S+D), divided into two groups of the fragmentation index χ : *a*, means for velocity groups when velocity is varied; *b*, means for mass groups when mass is varied; *c*, means for ablation coefficient groups when ablation coefficient is varied; *d*, means for zenith angle groups when zenith angle is varied.

aperture patrol cameras have been published by Jacchia (1952). Several more of such meteors have been reduced with precision techniques; altogether we now have data for 210 small-camera meteors. For many of these it was impossible to obtain reliable decelerations, not to speak of such quantities as σ and χ , which require first-class data. The first of these, σ , was computed for only 88 meteors, and the second, χ , for only 58. In spite of the heterogeneity and much lower quality of this material, we thought that it would be appropriate to run it through the analytical process so that the results could be compared with those of the Super-Schmidt meteors.

The results of the least-squares solutions (tables 3.16 and 3.17) are given after those for

the Super-Schmidt meteors. Even a cursory glance at these tables shows that the coefficients c_1 and c_2 undergo drastic changes when the mass is added to the variables, indicating a higher degree of interrelation among the first three variables ($\cos Z_R$, v_∞ , m_∞) than in the Super-Schmidt material. The further changes that occur in nearly all coefficients when $\log \sigma$ is added to the variables may be attributed, perhaps, to the fact that the meteors for which σ can be determined are a selective group, which cannot be directly compared with the average small-camera meteor. When χ is added to the variables, the coefficients again change appreciably; this time the cause must be sought in the relatively small range of χ and in its relations with mass and velocity.

Under such conditions it would be imprudent to draw any conclusions from these solutions. If anything, they can be considered an object lesson in the danger of applying a least-squares analysis to a nonhomogeneous material when the variables are anything but independent, and a justification for the laborious photographic program with the Super-Schmidt cameras. We shall limit ourselves to pointing out that the large discrepancy between the theoretical and the observed values of c_2 , the coefficient of $\log v_\infty$, in the beginning heights is found again here, just as for the Super-Schmidt meteors, when we consider only the solutions with the first three variables. When σ and χ are introduced in the solution, the discrepancy becomes smaller, but there is reasonable doubt that these solutions are really representative.

More significant is, perhaps, a comparison of the observed values of c_0 with those obtained from theory. Since the average values of most parameters, especially those of the mass, for small-camera meteors are considerably different from those of the Super-Schmidt meteors, we shall use here a different "standard" meteor, for which the parameters are as follows: $v_\infty = 30$ km/s; $\log \cos Z_R = -0.2$; $\log m_\infty = 0.77$; $\log \sigma = -11.52$; $\chi = 0$.

For the beginning heights we shall assume that the plate limit is -1 magnitude (photographic) (see below). As we can see, the agreement is quite good. From these data we derive a trajectory length of 30.0 km, which is 97 percent of the theoretical length. Since the limiting magnitude of the photographs cannot be determined with any degree of accuracy (it varies as much as two magnitudes for different cameras in different locations), this last comparison must be taken with more than a grain of salt.

e. Position of maximum light

The relative position of the maximum light on the trail can be described by the parameter F , defined as:

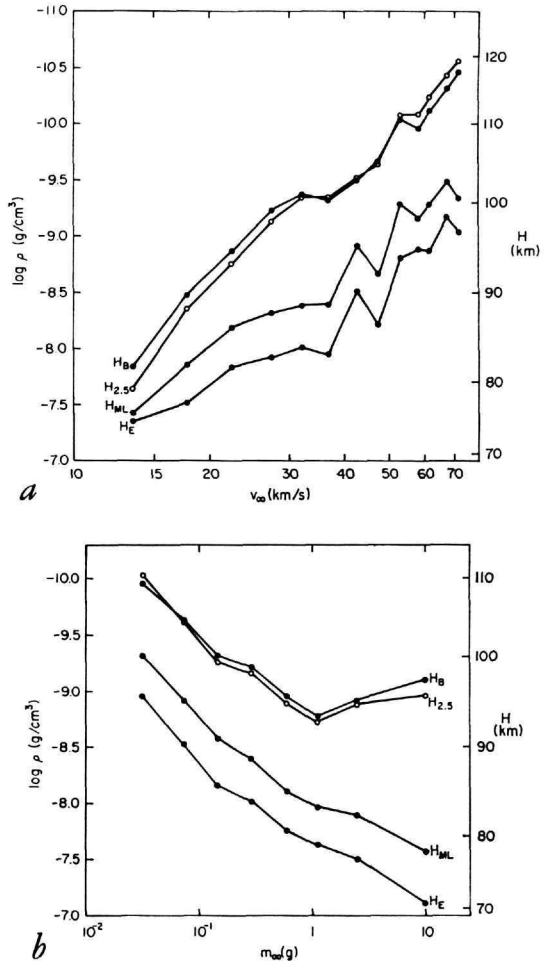


FIGURE 5.—Average observed heights of all Super-Schmidt meteors for: a, velocity groups; b, mass groups.

$$F = \frac{H_B - H_{ML}}{H_B - H_E} \tag{27}$$

The observed values of F range from 0.032 (abrupt meteor) to 0.965. The distribution of F is plotted in figure 6. The average value is 0.65 ± 0.01 . According to the data of table 4, the theoretical value of F for the standard meteor should be 0.684. According to the same

	Beginning		Maximum light		End	
	theor.	obs.	theor.	obs.	theor.	obs.
c_0	-8.76	-8.79	-7.85	-7.75	-7.28	-7.33
$H(\text{km})$	93.1	93.4	81.9	80.6	73.7	74.5

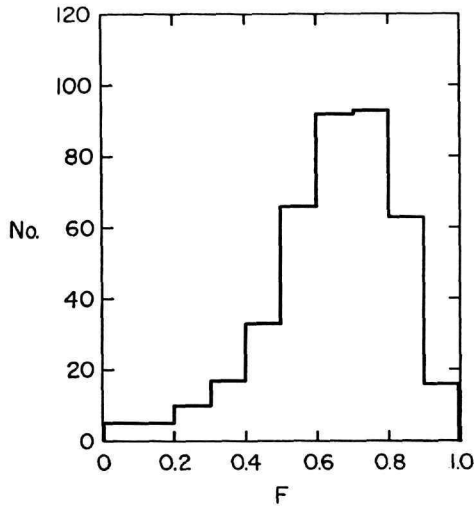


FIGURE 6.—Frequency distribution of F , the fraction of the trajectory corresponding to the position of maximum light, for all Super-Schmidt meteors.

table the observational value is 0.697.⁴ We should recall that the observed F always refers to the actual maximum light even if it occurs in a flare.

The average value of F has been computed for two of the principal showers, the Geminids and the Southern Taurids, which are known to differ rather widely in the physical characteristics of their members. The position of the maximum light proves, however, to be near to that of sporadic meteors (see table 7.1). For abrupt-beginning meteors, the maximum is, of course, much closer to the beginning. However, some of the A meteors reach their maximum light after the initial burst at a normal position in the trail. For the standard small-camera meteor \bar{F}_{obs} is 0.68, while the theoretical value of F is 0.58. This reflects the greater frequency of flares toward the end of the trajectory in bright meteors.

Table 7.2 shows F as a function of velocity. As we see also in figure 7a, F slightly increases with increasing v_{∞} . The result of a least-squares solution (v_{∞} in km/s) is $F = (0.64 \pm 0.01) + (0.0016 \pm 0.0006)(v_{\infty} - 30)$. The solution is not fully

⁴ The difference from the average value of 0.65 is essentially due to the difference between $\bar{F} = \frac{(\bar{H}_B - \bar{H}_{ML})}{(\bar{H}_B - H_B)}$ and $\frac{\bar{H}_B - \bar{H}_{ML}}{\bar{H}_B - \bar{H}_B}$.

adequate; the figure shows that between about 10 and 40 km/s we have $\frac{dF}{d \log v_{\infty}} = 0.03 \pm 0.01$, while $\frac{dF}{d \log v_{\infty}} \approx 0$ when $v_{\infty} > 40$ km/s.

Table 7.3 shows F as a function of $\log \sigma$. With the exception of the first point on the side of small values of σ there is a smooth decrease of F with increasing σ . The least-squares solution yields $F = (0.62 \pm 0.01) - (0.177 \pm 0.034)(\log \sigma + 11.0)$. However, between about -11.4 and -10.7 a better approximation (fig. 7c) is $F = 0.61 - 0.32(\log \sigma + 11.0)$.

Finally, table 7.4 shows F as a function of the fragmentation index χ . A least-squares solution yields $F = (0.67 \pm 0.01) - (0.065 \pm 0.032)\chi$. Tables 7.2 to 7.4 and figure 7 do not actually represent the behavior of F as a function of v_{∞} , σ , and χ because of the well-known intercorrelations between these parameters. The actual dependences can be found from tables 5.1.1 to 5.6.4 for meteors having standard values of all the parameters except the one that in each case is the variable.

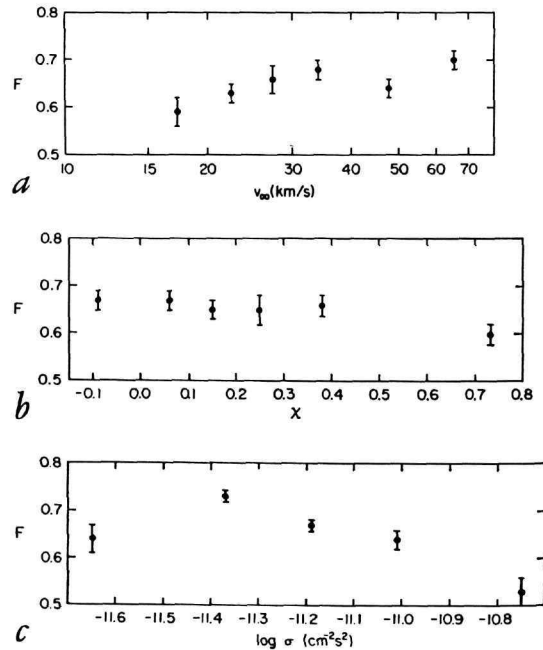


FIGURE 7.—The position of maximum light as a function of: a, velocity; b, fragmentation index; c, ablation coefficient. (F is the fraction of the trajectory corresponding to the position of maximum light. All Super-Schmidt meteors.)

From the analysis we can draw the following conclusions:

1. F varies strongly with velocity proceeding from 0.51 for 18 km/s to 0.86 for 68 km/s. The average value of $\frac{dF}{d \log v_{\infty}}$ is about

0.6 (compared with 0.03 quoted above). Recalling that for 30 km/s F is 0.70, it is clear that the increase of F with $\log v_{\infty}$ is not linear and becomes slower at high velocities.

2. F strongly increases with increasing mass, from 0.37 for $m_{\infty}=0.03$ g to 0.77 for $m_{\infty}=8.3$ g. Also in this case the relation between F and $\log m_{\infty}$ is not linear and the increase slows down for large masses. The average value of $\frac{dF}{d \log m_{\infty}}$ is about 0.15.

3. F increases with increasing $\cos Z_R$; it is 0.6 for $\cos Z_R=0.25$ and 0.71 for $\cos Z_R=0.95$.

Average value of $\frac{dF}{d \log \cos Z_R} \approx 0.15$.

4. F decreases with increasing σ for $\log \sigma > -11.2$; in the range from -10.8 to -11.2 we have $\frac{dF}{d \log \sigma} = -0.25$. For values of $\log \sigma$ smaller than about -11.2 , F is constant.

5. F is independent of χ . It is interesting and a little surprising to find that the degree of fragmentation does not on the average affect the relative position of the maximum light.

f. Duration

The duration of a meteor is clearly given by

$$D = \frac{H_B - H_E}{v \cos Z_R}, \quad (28)$$

where v is the average velocity between the heights of appearance and disappearance. Both the theoretical and the observed durations can be expressed in terms of the meteor parameters by means of equations (17) and (20), or equations (23) and (26), recalling that $H_B - H_E = \bar{H}_p (\ln \rho_B - \ln \rho_E)$, where \bar{H}_p is the average density scale height. We have

$$D_{obs} = \frac{\bar{H}_p \ln 10}{v \cos Z_R} (-16.26 + 2.1 \log v_{\infty} + 0.65 \log m_{\infty} + 1.2 \log \cos Z_R - 0.4 \log \sigma - 0.3\chi) \quad (29)$$

and

$$D_{th} = \frac{\bar{H}_p \ln 10}{v \cos Z_R} (-24.56 + 4 \log v_{\infty} + \log m_{\infty} + \log \cos Z_R - \log I_{itm}). \quad (30)$$

Equation (29) gives approximately the dependence of the duration on velocity, mass, zenith angle, and other parameters. Equation (30) has been used to provide a comparison with the observed durations.

The observed durations range from 0^h17 to 3^h84. The standard meteor should have a theoretical duration of 1^h13, while the observed duration is, according to table 4, only 0^h76, i.e., 67 percent of D_{th} . The average duration of all Super-Schmidt meteors is 0^h79 \pm 0.02.

The average ratio of durations $\frac{D_{obs}}{D_{th}}$ is 0.61 \pm 0.01. The two extremes are, respectively, 0.129 (A meteor) and 1.178. Table 8.1, which shows the average ratio for several characteristic groups of meteors, also contains the differences ΔH between observed and theoretical heights. The theoretical heights are obtained by equations (17) and (20) with the following numerical values: $C=4.01$ c.g.s. units; $\tau_{op}=10^{-19}$ c.g.s. units; $I_{itm}=10^{-0.4M_{itm}}$; $M_{itm}=M_{pm}+\Delta M$ = effective plate limit. For ΔM see the explanation to table 1.1.

For obvious reasons, S meteors have the lowest mean value (0.35) of $\frac{D_{obs}}{D_{th}}$. Also A meteors are, on the average, much shorter than required by theory ($\frac{D_{obs}}{D_{th}}=0.45$). In this matter, no difference is found between short- and long-period meteors. Shower meteors appear to have a duration a little less anomalous than sporadic meteors.

Table 8.2 shows the ratio of durations for groups of increasing velocity. With the exception of the first group, the meteors have a tendency to become shorter than expected when the velocity increases (fig. 8a). The discrepancy between observed and theoretical beginning heights increases strongly with v_{∞} , while ΔH_{ML} and ΔH_E remain practically constant.

Table 8.3 and figure 8b show $\frac{D_{obs}}{D_{th}}$ as a function of the mass. There is no significant dependence of this quantity on mass. The discrepancy between observed and theoretical beginning heights increases with mass, while ΔH_{ML} and ΔH_E do not vary much.

The ratio of the durations decreases rapidly with increasing σ (table 8.4, fig. 8c); $\frac{d}{d \log \sigma} \left(\frac{D_{obs}}{D_{th}} \right)$ is about -0.25 . From equations (29) and (30) we can compute $\frac{d}{d \log \sigma} \left(\frac{D_{obs}}{D_{th}} \right) = \frac{-0.4 \bar{H}_p \ln 10}{D_{th} v \cos Z_R}$, and the numerical agreement turns out to be quite good.

A similar decrease occurs in $\frac{D_{obs}}{D_{th}}$ when χ increases (table 8.5, fig. 8d). We find $\frac{d}{d\chi} \left(\frac{D_{obs}}{D_{th}} \right) \approx -0.2$, in agreement with the expression $\frac{d}{d\chi} \left(\frac{D_{obs}}{D_{th}} \right) = \frac{-0.3 \bar{H}_p \ln 10}{D_{th} v \cos Z_R}$ that can be obtained by equations (29) and (30).

The values of ΔH_B and ΔH_{ML} increase in modulus with both σ and χ . The dependence on σ is stronger, and ΔH_B does not vary appreciably.

Table 8.6 and figure 8e show $\frac{D_{obs}}{D_{th}}$ as a function of ϵ_∞ (it is almost a constant). A rapidly increasing discrepancy of ΔH_B between observed and theoretical heights is shown, while ΔH_{ML} and ΔH_B are nearly constant.

Among the showers, the Southern Taurids have an average value of $\frac{D_{obs}}{D_{th}} = 0.84 \pm 0.02$ and the Northern Taurids have $\frac{D_{obs}}{D_{th}} = 0.77 \pm 0.05$, rather high values, as could have been expected from less fragmenting objects. Also, three σ Hydrids have a high value of $\frac{D_{obs}}{D_{th}} : 0.87 \pm 0.10$. On the other side, a single Draconid has $\frac{D_{obs}}{D_{th}} = 0.18$; a Leonid has $\frac{D_{obs}}{D_{th}} = 0.44$, and the δ Aquarids have $\frac{D_{obs}}{D_{th}} = 0.50 \pm 0.05$.

The average difference $\Delta H_{2.5}$ between observed and theoretical heights at magnitude 2.5 is peculiar for each shower. For details on the peculiarities of individual showers, see section 10.

5. Decelerations

Before the systematic use of rockets made it possible to measure atmospheric densities and pressures at high altitudes, meteors provided

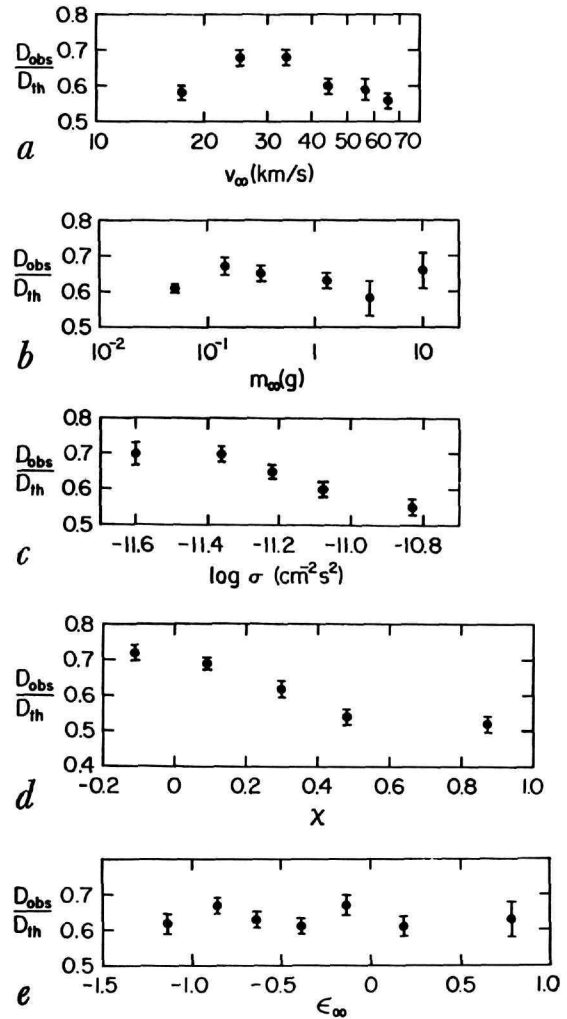


FIGURE 8.—Ratio D_{obs}/D_{th} of the observed and theoretical durations of all Super-Schmidt meteors as a function of: a, velocity; b, mass; c, ablation coefficient σ ; d, fragmentation index χ ; e, brightness.

the only means for deriving atmospheric densities at heights between roughly 50 and 100 km (Whipple, 1943; Jacchia, 1948, 1952). Now the approach can be reversed, and we can assume the atmospheric densities as known and can try to derive some information on the meteor process. Although the mean atmospheric-density profile can be considered as sufficiently well established in the meteor region, we can still use meteor decelerations to test the presence of seasonal fluctuations in the upper atmosphere.

A similar analysis had already been made earlier by Jacchia (1957a), who used 178 Super-Schmidt meteors. He also searched for the presence of lunisolar tidal oscillations in the atmosphere; the results showed no evidence of such oscillations, and we shall not attempt to repeat this part of his analysis. We will follow here essentially the same procedure of investigation.

From the drag equation, we have

$$\log \rho_{obs} = \log(-\dot{v}) + \frac{1}{2} \log m - 2 \log v - \log C. \quad (31)$$

To correct all the observed values of the atmospheric densities for the effects of fragmentation, we introduce the fragmentation index χ and reduce $\log \rho_{obs}$ to a given point on the trail where $s=s_0$. We have thus

$$\log \rho_{corr} = \log \rho_{obs} - \chi(s-s_0). \quad (32)$$

For each deceleration we can define $\Delta \log \rho_{corr}$ as

$$\Delta \log \rho_{corr} = \log \rho_{corr} - \log \rho_T, \quad (33)$$

where ρ_T is the atmospheric density corresponding in the U.S. Standard Atmosphere 1962 (1962) to the height where the meteor had velocity v , acceleration \dot{v} , and mass m . For each meteor we will define $\overline{\Delta \log \rho_{corr}}$ as

$$\overline{\Delta \log \rho_{corr}} = \frac{\sum_{i=1}^k p_i \Delta \log \rho_{corr i}}{\sum_{i=1}^k p_i}, \quad (34)$$

where k is the number of decelerations determined for the meteor and p_i is the weight of the i -th deceleration given by

$$p_i = 10 \psi \left(\frac{\dot{v}_i}{p.e._i} \right) [\psi(n_i - 3)] \left(\frac{m_i}{m_\infty} \right)^{1/2}, \quad (35)$$

where $p.e._i$ is the probable error of the deceleration \dot{v}_i , n_i is the number of segments used in the computation of \dot{v}_i , and $\psi(x)$ is defined as

$$\psi(x) = \frac{1}{2} [1 + \operatorname{erf}(2.5 \log x - 2.1)]. \quad (36)$$

The factor $\left(\frac{m_i}{m_\infty} \right)^{1/2}$ is introduced to decrease the importance of decelerations near the end of

trajectories, where fragmentation might be so severe as to make a correction meaningless. In the analysis of fragmentation effects we have not used this factor, of course; see, for example, equation (37).

We will select the value of s_0 in a way that the scatter in $\Delta \log \rho_{corr}$ reaches a minimum. First, a preliminary analysis is necessary to eliminate the meteors that display clearly anomalous values of $\Delta \log \rho_{corr}$. In doing this we have assumed $s_0=0$ from the results of Jacchia's (1957a) analysis. We have used all the Super-Schmidt meteors with the exception of (1) nine meteors without decelerations; (2) three meteors without χ ; (3) 20 Geminid meteors known to give systematically smaller values of $\Delta \log \rho_{corr}$ (Jacchia, 1952); (4) three Draconid meteors known to give very high values of $\Delta \log \rho_{corr}$ (Jacchia, 1956); (5) meteors nos. 3037, 8215, because of their uncommon values of χ , respectively +2.97 and -0.85. As a result of this preliminary analysis, we have eliminated from the final analysis 26 more meteors⁵ whose values of $\Delta \log \rho_{corr}$ differed from the overall average more than twice the standard deviation of an individual meteor with average weight. We are thus left with 350 meteors.

We now can find the value s_{0m} that minimizes the scatter in $\Delta \log \rho_{corr}$, i.e., the quantity

$$\eta = \sum_{i=1}^{N'} \lambda_i (\Delta \log \rho_{corr i} - \overline{\Delta \log \rho_{corr}})^2,$$

where

$$\lambda_i = p_i \left(\frac{m_i}{m_\infty} \right)^{-1/2}$$

and

$$\overline{\Delta \log \rho_{corr}} = \frac{\sum_{i=1}^{N'} \lambda_i \Delta \log \rho_{corr i}}{\sum_{i=1}^{N'} \lambda_i}; \quad (37)$$

N' is the total number of decelerations of our 350 meteors ($N'=1168$). It is easy to find the analytical expression of s_{0m} :

$$s_{0m} = - \frac{\sum_{i=1}^{N'} \lambda_i A_i B_i}{\sum_{i=1}^{N'} \lambda_i B_i^2},$$

⁵ Nos. 3288, 3651, 5273, 5370, 6429, 6961, 7002, 7052, 7067, 7609, 7188, 7734, 7946, 8054, 8147, 8192, 8294, 8415, 8668, 9284, 9833, 9955, 10064, 10173, 10279, 10480. Many of them have large negative values of $\overline{\Delta \log \rho_{corr}}$, and are slow or very slow meteors.

where

$$\begin{cases} A_i = A'_i - \bar{A}' ; & \bar{A}' = \frac{\sum_{i=1}^{N'} \lambda_i A'_i}{\sum_{i=1}^{N'} \lambda_i} \\ B_i = \chi_i - \bar{\chi} ; & \bar{\chi} = \frac{\sum_{i=1}^{N'} \lambda_i \chi_i}{\sum_{i=1}^{N'} \lambda_i} \\ A'_i = \log \rho_{obs\ i} - \log \rho_{T\ i} - \chi_i s_i. \end{cases} \quad (38)$$

Here, obviously, χ_i is the same for all the decelerations pertaining to the same meteor.

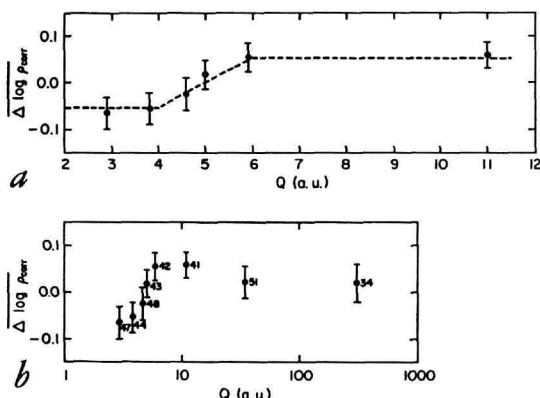


FIGURE 9.—Average residuals $\overline{\Delta \log \rho_{corr}}$ as a function of the aphelion distance Q : *a*, natural values; *b*, logarithms. [The broken line represents correction applied to $\overline{\Delta \log \rho_{corr}}$ in equation (42).]

The result is: $s_{0m} = 0.05 \pm 0.03$ and η is given by $\eta = \text{const} \times (1 - 0.13s_0 + 1.21s_0^2)$. The solution found by Jacchia (1957a) was $s_{0m} = 0.00$ and $\eta = \text{const} \times (1 + 0.96s_0^2)$ for 121 meteors. There seemed to exist a dependence of s_{0m} on the average fragmentation index of the group of meteors used to find s_{0m} itself. To reveal this dependence we have taken 78 meteors with χ comprised between -0.07 and 0.07 and combined them, in succession, with four groups of meteors divided according to χ . Solving for s_0 in the same manner as before, we obtain:

$$\begin{aligned} \text{meteors with } \chi \leq 0 & : s_{0m} = -0.20; \\ \text{meteors with } \chi \leq 0.2 & : s_{0m} = -0.01; \\ \text{meteors with } 0.2 > \chi \geq 0.4 & : s_{0m} = 0.07; \\ \text{meteors with } \chi > 0.4 & : s_{0m} = 0.10. \end{aligned}$$

As we see, the dependence of s_{0m} on χ is not very strong. We will adopt, henceforth, $s_{0m} = 0$. We will then choose C such that

$$\sum_{r=1}^N w_r \overline{\Delta \log \rho_{corr\ r}} = 0. \quad (39)$$

Here, N is the number of meteors ($N=350$) and w_r is the weight of the r -th meteor defined by

$$w_r = \left(\sum_{i=1}^k p_{ir} \right)^{1/2}.$$

The result is

$$\log C = 0.603 \pm 0.012. \quad (40)$$

According to the classical theory of meteors, C is given by $\frac{1}{2} C_D A_0 \rho_m^{-2/3}$, where C_D is the drag coefficient, A_0 the shape factor, and ρ_m the density of the meteor body. For the Super-Schmidt meteors we can assume $C_D = 2.2$, i.e., the value of C_D in free molecular flow. For a sphere we have $A_0 = (9\pi/16)^{1/3} = 1.21$. For any shape other than spherical, if we have random orientation, A_0 will have a somewhat larger value. Here we shall assume with Whipple (private communication) that for the average meteor $A_0 = 1.5$. Accordingly, the average meteor density turns out to be

$$\rho_m = 0.26 \pm 0.01 \text{ g cm}^{-3}. \quad (41)$$

Before we study the seasonal variations of the atmospheric densities, it is necessary to apply another correction to $\overline{\Delta \log \rho_{corr}}$ (and to $\Delta \log \rho_{corr}$) due to the variation of $\overline{\Delta \log \rho_{corr}}$ with the aphelion distance Q . Jacchia (1958, 1963) showed that the beginning heights of short-period meteors are lower than those of long-period meteors having the same mass, velocity, and zenith angle. Verniani (1964a, 1964b) found that meteors in elongated orbits have a lower density than those in short-period orbits. This difference is probably caused by the fact that large, loosely assembled meteor bodies have a greater probability of being disrupted in interplanetary space (by collisions, solar-wind erosion, and thermal effects) when they are in short-period orbits. We can, therefore, expect an increase of $\overline{\Delta \log \rho_{corr}}$ with increasing Q . This is what we find on the basis of table 9 and figure 9. Accordingly, we have considered the quantities $\Delta \log \rho_{corr}^*$ defined by

$$\Delta \log \rho_{corr}^* = \begin{cases} \overline{\Delta \log \rho_{corr}} + 0.053 & \text{when } Q \leq 4 \text{ a.u.} \\ \overline{\Delta \log \rho_{corr}} + 0.053 (5 - Q) & \text{when } \leq 4 Q \leq 6 \text{ a.u.} \\ \overline{\Delta \log \rho_{corr}} - 0.053 & \text{when } Q \geq 6 \text{ a.u.} \end{cases} \quad (42)$$

A similar relation defines also $\overline{\Delta \log \rho_{corr}^*}$. We have correlated the values of $\Delta \log \rho_{corr}^*$ with the height H and the values of $\overline{\Delta \log \rho_{corr}^*}$ with the mean velocity v_m (the velocity at the trajectory point where $s=0$) to check their independence from these quantities. The following correlations were obtained:

$$\frac{d\overline{\Delta \log \rho_{corr}^*}}{d \log v_m} = -0.051 \pm 0.063 \quad (v_m \text{ in km/s})$$

and

$$\frac{d\Delta \log \rho_{corr}^*}{dH} = 0.008 \pm 0.001 \quad (H \text{ in km}).$$

We have also computed

$$\frac{d\overline{\Delta \log \rho_{corr}^*}}{d\overline{H}},$$

where

$$\overline{H} = \frac{\sum_{i=1}^k p_i H_i}{\sum_{i=1}^k p_i}.$$

The result is

$$\frac{d\overline{\Delta \log \rho_{corr}^*}}{d\overline{H}} = 0.0075 \pm 0.0016.$$

There is no appreciable difference from the previous result in which individual decelerations were used. These derivatives can be considered satisfactorily insignificant. Jacchia (1957a) found for them values much closer to zero; this was due to more restricted conditions that the meteors accepted for the analysis had to satisfy.⁶ Tables 10.1 and 10.2 show, respectively, average values of $\overline{\Delta \log \rho_{corr}^*}$ and of $\Delta \log \rho_{corr}^*$ as functions of v_m and H . Table 10.3 shows $\overline{\Delta \log \rho_{corr}^*}$ as a function of \overline{H} . The data are also plotted in figures 10a and 10b. The dependence of $\Delta \log \rho_{corr}^*$ on v_m is negligible.

The dependence of $\Delta \log \rho_{corr}^*$ on the height H is very interesting. Between 85 and 103 km there is no dependence of $\Delta \log \rho_{corr}^*$ on H . Below 85 km, $\Delta \log \rho_{corr}^*$ decreases steadily when the height decreases. This should be

⁶ He used also a somewhat different procedure; weights were not employed and the corrections for Q not applied. Our data may be slightly overcorrected at values of $Q > 20$ a.u., and this explains the negative value of $\frac{d\overline{\Delta \log \rho_{corr}^*}}{d \log v_m}$.

due essentially to the deeper penetration in the atmosphere of denser bodies. Here apparently lies the principal obstacle to the determination of atmospheric densities from meteoric decelerations. The same phenomenon also precludes the possibility of effectively determining the exponent n of the luminosity law $\tau_p = \tau_0 v^n$ from an analysis of the systematic trend of the residuals $\Delta \log \rho$ with height. If we consider only meteors with $|\chi| \leq 0.2$ and vary n we find that $d\Delta \log \rho_{corr}^*/dH$ vanishes

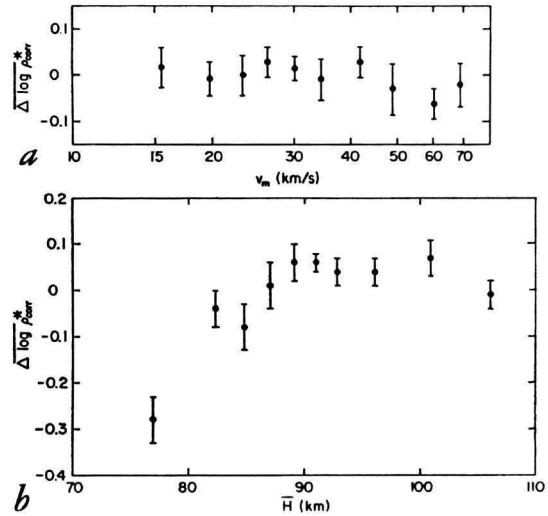


FIGURE 10.—Average residuals $\Delta \log \rho_{corr}^*$ as a function of: a, velocity v_m corresponding to the point at which the meteor has lost half of its mass; b, \overline{H} , the average for each meteor of the heights for which decelerations were determined.

when $n \approx 3$. We would not, however, attach any importance to this result; we would rather refer, in this connection, to the derivation of n by Verniani (1964a, 1966) using other methods.

We have further analyzed the 350 meteors by least squares for a possible seasonal variation in the atmospheric densities. The equation of condition is

$$\overline{\Delta \log \rho_{corr}^*} = \alpha \sin \left(\frac{2\pi t}{365.24} + \varphi_0 \right), \quad (43)$$

where t is the time in days, α is the semi-amplitude of the oscillation, and φ_0 is the phase angle. The weights w have been employed. The result is

$$\alpha = 0.026 \pm 0.016$$

$$\varphi_0 = -166^\circ \pm 42^\circ.$$

The semiamplitude is about 0.03, less than three times as large as its probable error; the amplitude of the seasonal variations is then about 14% in the natural value of the density. The phase angle puts the maximum on September 16 with a probable error of 27 days. The same amplitude was found in the preliminary analysis of Jacchia (1957a), which, however, gave a maximum on August 7 with a probable error of 35 days.

If we exclude from the analysis all meteors with $\chi > 0.40$, we are left with 267 meteors and we obtain

$$\alpha = 0.029 \pm 0.021$$

$$-\varphi_0 = -133^\circ \pm 37^\circ,$$

i.e., essentially the same amplitude, but a maximum on August 14. This solution is probably the better of the two.

These variations refer to a height corresponding to the average value of \bar{H} , which, according to table 10.3, is 91.0 km. This height practically coincides with that of a well-known isopycnic layer in the atmosphere, and this fact explains the small amplitude of the observed effect.

6. Magnitudes and "color index"

a. Magnitudes

According to classical theory, the maximum photographic luminous intensity I_{pm} is given by (Verniani, 1961)

$$I_{pm} = \frac{6f^2 \tau_{0p}}{(1+2f)^3 H_p} m_\infty \frac{v_m^6}{\bar{v}^2} \cos Z_R, \quad (44)$$

where

v_m = velocity at the point of maximum

$$\text{light} = v_\infty \left[1 + \frac{6}{\sigma v_\infty^2} \ln \frac{2f}{1+2f} \right]^{1/2},$$

\bar{v} = velocity at an intermediate point between beginning and maximum light,

H_p = pressure scale height (at maximum light),

$$f = 1 + \frac{9}{\sigma v_\infty^2}.$$

By assuming for \bar{v} an intermediate value⁷ be-

⁷ $\bar{v} = \sqrt{v_\infty v_m} = v_\infty \left[1 + \frac{6}{\sigma v_\infty^2} \ln \frac{2f}{1+2f} \right]^{1/4}$

tween v_m and v_∞ , adopting the usual value of τ_{0p} , and expressing the other parameters in c.g.s. units, we obtain from equation (44) a theoretical expression for the maximum absolute magnitude of a meteor as a function of its parameters:

$$\begin{aligned} M_{pm}^{(th)} = & 45.56 - 10 \log v_\infty - 2.5 \log m_\infty \\ & - 2.5 \log \cos Z_R + 2.5 \log H_p \\ & - 5 \log f + 7.5 \log (1+2f) \\ & - 6.25 \log \left[1 - \frac{6}{\sigma v_\infty^2} \ln \left(1 + \frac{1}{2f} \right) \right]. \quad (45) \end{aligned}$$

On the basis of equation (45), it appears reasonable to assume for the actually observed M_{pm} a dependence on the meteor parameters of the form

$$M_{pm} = k_0 + k_1 \log v_\infty + k_2 \log m_\infty + k_3 \log \cos Z_R, \quad (46)$$

and then find the values of the constants k_0, k_1, k_2, k_3 by least squares. To avoid the effects of the correlation between m_∞ and v_∞ we have also tried to use a simpler equation of condition that did not contain the mass; however, the dependence of M_{pm} on mass is so clear-cut that it cannot be ignored. Consequently, a solution that omits the mass does not have any meaning.

The results of the least-squares solutions with the condition equation (46) are listed in tables 11.1 to 11.6. Just as in the height analysis (section 4), the absolute term k_0 does not represent any realistic magnitude unless we subtract from each variable a constant close to its mean value. As before, we have taken the following constants: $v_\infty = 30$ km/s, $m_\infty = 0.3$ g, $\log \cos Z_R = -0.2$. For a meteor with these characteristics, equation (45) gives $M_{pm} = 0.63$; this is the theoretical value of k_0 , which should be compared with the least-squares results of tables 11.1 to 11.6.

An inspection of table 11.1 shows at a glance that for Super-Schmidt meteors k_0 is in all cases smaller than 0.63; i.e., the observed maximum brightness is greater than its theoretical value. The other coefficients, k_1 to k_3 , are all smaller in absolute value than their theoretical counterparts; in other words, the observed dependence of M_{pm} on the three parameters of equation (46) is smaller than predicted.

For the sake of comparison we have also included in table 11.4 the results of similar least-squares solutions for small-camera meteors. If uncritically accepted, these solutions would indicate that for small-camera meteors the dependence on the three basic parameters is closer to theory than for Super-Schmidt meteors. This agreement, however, must be considered fortuitous and caused by the presence of big flares in more than one-third of the small-camera meteors. If we exclude from the analysis the 80 meteors that had flares brighter than 0.5 magnitude above the general light-curve level, we find that the results agree with those from Super-Schmidt meteors.

One of the major differences between Super-Schmidt and small-camera meteors is to be found in their respective mean value of χ . The fact that the two groups do not behave too differently regarding the maximum brightness and its dependence on the basic parameters would indicate that χ is not very important in determining M_{pm} . This can be confirmed by dividing the sporadic Super-Schmidt meteors (classes A, S, and D excluded) into two groups of χ , one with $\chi \leq 0.2$ and the other with $\chi > 0.2$, and comparing the solutions (table 11.2). On the other hand, we see from table 11.2 that all coefficients are appreciably affected by differences in σ . The few Super-Schmidt meteors with $\log \sigma < -11.4$ show much better agreement with theory than those with larger σ . It should be remarked that, while it looks as if χ is less important than σ in modifying the coefficients k_1 to k_3 , it is only a little less efficient than σ in modifying k_0 , i.e., M_{pm} itself. From the various solutions for groups of σ and χ we obtain $dM_{pm}/d \log \sigma = -0.70$ and $dM_{pm}/d\chi = -0.45$. Since the standard deviations of a single observation, for Super-Schmidt and small-camera meteors combined, is ± 0.28 in σ and ± 0.29 in χ , we see that the effect on M_{pm} of the observed scatter in χ is about two-thirds as large as the effect of the scatter in σ .

Since it is a matter of geometry, we might expect to find a simple proportionality between I_{pm} and $\cos Z_R$ ($I \sim \dot{m} \sim \rho_a \sim \cos Z_R$). Instead we find a value of $-k_3$ remarkably smaller than 2.5. This could be due to the correlations, owing to selection, that affect all the principal quantities. The smaller values (in modulus)

of k_1 and k_2 could be due to this anomaly in k_3 . Therefore, we have computed another least-squares solution, postulating $k_3 = -2.5$. The results are practically the same as before, with a small improvement in the case of the Super-Schmidt meteors that can be considered negligible. Table 11.6 shows these results in some detail, for both Super-Schmidt and small-camera meteors. It becomes clear now that the deviations from theory of the values of k_1 and k_2 do not depend on the anomalous value of k_3 . Even the standard deviations are the same in both cases.

From the results of table 11.1 we can obtain the empirical dependence of I_{pm} on mass, velocity, and zenith angle. On the average, for Super-Schmidt meteors we find, in c.g.s.,

$$I_{pm} = 7.3 \times 10^{-23} v_{\infty}^{3.5} m_{\infty}^{0.9} \cos^{0.6} Z_R. \quad (47)$$

Introducing magnitudes, we have

$$M_{pm} = 55.34 - 8.75 \log v_{\infty} - 2.25 \log m_{\infty} - 1.5 \log \cos Z_R. \quad (48)$$

According to equation (48) the initial mass of a zero visual magnitude meteoroid (color index $= -1^m 86$) with a velocity of 40 km/s and a zenith angle of $\sim 50^\circ$ ($\log \cos Z_R = -0.2$) is 0.76 g. Previously, and using the same value of τ_0 as here, Verniani (1964a) had found for such a meteor a mass of 0.84 g. His computation was based on the relationship between luminous intensity and integrated brightness empirically derived by Jacchia (1958) that we can now improve by means of equations (47) and (48). We have

$$E_{\infty} = \frac{1.96 \times 10^5 I_{pm}^{1.11}}{v_{\infty}^{0.89} \cos^{2/3} Z_R}, \quad (49)$$

or in logarithmic form,

$$\epsilon_{\infty} = 5.29 - 0.89 \log v_{\infty} - 0.444 M_{pm} - \frac{2}{3} \log \cos Z_R. \quad (50)$$

These equations hold approximately also for nonflaring small-camera meteors and for Super-Schmidt and nonflaring small-camera meteors taken together (table 11.5). Table 12 shows the mass of a zero visual magnitude

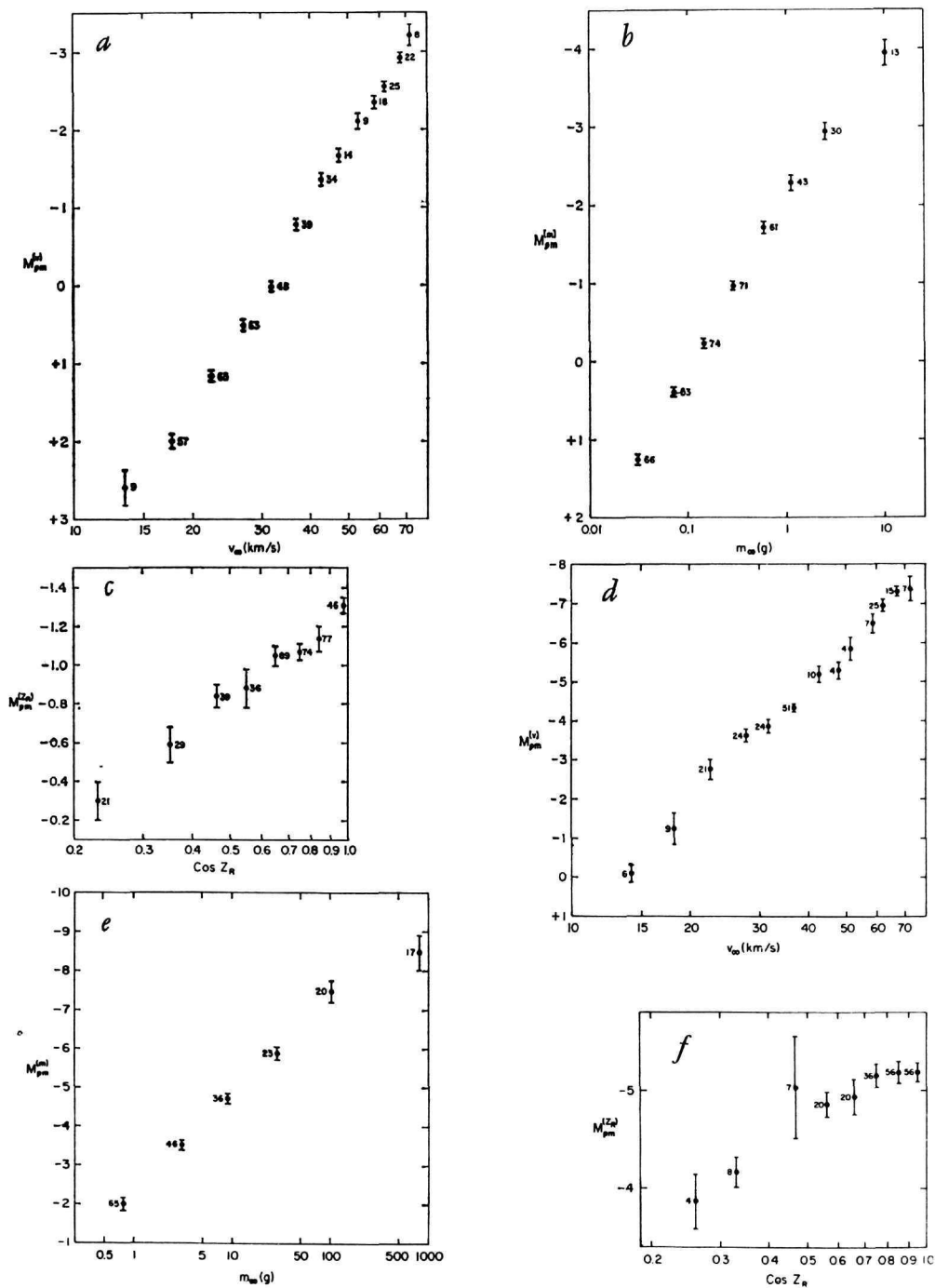


FIGURE 11.—Photographic magnitude: *a-c*, Super-Schmidt meteors reduced to: *a*, $m_{\infty}=0.3$ g and $\cos Z_R=0.63$ as a function of velocity; *b*, $v_{\infty}=40$ km/s and $\cos Z_R=0.63$ as a function of mass; *c*, $v_{\infty}=40$ km/s and $m_{\infty}=0.3$ g as a function of zenith angle of the trajectory. *d-f*, Small-camera meteors reduced to: *d*, $m_{\infty}=10$ g and $\cos Z_R=0.63$ as a function of velocity; *e*, $v_{\infty}=40$ km/s and $\cos Z_R=0.63$ as a function of mass; *f*, $v_{\infty}=40$ km/s and $m_{\infty}=10$ g as a function of the zenith angle of the trajectory.

meteoroid as a function of initial velocity and zenith angle. As we have seen from the results in table 11.4, different relationships hold for all small-camera meteors:

$$I_{pm} = 5.0 \times 10^{-26} v_{\infty}^{4.0} m_{\infty}^{1.0} \cos^{0.7} Z_R \quad (51)$$

$$M_{pm} = 63.26 - 10 \log v_{\infty} - 2.5 \log m_{\infty} - 1.75 \log \cos Z_R \quad (52)$$

$$E_{\infty} = \frac{2.8 \times 10^7 I_{pm}}{v_{\infty} \cos^{0.7} Z_R} \quad (53)$$

$$\epsilon_{\infty} = 7.44 - \log v_{\infty} - 0.4 M_{pm} - 0.7 \log \cos Z_R. \quad (54)$$

From equation (52) we obtain $m_{\infty} = 0.60$ g for a zero visual magnitude meteor with $v_{\infty} = 40$ km/s and $\log \cos Z_R = -0.2$. This result is less reliable than that obtained from Super-Schmidt meteors owing to the nonhomogeneity of the observational material and the difficulty of eliminating flares.

Because of the observational correlations between mass, velocity, and zenith angle, it is useless to consider the functions $M_{pm}(v_{\infty})$, $M_{pm}(m_{\infty})$, $M_{pm}(Z_R)$ directly derived from the observations, unless we reduce them to constant values of the other two variables. This can be done by means of equation (48) for Super-Schmidt meteors and of equation (52) for small-camera meteors. Table 13.1 shows M_{pm} as a function of the velocity for Super-Schmidt meteors reduced to $m_{\infty} = 0.3$ g and $\log \cos Z_R = -0.2$. The results are plotted in figure 11a. Similarly, tables 13.2 and 13.3 show M_{pm} as a function, respectively, of the mass and of the zenith angle; in the first, the observed absolute magnitudes have been reduced to $v_{\infty} = 40$ km/s and $\log \cos Z_R = -0.2$; in the second, to $v_{\infty} = 40$ km/s and $m_{\infty} = 0.3$ g. These results are plotted in figures 11b and 11c. Figure 11a also clearly shows the small systematic difference in brightness between low- and high-velocity meteors due to the difference between short- and long-period meteors. Long-period meteors are roughly one-fourth to one-half magnitude brighter than short-period meteors.

Tables 13.4 to 13.6 and figures 11d-f show similar results for small-camera meteors. The only difference is that they have been reduced to $m_{\infty} = 10$ g instead of $m_{\infty} = 0.3$ g.

The discrepancy between observed and theoretical magnitudes has been investigated for both Super-Schmidt and small-camera meteors. The differences $\Delta M_{pm} = M_{pm} - M_{pm}^{(th)}$ for sporadic and shower meteors are listed in tables 14.1 and 14.2. At first glance it may be surprising that the average values of ΔM_{pm} for Super-Schmidt and small-camera meteors should be roughly the same. Actually, the presence of big flares completely distorts the results for small-camera meteors. When there are no flares, the observed magnitude of a small-camera meteor is often close to the theoretical value, while flares can produce a difference of as much as three magnitudes.

The average value of ΔM_{pm} is -0.3 ± 0.1 for meteors with flares smaller than $0^{\circ}.5$ and -1.0 ± 0.3 for meteors with flares greater than $0^{\circ}.5$. These figures indicate a good agreement with theory; a small flare of $0^{\circ}.3$ occurs quite often in the smoother light curves. The discrepancy is much more systematic for Super-Schmidt meteors; this is shown also by the smaller value of the standard deviation of one observation, 0.50 instead of 0.76. Among the showers (Super-Schmidt) the Taurids show a very small value of ΔM_{pm} . The same is true also for σ Hydrids and for Lyrids, but these two showers have only three meteors each on our list. Geminids also show a moderate value of ΔM_{pm} . On the other hand, the δ Aquarids are about one magnitude brighter than the theoretical value. The Draconids, of course, are very anomalous. As a curiosity, the only member of the Leonid shower contained in our list appears less bright than predicted by theory. Among all meteors only 27 have a positive ΔM : among these, 12 are sporadic, 5 are Taurids, and 5 are Geminids.

The departure from theory appears to be greater for short-period meteors than for those in long-period orbits.

The difference ΔM_{pm} turns out to be independent of mass, velocity, zenith angle, and height. There is, however, as we expected, a clear-cut dependence on the fragmentation index χ , shown in table 14.3. The small-camera meteors do not show such a correlation, but those having all the data for computing $M_{pm}^{(th)}$ are too few and the flares are present also among meteors with a value of χ close to

zero. We can also see that those Super-Schmidt meteors that do not show progressive fragmentation are about half a magnitude brighter than expected on theoretical ground.

b. "Color index"

Visual estimates of brightness were recorded for 390 out of the 413 precisely reduced Super-Schmidt meteors. For these 390 meteors we can compare photographic and visual magnitudes and analyze the difference between the two, the so-called "color index." A previous analysis of the color index (Jacchia, 1957b) covered 336 of these same meteors, or about 86 percent of the present material. The present analysis is conducted along the same line as the previous investigation, and the numerical results are essentially the same. We refer the reader to the aforementioned paper for a description of the techniques used to derive photographic magnitudes to be compared with the visual estimates. Here we shall simply repeat that the emulsion used in the photography was the blue-sensitive Kodak X-ray for the Super-Schmidt meteors. For small-camera meteors it was mostly Cramer Hi-speed or Kodak 103a-o emulsion with spectral-sensitivity curves similar to that of Kodak X-ray.

The analysis was made twice, first with all the 390 meteors and then discarding the meteors of classes A, F, and S (48 meteors). The results are quite similar in both cases, and we present here those obtained from all 390 meteors. Table 15.1 shows the color index as a function of the velocity (fig. 12a) and its distribution for five velocity groups. Little dependence, if any, is found on the velocity; $C.I. = -1.37 \pm 0.04$ for all velocities seems the best conclusion.

Table 15.2 shows the color index as a function of the absolute photographic magnitude (fig. 12b) and its distribution for seven magnitude groups. In figure 12b we have plotted also the dot corresponding to the mean C.I. for small-camera meteors (Jacchia, 1957b). The color index turns out to be almost a linear function of the magnitude between $M_{pm} = -1.5$ and $M_{pm} = +1.0$ and can be represented by

$$C.I. = \frac{1}{2}M_{pm} - 1.36 \quad (-1.5 \leq M_{pm} \leq 1.0). \quad (55)$$

For fainter magnitudes C.I. seems to reach a

constant value of about -1.0 . For $M_{pm} \leq -2$ the color index is roughly constant and its value is close to -1.95 .

In its range of validity equation (55) is equivalent to

$$M_p = \frac{1}{2}M_v - 2.04 \quad (56)$$

or to

$$M_v = \frac{1}{2}M_p + 1.36. \quad (57)$$

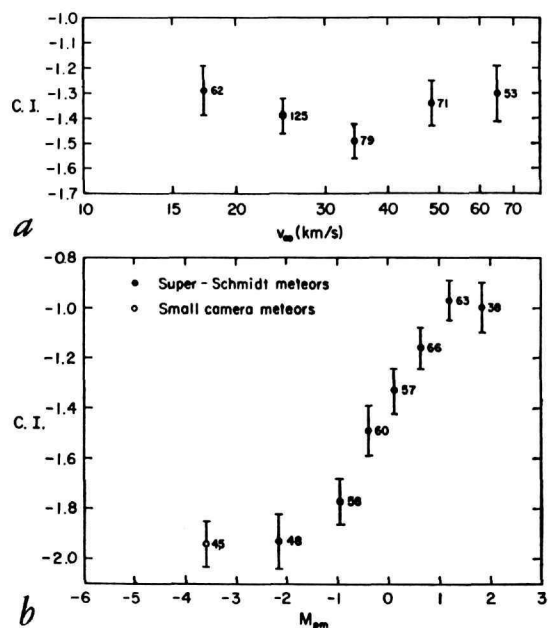


FIGURE 12.—Color index as a function of: *a*, velocity for Super-Schmidt meteors; *b*, absolute photographic magnitude for Super-Schmidt and small-camera meteors.

7. The ablation coefficient σ

a. Dependence of the mean σ on the other parameters

For all Super-Schmidt meteors, "instantaneous" values of σ were computed from equation (11) from each observed deceleration. In addition, equation (12) was used whenever more than one deceleration from the same plate was available on the meteor trajectory. A mean value of σ was derived for each meteor on the basis of all these determinations; those derived from equation (12) were given greater weight in calculating the mean. Since σ generally varies during the trajectory, the value obtained for those meteors for which only one deceleration was available for each

film depends on the location on the trajectory of the point to which the deceleration refers. Therefore, a correction had to be applied to make the σ 's of those meteors comparable with those obtained mainly from the "integrated" equation (12). Let us suppose for a moment that the only anomaly introduced by fragmentation concerns \dot{v} . From equation (10) we should then have

$$\sigma_T = \sigma \frac{\dot{v}}{\dot{v}_T}$$

when σ_T corresponds to the theoretical value \dot{v}_T of the deceleration. We can assume that σ_T is approximately constant during the trajectory. Therefore, differentiating with respect to the mass-loss parameter s (equation (14)), we have

$$0 = \frac{d \log \sigma}{ds} + \frac{d}{ds} \log \frac{\dot{v}}{\dot{v}_T},$$

and recalling the definition of the fragmentation index χ (equation (15)),

$$\frac{d \log \sigma}{ds} = -\chi. \quad (58)$$

Since equation (58) suggests that there might be a linear dependence on χ , we have put

$$\frac{d \log \sigma}{ds} = a\chi + b, \quad (59)$$

and determined a and b by least squares for the 143 Super-Schmidt meteors with more than two decelerations and thus several instantaneous values of σ . Each value of $d \log \sigma/ds$ was given a weight $\Delta s/D^2$, Δs being the maximum difference between the values of s employed in the computation of the derivative and D the standard deviation of the derivative itself. The result was: $a = -0.84 \pm 0.05$; $b = 0.02 \pm 0.01$. The correlation coefficient between $d \log \sigma/ds$ and χ is -0.81 . The average value of $d \log \sigma/ds$ is -0.09 ± 0.01 , in perfect agreement with the mean value $\chi = 0.13$ obtained from these 143 meteors. The complete theoretical derivation of $d \log \sigma/ds$ is given in section 7b; here we are just concerned with the correction to apply to the values of σ for the meteors with only two decelerations (or less). Clearly these σ 's must be reduced to a

standard value s' of s by means of equation (59). The value of s' was determined as follows. For each multideceleration meteor, there are available several instantaneous values of σ , which correspond to different values s_i of the mass-loss parameter s . Moreover we have the average value $\overline{\log \sigma}$ determined mainly through the use of equation (12). From these meteors we selected the sporadic ones with $\chi > 0.15$ or $\chi < -0.1$ so that the corrections were greater than or equal to 0.1. There are 59 such meteors and for each of them a value s'_0 has been computed such that:

$$\overline{\log \sigma} = \frac{1}{k} \sum_{i=1}^k (\log \sigma_i)_{s=s'_0},$$

where k is the number of the decelerations of the meteor and $(\log \sigma_i)_{s=s'_0}$ is given by

$$(\log \sigma_i)_{s=s'_0} = \log \sigma_i + (s'_0 - s_i)(a\chi + b).$$

Then we computed $\overline{s'_0} = \frac{1}{n} \sum_{l=1}^n s'_{0l}$. Here, n is

the number of meteors with multiple decelerations ($n=59$). The result is 0.03 ± 0.04 . A check on the reliability of this value was made by computing the quantity s'_1 that minimizes the sum

$$\sum_{l=1}^n (\Delta \log \sigma_l)^2,$$

where

$$\Delta \log \sigma_l = \overline{\log \sigma}_l - \frac{1}{k} \sum_{i=1}^k (\log \sigma_i)_{s=s'_1}.$$

We find $s'_1 = 0.07 \pm 0.04$. On the basis of these results we have assumed the round value $s'_1 = 0$. The final $\log \sigma$ for a meteor with two decelerations is therefore:

$$\overline{\log \sigma} = \frac{\lambda_1 (\log \sigma_1)_{s=0} + \lambda_2 (\log \sigma_2)_{s=0}}{\lambda_1 + \lambda_2},$$

where λ_i is the weight for individual decelerations, defined by equation (37).

The observed values of $\log \sigma$ for Super-Schmidt meteors range from -10.42 to -12.02 . Meteors of the classes A and S have been systematically excluded from the present analysis, as well as those meteors for which the determination of σ was deemed to be too unreliable. Table 16.1 shows the distribution

of $\log \sigma$, both for all meteors (fig. 13a) and for sporadic meteors only. Table 16.2 and figure 13b cover small-camera meteors; a comparison will show the difference in the two distributions. It is known that σ is a function of the velocity and of the integrated brightness (Jacchia, 1958). Tables 17.1.2 and 17.2 show the dependence of σ on these quantities, both for all meteors and for sporadic meteors only. The latter have been also divided into two groups, $Q \leq 6$ a.u.

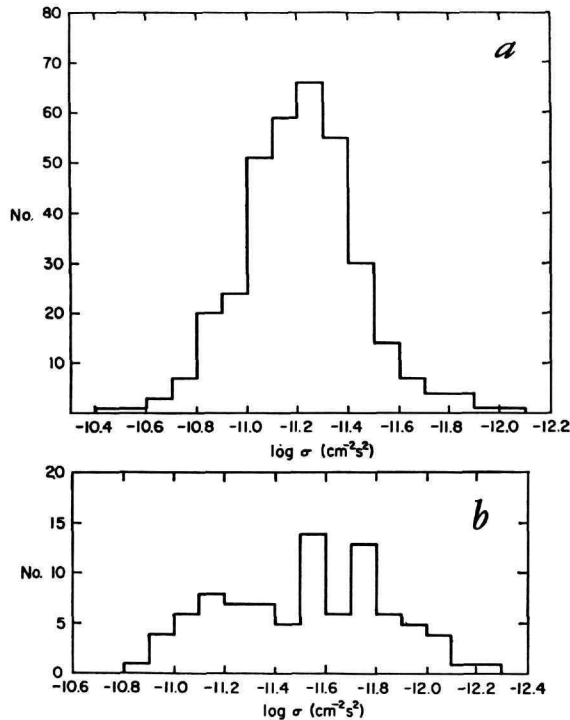


FIGURE 13.—Frequency distribution of the ablation coefficient σ for: *a*, Super-Schmidt meteors; *b*, small-camera meteors.

and $Q > 6$ a.u.; there is no appreciable difference in the behavior of $\log \sigma$ for these two groups (table 17.1.1 and fig. 14b). The apparent differences between the values of $\log \sigma$ for the two groups in the same range of ϵ_{∞} are due only to the different mean velocities and masses of the two groups. As was already known, σ decreases when v_{∞} or ϵ_{∞} increases. The variation of σ with v_{∞} is quite similar both for all meteors and for sporadic meteors only (fig. 14a). The latter group seems more regular since it is not affected by the peculiarities of the

individual showers. If we limit our attention to sporadic meteors, we see that the decrease of $\log \sigma$ with velocity appears to be linear up to about 40 km/s; thereafter σ is roughly a constant (around -11.33). From 15 to 40 km/s, we have approximately $\log \sigma = -10.24 - 0.65 \log v_{\infty}$ (v in km/s). A least-squares solution for the whole range of velocity gives $\log \sigma = (-10.40 \pm 0.11) - (0.51 \pm 0.07) \log v_{\infty}$. If we also introduce the mass as an independent variable, we get $\log \sigma = (-10.29 \pm 0.13) - (0.63 \pm 0.11) \log v_{\infty} - (0.05 \pm 0.03) \log m_{\infty}$.

As a result of selection effects, mass and velocity are correlated, as is shown in table 2.1. Therefore, the preceding solution has little, if any, meaning. Moreover, this correlation makes it necessary to correct the preceding results. Since the brightness is not an independent variable, σ must be regarded essentially as a function of mass and velocity: $\sigma = \sigma(v_{\infty}, m_{\infty})$. Table 17.3 shows σ as a function of mass. It appears that for the Super-Schmidt material σ depends more on v_{∞} than on m_{∞} . By using a method of successive approximation we can find the values of $\sigma = \sigma(v_{\infty})$ at $m_{\infty} = \text{const}$ and $\sigma = \sigma(m_{\infty})$ at $v_{\infty} = \text{const}$. These functions are listed in tables 17.1.2 and 17.3 for the values $m_{\infty} = 0.8$ g and $v_{\infty} = 30$ km/s. In the reduction to $m_{\infty} = 0.8$ g of the uncorrected $\sigma(v_{\infty})$, the values of σ of the small-camera meteors have been very useful. The functions $\sigma(v_{\infty})$ at $m_{\infty} = \text{const}$ and $\sigma(m_{\infty})$ at $v_{\infty} = \text{const}$ have been determined by successive approximations also for small-camera meteors; unfortunately only for 88 among more than 200 small-camera meteors has σ been determined. Tables 17.4 and 17.5 show results of small-camera meteors, while table 17.6 gives results of shower meteors, both Super-Schmidt and small-camera.

Figure 14c shows $\sigma(v_{\infty})$ for Super-Schmidt and small-camera meteors, for a constant mass of 0.8 g. This value for the mass has been chosen because it is the average mass for Super-Schmidt meteors and is still on the plateau where σ does not vary with mass (see below). The results of the small-camera meteors do not agree very well with those of the Super-Schmidt. For the Super-Schmidt we can describe approximately σ as a function of v_{∞} as follows:

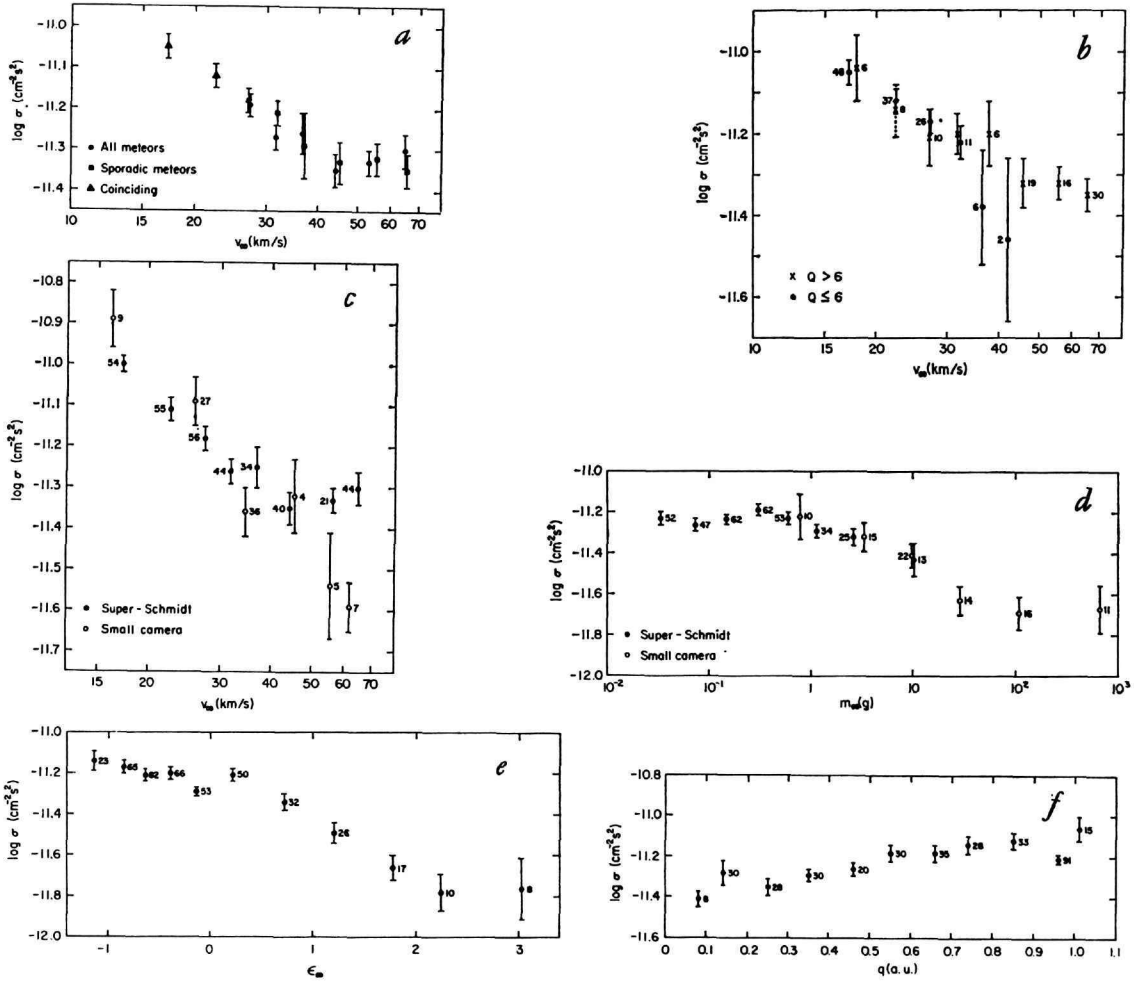


FIGURE 14.—Ablation coefficient as a function of: *a*, velocity for Super-Schmidt meteors; *b*, velocity for sporadic Super-Schmidt meteors in short-period and long-period orbits; *c*, velocity for Super-Schmidt and small-camera meteors, reduced to standard mass of 0.8 g; *d*, mass for Super-Schmidt and small-camera meteors, reduced to standard velocity of 30 km/s; *e*, brightness for Super-Schmidt and small-camera meteors together; *f*, perihelion distance q for all Super-Schmidt meteors.

for $m_{\infty} = 0.8$ g,

$$\log \sigma = -9.90 - 0.90 \log v_{\infty} \quad (v_{\infty} \leq 40 \text{ km/s})$$

$$\log \sigma = -11.33 \quad (v_{\infty} > 40 \text{ km/s}).$$

For the small-camera meteors an approximate representation of $\sigma(v_{\infty})$ is:

for $m_{\infty} = 0.8$ g,

$$\log \sigma = -9.46 - 1.20 \log v_{\infty}.$$

Figure 14d shows $\sigma(m_{\infty})$ for Super-Schmidt and small-camera meteors reduced to a velocity of 30 km/s. In the overlapping region (between 1 and 10 g) the results of the Super-Schmidt agree very well with those of the small camera. Average values of $\log \sigma$ for groups of increasing mass for all meteors (Super-Schmidt and small-camera) are given in table 17.7. Between about 10^{-2} and 1 g there seems to be no dependence of σ on mass. A clear dependence is noticeable, however, between 1 and about 70 g, at which point σ again becomes

practically independent of mass. Between 0.01 and 0.9 g, the results are well represented by ($v_\infty = 30$ km/s), $\log \sigma = -11.23$ ($0.01 < m_\infty \leq 0.9$ g) for both Super-Schmidt and small-camera meteors. When m is greater than 0.9 g, a curve is more adequate than a straight line to describe the function $\sigma(m_\infty)$; however, a rough linear approximation is ($v_\infty = 30$ km/s), $\log \sigma = -11.24 - 0.23 \log m_\infty$ ($0.9 \leq m_\infty \leq 70$ g); ($v_\infty = 30$ km/s), $\log \sigma = -11.67$ ($70 \leq m_\infty < 1000$ g). Combining together these and the previous results for $\sigma(v_\infty)$ we find an approximation of the function $\sigma(m_\infty, v_\infty)$ [see formula (60)].

Table 17.8 and figure 14e show $\sigma(\epsilon_\infty)$ for Super-Schmidt and small-camera meteors. These results are quite similar to the previous ones obtained by Jacchia in 1958. Table 17.9 presents $\log \sigma$ as a function of the zenith angle Z_R for Super-Schmidt meteors. We see that σ is practically independent of $\cos Z_R$. The same conclusion is reached if we reduce the results to the same mass and velocity. Table 17.10 shows $\log \sigma$ as a function of the aphelion distance Q ; σ decreases when Q increases, but this is only the consequence of the variation of Q with the velocity v_∞ , as can be seen from the column that gives $\log \sigma$ reduced to a standard velocity of 30 km/s. Table 17.11.1 shows $\log \sigma$ as a function of the perihelion distance q (see also fig. 14f). It appears that $\log \sigma$ increases rather regularly with q ; again the slight decrease of v_∞ with q contributes partially to this effect. Table 17.11.2 shows $\log \sigma$ versus q for short-period and long-period meteors.

Lastly, table 17.12 shows that σ is, surprisingly, quite independent of χ and vice versa. This result is quite important for a better understanding of the different meaning of σ and χ . We cannot describe the behavior of a meteor if we do not know both of these basic parameters. For a discussion of the different manner in which σ and χ may be related to fragmentation, see section 8.

$$\log \sigma = \begin{cases} -9.90 - 0.9 \log v_\infty & (v_\infty \leq 40 \text{ km/s}; 0.01 < m_\infty \leq 0.9 \text{ g}) \\ -9.91 - 0.9 \log v_\infty - 0.23 \log m_\infty & (v_\infty \leq 40 \text{ km/s}; 0.9 \leq m_\infty \leq 70 \text{ g}) \\ -10.34 - 0.9 \log v_\infty & (v_\infty \leq 40 \text{ km/s}; 70 \leq m_\infty < 1000 \text{ g}) \\ -11.33 & (v_\infty > 40 \text{ km/s}; 0.01 < m_\infty \leq 0.9 \text{ g}) \\ -11.34 - 0.23 \log m_\infty & (v_\infty > 40 \text{ km/s}; 0.9 \leq m_\infty \leq 70 \text{ g}) \\ -11.77 & (v_\infty > 40 \text{ km/s}; 70 \leq m_\infty \leq 1000 \text{ g}) \end{cases} \quad (60)$$

b. The variation of σ along the trajectory

Although σ turns out to be independent of χ , we have seen that fragmentation must be responsible for the variation of σ in the course of the trajectory. We have seen also that in first approximation $d \log \sigma / ds$ is equal to $-\chi$ [equation (58)]. Let us now evaluate correctly this variation. From equation (10) we have:

$$\frac{d \log \sigma}{ds} = \frac{1}{\ln 10} \left[\frac{d}{ds} \ln(-\dot{m}) - \frac{d}{ds} \ln m - \frac{d}{ds} \ln(-v\dot{v}) \right].$$

Recalling the definitions of s [equation (14)], χ [equation (15)], and the drag equation (2), we have also:

$$\begin{aligned} \frac{d}{ds} \ln(-\dot{m}) &= \frac{1}{-\dot{m}} \left[-\frac{d^2 m}{ds^2} \dot{s} - \frac{dm}{ds} \ddot{s} \right], \\ -\frac{d}{ds} \ln m &= \frac{10^* \ln 10}{10^* + 1}, \\ -\frac{d}{ds} \ln(-v\dot{v}) &= -(\ln 10) \left(\chi + \frac{d}{ds} \log \rho r \right) \\ &\quad + \frac{1}{3} \frac{d \ln m}{ds} - \frac{3 d \ln v}{ds}. \end{aligned}$$

Moreover, we have

$$\begin{aligned} \frac{dm}{ds} &= -\frac{m_\infty 10^* \ln 10}{(10^* + 1)^2}, \\ \frac{d^2 m}{ds^2} &= \frac{-m_\infty 10^* (\ln 10)^2 (1 - 10^*)}{(10^* + 1)^3}, \\ \dot{s} &= \frac{-m_\infty \dot{m}}{(\ln 10) m (m_\infty - m)}, \\ \ddot{s} &= \frac{(m_\infty - m) \left[\frac{m_\infty}{m^2} \dot{m}^2 - \frac{m_\infty}{m} \ddot{m} \right] - \frac{m_\infty}{m} \dot{m}^2}{(\ln 10) (m_\infty - m)^2}, \end{aligned}$$

and from equation (3)

$$\ddot{m} = \frac{2I_p}{\tau_0 v^3} \left(3 \frac{v}{v} + 0.4 M_p \ln 10 \right).$$

The expressions written above allow the determination of $d \log \sigma / ds$. Considering this derivative at the point $s=0$ (i.e., when $m = \frac{m_\infty}{2}$) and indicating with the subscript 0 all the quantities taken in the points $s=0$, we have (H_p =pressure scale height)

$$\left(\frac{d \log \sigma}{ds}\right)_{s=0} = -\chi + \frac{1}{3} + \frac{1}{\sigma_0 v_0 \dot{v}_0} \left(0.46 \dot{M}_{p0} + 3 \frac{\dot{v}_0}{v_0} + \frac{1}{2H_{p0}} v_0 \cos Z_R\right). \quad (61)$$

We have randomly selected 12 meteors and computed $\left(\frac{d \log \sigma}{ds}\right)_{s=0}$ according to the preceding equation. The result,

$$\left(\frac{d \log \sigma}{ds}\right)_{s=0} = (0.01 \pm 0.04) - \chi,$$

was in good agreement with the least-squares solution obtained before.

Using the 143 meteors with more than two decelerations, we have searched for a dependence of $d \log \sigma / ds$ on v_∞ and $\log \sigma$ itself. No dependence has been found:

$$\frac{d}{d \log v_m} \left(\frac{d \log \sigma}{ds}\right) = -0.008 \pm 0.002$$

$$\frac{d}{d \log \sigma} \left(\frac{d \log \sigma}{ds}\right) = -0.01 \pm 0.13.$$

8. The fragmentation index χ

Whenever several decelerations are available along the trajectory of a meteor, χ can be evaluated directly from equation (15) by plotting

$$\Delta \log \rho_{obs} = \log \rho_{obs} - \log \rho_T = \log \frac{\dot{v}}{\dot{v}_T}$$

against s and fitting the best straight line through the points of the diagram. When only one deceleration per plate is available, or the different decelerations correspond to points too close to each other, the value of χ can be computed approximately by an equation that can be obtained by differentiating the drag equation and reads (Jacchia, 1955)

$$\chi = \frac{m}{\dot{m}} \left(1 - \frac{m}{m_\infty}\right) \left(2 \frac{\dot{v}}{v} + \frac{v \cos Z_R}{H_p} \frac{\dot{v}}{v} - \frac{\dot{m}}{3m}\right), \quad (62)$$

where H_p is the density scale height. From equation (13) we have $\frac{\dot{v}}{v} = k$, and from equation (3)

$$\frac{\dot{m}}{m} = - \frac{I_p / v^3}{\int_t^{+\infty} \frac{I_p}{v^3} dt}.$$

The fragmentation index χ is zero when $\frac{\dot{v}}{v} = \frac{\dot{v}_T}{v_T}$; that is, when the relative rate of change in the "dynamic" mass of the meteor coincides with the relative rate of change of the "photometric" mass. It takes positive or negative values according to whether the former is larger or smaller than the latter. If a faster rate of change of the dynamic mass is interpreted as due to fragmentation, χ emerges as a measure of the fragmentation process. It should also be clear that χ will always be positive when the meteor is fragmented. A negative value of χ cannot be physically justified any more than a negative meteor deceleration. Negative values of χ , however, are much more frequent than negative decelerations. The negative values of χ that are occasionally observed must be ascribed to (a) observational errors, (b) variations in the atmospheric density profile, (c) systematic errors in the standard atmospheric density profile, (d) variations either in the shape of the meteor or in the drag coefficient γ (for small-camera meteors, which on the average are larger and lower; the latter is a distinct possibility; for some of them there probably occurs a transition from free-molecule to continuum flow in the course of the trajectory), and (e) the presence of a residual mass, which, according to equation (6), is always assumed to be zero.

Whenever fragmentation is present, a knowledge of χ is necessary for the correction of all the quantities computed by means of the decelerations. This correction is made simple by the near constancy of χ during the observable part of the meteor flight. We have employed χ in the analysis of the atmospheric densities (as Jacchia already did in 1957a), in the reduction to $s=0$ of all the values of $\log \sigma$, and in the heights analysis. The determination of the luminous efficiency τ_p by Verniani

(1964a) has been made possible by the knowledge of the fragmentation index. Otherwise, the scatter in the computed quantities would be so large as to make it impossible to draw any meaningful and reliable conclusion. The study of the correlations of χ with the physical parameters of meteors permits us to relate them to the physical behavior of meteors in the atmosphere; we will find, for instance, that the relative degree of fragmentation is high for small meteors and decreases when the mass increases. It should be clear then that the fragmentation index is an important characteristic of each meteor as well as an efficient tool in handling the observed decelerations. For a nonfragmenting body, the ablation coefficient σ is presumably a constant and χ is zero. In an ordinary, crumbling meteor, however, the meaning of σ becomes obscure and is reduced more or less to a parameter of the smoothed light curve. On the other hand, χ tells at a glance how much the presence of fragmentation contributed to the discrepancy between observation and theoretical behavior.

Differences in fragmentation must result in different values of both σ and χ ; each of these parameters, however, reflects a different effect of fragmentation. If a meteor keeps shedding fragments during its flight, but maintains a single main body, the ablation rate may become noticeably larger than for a nonfragmenting body, while the deceleration, which contains an $m^{-1/3}$ factor in its expression, may not be too anomalous. The increased ablation rate, which results in a greater σ , will raise the maximum brightness and the height at which it occurs. In those cases when the disintegration of a meteor is more complete, to the point where it may become difficult to identify a main body, χ will generally be noticeably different from zero and σ will be even larger—although it is conceivable that beyond a certain level of crumbling σ may not appreciably increase. That this may actually be the case is suggested by the comparison of the mean values of σ and χ for all meteors as a function of ϵ_∞ (figs. 14e and 16d; see also Jacchia, 1958, fig. 1), from which it appears that, proceeding to fainter meteors, σ increases earlier than χ and reaches a near-constant maximum value long before χ has stopped rising.

An analysis of the fragmentation index for most of these Super-Schmidt meteors has been published earlier (Jacchia, 1958). It confirmed the dependence of χ on the integrated brightness (Jacchia, 1955) and showed the existence of a clear correlation between fragmentation and zenith angle ($\bar{\chi}=0.5-0.27 \cos Z_R$). It also established a dependence of χ on velocity and suggested a difference of fragmentability between long-period and short-period meteors (χ near 0.30 for meteors with $v_\infty < 40$ km/s and $\chi \approx 0.38$ for meteors with $v > 40$ km/s).

The present analysis repeats the earlier investigations in somewhat greater detail. The present values of χ are appreciably different from those of the earlier investigations that were computed on the basis of the ARDC 1956 atmosphere (Minzner and Ripley, 1956); the values used in the present analysis have been computed using the U.S. Standard Atmosphere 1962 (1962). The present values of χ are, on the average, smaller than the preceding ones; the mean value of χ was close to 0.32, while the present average for all Super-Schmidt meteors is 0.27.

The values of χ for Super-Schmidt meteors range from -0.85 to $+2.97$. The distribution of χ for these meteors is given in table 18.1 and plotted in figure 15a. In figure 15b (see also table 18.2) we have plotted also the distribution of χ for small-camera meteors. In the following general analysis we have not used all the 401 Super-Schmidt meteors for which a value of χ was computed; the meteors of classes A (abrupt beginning) and S (flarelike meteors) have been excluded from the general analysis and studied separately. We have also excluded four meteors whose values of χ were quite exceptional (meteor no. 8215: $\chi = -0.85$; no. 8817: $\chi = 1.73$; no. 8951: $\chi = 2.46$; no. 3037: $\chi = 2.97$). [Meteor no. 8951, however, a member of the Draconid shower, has been used to determine $\bar{\chi}$ for the shower itself in table 19.7.] We are, therefore, left with 359 Super-Schmidt meteors, 249 of which are sporadic. We have also 58 values of χ for small-camera meteors; since a comprehensive analysis of these data has never been made; it seemed proper to do it here. Though they are quite few, these small-camera meteors provide a useful basis of com-

parison with meteors of much larger mass and greater brightness.

Table 19.1.1 shows the dependence of χ on the velocity both for all Super-Schmidt meteors (fig. 16a) and for sporadic Super-Schmidt meteors. We see that the trend is irregular. Meteors with $v < 40$ km/s have a mean value of about 0.22, while fast meteors ($v > 40$ km/s) have $\chi \approx 0.33$ on the average; however, most of this otherwise remarkable difference appears

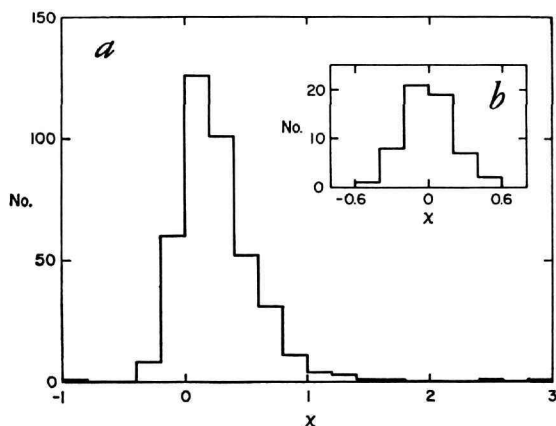


FIGURE 15.—Frequency distribution of the fragmentation index χ for: *a*, Super-Schmidt meteors; *b*, small-camera meteors.

to be due to the different mass distribution of the two groups. Table 19.1.1 also lists mean values of χ reduced to a mass of 0.8 g. If we take these values, we find the average values of χ to be respectively 0.23 for slow meteors and 0.26 for fast meteors, with a difference roughly equal to the standard deviation of the second value alone (sum of standard deviation of both groups ≈ 0.05). For sporadic meteors we have:

$$v_{\infty} < 40 \text{ km/s, mean } \chi = 0.23 \pm 0.02, \\ (\text{mean } \chi)_{m_{\infty} = 0.8\text{g}} = 0.24$$

$$v_{\infty} > 40 \text{ km/s, mean } \chi = 0.30 \pm 0.03, \\ (\text{mean } \chi)_{m_{\infty} = 0.8\text{g}} = 0.23.$$

There is no difference here between corrected averages. It therefore seems that in the mass range of the Super-Schmidt meteors, χ is

independent of velocity. However (see table 19.4), χ shows a clear decrease with velocity for small-camera meteors, being equal to 0.07 ± 0.04 at $v_{\infty} = 15$ km/s and to -0.12 ± 0.04 at $v = 57$ km/s. Values, corrected for mass dependence, are, respectively, 0.08 and -0.18 (at $m_{\infty} = 30$ g). Table 19.1.2 lists χ versus v_{∞} separately for short-period and long-period meteors. Again the trend is irregular for both groups (see also fig. 16b), but we find a rather surprising result: Short-orbit meteors seem to have a greater χ than those in elongated orbits, at variance with the result of Jacchia's (1958) analysis. If we look at uncorrected results, this difference is negligible: $\chi = 0.26 \pm 0.03$ for meteors with $Q \leq 6$ a.u. and $\chi = 0.24 \pm 0.03$ for meteors with $Q > 6$ a.u.; however, the mean values reduced to constant mass of 0.8 g are, respectively, 0.27 and 0.20. It should be noted that in the present analysis the critical aphelion distance for dividing the orbits into long-periodic and short-periodic is 6 a.u., whereas it was 7 a.u. in Jacchia's (1958) paper.

Table 19.2.1 shows the dependence of χ on the integrated brightness ϵ_{∞} both for all and for sporadic meteors only. At faint magnitudes the results look more scattered than those previously obtained by Jacchia; otherwise there are no remarkable differences (except, of course, for the systematic difference caused by the difference in the reference atmosphere). Table 19.2.2 gives χ versus ϵ_{∞} for the two groups of short- and long-period meteors. No particular comment is needed, except for recalling that on the same row the meteors have the same brightness but quite different masses and velocities.

Table 19.3 gives the dependence of the fragmentation index χ on mass for all Super-Schmidt meteors and for sporadic Super-Schmidt only. There is no difference between "all" and "sporadic" in the dependence on mass. For masses comprised between 0.05 and 5 g, we conclude that χ is constant and on the average equal to 0.23 ± 0.02 . For meteors with m between 0.01 and 0.05 g we have $\chi = 0.40 \pm 0.04$, while on the other side of the distribution for meteors with $m_{\infty} > 5$ g, we have $\chi = 0.08 \pm 0.04$. For these few big meteors the standard deviation of the individual value of

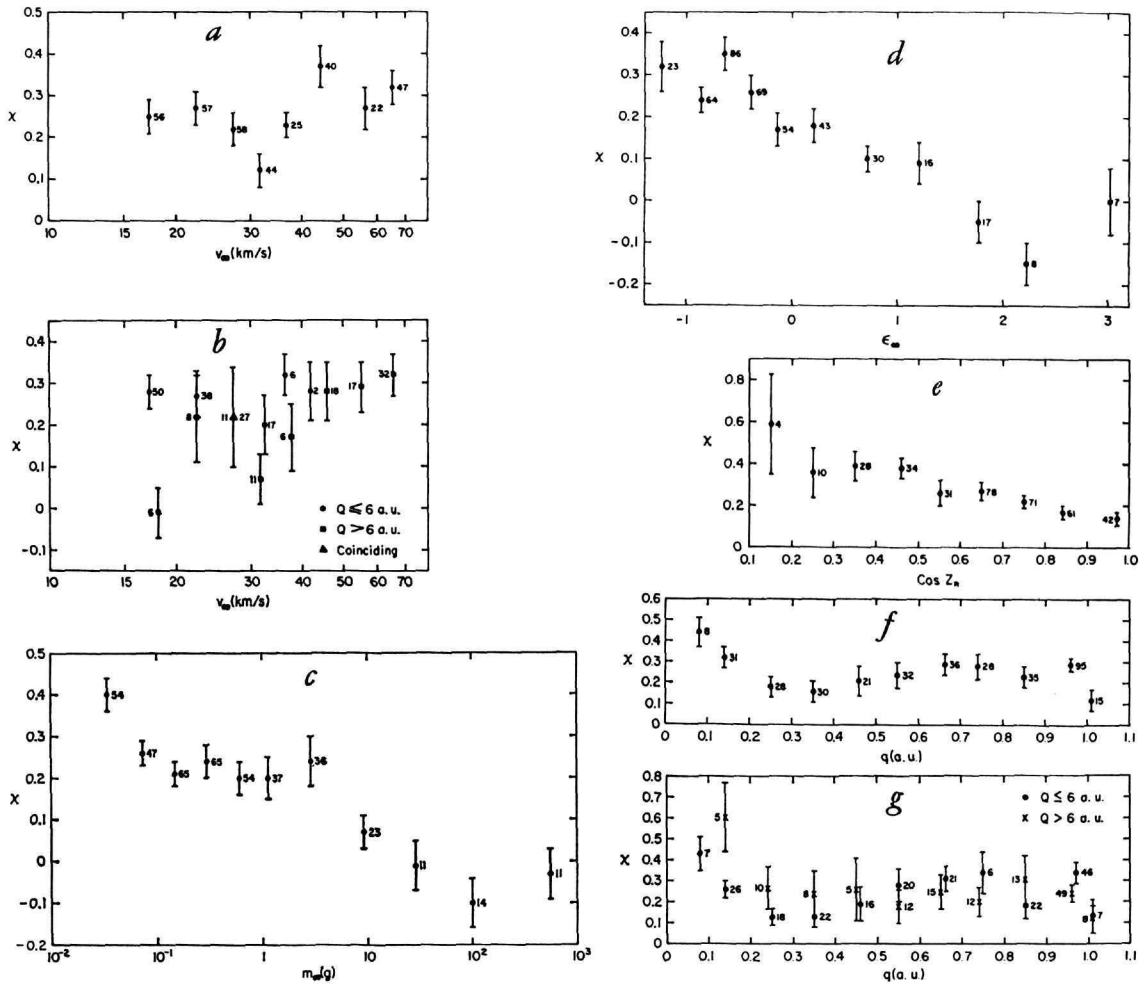


FIGURE 16.—Fragmentation index χ as a function of: *a*, velocity for all Super-Schmidt meteors; *b*, velocity for short-period and long-period sporadic Super-Schmidt meteors; *c*, mass for Super-Schmidt and small-camera meteors together; *d*, brightness ϵ_{∞} for Super-Schmidt and small-camera meteors together; *e*, zenith angle Z_R of the trajectory for all Super-Schmidt meteors; perihelion distance q for: *f*, all Super-Schmidt meteors; *g*, two groups of Super-Schmidt meteors, short-period and long-period orbits. The points at $q < 0.2$ a.u. for short-period meteors are strongly influenced by two showers: Geminids (mean $q = 0.142$ a.u.; 20 meteors) and δ Aquarids (mean $q = 0.084$ a.u.; 8 meteors).

χ is less than half the average, ± 0.14 instead of ± 0.29 . It may also be worth noting that the standard deviation of the individual values of χ for small-camera meteors is smaller than for Super-Schmidt meteors (± 0.20 against ± 0.29). As previously stated (Jacchia, 1958), this difference reflects the fact that the relative amount of fragmentation greatly varies among fainter meteors.

Tables 19.4, 19.5, and 19.6 contain results concerning small-camera meteors. They show

that for these meteors χ decreases both with mass and with velocity; the data must, therefore, be reduced respectively to a constant mass and a constant velocity. There is a small region of overlap in mass for Super-Schmidt and small-camera meteors; the agreement in this region is quite good, although the data are few. No dependence of χ on $\cos Z_R$ is found among the small-camera meteors.

Table 19.7 gives the mean value of χ for each shower, for both Super-Schmidt and

small-camera meteors. Each shower has its own peculiar mean value (the same happens for $\log \sigma$). The low value ($\chi=0.04\pm 0.05$) of the Southern Taurids, whose light curves are known to be generally smooth (Jacchia, 1955), is remarkable. Small values of χ are found also for the Northern Taurids (5 meteors: $\chi=0.03\pm 0.07$); σ Hydrids (3 meteors: $\chi=0.04\pm 0.04$); Lyrids (3 meteors: $\chi=0.08\pm 0.09$); κ Cygnids (4 meteors: $\chi=0.11\pm 0.09$); for the lone member of the η Aquarid shower ($\chi=0.09$); and the two Northern ι Aquarids ($\chi=0.10\pm 0.26$).

Values of χ for small-camera shower meteors are available for a few showers: Geminids have $\chi=0.00\pm 0.07$, but if we reduce this value to $v_\infty=30$ km/s and to $m=0.8$ g (standard Super-Schmidt mass), we get $\chi_{st}\approx 0.15$, in good agreement with the value for Super-Schmidt Geminids. For Southern Taurids we have $\chi=-0.17\pm 0.07$, which, after reduction, becomes $\chi_{st}=0.02$, in excellent agreement with the Super-Schmidt value. Very good agreement is also found for Northern Taurids ($\chi=-0.13\pm 0.10$, which after reduction becomes $\chi_{st}\approx 0.10$). There is fair agreement for the Perseids ($\chi=-0.13\pm 0.10$, i.e., $\chi_{st}\approx 0.15$, which compares with $\chi_{st}\approx 0.22$ for Super-Schmidt meteors). A shower not present among Super-Schmidt meteors is that of the χ Orionids, four members of which were photographed by small cameras and permitted the determination of an average value of χ . The result is $\chi=0.06\pm 0.05$ and $\chi_{st}\approx 0.25$. On the average, there are no differences between sporadic and shower meteors with regard to χ .

When Super-Schmidt and small-camera meteors are considered together, we have values of χ for masses ranging from 10^{-2} to 2×10^3 g (extreme averages 0.03 and 555 g) and for a range in integrated brightness between -1.4 and 3.4 (extreme averages -1.14 and 3.02). The resulting mean values are listed respectively in tables 19.8 and 19.9 and plotted in figures 16c and 16d. From an inspection of the tables we see that χ remains approximately constant up to a mass of about 5 g ($\chi\approx 0.23\pm 0.02$) and then decreases to zero for a mass comprised between 25 and 30 g. The dependence of χ on ϵ_∞ looks roughly linear for $\epsilon_\infty < 2$.

For brighter meteors one would expect χ to level off to a value near zero, and this seems to be corroborated by the few meteors with $\epsilon_\infty > 2$, although the data for them are very scanty.

Table 19.10.1 shows mean values of χ as a function of the zenith angle both for all Super-Schmidt meteors (fig. 16e) and for sporadic meteors only. We confirm that the fragmentation index decreases when $\cos Z_R$ increases. The correlation can be expressed by the linear expression, mean $\chi=0.53-0.4 \cos Z_R$, or, if we use values reduced to a constant mass of 0.8 g,

$$\text{mean } \chi=0.49-0.37 \cos Z_R. \quad (63)$$

Since the correlation of χ with $\cos Z_R$ is rather clear-cut, it may seem necessary to correct the other correlations for this effect. Fortunately, there is practically no correlation of $\cos Z_R$ with the mass nor can the slight correlation of $\cos Z_R$ with v_∞ affect the preceding results on $\chi(v_\infty)$. Table 19.10.2 shows $\chi(\cos Z_R)$ for sporadic Super-Schmidt meteors in groups $Q\leq 6$ a.u., $Q> 6$ a.u.

Table 19.11 shows χ as a function of the aphelion distance Q . There is nothing to add to the remarks made earlier in this section.

The correlation, or better, the lack of correlation, between χ and $\log \sigma$ among the Super-Schmidt meteors has been fully discussed in the section on $\log \sigma$; however, we may add here that a slight correlation between χ and $\log \sigma$ exists among small-camera meteors (table 19.12). Meteors having $\log \sigma$ close to -12.0 show a mean value of χ of -0.11 ± 0.05 , while those with $\log \sigma$ greater than -11.6 have $\chi=0.03\pm 0.03$. On the other hand, meteors with $\chi\leq 0$ have $\log \sigma=-11.65\pm 0.05$, while those with positive χ have $\log \sigma=-11.45\pm 0.08$.

Table 19.13.1 shows χ as a function of the perihelion distance q both for all Super-Schmidt meteors (fig. 16f) and for sporadic meteors only. In table 19.13.2, $\chi(q)$ is given for sporadic meteors with $Q\leq 6$ a.u. and $Q> 6$ a.u., respectively, while table 19.13.3 is a similar listing for all and not only sporadic meteors (fig. 16g).

While no clear trend is visible among the meteors with $q>0.2$ a.u., it appears significant

that those meteors that approach the sun to a distance less than 0.2. a.u. have a considerably larger fragmentation index.

9. Wake and blending

We define "wake" as the short train that follows the meteor head. On Super-Schmidt films it shows as a tapering appendage of the bright segments cut out by the shutter on the meteor trail and gives these segments a characteristic teardrop appearance. The brightness of the wake relative to the head varies from meteor to meteor. As a rule, it is always visible when the meteor brightness is five magnitudes or more above the plate limit. Occasionally, however, a meteor only two magnitudes brighter than the plate limit may display a conspicuous wake.

We define "blending" as the gradual increase in length of the bright trail segments, which occasionally results in their blending together into a continuous-appearing trail. A considerable number of meteor trails show complete blending on Super-Schmidt films toward the end of the trajectory. In very rare cases blending may follow the occurrence of a flare and then clear up before the end.

We have tried to give a rough quantitative estimate of the intensity of wake and of blending, by assigning to each meteor a grade for each of the two phenomena in a memory-based scale ranging from zero to four. These grades are listed in table 1.1 as W (wake) and B (blending), respectively. Although in most instances W and B were recorded as integers, we sometimes found it necessary to use finer subdivisions such as 0^+ , $0-1$, 1^- ; for the most exceptional cases of blending we have used 4^+ . The subdivisions were transformed to approximate decimal fractions in table 1.1.

Mean values of B and W and their distributions for all meteors and for sporadic meteors only, as well as for particular groups, are listed in table 20.1. The same quantities are given in table 20.2 for shower meteors. The mean values for all meteors are $\bar{B}=0.51\pm 0.05$, $\bar{W}=0.74\pm 0.05$. Of all meteors 53 percent show some wake, while only 32 percent show some blending. The sporadic meteors show less blending and more wake than shower

meteors do; however, according to the following figures, these differences do not appear important.

	$\bar{B}\pm\text{s.d.}$	$\bar{W}\pm\text{s.d.}$
Sporadic meteors	0.47 ± 0.05	0.77 ± 0.06
Shower meteors	0.63 ± 0.08	0.67 ± 0.08
All meteors	0.51 ± 0.05	0.74 ± 0.05

While meteors in short-period orbits have slightly larger values of B and W than long-period meteors, the results are not conclusive. For sporadic meteors we find:

$$Q\leq 6 \text{ a.u. } \bar{B}=0.46\pm 0.08 \quad \bar{W}=0.73\pm 0.08$$

$$Q>6 \text{ a.u. } \bar{B}=0.37\pm 0.07 \quad \bar{W}=0.70\pm 0.09.$$

Meteors of classes A and S were excluded in these two groups, so that the preceding values agree with the overall average: $\bar{B}=0.42$, $\bar{W}=0.71$, slightly smaller than the averages for all sporadic meteors.

Of the class A meteors (abrupt beginning), 77 percent show some blending; their average value of B is 1.35 ± 0.24 , almost three times the average of all other meteors. This is in agreement with what might be expected if the sudden increase in brightness that makes the meteor become visible is caused by a complete disintegration of the meteor body into fragments of different sizes. With respect to wake, however, class A meteors are normal ($\bar{W}=0.59\pm 0.13$).

Opposite behavior is shown by meteors of class F, i.e., those from which one or more large fragments become detached from the main body in the course of the trajectory. Of these meteors, which presumably represent a hardier group whose members are less apt to be pulverized, 10 out of 11 showed no blending at all. On the other hand, 82 percent of them showed some degree of wake, and their average value of W (2.1 ± 0.4) is nearly three times the mean of all meteors. This feature, however, may simply reflect the fact that most class F meteors are quite bright.

Among the showers the Taurids are the most remarkable. All 18 Southern Taurids have $B=0$ and 15 of them also have $W=0$. The five Northern Taurids also have $\bar{B}\approx 0$ (four of them have $B=0$, and the remaining one has $B=0.3$, or 0^+). The wake of the Northern Taurids is normal. The results for the Southern

Taurids are in agreement with the well-known smoothness of the light curves of these meteors. The 11 Perseids have $\bar{B} \approx 0$ (10 out of 11 have $B=0$) and normal wake ($\bar{W}=0.96 \pm 0.35$). The absence of blending is probably just a consequence of the short duration of the trajectory, which prevents the fragments from becoming widely dispersed. Both Draconids have $B=4$ and $W=0$.

The 11 δ Aquarids show a high value of the blending ($\bar{B}=1.55 \pm 0.27$) and low wake ($\bar{W}=0.21 \pm 0.12$). Only one out of 11 has $B=0$, while eight out of 11 have $W=0$. The 14 α Capricornids also have a large value of \bar{B} (1.0 ± 0.3) and normal W , while on the contrary, the Geminids (20 members) have a large \bar{W} (1.5 ± 0.3) and normal \bar{B} .

The dependence of wake and blending on the various meteor parameters has been investigated. Table 20.3 shows the variations with the velocity of \bar{B} and \bar{W} and of the percentages of the different groups. As was expected, both \bar{B} and \bar{W} decrease, although somewhat irregularly, when v_∞ increases (fig. 17a). Table 20.4 gives the mean values of B and W and their distribution as a function of the mass. The behavior of \bar{B} is irregular, while the dependence of \bar{W} on mass is quite strong. There is practically no wake for small meteors; then \bar{W} increases regularly with mass and the wake is generally well developed for the largest meteors ($\bar{W}=2.5 \pm 0.3$). This is apparently just an effect of relative brightness, not of the mass itself. Figure 17b shows the plotting of these results. Table 20.5 lists the same quantities as functions of the difference ΔM between the plate limit and the maximum photographic magnitude. As we can see also in figure 17c, \bar{W} increases strongly with ΔM , from about zero for $\Delta M \approx 1$ to about 3 for $\Delta M > 5$. \bar{B} shows a parabolic trend with ΔM ; it could also be considered roughly as a constant. Tables 20.6 to 20.10 show the mean values of B and W and their distributions as a function of ϵ_∞ , $\log \sigma$, χ , $\cos Z_R$, and Q , respectively. These results are plotted in figures 17d-h. Since the integrated brightness ϵ_∞ is a function of m_∞ and v_∞ , $\bar{B}(\epsilon_\infty)$ and $\bar{W}(\epsilon_\infty)$ are functions that could be derived from the results of tables 20.1 and 20.2. \bar{W} increases with ϵ_∞ , while \bar{B} has a parabolic trend. The dependence of \bar{B}

and \bar{W} on $\log \sigma$ is quite interesting. Meteors with $\log \sigma < -11.45$ ($\log \sigma = -11.66$) show normal values for both \bar{B} and \bar{W} . They do not follow the trend of all the other groups. As a matter of fact, if we exclude them, we note a clear-cut and regular increase of \bar{B} and \bar{W} when $\log \sigma$ increases: \bar{B} rises from 0.22 at $\log \sigma = -11.37$ to 0.74 at $\log \sigma = -10.83$, while \bar{W} increases from 0.54 to 1.02. The behavior of \bar{W} for sporadic meteors is just about the same as that for all meteors; however, the value of \bar{B} for sporadic meteors with $\log \sigma < -11.45$ is smaller than the corresponding one for all meteors and is not in disagreement with the general trend.

In table 20.8 we see that the wake is independent of the fragmentation index χ , while \bar{B} increases with χ . This increase is very slow for sporadic meteors from $\bar{\chi} = -0.1$ to $\bar{\chi} = 0.5$, since \bar{B} increases only from 0.31 to 0.40. Then \bar{B} jumps to 1.1 ± 0.2 for the last group ($\bar{\chi} = 0.89$). The behavior of all meteors is more regular; there is an increase from 0.3 to 0.6 when $\bar{\chi}$ increases from -0.1 to 0.5 and then a jump to $\bar{B} = 1.2 \pm 0.2$ for $\bar{\chi} = 0.9$.

The wake is also almost independent of the zenith angle. There is, however, a very regular decrease of the blending with the increase of $\cos Z_R$. This is in accordance with expectation, because meteors with low angles of incidence have longer durations; also, the effect will be more conspicuous on photographs taken near the zenith, as was the case of the Super-Schmidt photographs.

The list of results ends with table 20.10, which is devoted to the correlations of \bar{B} and \bar{W} with the aphelion distance Q . The wake does not seem to depend at all on the type of the orbit; however, there are some differences in the blending. If we examine all meteors, there is a small difference between the first three groups ($Q \leq 7$ a.u.) and the remaining two ($Q > 7$ a.u.), since the average value of B for the former is around 0.6, while for the latter it is 0.3. If we look at sporadic meteors only, the picture is different. There is a large difference between the first group ($Q \leq 3.5$ a.u.) and the others. In fact, we have $\bar{B} = 1.0 \pm 0.2$ for $Q = 2.6$ and $\bar{B} = 0.38 \pm 0.05$ for all the other meteors (Q from 3.5 a.u. to ∞). A further

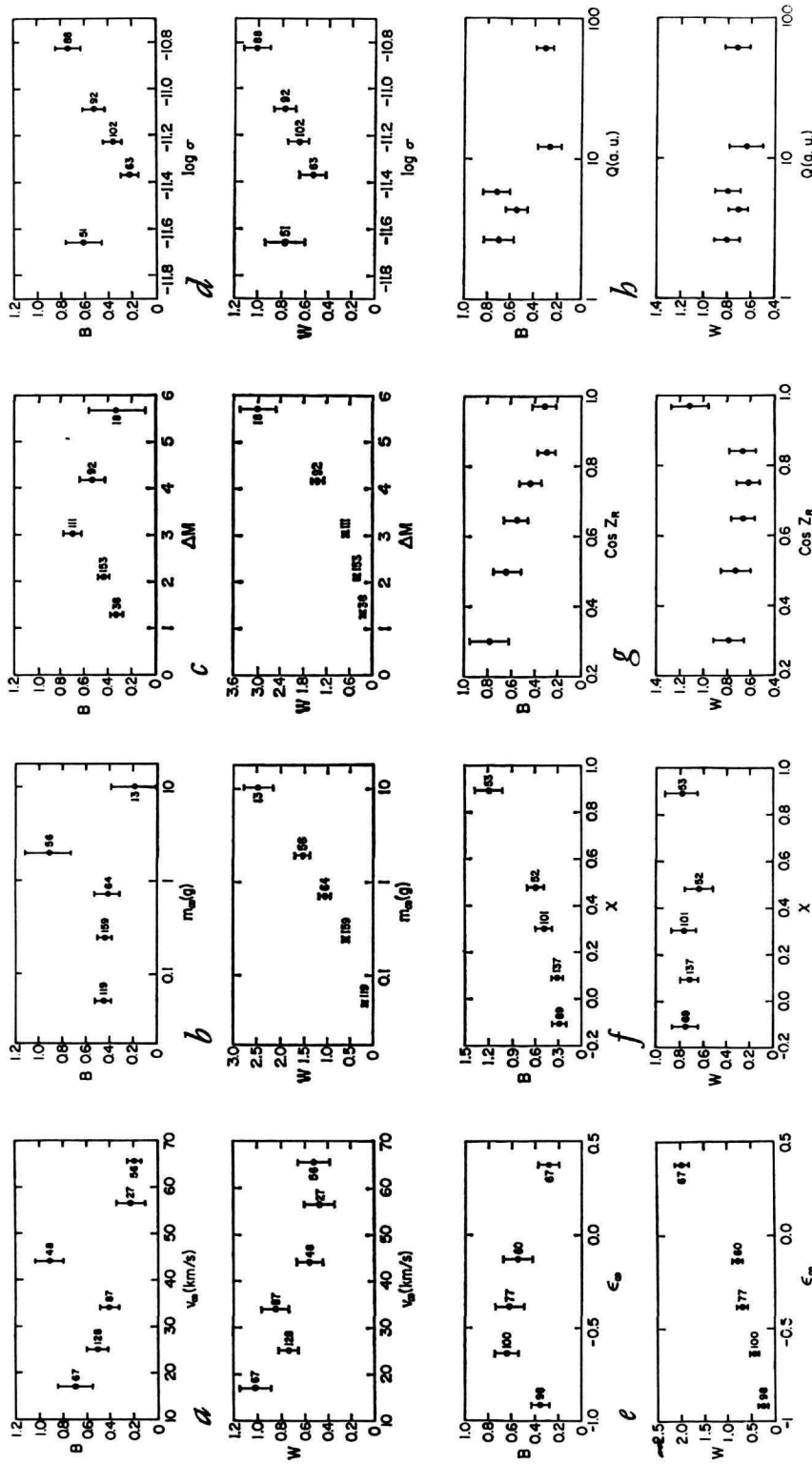


FIGURE 17.—Blending (*B*) and wake (*W*) indices as functions of: *a*, velocity; *b*, mass; *c*, difference ΔM between the plate limit and maximum photographic magnitude; *d*, ablation coefficient σ ; *e*, brightness; *f*, fragmentation index X ; *g*, zenith angle Z_R of the trajectory; *h*, aphelion distance Q .

subdivision among these meteors shows that for meteors having Q comprised between 3.5 and 7 a.u., \bar{B} is about 0.4 and decreases to 0.33 for meteors with $Q > 7$ a.u. The difference between the behavior of the sporadic meteors and all meteors is, of course, due to the showers; Taurids and Geminids lower the value of \bar{B} in the group with $Q < 3.5$ a.u., while α Capricornids, Quadrantids, and δ Aquarids increase it in the group between 3.5 and 7 a.u.

10. Peculiarities of individual showers; meteors with abrupt beginnings; asteroidal meteors

a. Showers

Table 21 gives a synoptic survey of the physical characteristics of those of our Super-Schmidt meteors that belong to major showers. In the upper part of the table we have compared means for shower meteors with means for all meteors, for sporadic meteors, and for meteors with abrupt beginnings (A) and short trails (S).

The number of observations refers to quantities such as v_{∞} and $\cos Z_R$, which were available for all meteors (413) without exception. For each individual parameter the mean was taken over the available data, the number of which was occasionally smaller than the number in the last columns. (For example, we had only 400 values of the duration D and 396 values of $\log \sigma$.) The mean value of $\Delta \log \rho_{corr}$ for "all" meteors refers to the 350 meteors that were used in the analysis of the decelerations. The same is true for the mean $\Delta \log \rho_{corr}$ for sporadic meteors.

For two parameters, $\log \sigma$ and χ , means for individual showers were computed and listed in the respective sections dealing with the analysis of these quantities (secs. 7 and 8). These means are not necessarily identical with the means listed in table 21, because meteors of classes A and S were excluded in their formation in harmony with the analysis of sporadic meteors. The means of table 21 apply to all meteors.

The means are all unweighted except the ones of $\Delta \log \rho_{corr}$ for which we have used the weight w . Draconids and Geminids, which have large systematic peculiarities in $\Delta \log \rho_{corr}$, were eliminated in computing the mean of this quan-

tity for shower meteors (actually, their inclusion would not have changed the mean although it would have increased the standard deviation by a factor of three).

Meteors whose membership in a shower may be subject to some doubt (those marked with a Q after the shower code number in table 1.1) were included in the means of individual showers, except for meteor no. 4513, whose physical characteristics are so different from those of the two *bona fide* Draconids that its inclusion would have spoiled the uniqueness of the Draconid data. On the other hand, we have eliminated meteor no. 5180 from the means of the Northern Taurids because of its drastically different physical characteristics, although its membership in the shower does not seem to be in question.

In the column headed $\Delta' H_{2.5}$, we have listed the difference between the mean value of $H_{2.5}$ for individual showers and meteor groups and the means of $H_{2.5}$ for sporadic meteors. These means are all reduced to a standard meteor mass of 0.3 g using the coefficient of $\log m_{\infty}$ from table 4. [$\log \rho_{2.5}$ standard = $\log \rho_{2.5}$ observed + 0.28 ($\log m_{\infty} + 0.52$); the mean mass for each group is a logarithmic mean.] The means were plotted on a diagram (fig. 18), in which smooth curves were drawn through the points representing sporadic meteors separating those with aphelion distances larger than 6 a.u. from those in short-period orbits. The differences $\Delta' H_{2.5}$ were taken from these smooth curves. For the sake of completeness we have also given $\Delta' H_{2.5}$ for meteors of classes A and S; the residuals were taken from a smooth curve through points representing the sporadic meteors without those of classes A and S.

The parameters that best characterize the physical peculiarities of each shower are $\Delta' H_{2.5}$, $\Delta \log \rho_{corr}$, $\log \sigma$, χ , and B . The means of these quantities for individual showers are plotted in figure 19, which enables us to tell at a glance how one shower differs from another. Thus we can see that the Draconids are exceptional in just about every respect, and the Geminids are nearly four times denser than the average ($\Delta \log \rho_{corr} = -0.39$), but crumble just as easily as any ordinary meteor (normal χ and B) and appear at normal heights ($\Delta H_{2.5} = -0.5$ km). Delta Aquarids are crumbly (large χ ,

large B) and appear lower than the average ($\Delta'H_{2.5} = -3.1$ km), but their decelerations are normal. The Southern Taurids have great tensile strength (χ and B just about zero), but apparently are not denser than the average since their decelerations are perfectly normal ($\overline{\Delta \log \rho} = 0$).

All these clues are far from adding up to the picture of meteor structure and composition that we could have by studying specimens in the laboratory, but at least they tell us something about the diversity to be found in the meteor population and may be useful in reconstructing the processes of comet formation and disintegration.

b. Meteors with abrupt beginnings

The results of least-squares solutions for the heights of meteors with abrupt beginnings

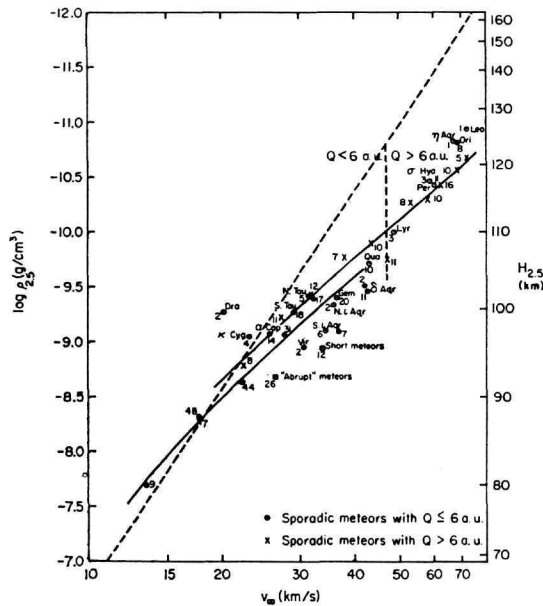


FIGURE 18.—The height $H_{2.5}$ at which meteors reach absolute magnitude $+2.5$ while brightening, as a function of velocity. Logarithms of the atmospheric density ρ (g/cm^3) in ordinates at left; heights, in km, at right. Dots: sporadic meteors with $Q \leq 6$ a.u.; crosses: sporadic meteors with $Q > 6$ a.u.; circled dots: meteors in individual showers. Smooth curves have been drawn, for reference, through the points representing sporadic meteors. Theoretical values from equation (18) are represented by the broken straight line.

(class A meteors), involving all the five basic parameters, are given in table 3.13; comments on these solutions are found in section 4b. In view of the statement often repeated in meteor literature, that the abrupt increase in brightness in such meteors, which clearly indicates a break-up of the meteor body, occurs at a point in the trajectory corresponding to a constant value of ρv^2 (McCrosky, 1955a; Whipple, 1959; McKinley, 1961), we have tried to see if we could confirm or disprove this assertion on the basis of our material.

Altogether our Super-Schmidt material includes 26 meteors with an abrupt beginning, or about 6 percent of the total number. McCrosky (1955b) estimates that 13 percent of all Super-Schmidt meteors belongs to this category; the smaller percentage in our material is probably due partly to selection (many meteors of class A are of too short duration to yield good decelerations) and partly to a more stringent rule for classification (several meteors of class S display a fast rise to maximum and could almost be classified as A's). Even among our 26 class A meteors some have a less abrupt beginning than others; for 12 of them the rise is almost instantaneous.

If we take the atmospheric density ρ_{AB} corresponding to the abrupt beginning of all class A meteors and put $\rho_{AB} v_{\infty}^K = \text{const}$, we find by least squares $K = 3.6 \pm 0.3$. Using only the 12 ultra-abrupt meteors, we obtain $K = 3.0 \pm 0.5$. Taking the density ρ_B corresponding to the beginning heights of all Super-Schmidt meteors and putting $\rho_B v_{\infty}^K = \text{const}$, we find $K = 3.0 \pm 0.1$; this compares with $K = 3.7 \pm 0.3$ for the actually observed beginnings of all class A meteors.

We see, then, that fragile meteors tend to break up at a point corresponding to a constant value of ρv^3 rather than of ρv^2 , and that the power of v is not too different from that found from the beginning points of ordinary meteors. Abrupt meteors do, however, begin 4 km lower, on the average, than ordinary meteors (see sec. 4b).

The $\rho v^3 = \text{const}$ relation would suggest heat transfer rather than pressure as the trigger for the breakup of meteors. This could be the case if we have to deal with a body so porous that air molecules will penetrate deep inside to do

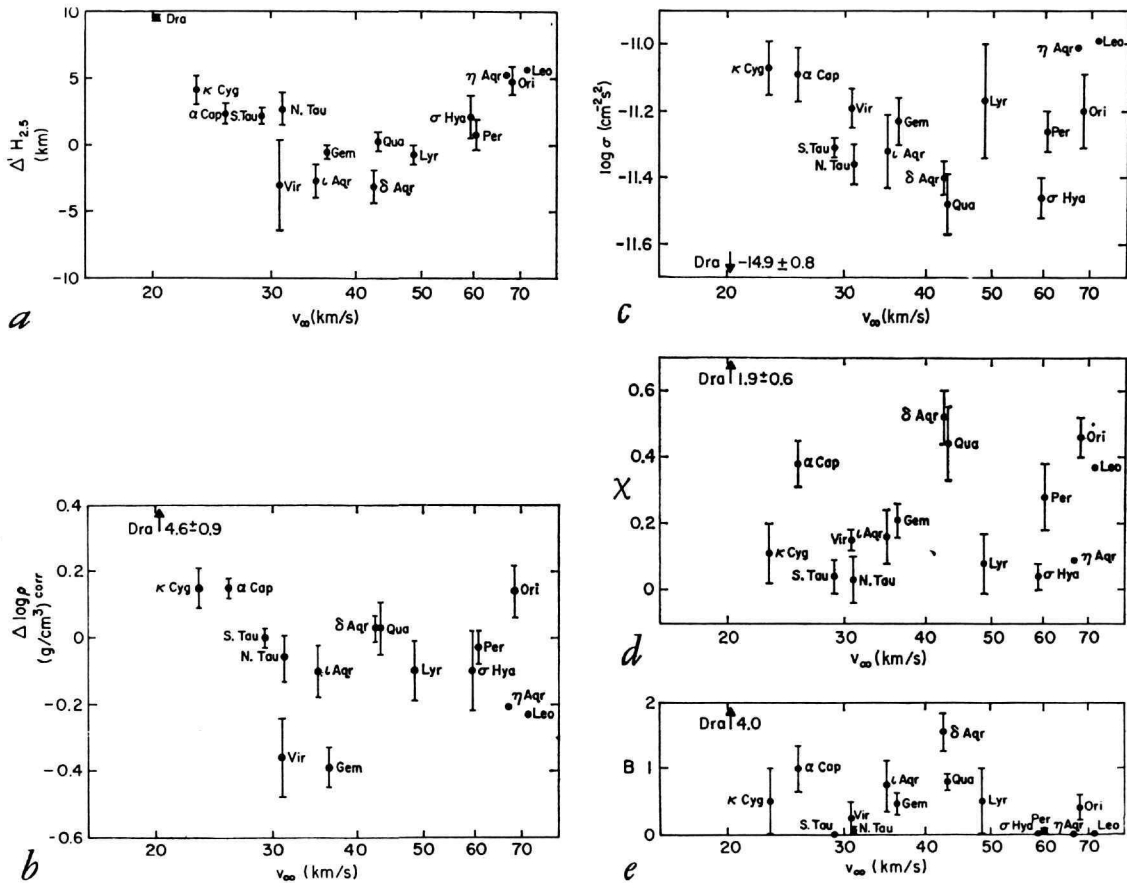


FIGURE 19.—Physical characteristics of individual meteor showers arranged in order of increasing velocity: *a*, deviation of the height $H_{2.5}$ from the mean curve corresponding to sporadic meteors (see fig. 18), taking into account the aphelion distance Q ; *b*, acceleration values (see table 1.2; a high value means that the meteor had an abnormally high deceleration; the opposite is true for low values); *c*, logarithm of the ablation coefficient σ ; *d*, fragmentation index χ ; *e*, blending index B . (The standard deviations of the mean value of B for Southern Taurids (18 meteors) and σ Hydrids (3 meteors) are equal to zero.)

their heating and melting, thus destroying the precarious cohesion of the body as a whole. In larger meteors the penetration of air molecules will be relatively smaller, owing to the shielding by the outer layers; this could explain why no meteors with abrupt beginnings are found among small-camera meteors. This process of flaking off of large meteors and complete breakup of small meteors was described by Jacchia (1955) in his first paper on fragmentation.

c. Search for asteroidal meteors

Since several of the major meteor showers are associated with comets and since the heights,

decelerations, and other physical characteristics of shower meteors, taken in their totality, do not differ from those of most sporadic meteors, we must conclude that the overwhelming majority of the photographic meteors are of cometary origin. This does not exclude the possibility that a few asteroidal meteors might be included in our sampling.

In comparison with a cometary meteor, an asteroidal meteor should presumably be much more dense and of greater tensile strength. For such a meteor, then, we must expect to find some peculiar characteristics, such as

1. an abnormally small deceleration, i.e., a strongly negative value of $\Delta \log \rho_{corr}$;

2. low fragmentation index χ ;
3. low ablation coefficient σ ;
4. long trajectory, resulting in an exceptionally low end height;
5. absence of terminal blending;
6. rather smooth light curve, at least in the early part of the trajectory; never an abrupt beginning.

In addition, on the basis of what we know about asteroids, we would expect the orbit of such a meteor to have an aphelion well inside Jupiter's orbit.

Only one of our 413 Super-Schmidt meteors satisfies all these requirements, namely meteor no. 7946. This meteor entered the atmosphere with a velocity of 18.5 km/s at an angle of $26^{\circ}6$ with respect to the vertical. It became visible on the photographs at a height of 88.1 km, reached a maximum brightness of $-0^m.7$ (photographic, absolute), and disappeared after 2.55 seconds at the height of 49.3 km, the lowest on record for any of our Super-Schmidt meteors. A single fragment became detached a little before midtrajectory and could be followed on the photograph for $0^s.10$. The orbit has a major axis of 2.49 a.u., a perihelion distance of 0.94 a.u., and an aphelion distance of 4.04 a.u. The deceleration is much smaller than the average for a meteor with comparable mass, velocity, and angle of incidence. The mean value of $\Delta \log \rho$ for the whole trajectory is -0.85 , which compares with a mean value of -0.05 for meteors with $Q=4$ a.u. The trail shows no trace of terminal blending. The mean value of the fragmentation index χ for the whole trail is $+0.08$; but in the early portion of the trail, before the loss of the fragment, it is about -0.1 ; after the loss of the fragment it jumps to $+0.3$. The mean value of $\log \sigma$ is -11.46 . The light curve is quite smooth, except for some minor flaring during the last half second of the visible trajectory. The ratio of the observed duration to the theoretical duration is 0.93, while the mean for all Super-Schmidt meteors is 0.61, and the mean for meteors with a velocity of 18 km/s is 0.58.

According to equation (41) the mean density of all Super-Schmidt meteors is 0.26 g/cm^3 . For standard conditions of meteor shape and

atmospheric density a value of -0.85 in $\Delta \log \rho_{corr}$ corresponds to a factor of 19 in the density; this would result in a density of 4.9 g/cm^3 for meteor no. 7946. While we would not give any weight to this individual density determination as such, we want to point out that it is of the right order of magnitude for an asteroidal meteor.

Acknowledgments

Aspects of this research were supported in the past by the Office of Naval Ordnance, the Office of Naval Research, the Air Force Cambridge Research Center, Geophysics Research Directorate, and the U.S. Army Office of Ordnance Research.

As stated in the orbital analysis of the present meteor material (Jacchia and Whipple, 1961), a great many people contributed to the success of this meteor program, in its manifold aspects, involving instrumental design and construction, station operation, photography, visual observing, measuring, and computing. For a list of the principal persons and agencies involved we refer to the paper quoted above. In addition, the present analysis required a great deal of electronic computing, which was programmed principally by J. C. Cherniack, R. L. Emerson, and B. M. Fardon.

References

JACCHIA, L. G.

1948. Ballistics of the upper atmosphere. Harvard Coll. Obs. and Center of Analysis M.I.T. Tech. Rep., no. 2; Harvard Reprint Ser. II, no. 26, 30 pp.
- 1949a. Photographic meteor phenomena and theory. Harvard Coll. Obs. and Center of Analysis M.I.T. Tech. Rep., no. 3; Harvard Reprint Ser. II, no. 31, 36 pp.
- 1949b. Atmospheric density profile and gradients from early parts of photographic meteor trails. Harvard Coll. Obs. and Center of Analysis M.I.T. Tech. Rep., no. 4; Harvard Reprint Ser. II, no. 32, 12 pp.
1952. A comparative analysis of atmospheric densities from meteor decelerations observed in Massachusetts and New Mexico. Harvard Coll. Obs. and Numerical Analysis Laboratory of M.I.T. Tech. Rep., no. 10; Harvard Reprint Ser. II, no. 44, 37 pp.

1955. The physical theory of meteors, VIII: Fragmentation as a cause of the faint-meteor anomaly. *Astrophys. Journ.*, vol. 121, pp. 521-527.
1956. On two 1953 Giacobinids and on some physical characteristics of shower meteors (abstract). *Astron. Journ.*, vol. 61, pp. 6-7; see also *Sky and Telescope*, vol. 15, p. 207.
- 1957a. A preliminary analysis of atmospheric densities from meteor decelerations for solar, lunar and yearly oscillations. *Journ. Meteorol.*, vol. 14, pp. 34-37.
- 1957b. On the "color-index" of meteors. *Astron. Journ.*, vol. 62, pp. 358-362.
1958. On two parameters used in the physical theory of meteors. *Smithsonian Contr. Astrophys.*, vol. 2, no. 9, pp. 181-187.
1960. Individual characteristics of meteor families (abstract). *Astron. Journ.*, vol. 65, p. 53.
1963. Meteors, meteorites and comets; interrelations. *In The Solar System*, vol. IV, ed. by B. M. Middlehurst and G. P. Kuiper, University of Chicago Press, Chicago, pp. 774-798.
- JACCHIA, L. G.; KOPAL, Z.; and MILLMAN, P. M.
1950. A photographic study of the Draconid meteor shower of 1946. *Astrophys. Journ.*, vol. 111, pp. 104-133.
- JACCHIA, L. G., and WHIPPLE, F. L.
1961. Precision orbits of 413 photographic meteors. *Smithsonian Contr. Astrophys.*, vol. 4, no. 4, pp. 97-129.
- LEVIN, B. J.
1961. *Physikalische Theorie der Meteore und die Meteoritische Substanz in Sonnensystem*. Akademie-Verlag, Berlin.
- McCROSKY, R. E.
1955a. Fragmentation of faint meteors (abstract). *Astron. Journ.*, vol. 60, p. 170.
1955b. Physical and statistical studies of meteor fragmentation. Thesis, Harvard University.
- McKINLEY, D. W. R.
1961. *Meteor Science and Engineering*. McGraw-Hill, New York, 309 pp.
- MILLMAN, P. M.
1935. An analysis of meteor spectra: second paper. *Ann. Harvard Coll. Obs.*, vol. 82, pp. 149-177.
- MILLMAN, P. M., and McKINLEY, D. W. R.
1963. Meteors. *In The Solar System*, vol. IV, ed. by B. M. Middlehurst and G. P. Kuiper, University of Chicago Press, Chicago, pp. 674-773.
- MINZNER, R. A., and RIPLEY, W. S.
1956. The ARDC model atmosphere, 1956. *Air Force Surveys and Geophys.*, TN 56-204 (no. 86), p. 15.
- ÖPIK, E.
1933. Atomic collisions and radiation of meteors. *Harvard Reprint Ser. I*, no. 100, 39 pp.
- RUSSELL, J. A.
1960. A time-resolved spectrum of the terminal burst of a Perseid meteor. *Astrophys. Journ.*, vol. 131, pp. 34-37.
- U.S. STANDARD ATMOSPHERE 1962
1962. Prepared under NASA, USAF, and U.S. Weather Bureau, Washington, D.C., 278 pp.
- VERNIANI, F.
1961. On meteor ablation in the atmosphere. *Il Nuovo Cimento*, vol. 19, pp. 415-442.
1964a. On the luminous efficiency of meteors. *Smithsonian Astrophys. Obs. Spec. Rep.*, no. 145, 62 pp.; also *Smithsonian Contr. Astrophys.*, vol. 8, no. 5, pp. 141-172, 1965.
1964b. On the density of meteoroids, II: The density of faint photographic meteors. *Il Nuovo Cimento*, vol. 33, pp. 1173-1184.
1966. Meteor masses and luminosity. *Smithsonian Astrophys. Obs. Spec. Rep.*, no. 219, 46 pp.
- WHIPPLE, F. L.
1943. Meteors and the earth's upper atmosphere. *Rev. Mod. Phys.*, vol. 15, pp. 246-264.
1959. Solid particles in the solar system. *Journ. Geophys. Res.*, vol. 64, pp. 1653-1664.
- WHIPPLE, F. L., and JACCHIA, L. G.
1957. Reduction methods for photographic meteor trails. *In Smithsonian Contr. Astrophys.*, vol. 1, no. 2, pp. 183-206.

Abstract

In this paper we present a statistical evaluation of the atmospheric trajectories of the 413 precision-reduced meteors, doubly photographed with the Super-Schmidt cameras in New Mexico, for which orbital data have been previously published and analyzed by Jacchia and Whipple (1961). We have studied the dependence of heights, lengths, decelerations, and magnitudes on such basic parameters as velocity, angle of incidence, and mass, as well as on derived parameters such as the ablation coefficient and the fragmentation index; the latter are in turn related to the other geometric and physical characteristics, including the phenomena of wake and terminal blending. A comparison with classical meteor theory shows again and again that fragmentation is the most important factor in causing the wide discrepancies between theory and observation.

Owing to strong interrelations among the basic parameters, mostly inherent in the meteor phenomenon, we have tried not to rely entirely on the least-squares process for the analysis; where the least-squares method was used, we have often added the variables one at a time in the solution, in order to evaluate the effect of the interrelations and the reliability of the solutions. Our analysis confirms the results previously obtained by Jacchia (1955, 1956, 1957a, 1957b, 1958, 1960, 1963) using part of the present material, concerning the systematic variation in the accelerations, the ablation coefficient, the fragmentation index, and the color index, with meteor brightness, as well as the physical peculiarities of individual meteor showers and the systematic differences between meteors in short-period and in long-period orbits. The maximum brightness of fragmenting meteors is greater than for nonfragmenting ones; Super-Schmidt meteors are, on the average, half a magnitude brighter at maximum than predicted by single-body theory and are about one-third shorter in duration and length.

For meteors that suddenly break up (abrupt-beginning meteors) we find that the breakup occurs at a point in the trajectory that corresponds to a constant value of ρv^3 (ρ =air density, v =velocity). This suggests heat transfer rather than dynamic pressure as the break up trigger and leads to the picture of a meteor body so porous that air molecules can penetrate to its core; shielding by the outer layers prevents the complete breakup of larger meteors.

Using Verniani's (1964a) value, 1.0×10^{-19} zero mag $\text{g}^{-1} \text{cm}^{-3} \text{s}^4$, for the photographic luminous-efficiency coefficient τ_{0p} , we find that the average Super-Schmidt meteor has a density of 0.26 g/cm^3 ; a meteor that enters the atmosphere with a velocity of 40 km/sec and makes an angle of 45° with the vertical must have a mass of 0.69 g to reach visual magnitude zero at maximum. Among showers we find that the Geminids are four times denser than the average meteor, but crumble just as easily, while the Southern Taurids have normal densities but do not fragment much; the Draconids are unique in their extraordinary fragility.

A search for meteors of asteroidal origin has led us to conclude that only one of our 413 Super-Schmidt meteors, namely no. 7946, possesses all the requisites to qualify as a member of this group.

Tables 1.1-21

TABLE 1.1.—Basic physical data for 413 Super-Schmidt meteors: Trajectories

Trail No.	Date	Sh.No.	Apparent radiant α , δ	sin Q	cos Z_R	v_m	M_{pm}	H_B	H_{BD}	$H_{2.5}$	H_{HL}	H_{ED}	H_Z
2961	51 10	2.22043	20 15 51 +10 12	.205	.790	31.22	-2.2	94.4	94.3	94.1	88.9	78.7	78.0
3000	52 4	3.45698	289 14 +36 51	.311	.848	49.58	-0.9	109.6	108.7	111.9	97.9	93.1	92.6
3024	52 4	1.33078	272 36 -6 13	.155	.219	68.85	+0.4	112.6	112.4		104.9	102.2	102.2
3037	52 3	30.39983	235 9 -45 36	.155	.196	59.92	+0.2	116.36	115.1	119.8	107.8	105.4	105.4
3053	52 3	20.16674	117 27 -13 58	.608	.666	16.10	-0.5	94.5	94.5	92.3	80.3	73.6	73.6
3072	52 3	21.40481	210 20 -5 53	.137	.777	38.90	-0.6	97.9	97.4	97.9	89.0	86.9	84.8
3074	52 3	21.41403	213 46 -31 9	.188	.438	55.35	-0.8	100.5	100.5	102.0	93.7	87.7	87.7
3076	52 3	22.41288	167 43 +33 0	.072	.709	16.82	+0.9	92.0	92.0	90.9	78.9	76.9	76.9
3088	52 3	28.34066	280 14 +67 37	.282	.560	25.93	+1.2	99.8	99.6	99.2	89.8	85.5	85.5
3217	52 4	22.43214	6 271 39 +33 15	.451	.983	48.04	-0.6	106.7	105.9	107.1	100.2	92.4	92.5
3228	52 4	23.32587	265 40 +42 29	.501	.811	40.76	+1.3	105.4	105.3	104.8	94.8	90.0	89.6
3234	52 4	23.36348	227 59 -1 50	.271	.819	28.94	+0.4	89.4	88.9	89.4	86.2	78.5	78.5
3250	52 4	26.32654	222 6 -3 55	.309	.803	29.37	+1.0	101.6	101.6	99.6	92.7	85.5	85.5
3265	52 5	1.36734	326 41 +51 30	.288	.493	41.45	+0.1	105.5	105.5	106.6	96.7	94.7	94.7
3271	52 4	22.35236	6 271 44 +33 27	.330	.824	47.37	-1.5	105.7	104.4	107.3	92.1	85.7	85.3
3277	52 5	31.33476	309 29 +41 42	.348	.787	50.70	-0.9	108.9	108.9	108.9	98.4	92.6	92.6
3286	52 5	25.22660	273 10 -33 20	.031	.102	41.37	+1.1	99.4	99.4	99.4	98.2	95.1	95.1
3288	52 5	24.28819	229 46 -34 47	.281	.377	21.02	+1.5	86.4	85.7	83.8	78.6	77.0	77.0
3295	52 5	23.40982	261 15 -6 14	.333	.727	32.27	+1.1	101.3	101.3	100.3	91.5	89.4	89.3
3299	52 5	23.35833	252 9 -7 37	.431	.749	29.05	+1.0	101.1	99.1	97.9	92.6	88.1	88.1
3303	52 5	22.28093	222 28 -4 41	.390	.779	17.33	+2.2	85.7	84.1	83.7	83.0	77.0	77.0
3307	52 5	22.27047	225 15 +61 25	.140	.871	19.24	+1.2	93.7	93.3	93.5	81.5	80.5	80.5
3312	52 5	22.25789	193 39 +61 75	.090	.812	16.57	+2.1	91.7	89.1	84.6	84.0	80.0	80.0
3327	52 5	21.36274	257 10 -23 5	.222	.950	35.96	+1.3	100.8	100.8	100.2	95.6	93.3	93.3
3332	52 5	21.34855	242 6 +10 57	.617	.900	24.60	+0.4	93.9	93.9	91.7	80.4	76.1	76.1
3334	52 5	21.32504	283 31 +14 14	.174	.807	53.57	-0.6	112.9	110.4	113.2	102.2	94.0	91.8
3340	52 5	21.30844	306 47 +14 43	.299	.498	62.80	-0.9	102.9	102.9	103.9	91.7	89.6	88.7
3342	52 5	21.31213	218 52 -29 33	.388	.397	19.54	-0.7	86.5	85.8	84.9	76.0	74.4	74.4
3344	52 5	21.21701	209 56 +68 31	.392	.809	19.25	+2.3	93.5	93.5	90.3	89.2	85.4	85.3
3355	52 7	19.41152	3 316 58 -16 7	.504	.605	34.28	+0.9	89.5	89.5	89.1	86.5	83.1	81.6
3360	52 7	21.35983	5 334 8 -16 59	.291	.631	44.34	-0.8	92.1	91.6	92.3	90.0	85.7	85.6
3377	52 7	24.34757	10 22 +36 40	.552	.755	65.33	-0.8	117.8	111.9	117.6	97.1	93.9	93.8
3379	52 7	24.36850	1 302 28 -7 43	.385	.683	24.84	+1.0	96.3	96.3	96.0	92.3	88.2	88.0
3386	52 7	25.27043	1 303 34 -7 19	.147	.755	24.72	+1.0	94.0	94.0	91.9	88.5	85.7	85.7
3393	52 7	25.42131	311 11 +20 42	.309	.822	36.05	+0.6	98.6	98.6	100.1	90.5	85.6	85.6
3399	52 7	25.44425	5 336 45 -16 14	.517	.613	43.05	+0.1	97.3	96.9	96.1	93.4	86.1	86.1
3405	52 7	26.22340	1 304 9 -7 47	.036	.674	26.10	-1.7	97.1	97.0	95.8	85.0	80.7	80.7
3407	52 7	26.25526	3 320 19 -15 13	.082	.554	35.16	-0.9	92.2	92.2	92.4	91.3	87.4	87.4
3411	52 7	26.27789	1 305 23 -9 48	.035	.731	24.47	+1.5	94.0	94.0	93.5	89.0	87.9	87.9
3416	52 7	26.35994	1 305 19 -8 11	.339	.701	25.34	+1.0	96.5	96.2	96.5	91.0	88.3	87.5
3424	52 7	27.27810	5 336 39 -15 43	.008	.490	43.23	-1.4	102.0	100.5	105.6	91.6	88.9	88.9
3450	52 7	28.31172	5 339 36 -15 29	.068	.572	42.71	-0.7	96.8	96.7	98.2	92.3	89.3	88.9
3463	52 7	28.31997	5 338 1 -15 1	.118	.607	43.42	-0.8	102.4	102.4	102.0	92.6	90.8	88.8
3487	52 7	29.42639	5 341 20 -15 9	.466	.655	41.82	+0.1	97.7	97.7	97.4	92.7	87.8	87.8
3497	52 8	4.46209	271 57 +76 46	.072	.488	28.17	+0.5	92.3	92.3	92.4	92.1	87.4	87.1

TABLE 1.1.—Basic physical data for 413 Super-Schmidt meteors: Trajectories.—Continued

Tr-ill No.	L _A o	L _B o	D	n _A	n _B	ΔM	Vis.A	Vis.B	C.I.	ε _∞	m _∞	m _{∞1}	log σ	x	W	B	Rem.
2961	4.7	8.3	.68	C	40					+5.45	2.3889	.37000	-11.09	+3.6	1Q	0	
3000	8.5	7.9	.42	22	22	3.7	-2	+1	-1.7	-2.263	0.0891	.01380	-11.15	+2.8	1	0	
3024	19.4	21.5	.70	35	33	1.8	+2.5	+1	-1.0	-5.17	0.0187	.00290	-11.47	+3.6	0	0	
3037	18.0G	13.8G	.97G	40	32	2.2	+2.5			-1.170	0.0626	.00970	-10.52	+2.97	2	2	
3053	6.5	9.7	2.02	109	113	4.1				+0.099	6.7148	1.04000	-10.96	-.02	1.5Q	0	
3072	5.1	6.7	.45	20	22	3.8				-4.457	0.1201	.01860	-11.45	+3.9	1	1	
3074	15.7	15.3	.53	31	29	2.8		+2	-2.8	-1.154	0.0839	.01300	-11.23	+1.5	0	0	
3076	7.6	4.9	1.33	70	80	2.4				-3.89	1.9370	.30000	-11.29	+2.5	0	0	
3088	11.8	10.5	1.01	58	57	1.8	+3		-1.8	-5.83	0.3164	.04900	-11.12	+0.7	1	0	
3217	4.2	3.8	.30	16	17	3.2		+2	-2.3	-4.442	0.0646	.01000	-10.93	+2.3	0.3	1.5	
3228	4.8	5.2	.48	25	27	1.5		+1.5	-0.2	-9.46	0.0336	.00520	-11.20	+3.1	0	0	
3234	4.9	5.4	.47	25	24	2.5	+2.5		-2.2	-6.76	0.1808	.02800	-11.14	+0.2	0	1	A
3250	8.3	7.6	.70	41	32	2.3		+1.8	-0.8	-7.85	0.1388	.02150	-11.24	-.13	1	0	
3265	11.7	8.1	.54	32	23	2.4		+1	-0.8	-4.99	0.0904	.01400	-11.38	+4.4	0	2	
3271	10.7	11.7	.52	28	29	4.0	-1	+1	-1.5	+0.034	0.2066	.03200	-11.08	-.07	1	0	
3277	8.7	8.8	.42	25	22	3.7	+2		-2.6	-2.79	0.0814	.01260	-11.42	+0.0	0	0	
3286	16.5	15.3	.94	54	35	1.3	+1.5	+2	-0.5	-2.14	0.0968	.01500	-11.57	+4.1	1	2.5Q	
3288	13.2	12.2	1.20	63	50	1.8				-6.41	0.5036	.07800	-10.63	+8.6	0	0	
3295	7.8	7.5	.52	28	28	2.0		+1.8	-0.6	-9.18	0.0749	.01160	-11.15	+0.0	0	0	
3299	5.7	5.9	.61	26	29	2.0		+2	-1.1	-8.45	0.1207	.01870	-11.05	+0.0	0.5Q	0	
3303	4.8	3.3	.65	27	14	1.1		+2	-0.1	-1.089	0.3164	.04900	-11.20	+3.0	0	0	
3307	6.1	4.6	.81	42	45	2.0		+1.7	-0.7	-6.63	0.6457	.10000	-11.29	+3.4	0	0	
3312	5.3	2.6	.92	38	46	1.3	+2		-0.1	-9.34	0.5863	.09080	-11.42	+3.0	0	0	
3327	5.4	5.8	.38	24	18	1.7		+1	+0.4	-1.039	0.0400	.00620	-11.17	+3.0	0	0	
3332	5.1	3.0	.82	47	39	2.4		+2	-1.5	-6.43	0.3293	.05100	-11.14	-.29	0	0	
3334	6.3	7.4	.49	0	24	3.4				-3.66	0.0563	.00872	-11.24	+0.9	1	2	
3340	11.5	12.7	.46	24	25	3.1	+0.5	+1.3	-1.7	-2.14	0.0491	.00760	-11.57	+4.1	1	2.5	
3342	14.0	12.1	1.56	87	84	4.1	+1.3	+1.8	-2.4	+0.084	3.4420	.53310	-11.06	+4.7	2	0	
3344	3.2	3.2	.54	21	28	1.5	+2		+0.2	-1.296	0.1550	.02400	-10.83	-1.4	0	0	
3355	3.9	3.8	.40	20	16	2.6				-1.199	0.0426	.00660	-11.74	+2.5	0	3	
3360	3.0	4.4	.22	14	13	4.0		+1	-1.8	-5.29	0.0730	.01130	-11.70	+2.4	0	2	S
3377	5.8	6.0	.38	23	21	3.7	0	+1.5	-1.5	-3.03	0.0362	.00560	-11.22	+3.2	0.3	0	
3379	5.1	3.8	.51	28	17	2.5	+2.3	+3	-1.7	-8.19	0.2002	.03100	-10.83	+5.5	1	2	
3386	2.0	2.6	.45	27	18	2.5	+2		-0.9	-1.024	0.1324	.02050	-11.06	+0.9	0	0	
3393	7.2	7.2	.45	24	25	2.3	+1.5	+2	-1.2	-7.10	0.0839	.01300	-11.27	+4.1	0	1	
3399	4.7	3.8	.44	25	15	2.5	+2.3	+3	-2.0	-7.722	0.0484	.00750	-11.50	+3.1	0	3	A
3405	10.3	12.2	.95	56	50	5.0	-1		-1.1	+4.460	3.3574	.52000	-11.28	+3.1	3	0	
3407	3.3G	4.7	.25	7	16	3.6		+2	-2.5	-5.88	0.1201	.01860	-10.82	+0.9	0	0	S
3411	3.4	2.2	.35	20	9	1.9	+3		-1.5	-1.164	0.1020	.01580	-11.24	+0.5	0	0Q	
3416	1.4	6.3	.54	8	26	2.2		+1.5	-0.5	-7.78	0.2066	.03200	-10.85	+4.2	0.5Q	1.5	
3424	12.6	13.0	.62	35	34	3.9	+0.5	+0.5	-2.0	+1.25	0.3357	.05200	-11.26	+6.7	0	1.5	
3450	5.5	6.8	.29	14	17	3.3	0	+2	-1.7	-4.67	0.0878	.01360	-11.38	+7.4	0	2	
3463	7.4	8.1	.52	26	23	3.6		+1.5	-2.2	-4.07	0.0968	.01500	-11.33	+5.8	1	2.5	
3487	4.2	4.1	.37	21	17	3.2	+1.5	+3	-2.0	-7.50	0.0510	.00790	-11.50	+3.0	0	1.5	
3497	4.0	6.1	.38	16	23	2.5		+2.5	-2.0	-8.446	0.1291	.02000	-10.83	+5.5	0	2	A

TABLE 1.1.—Basic physical data for 418 Super-Schmidt meteors: Trajectories.—Continued

Trail No.	Date	Sh.No.	Apparent radiant α , δ		sin Q	cos Z_R	v_{∞}	M_{pm}	H_B	H_{ED}	$H_{2.5}$	H_{ML}	H_{ED}	H_E
3567	52 8 15.32162	1	326 21	-11 18	.427	.717	26.85	+0.3	100.1	99.4	98.8	90.3	87.2	86.0
3573	52 8 15.37878		350 27	+5 0	.462	.886	36.80	-1.6	100.3	100.3	99.5	83.6	81.0	81.0
3604	52 8 18.25543		277 28	+65 9	.309	.781	31.01	-0.3	103.7	103.7	105.2	96.4	93.3	93.2
3610	52 8 18.34726		352 14	+2 10	.134	.856	41.56	+0.2	100.9	99.1	97.5	91.5	85.9	84.8
3612	52 8 18.35793	7	52 20	+61 5	.322	.651	58.71	-0.3	112.2	111.2	112.4	100.1	96.3	96.3
3629	52 8 18.46233	20	345 34	-2 25	.329	.614	34.20	+1.4	100.6	99.9	100.2	93.7	89.0	88.7
3633	52 8 20.21140	120	275 50	+58 7	.255	.806	23.91	+0.8	99.1	98.4	95.3	86.0	82.2	82.2
3636	52 8 20.24167	1	324 19	-11 5	.121	.694	23.46	+0.1	99.5	99.5	98.8	83.0	77.1	77.1
3640	52 8 20.27477		273 28	+15 36	.355	.697	15.59	-2.0	87.8	87.8	90.9	74.3	67.0	67.0
3643	52 8 21.19139	1	329 22	-4 45	.083	.620	27.00	+1.6	99.2	99.2	99.7	92.8	89.1	89.1
3651	52 8 21.29165	1Q	329 3	-8 55	.439	.750	25.12	+0.8	92.1	91.7	91.5	89.0	81.0	79.9
3655	52 8 21.30888	1Q	323 3	-2 19	.543	.806	26.74	+0.3	100.8	100.8	98.2	83.1	82.1	82.1
3657	52 8 21.40200		68 0	+66 55	.280	.657	55.84	-0.1	107.4	107.4	107.5	99.8	97.1	97.1
3663	52 8 21.46684		349 10	+0 56	.408	.638	30.35	+0.5	101.2	101.2	101.2	87.2	84.3	84.3
3784	52 8 22.24496	3	353 1	-8 53	.055	.544	37.50	-0.6	96.7	96.0	97.0	93.0	89.9	89.3
3786	52 8 22.27604		333 2	-14 2	.278	.676	21.28	-0.3	89.2	89.2	88.6	85.1	80.2	80.2
3813	52 8 25.44441	120	266 58	+65 18	.107	.313	23.11	+1.6	98.1	98.1	97.7	94.0	89.9	89.9
3847	52 8 30.36452		51 27	+63 29	.283	.730	59.03	-0.2	96.2	96.2	97.1	92.4	89.0	89.0
3861	52 8 30.46355		18 29	+61 21	.241	.851	52.24	-2.4	111.1	111.1	111.4	89.7	88.2	87.9
3877	52 8 31.47361		4 56	+6 32	.314	.719	25.95	+1.2	100.0	100.0	98.9	88.1	84.8	84.8
3886	52 9 1.47897	2	356 18	+0 35	.292	.549	29.16	+0.7	101.5	101.5	101.4	88.5	83.4	83.4
4103	52 6 1.37781		242 11	+43 0	.266	.860	18.98	+2.3	90.9	90.9	88.9	85.5	83.8	83.8
4111	52 6 14.19977		227 52	-21 46	.414	.584	16.82	-0.8	85.7	85.7	84.2	74.6	72.7	72.6
4125	52 6 19.30147		244 39	+30 16	.427	.934	18.37	+1.3	84.0	84.0	83.3	77.7	74.8	74.7
4136	52 6 21.41546		319 53	+35 31	.147	.993	53.45	-1.2	108.5	108.5	109.1	91.8	89.6	89.3
4138	52 6 21.42265		5 37	+18 32	.327	.677	68.79	-0.6	113.4	113.4	114.3	102.6	95.7	95.7
4141	52 6 22.18470		191 15	+59 50	.099	.795	16.92	+0.3	83.7	83.7	83.6	79.8	76.6	75.0
4143	52 6 22.19380		275 39	-7 15	.198	.550	29.90	+1.4	99.5	99.5	97.0	90.6	86.7	86.6
4147	52 6 22.22390		264 44	-14 6	.086	.635	22.70	-1.9	86.3	86.3	86.3	77.5	70.9	70.9
4151	52 6 22.38093		3 32	+12 24	.229	.493	70.97	-0.7	111.7	111.2	121.3	95.9	95.3	95.3
4153	52 6 23.28640		259 3	-13 1	.393	.689	20.58	+0.1	95.2	95.2	95.5	86.4	83.9	83.9
4181	52 6 25.22210		277 37	-8 42	.058	.632	30.45	-1.6	101.3	101.3	103.0	87.4	86.5	86.2
4199	52 6 29.43208		300 49	-14 34	.466	.602	32.12	+1.5	98.9	98.9	96.8	88.4	86.2	86.2
4216	52 8 25.26884	7Q	43 14	+59 32	.332	.539	60.51	+0.2	109.6	109.5	110.2	102.9	94.0	94.0
4229	52 9 19.20433		218 59	+74 45	.123	.458	34.18	+1.0	103.8	103.8	103.5	97.4	92.0	92.0
4289	52 9 10.15042		315 57	+1 54	.114	.812	18.82	+0.5	90.8	90.3	90.0	82.8	76.4	76.4
4311	52 9 13.27009		347 13	-26 8	.167	.518	20.13	-1.1	86.7	86.0	86.0	85.3	82.4	82.4
4313	52 9 13.32250		308 20	+12 50	.363	.612	15.37	+1.6	83.4	83.4	81.7	76.4	73.3	73.0
4328	52 9 14.21329		341 11	+13 20	.423	.904	25.81	-0.3	94.0	92.5	91.4	79.8	77.2	77.2
4330	52 9 14.23858		57 15	+51 41	.253	.467	64.16	-2.5	115.9	115.9	118.4	108.3	98.5	98.5
4340	52 9 14.31121		352 54	-11 8	.553	.720	22.74	+0.0	100.0	98.1	99.3	86.5	82.2	82.2
4351	52 9 14.37389		4 22	-13 9	.570	.665	24.98	+0.3	92.4	92.4	91.4	84.9	80.7	80.6
4360	52 9 16.15238		10 42	+45 49	.326	.609	45.40	+0.1	95.5	95.5	97.4	90.3	86.4	86.4
4369	52 9 16.33235		353 11	+7 5	.430	.875	26.73	+1.1	101.0	101.0	98.9	85.6	83.4	83.4
4388	52 9 17.27972		316 53	-0 54	.530	.697	16.02	+1.6	83.5	83.5	82.2	75.0	72.1	72.1

TABLE 1.1.—Basic physical data for 413 Super-Schmidt meteors: Trajectories.—Continued

Trail No.	L_A o	L_B o	D	n_A	n_B	ΔM	Vis.A	Vis.B	C.I.	ϵ_∞	$m_{=0}$	$m_{=1}$	log σ	x	W	B	Rem.
3567	5.8	7.3	.74	38	34	2.8	0	+1.5	-0.6	-510	0.3293	.05100	-11.12	+62	2.5	2.5	
3573	6.5	8.4	.60	37	36	4.9		+1	-2.8	+073	0.4842	.07500	-11.12	+28	2	0	
3604	5.0	3.4	.44	23	21	3.0	0	+2.5	-1.4	-388	0.2776	.04300	-10.94	+22	00	00	
3610	3.1	4.7	.46	24	20	2.8	+1	+1	-0.8	-781	0.0478	.00740	-11.66	+21	4	1.3	
3612	11.1	1.8G	.43	24	5	2.8	-1	+1.5	-0.5	-414	0.0381	.00590	-11.19	+34	0	0	
3629	9.7	8.1	.55	30	25	1.8	+2	+3	-1.3	-872	0.0710	.01100	-11.23	-16	0	00	
3633	8.0	5.8	.83	42	44	2.9	0	+2	-0.3	-756	0.2738	.04240	-11.20	+05	1	0	
3636	10.3	14.9	1.42	87	46	3.0	+0.5	+1	-1.1	-072	1.4269	.22100	-11.47	+10	0.5	0	
3640	18.8	13.8	2.06G	125	92	5.0	-1	0	-1.5	+750	33.5094	5.19000	-11.19	+21	4	0	F
3643	7.7	7.1	.62	37	28	1.6				-890	0.1324	.02050	-11.13	+56	0	2	
3651	4.9	5.6	.65	35	29	2.2		+2	-1.5	-692	0.2544	.03940	-10.42	+86	0.5	3	
3655	4.8	6.6	.88	52	47	2.8	+1	+1.5	-1.2	-521	0.3422	.05300	-11.23	-01	0	0	
3657	7.8	6.6	.29	17	14	2.6	+0.5	+1.5	-1.1	-628	0.0278	.00430	-11.49	+37	0	0	
3663	8.4	6.6	.89	49	43	2.6	+1.5	+2	-1.3	-432	0.2776	.04300	-11.42	+18	0	0	
3784	7.5	6.6	.37	18	17	3.5	+1	+1	-1.5	-427	0.1433	.02220	-11.13	+54	1	2	
3786	5.3	7.1	.64	39	39	4.0	+1	+1	-1.5	-472	0.7102	.11000	-10.61	+16	1.5	3	
3813	15.1	13.7	1.18	66	63	1.2	+3	+1.9	-0.8	-689	0.3564	.05520	-10.87	-13	1	2	
3847	5.1	5.0	.17	10	11	2.9	+2.3	+2	-2.0	-925	0.0119	.00185	-11.91	+42	0	1.3	S
3861	8.8	9.2	.52	30	28	5.1		0	-2.1	+313	0.2938	.04550	-11.37	+31	1.3	0	
3877	10.4	8.1	.83	46	35	2.1	+1.7	+1	-0.3	-732	0.2221	.03440	-11.24	+06	0	00	
3886	16.7	16.6	1.16	63	67	2.4	+2	+0.5	-0.7	-388	0.3487	.05400	-11.34	-11	0	0	
4103	3.8	2.7	.43	26	24	1.3		+2.3	-0.3	-1340	0.1420	.02200	-11.05	+36	0	0	
4111	6.8	9.7	1.34	76	71	4.7	+0.3		-1.4	+101	5.8109	.90000	-11.04	+33	2	0	
4125	4.5	3.9	.56	29	33	2.5	+2		-1.1	-891	0.4197	.06500	-10.98	+50	0	0	
4136	4.7	2.5	.37	21	22	3.9		+1	-2.1	-212	0.0826	.01280	-11.49	+14	0	0	
4138	7.8	8.4	.38	24	18	3.4	-2	0	-0.3	-445	0.0225	.00348	-11.52	+16	0	0	
4141	6.0	3.5	.70	31	29	3.4		+2	-2.0	-560	1.2138	.18800	-11.10	+44	0	0	
4143	6.7	7.8	.79	38	29	1.5	+2	+1	+0.1	-817	0.1162	.01800	-11.14	+69	0	0	
4147	6.8	11.4	1.08	64	63	5.4	+1	-1	-2.1	+526	5.9400	.92000	-11.16	+23	3	0	
4151	11.8	10.6	.47	28	15	3.0		0	-0.6	-122	0.0420	.00650	-11.32	+50	0	0	
4153	6.2	7.4	.81	37	47	3.4	+1	+1	-1.1	-370	1.0330	.16000	-11.07	+43	2	1	
4181	12.8	10.8	.79	46	40	4.6				+180	1.0847	.16800	-11.22	+44	2	0.5	
4199	6.7	6.7	.67	27	34	1.5				-957	0.0684	.01040	-11.39	+12	0	0	
4216	13.3	12.6	.48	25	21	2.6	+1.5	+1.5	-1.2	-564	0.0245	.00380	-11.28	+13	0	0	
4229	13.0	10.6	.76	40	38	2.2	+2.5	+1.5	-1.0	-686	0.1072	.01660	-11.20	-01	0	0	
4289	6.4	4.7	1.00	54	35	2.6	+1.8	+2.5	-1.4	-442	1.2138	.18800	-11.15	-11	0.50	0	
4311	5.2	4.0	.43	23	20	4.6	+1	+1	-2.2	-427	0.9782	.15150	-10.80	+04	0.5	2	A
4313	8.8	7.0	1.14	65	68	1.6	+1.5	+2	-0.6	-687	1.2267	.19000	-11.00	+24	0	0	
4328	3.9	6.3	.73	39	36	4.1	+1	+2	-1.8	-536	0.3564	.05520	-11.22	+10	1	0	
4330	17.5	18.1	.60	32	31	4.9	0	0	-2.1	+519	0.2518	.03900	-10.48	+41	1.5	1	
4340	5.2	7.3	1.10	59	56	2.6		+0.5	-0.8	-166	1.2590	.19500	-11.36	+15	0	0	
4351	4.2	5.2	.72	38	34	3.2	+1.5	+1	-1.0	-600	0.3441	.05330	-11.14	+01	1	0	
4360	8.2	8.1	.34	21	19	2.6		+1	-1.0	-674	0.0478	.00740	-11.70	+67	0	1	
4369	7.9	7.2	.77	46	36	2.2	+1.5	+1.5	-0.6	-780	0.1827	.02830	-11.27	+03	0	0	
4388	6.8	6.3	1.08	66	52	2.0	+2	+2	-0.9	-724	1.0976	.17000	-10.98	-07	0	0	A

TABLE 1.1.—Basic physical data for 418 Super-Schmidt meteors: Trajectories.—Continued

Trail No.	Date	Sh.No.	Apparent radiant α / δ	$\sin Q$	$\cos Z_R$	v_{∞}	M_{km}	H_B	H_{BD}	$H_{2.5}$	H_{ML}	H_{ED}	H_E
4394	52 9 17.31692		11 8 +2 17	.174	.857	33.85	+0.8	97.5	96.2	95.3	85.6	84.2	83.8
4454	52 9 19.36752		89 29 +43 59	.250	.622	69.05	+0.0	111.6	111.6	114.0	103.8	101.0	101.0
4464	52 9 19.43364		350 48 +10 16	.355	.551	21.89	-0.9	99.9	99.9	98.7	76.2	73.8	73.8
4472	52 9 20.25706	120	262 59 +57 43	.016	.667	23.50	+0.8	101.6	100.9	100.1	91.6	87.7	87.7
4505	52 9 20.37880		359 3 -1 8	.525	.722	25.66	+1.9	101.4	100.2	96.5	92.6	89.2	86.8
4507	52 9 20.38472	20	16 40 +0 15	.636	.820	29.03	+2.0	99.5	98.6	95.8	92.3	86.7	86.5
4513	52 9 20.39448	90	267 31 +58 29	.083	.193	19.30	-0.3	90.3	90.3	90.3	90.2	88.4	87.2
4534	52 9 25.28963		301 42 +72 18	.156	.641	31.78	-1.8	104.7	104.5	104.5	86.9	84.9	84.9
4542	52 9 25.33709		8 6 -3 42	.307	.793	23.86	+1.2	98.1	98.1	95.1	88.5	86.9	86.9
4574	52 9 26.22639	2	23 52 +7 16	.177	.667	28.62	+1.9	103.3	102.1	99.1	95.4	88.5	88.2
4596	52 9 26.36991		326 5 +54 34	.005	.641	22.41	+2.0	94.3	94.3	91.9	88.0	81.5	81.5
4618	52 9 27.28448		357 47 -2 32	.298	.817	20.50	+1.9	98.4	97.8	94.9	87.8	85.2	85.2
4622	52 9 27.29697		107 32 +46 49	.203	.277	67.87	+0.3	113.8	113.6	115.1	108.6	106.6	106.6
4624	52 9 27.30209		344 37 -0 5	.529	.774	18.57	+0.9	95.2	95.2	93.0	86.9	82.8	82.8
4645	52 9 27.40903		62 15 -5 42	.114	.756	58.85	-1.1	111.5	109.2	112.5	96.7	93.0	91.6
4657	52 9 27.46457		6 50 -5 24	.317	.372	23.79	+0.8	100.9	100.9	99.3	87.2	82.9	82.8
4659	52 9 27.46431		16 42 -4 30	.387	.501	18.16	+0.4	87.4	87.4	86.5	82.4	80.5	78.9
4677	52 9 28.38340		260 20 +85 16	.149	.484	41.15	-0.5	109.0	108.3	109.5	96.6	92.4	91.8
4679	52 9 28.39461		340 4 +2 43	.274	.426	17.50	-0.2	95.8	95.8	93.6	85.2	82.9	82.2
4683	52 9 28.41338		110 36 +48 5	.433	.669	67.16	-1.2	114.2	114.2	114.5	105.1	97.3	96.2
4701	52 9 30.48305	2	25 44 +5 53	.414	.589	30.01	+1.5	99.7	99.4	97.8	89.8	83.8	83.8
4702	51 9 24.14407		313 56 +70 27	.288	.787	31.62	-2.1	101.3	101.2	102.8	89.5	83.9	82.4
4952	52 10 19.44153		62 2 +7 31	.564	.866	11.49	+1.4	77.2	77.2	75.1	73.0	69.7	69.7
4962	52 10 21.20082		339 16 +46 18	.058	.949	21.65	+0.0	97.0	97.0	96.9	89.1	81.7	80.7
4964	52 10 21.20117		292 45 +28 44	.246	.601	15.92	+1.7	92.5	92.5	91.2	88.0	83.4	83.3
4966	52 10 21.22682		33 24 +6 28	.121	.801	26.29	+1.4	101.9	101.2	98.6	89.4	87.0	87.0
4974	52 10 21.27695	80	94 59 +6 12	.199	.311	67.05	-0.5	117.7	116.7	116.7	103.3	101.5	101.5
5006	52 10 21.34780	8	95 57 +16 2	.185	.692	68.17	-0.3	115.5	115.4	118.0	107.1	99.6	98.0
5022	52 10 21.40054	2	41 14 +11 12	.442	.849	30.13	-0.6	100.5	100.0	101.1	85.3	78.1	78.1
5045	52 10 21.48504		126 25 +84 3	.197	.611	42.42	-1.2	99.9	99.9	101.1	93.9	88.9	88.9
5047	52 10 22.13463		11 43 +0 17	.321	.653	16.26	+0.3	86.5	86.5	85.8	83.0	79.9	79.0
5063	52 10 22.26372	80	103 45 +26 38	.252	.306	70.64	+0.1	118.9	118.9	121.3	109.8	107.1	107.1
5073	52 10 22.29003		330 20 +51 40	.102	.700	20.26	-1.0	102.1	102.1	98.4	80.6	76.8	76.8
5079	52 10 22.31903	8	96 6 +15 56	.205	.584	67.83	-1.1	118.4	118.4	123.3	109.2	103.3	103.3
5083	52 10 22.33811	8	93 52 +16 3	.278	.688	67.27	-2.4	117.6	117.6	120.1	106.8	96.2	96.1
5101	52 10 22.37746	8	95 47 +15 46	.317	.803	67.40	-1.3	116.7	116.0	118.2	111.3	98.2	98.1
5112	52 10 22.43449	8	94 44 +16 43	.739	.937	67.51	-2.3	114.9	114.9	115.2	96.8	90.7	90.7
5124	52 10 22.47095	20	36 20 +9 0	.304	.535	27.88	+0.4	101.4	101.3	101.9	86.2	80.5	80.1
5176	52 10 23.42685	2	44 4 +12 30	.370	.795	30.47	-0.8	102.3	102.3	102.3	84.2	80.1	80.1
5180	52 10 23.44002	17	42 35 +19 39	.149	.783	31.88	-0.6	93.4	93.0	93.3	81.7	80.9	78.7
5195	52 10 23.48194	2	42 23 +12 3	.306	.572	28.92	+0.9	102.1	102.1	102.1	93.0	86.8	86.8
5231	52 10 24.27733	80	99 5 +33 48	.230	.498	67.83	-0.6	116.7	116.7	120.8	102.8	99.4	99.4
5237	52 10 24.30020		32 32 -6 29	.636	.777	28.61	+0.8	102.0	102.0	100.7	88.6	85.1	85.1
5257	52 10 24.38896	17	45 17 +19 35	.360	.924	32.87	-1.7	102.4	102.4	102.1	82.1	79.0	79.0
5273	52 10 24.42539		161 33 +36 48	.239	.410	63.05	-0.8	113.1	113.1	118.2	108.4	104.6	104.6

TABLE 1.1.—Basic physical data for 413 Super-Schmidt meteors: Trajectories.—Continued

Trail No.	L _A °	L _B °	D	n _A	n _B	ΔM	Vis.A	Vis.B	C.I.	ε _m	m ₂	m ₁	log σ	x	W	B	Rem.
4394	3.9	5.9	.48	26	25	2.4	+2	+2	-1.3	-.864	0.0710	-.01100	-10.94	+.51	0	0	
4454	8.0	7.3	.25	16	13	2.3		+1	-0.6		0.0128	-.00198			0	0	
4464	27.3	23.8	2.27	137	129	4.6	+1	0	-1.9	+.388	5.5139	-.85400	-11.48	+.07	1.7	0	F
4472	11.0	8.4	.51	51	52	2.3	+2	+0.5	-0.6	-.602	0.3958	-.06130	-11.01	+.23	1.5	0	
4505	5.7	4.6	.82	34	31	0.9	+3	+2.5	-0.9	-.964	0.1349	-.02090	-11.33	+.12	0	0	
4507	3.7	4.2	.55	31	27	0.9				-1.172	0.0565	-.00875	-11.16	+.34	0	0	
4512	6.3	6.5	.84	33	29	3.5	+2.3	+2	-2.4	-.328	1.4204	-.22000	-11.15	+.32	1	4	A
4534	16.0	15.1	1.00	59	59	4.4	0	0	-1.6	+.331	1.3817	-.21400	-11.27	+.13	1	0	
4542	3.1	4.1	.60	35	29	2.2	+2	+2	-0.9	-.935	0.1814	-.02810	-11.29	+.29	0	0	
4574	8.9	8.6	.80	41	36	1.6	+2.5	+3	-0.9	-.954	0.0981	-.01520	-11.06	+.20	0	0	
4596	10.4	11.1	.92	50	49	1.2		+3.5	-1.6	-.782	0.3190	-.04940	-11.28	-.03	0.5	0	0
4618	4.3	5.5	.80	46	39	1.8	+2	+2	-0.4	-1.023	0.2286	-.03540	-11.12	+.61	1	0	
4622	12.7	11.7	.37	21	22	2.0	+1	+1	-0.4	-.670	0.0136	-.00211	-11.11	+.63	0	0	0.3
4624	3.9	4.9	.88	53	46	2.3	+1.8	+1	-0.7	-.654	0.7296	-.11300	-11.00	+.01	1.5	0	
4645	9.9	10.3	.45	23	22	3.9	+1	0	-1.6	-.124	0.0697	-.01080	-11.36	+.34	0.3	1	
4657	27.3	26.7	2.11	94	85	2.3	+1.5		-0.9	-.161	1.0912	-.16900	-11.24	-.05	0.7	0	
4659	5.2	8.2	.88	44	47	3.2	+1		-0.8	-.548	1.0137	-.15700	-11.45	+1.06	2	3	
4677	18.8	17.2	.87	49	47	3.4	0	0	-0.5	-.107	0.2286	-.03540	-11.19	+.12	1	2	A
4679	17.0	16.1	1.89	104	98	3.9	+2	+1	-1.8	-.209	2.5181	-.39000	-11.06	+.12	3	2	
4683	8.3	7.0	.40	22	20	4.2	+1.8	0	-1.9	-.142	0.0478	-.00740	-10.92	+.37	0.3	0	
4701	8.4	7.5	.92	45	54	1.7				-.753	0.1369	-.02120	-11.36	+.04	0	0	
4702	9.2	10.6	.78	0	38	5.1	-1		-1.2	+.475	1.3240	-.29800	-11.29	+.97	3	3	
4952	3.0	2.5	.79	39	42	2.0				-.995	1.6012	-.24800	-10.88	+.08	0	1.5	
4562	6.6	6.7	.82	40	43	2.5	+1.5	+1.5	-1.4	-.309	0.9039	-.14000	-11.27	-.34	1	0	
4584	6.9	6.6	1.00	48	53	1.5	+2	+2	-0.5	-.784	0.8523	-.13200	-10.92	+.24	1	0	0
4966	7.4	6.7	.72	41	26	2.2	+1	+2	-0.2	-.819	0.1679	-.02600	-10.91	+.37	0	0	0
4974	22.1	23.7	.77	41	43	2.5	+1.5	+1.6		-.002	0.0659	-.01020	-11.24	+.73	0	0	
5006	8.7	8.5	.37	21	19	3.1	+0.5	+2	-1.3	-.511	0.0194	-.00300	-11.04	+.45	0	0	
5022	11.7	10.9	.90	42	42	4.1	+1.5	+2	-2.5	-.025	0.8716	-.13500	-11.31	-.12	1	0	
5045	9.2	8.4	.44	24	21	4.1	+1	+1.2	-2.1	-.235	0.1550	-.02400	-11.20	+.60	0.5	1.5	
5047	3.4	4.0	.73	37	32	3.4		+3	-2.0	-.855	0.7231	-.11200		+.17	0	3	
5063	15.9	17.2	.55	28	32	1.9	+1	+1	-0.5	-.471	0.0194	-.00300	-11.18	+.53	0	1	
5073	17.1	11.5	1.82	104	106	4.9	-1	0	-0.9	+.290	4.9070	-.76000	-11.04	+.02	3	0	F
5079	8.5	12.0	.38	17	23	3.4	+1	+1.8	-1.9	-.221	0.0387	-.00600		+.60	0	0.3	
5083	9.5	11.1	.46	26	25	5.0	+0.5		-2.1	+.319	0.1356	-.02100	-10.96	+.33	0.7	0.7	A
5101	6.5	8.2	.34	20	20	4.2	+1	+1.8	-2.2	-.260	0.0355	-.00550		+.46	0	1.3	A
5112	2.9	4.9	.39	22	24	5.1	0	0	-2.1	+.107	0.0859	-.01330	-11.73	+.14	2	0	A
5124	23.0	16.4	1.50	85	66	2.5	+1	+1.5	-1.0	-.120	0.7748	-.12000	-11.40	-.31	0	0	
5176	12.4	12.3	.90	53	53	4.0	+1	+2	-2.3	-.015	0.7231	-.11200	-11.26	-.02	0	0	
5180	6.7	6.8	.60	25	30	3.8		+2	-2.7	-.401	0.2518	-.03900	-11.41	+.68	1	2	
5195	13.6	13.4	.95	45	55	2.3	+2	+2	-1.2	-.474	0.2905	-.04500	-11.30	+.02	0	0	
5231	13.9	15.9	.52	31	27	2.2	+1	+1	-1.2	-.122	0.0484	-.00750	-11.03	+.41	0	0	
5237	3.6	5.1	.77	46	42	2.2	+4	+2	-2.2	-.652	0.1937	-.03000	-11.22	+.17	0	0	
5257	9.5	8.1	.78	43	41	4.9	+1	+1	-2.8	+.257	1.0589	-.16400	-11.15	+.26	1.3	0.3	A
5273	7.4	10.1	.34	15	20	2.7				-.263	0.0433	-.00670	-11.39	+.75	0	0.3	0

TABLE 1.1.—Basic physical data for 418 Super-Schmidt meteors: Trajectories.—Continued

Trail No.	Date	Sh.No.	Apparent radiant α , δ		$\sin Q$	$\cos Z_R$	v_s	M_{pm}	H_B	H_{BD}	$H_{2.5}$	H_{ML}	H_{ED}	H_E
5289	52 10 24.49407		159 53	+7 41	.223	.539	63.40	+0.2	110.5	110.5	115.1	102.8	98.7	98.7
5332	52 11 7.09028		17 41	+41 42	.375	.797	23.08	+1.1	92.8	92.5	92.4	82.2	77.7	77.7
5346	52 11 11.21208	2	56 51	+15 4	.274	.790	28.75	+0.7	102.3	102.3	100.4	87.7	83.8	83.8
5370	52 11 12.18972		341 20	+23 57	.409	.876	15.58	+1.3	75.8	75.6	74.8	73.9	67.3	67.3
5450	52 11 15.48622	13	152 8	+22 47	.435	.885	71.73	-3.3	127.8	127.8	125.9	89.1	87.2	87.2
5472	52 11 19.50249		180 2	+67 54	.394	.712	46.75	-1.2	104.7	104.7	105.3	92.0	89.5	85.4
5511	52 11 21.44139	17	67 3	+21 56	.287	.750	31.00	-0.2	104.9	104.5	105.4	81.9	80.8	80.8
5551	52 12 9.25420		133 25	+31 40	.261	.518	60.76	+0.6	112.6	112.6	113.4	104.8	100.2	100.2
5557	52 12 9.27326		68 47	-7 24	.192	.767	22.67	-0.6	99.5	99.5	98.3	82.2	78.7	78.7
5572	52 12 10.21182		3 18	+53 12	.146	.788	17.19	+1.4	92.7	92.5	89.4	80.2	77.8	77.8
5601	52 12 11.19612	4	108 49	+33 7	.301	.579	36.66	+0.4	100.7	100.7	100.5	93.0	88.5	88.5
5605	52 12 11.21585	4	109 31	+32 44	.366	.658	36.18	-2.7	101.3	101.3	101.4	82.3	74.6	74.5
5640	52 12 12.21300	4	109 32	+32 39	.318	.657	37.13	+0.9	101.4	101.2	100.0	92.6	90.6	90.6
5644	52 12 12.22909	4	110 27	+32 10	.390	.705	35.56	-0.4	99.2	98.8	99.2	88.7	84.6	84.6
5648	52 12 12.23334	4	110 37	+32 49	.438	.722	36.21	-0.7	107.1	107.1	107.8	89.0	84.4	83.2
5688	53 3 20.39372		265 26	-5 54	.125	.450	68.64	-5.7	114.4	114.4	115.3	84.1	78.6	78.61
5759	52 12 13.14203	4	110 28	+33 9	.273	.362	36.41	+1.0	100.8	100.8	100.6	94.0	92.1	92.1
6062	53 1 10.13459		58 53	-23 57	.191	.629	15.33	+1.2	84.6	84.6	84.3	82.0	80.0	79.9
6093	53 1 13.39400	10Q	250 16	+43 19	.279	.234	43.50	+0.7	107.9	107.6	107.8	106.0	102.8	102.8
6095	53 1 13.41927		220 37	+43 44	.322	.639	29.73	-0.3	95.0	95.0	95.3	89.5	82.2	82.2
6105	53 1 13.46463	10Q	242 45	+35 58	.344	.553	43.95	+0.7	101.8	100.2	100.9	96.3	85.9	85.9
6218	53 1 16.44630		210 45	-0 49	.113	.625	72.78	-1.4	115.2	115.2	115.9	100.8	96.3	96.3
6275	53 1 20.31662		198 17	+29 21	.297	.494	61.60	-1.1	113.0	113.0	114.6	103.9	96.4	96.4
6329	53 1 23.38956		120 52	+15 34	.412	.810	22.70	+1.7	95.8	95.7	93.8	86.3	84.4	84.4
6376	53 2 5.14883		145 35	+13 24	.260	.486	31.67	-0.1	102.2	101.4	102.2	93.4	89.2	88.6
6398	53 2 10.27808		142 52	+38 29	.412	.985	27.35	-2.9	104.9	104.1	104.9	74.4	69.0	68.8
6429	53 2 12.47257		175 36	+10 3	.652	.814	35.40	-0.1	92.4	92.4	92.9	85.7	78.8	78.8
6433	53 2 12.49419		236 35	+9 55	.101	.856	66.06	-0.7	113.2	113.2	114.5	97.5	90.8	90.8
6437	53 2 12.50608		217 24	-29 36	.226	.468	71.07	-0.6	115.8	115.8	117.8	106.6	100.8	100.8
6491	53 2 18.40527		159 11	+49 2	.157	.894	22.69	+0.4	90.3	90.3	90.8	80.9	74.2	74.2
6546	53 2 21.46448		254 51	+9 5	.207	.690	64.45	-0.6	108.0	108.0	108.3	94.5	90.4	90.4
6795	53 3 12.22319		130 27	+78 35	.274	.690	17.39	-0.1	85.7	85.7	85.8	84.0	82.4	82.4
6802	53 3 12.27808		234 58	+22 35	.238	.446	54.84	+0.9	109.0	109.0	109.4	102.9	99.5	99.5
6811	53 3 12.30740		217 12	-21 26	.013	.371	61.25	+0.9	100.4	100.4	100.7	96.9	92.3	92.0
6842	53 3 13.38101		218 52	-24 9	.111	.512	57.90	+0.5	109.6		110.6	101.7		97.4
6882	53 3 14.30065		140 37	+61 1	.346	.815	12.72	+2.2	78.3	78.2	73.7	68.7	67.4	67.4
6904	53 3 14.44660		294 56	-0 46	.176	.301	59.86	+0.8	110.3	110.3	112.2	105.1	100.1	100.1
6915	53 3 18.21645		172 4	+30 6	.566	.928	20.36	+2.2	91.8	91.8	90.3	88.5	83.5	83.5
6932	53 3 18.34978		239 28	+57 57	.248	.773	31.77	+0.3	100.5	99.7	99.8	91.1	87.1	85.8
6949	53 3 18.43249	11Q	185 6	+6 58	.442	.711	27.07	-0.5	101.4	100.7	99.4	82.9	76.9	76.6
6959	53 3 18.47712		307 24	+23 34	.276	.520	48.71	-0.5	109.4	109.4	110.9	96.6	91.1	91.1
6961	53 3 19.22288		123 59	-44 50	.282	.159	20.12	+0.8	94.0	94.0	93.9	91.3	90.1	88.1
6971	53 3 19.31853		176 35	+26 51	.675	.988	21.60	+1.9	86.6	85.9	84.3	81.0	78.6	78.6
6992	53 3 19.39518		174 54	+21 8	.450	.821	24.68	+2.1	99.8	97.5	90.8	87.4	82.8	82.7
6998	53 3 19.43246		176 30	-6 28	.378	.489	30.25	+1.3	104.3	104.0	102.5	96.1	90.8	90.1

TABLE 1.1.—Basic physical data for 413 Super-Schmidt meteors: Trajectories.—Continued

Trail No.	L_A o	L_B o	D	n_A	n_B	ΔM	Vis.A	Vis.B	C.I.	ϵ_m	m_{∞}	$m_{\infty 1}$	log σ	χ	W	B	Rem.
5289	9.2	9.7	.35	21	19	2.4	+1	+2.5	-1.3	-.582	0.0207	-.00320	-11.36	+.58	0	0	
5332	9.8	10.0	.85	49	44	1.6	+2	+1.5	-0.9	-.671	0.3725	-.05770	-11.24	+.01	0	0	
5346	9.7	11.3	.83	49	44	2.5	+2	+2	-1.4	-.658	0.1918	-.02970	-11.30	+.05	0	0	
5370	5.8	5.1	.65	37	37	2.1	+1	+3	-1.1	-.955	0.6231	-.09650	-10.94	+.54	2	0	A
5450	11.0	13.9	.64	35	32	6.1				+.719	0.2893	-.04480	-10.99	+.37	40	0	
5472	11.3	10.0	.60	26	26	4.5	0	+0.5	-1.5	-.057	0.1756	-.02720	-11.30	+.16	1.5	2	
5511	14.8	12.2	1.05	61	56	3.0	+1.5		-1.6	-.168	0.4720	-.07310	-11.40	-.10	0	0	
5551	10.2	8.2	.40	21	20	1.9	+2.5		-1.5	-.803	0.0142	-.00220	-11.21	+.41	0	0	
5557	4.3	8.5	1.22	71	61	3.9		+1	-1.6	-.001	1.8337	-.28400	-11.32	+.22	1.7	0	
5572	8.7	5.1	1.15	64	61	2.0	+3	+2.5	-1.6	-.769	0.7683	-.11900	-11.08	+.00	0	0	
5601	11.2	10.6	.58	34	31	2.9	+1	+2	-1.2	-.615	0.0988	-.01530	-10.79	+.09	0.3	1	
5605	20.7	21.8	1.14	67	67	5.9	-1	-1.5	-1.8	+.880	3.2928	-.51000	-11.33	+.08	4	0	
5640	8.0	6.2	.44	20	18	2.2	+2	+2.5	-1.4	-.960	0.0433	-.00670	-11.35	+.52	0	0	
5644	8.2	5.6	.60	33	32	3.5	+1		-1.2	-.414	0.1743	-.02700	-11.11	+.63	1	0	
5648	9.3	10.5	.74	42	38	3.7	+1	+0.5	-1.6	-.155	0.3022	-.04680	-11.01	-.08	2	2.5	
5688	37.16	39.86	1.166	68	65	8.5	+0.5	-5	-1.0	+1.909	5.1007	-.79000	-11.88	+.23	4	00	
5759	14.0	10.9	.67	37	33	2.0		+3	-1.8	-.831	0.0626	-.00970	-11.24	+.44	0	0.30	
6062	3.7	5.0	.58	34	33	2.2	+3	+3	-1.5	-.967	0.6521	-.10100	-11.23	+.84	1	2	
6093	11.3	10.3	.51	29	27	2.2	+2		-1.3	-.721	0.0460	-.00713		+1.06	0	1	
6095	11.4	10.2	.69	40	39	3.2		+3	-3.3	-.360	0.3409	-.05280	-10.89	+.06	0.3	0.3	
6105	14.4	14.0	.67	32	35	2.3	+0.5	+3	-1.1	-.649	0.0553	-.00856	-11.74	+.07	0	1	
6218	12.1	14.1	.42	24	24	3.8	0	0	-1.2	-.171	0.0351	-.00543	-11.36	+.37	0.3	0	
6275	12.9	8.5	.55	34	0	3.6	+2.5	-3.5		-.129	0.0652	-.01010	-11.29	-.11	0	0	
6329	5.2	3.7	.65	38	34	2.0	+2	+3	-1.0	-.960	0.1956	-.03030	-11.29	+.36	0	0.3	
6376	10.8	13.6	.89	44	45	3.4		+2	-2.0	-.239	0.3738	-.05790	-11.08	+.26	2	1.5	
6380	12.7	10.5	1.40	81	75	5.6		0	-3.3	+.940	9.4717	1.46700	-11.60	+.07	2	0	F
6429	5.5	5.4	.48	30	30	2.8	+1.5	+2	-1.9	-.611	0.1130	-.01750	-11.25	+.48	0	0.3	
6433	7.7	10.1	.40	25	23	3.5		0	-0.5	-.356	0.0310	-.00480	-11.50	-.03	0	0	
6437	11.4	12.0	.45	28	25	3.0	+2		-2.1	0.0258	-.00400			0	1		
6491	8.5	7.6	.82	44	49	2.5		+1	-0.9	-.421	0.7038	-.10900	-11.21	+.05	0	0	
6546	10.3	12.6	.40	21	22	2.9		+0.5	-1.0	-.435	0.0275	-.00426	-11.43	+.11	1	1.3	
6795	2.8	2.3	.28	18	17	3.2	+4	+3	-3.5	-.881	0.5488	-.08500	-10.79	+.14	0	0	S
6802	11.0	10.3	.39	23	20	1.4	+2	+1.5	-0.6	-.883	0.0161	-.00250	-11.25	+.60	0	0	
6811	8.7	10.8	.37	22	20	1.7	+3	+2	-1.5	-.875	0.0119	-.00184	-11.97	+.74	0	1	
6842	11.2	12.0	.42	25	25	1.7	+3	+1	-1.4		0.0207	-.00320			0	0	
6882	7.4	4.8	1.12	64	59	1.4	+3.5	+1	-1.5	-1.040	1.0266	-.15900	-11.09	+.15	1	0	
6904	12.7	16.1	.56	28	31	1.1	+2	+1	-0.2	-.644	0.0213	-.00330	-11.38	+.69	0	0	
6915	2.7	3.3	.45	22	27	1.1	+3	+3	-1.0	-1.394	0.1395	-.02160	-10.93	+.59	0	0	
6932	7.0	8.2	.61	30	33	2.4	+2	+3	-2.0	-.567	0.1698	-.02630	-11.06	+.31	0	1.5	
6949	15.5	15.2	1.30	74	72	3.6		+1	-1.7	+.001	1.0647	-.16490	-11.24	+.12	2.3	0	
6959	14.7	16.7	.73	43	42	2.6		+1	-1.4	-.162	0.1233	-.01910	-11.48	+.07	0	0	
6961	17.3	18.5	1.90	50	68	2.6		+3	-2.2	-.071	2.2210	-.34400	-11.97	+1.01	1.5	4	
6971	2.5	2.1	.38	21	20	1.7	+3	+2.5	-1.1	-1.291	0.1098	-.01700	-11.03	+.08	00	0	
6992	8.0	7.6	.87	44	44	1.3	+3	+2.5	-0.8	-1.084	0.1188	-.01840	-11.37	+.04	0	0	
6998	11.7	10.9	.97	45	55	1.5	+3	+2.5	-1.3	-.712	0.1466	-.02270	-11.24	-.07	0	0	

TABLE 1.1.—Basic physical data for 413 Super-Schmidt meteors: Trajectories.—Continued

Trail No.	Date	Sh.No.	Apparent radiant α , δ	$\sin Q$	$\cos Z_R$	v_m	M_{pm}	H_B	H_{BD}	$H_{Z,5}$	H_{ML}	H_{ED}	H_E
7002	53 3 19.44747	210 46	-12 13	.392	-.660	31.40	+1.3	89.8	87.3	89.5	83.3	79.1	79.1
7022	53 3 20.35965	262 2	+56 24	.316	-.652	27.29	+1.1	100.8	100.8	99.9	94.4	88.1	86.4
7026	53 3 20.38008	223 58	+37 5	.778	-.970	39.99	+0.8	101.0	101.0	100.3	95.3	83.5	83.0
7040	53 3 20.45639	190 45	+37 58	.238	-.806	22.15	+0.6	89.1	88.5	87.7	84.3	80.9	80.0
7044	53 3 20.47410	228 34	+30 28	-.544	-.981	44.95	-0.9	108.1	108.1	109.0	96.2	92.8	92.8
7046	53 3 21.35019	158 54	+0 13	-.439	-.658	18.72	+1.1	95.2	95.2	93.7	86.6	84.0	83.9
7052	53 3 21.38915	252 8	+26 0	.318	-.814	54.40	-0.3	110.9	110.9	111.5	104.2	98.6	98.6
7067	53 4 3.13834	173 22	+28 55	.387	-.832	18.58	+0.5	86.5	86.3	86.2	84.9	76.8	76.5
7069	53 4 3.19325	219 10	+48 57	-.322	-.638	27.65	+0.7	90.3	90.3	89.1	83.0	81.7	78.7
7073	53 4 4.17184	205 9	-8 12	-.170	-.366	34.14	+1.7	96.0	95.2	95.3	93.5	87.0	87.0
7075	53 4 4.17230	173 10	+54 39	-.694	-.878	18.04	+1.8	86.4	85.7	83.9	80.8	77.6	76.8
7097	53 4 7.28372	218 13	+8 39	-.269	-.819	32.71	+0.0	103.9	103.5	103.7	93.7	86.7	85.7
7158	53 4 9.37394	193 20	-3 9	-.366	-.686	23.07	-0.7	88.0	88.0	88.0	84.0	81.7	80.9
7161	53 4 9.38246	315 59	+32 56	-.272	-.319	49.19	-2.0	113.9	113.6	113.8	94.0	91.3	90.9
7169	53 4 10.14076	45 31	+55 8	-.052	-.388	18.00	+1.2	86.5	86.5	85.6	84.8	81.3	80.8
7184	53 4 10.27490	197 11	-2 31	-.006	-.813	23.12	+0.6	89.1	88.8	86.3	85.5	76.3	76.3
7188	53 4 10.33836	232 13	+29 37	-.430	-.959	38.93	-1.3	106.0	105.9	105.9	97.5	91.7	89.7
7190	53 4 10.35115	210 2	+27 32	-.831	-.989	29.49	-1.6	106.2	104.4	103.4	83.1	79.9	79.4
7210	53 4 11.18466	111 39	+38 41	-.301	-.784	13.71	+1.5	80.5	80.5	79.2	74.1	72.1	71.7
7216	53 4 11.20551	194 59	-23 40	-.020	-.461	31.89	-1.9	106.8	106.8	106.0	88.9	82.8	82.8
7240	53 4 11.34984	197 17	+3 40	-.409	-.819	21.89	-0.6	86.6	86.4	86.2	83.8	79.2	79.2
7272	53 4 13.38363	216 39	+0 24	-.450	-.815	30.92	-0.9	104.2	104.2	103.8	82.2	81.1	81.1
7277	53 4 13.40978	250 55	-28 8	-.154	-.481	60.68	-0.6	111.8	110.4	112.5	95.5	95.2	95.2
7331	53 4 15.27683	218 8	+34 51	-.485	-.948	25.65	+0.6	86.9	86.3	85.8	78.9	75.9	75.9
7333	53 4 15.28568	212 30	-9 25	-.267	-.721	31.46	+1.3	104.6	104.6	103.6	94.2	90.2	90.2
7339	53 4 15.32599	220 24	-35 44	-.131	-.366	44.63	+1.2	108.3	108.3	109.1	104.2	102.1	102.1
7367	53 4 16.13411	179 44	-8 13	-.028	-.612	21.94	+1.0	94.8	94.8	93.1	87.5	84.4	84.4
7372	53 4 16.15595	187 57	-6 45	-.224	-.626	21.12	+0.7	96.5	94.6	96.5	90.2	87.8	87.1
7388	53 4 16.30122	204 7	-2 19	-.359	-.820	23.51	-0.7	87.5	87.2	87.5	84.5	80.8	80.8
7392	53 4 16.33582	282 19	+64 55	-.275	-.643	27.56	-0.2	93.8	93.8	92.9	86.7	83.0	82.4
7454	53 4 21.44645	346 17	+25 40	-.307	-.323	47.21	+0.1	99.0G	98.7		91.6	89.2	88.6
7474	53 5 5.28417	239 11	-20 46	-.160	-.546	36.83	+0.8	104.5	103.9	104.5	96.1	91.4	91.4
7476	53 5 5.30743	241 43	-14 23	-.171	-.655	33.77	+0.2	105.4	105.4	105.2	90.8	84.9	84.9
7478	53 5 5.30847	233 28	-26 17	-.195	-.513	31.95	+1.4	103.6	102.7	103.5	97.0	91.4	91.4
7480	53 5 6.15238	198 4	-7 10	-.064	-.683	18.91	+0.8	95.2	95.2	93.0	85.9	83.3	83.3
7494	53 5 6.28495	216 6	-11 20	-.151	-.720	21.45	+1.4	90.2	90.2	89.6	85.1	81.1	81.1
7496	53 5 6.29001	232 48	+67 48	-.331	-.810	13.67	+0.7	81.4	81.4	81.4	79.0	77.8	77.8
7499	53 5 6.29997	234 35	-6 49	-.132	-.761	28.11	+0.8	100.9	100.6	99.0	86.4	84.9	84.6
7520	53 5 7.27400	204 27	+3 18	-.593	-.854	18.13	+1.5	92.4	92.4	89.3	83.8	78.5	78.5
7522	53 5 7.27581	239 36	+66 8	-.390	-.807	21.03	+0.0	85.4	84.8	84.2	76.9	75.0	74.2
7524	53 5 7.28445	274 20	+53 54	-.305	-.727	36.11	-1.8	110.0	107.6	109.9	98.0	91.1	87.9
7534	53 5 7.31955	241 3	-11 42	-.164	-.708	35.05	+1.1	92.7	92.3	91.6	87.9	81.9	81.9
7560	53 5 8.26788	251 36	+27 2	-.401	-.850	37.75	+0.2	106.0	105.3	105.4	96.6	91.0	91.0
7562	53 5 8.27766	225 43	-2 0	-.114	-.818	26.43	+1.1	100.0	99.2	98.3	85.6	81.6	81.6
7592	53 5 9.33792	160 22	+35 16	-.155	-.614	13.25	+1.5	91.7					88.0

TABLE 1.1.—Basic physical data for 413 Super-Schmidt meteors: Trajectories.—Continued

Trail No.	L_A σ	L_B σ	D	n_A	n_B	ΔM	Vis.A	Vis.B	C.I.	ϵ_m	m_{∞}	m_{m1}	log σ	x	W	B	Rem.
7002	5.9	7.8	.52	22	24	1.9	+2.5		-1.5	-1.047	0.0607	.00940	-11.07	+.25	0	0	
7022	8.5	7.6	.74	41	42	1.9		+2	-0.8	-.756	0.1769	.02740	-11.15	-.08	0	0	
7026	4.1	2.4	.48	27	28	2.5		+3	-1.6	-.961	0.0355	.00550	-11.41	+.08	0	1	
7040	5.6	3.7	.53	28	25	2.9		+2	-1.5	-.905	0.2937	.03930	-11.02	+.00	0.3	1.3	
7044	4.3	3.7	.35	22	22	3.5		+2.5	-3.1	-.455	0.0768	.01190	-11.46	+.57	0	0	S
7046	7.1	7.6	.94	50	53	2.3				-.750	0.5675	.08790	-11.12	+.48	1.5	0	
7052	5.0	5.9	.28	15	16	2.8	+1		-1.0	-.797	0.0200	.00310	-11.46	+.19	0	0	S
7067	5.3	5.3	.65	37	30	3.3	+2.5	+2	-1.9	-.794	0.5081	.07870	-10.34	+.21	0.5	1	A
7069	10.2	10.4	.70	30	30	2.3	0	+1.5	-0.2	-.644	0.2996	.04640	-12.55	+1.40	0.5	3.5	
7073	6.2	14.6	.72	22	33	0.9		+3	-1.3	-.921	0.0600	.00930			0	0	0W
7075	3.3	2.8	.63	31	31	2.2		+3	-1.5	-1.172	0.2731	.04230	-11.10	+.81	0.3	1.5	
7097	6.7	8.8	.65	36	37	3.0		+2	-1.8	-.517	0.1750	.02710	-11.09	+.25	0.3	0	
7158	4.4	5.3	.46	25	25	3.8	+1.5		-2.0	-.411	0.6392	.09900	-10.86	+.57	1	0	
7161	35.6	36.8	1.49	78	86	4.4	0	-1	-1.2	+.510	0.5604	.08680	-11.45	-.01	1.3	0	
7169	8.3	8.5	.83	45	47	2.1	+2	+2	-0.8	-.803	0.5604	.08680	-10.80	+.36	0.0	1	
7184	2.4	4.5	.70	38	33	2.9		+2	-1.6	-.755	0.2912	.04510	-10.92	+.16	0.70	1	A
7188	5.1	5.3	.44	23	22	4.1	+1.5	+1	-2.2	-.195	0.2195	.03400	-11.13	+.14	2	2	S
7190	5.0	2.7	.93	51	57	5.2	+1	0	-1.9	+.088	0.9820	.15210	-11.33	+.23	1.7	0	
7210	5.3	3.2	.85	48	48	2.0	+2	+2	-1.0	-.836	1.2332	.19100	-10.83	+.21	0.50	0.30	
7216	22.1	26.2	1.64	97	94	4.7		+1	-2.7	+.522	2.1500	.33300	-11.30	+.06	1	0	
7240	4.4	4.4	.42	26	24	4.4	+2	+3	-3.0	-.460	0.6779	.10500	-10.79	+.35	1	0.5	S
7272	10.6	12.0	.93	56	57	4.5				+.000	0.7005	.10850	-11.40	+.07	1.5	0	
7277	8.1	11.3	.56	30	28	3.1		+1	-1.2	-.362	0.0394	.00610	-11.24	+.77	0	0	
7331	4.2	5.1	.47	24	28	2.5	+3		-2.4	-.880	0.1653	.02560	-11.31	+.34	0	0	
7333	5.3	7.4	.64	38	36	1.5	+3	+3.5	-1.9	-.857	0.0936	.01450	-11.18	-.02	0	0	
7339	8.1	8.8	.38	20	24	1.2	+2		-0.6	-.883	0.0297	.00460	-11.05	+.87	0	0	
7367	6.7	8.6	.79	46	46	2.0		+2	-1.0	-.762	0.3409	.05280	-11.12	+.25	0	0	
7372	3.1	5.8	.74	23	30	2.0		+3	-2.0	-.716	0.4139	.06410	-10.80	+1.28	0.50	1	
7388	3.5	4.2	.36	21	20	4.2		+1.5	-2.2	-.582	0.4152	.06430	-11.16	+.64	0.7	0.30	
7392	7.8	8.1	.66	29	35	3.0		+3	-3.2	-.530	0.2964	.04590	-11.18	+.19	0.3	0.5	
7454	12.7	9.9	.69G	37	25	1.9	0	0	+0.2	-.378	0.0820	.01270	-11.69	+.74	1.5	1	
7474	8.9	10.5	.65	37	36	2.2		+1	-0.1	-.609	0.0994	.01540	-11.25	+.12	0	0	
7476	7.0	13.6	.94	47	58	2.7	+1.5	+0.5	-0.8	-.319	0.2583	.04000	-11.34	-.03	0.5	0	
7478	11.6	11.5	.75	42	39	1.2	+2.5	+2	-0.8	-.665	0.1369	.02120	-11.24	+.14	0	0.0	
7480	7.7	8.3	.94	55	46	2.5		+2	-1.2	-.664	0.6831	.10580	-11.06	+.32	1.5	0	
7494	5.1	5.1	.60	37	28	1.7	+3	+1	-0.7	-.899	0.2686	.04160	-10.93	+.12	0	0.0	
7496	2.5	2.3	.33	21	21	2.9	+2.5	+3	-2.1	-1.000	0.8781	.13600	-10.93	+.38	1	1.0	S
7499	3.2	6.4	.78	38	39	2.4		+1.5	-0.6	-.734	0.1769	.02740	-11.32	-.04	0	0	
7520	4.4	4.6	.93	53	52	2.0		+3.5	-2.2	-.846	0.5301	.08210	-11.10	+.02	0	0	
7522	7.0	7.0	.69	35	37	3.5		+1	-1.5	-.447	0.9304	.14410	-11.34	+.74	2	2	A
7524	8.9	12.4	.87	31	38	4.6		0	-1.7	+.152	0.6127	.09490	-10.86	-.02	2.3	2	
7534	5.3	7.0	.46	27	25	2.1		+4	+1.5	-.935	0.0809	.00944	-12.02	+.35	0.3	0.3	
7560	5.1	6.7	.48	27	28	3.2	+2	0	-0.7	-.653	0.0859	.01330	-11.21	+.11	1.3	0	
7562	2.2	6.4	.87	37	49	2.1	+4	+3	-2.2	-.683	0.2376	.03680	-11.37	+.09	0	0	
7592	4.9	5.1		13	10	1.2	+1	+2.8							0.0	4.3	

TABLE 1.1.—Basic physical data for 418 Super-Schmidt meteors: Trajectories.—Continued

Trail No.	Date	Sh.No.	Apparent radiant		sin Q	cos Z _R	v _∞	M _{pm}	H _B	H _{BD}	H _{2.5}	H _{ML}	H _{ED}	H _E
			α °	δ °										
7607	53 5 9.37370		308 51	+68 6	-.293	.682	31.58	+0.2	92.9	92.6	93.0	89.5	84.0	84.0
7635	53 5 12.24694		236 21	-8 32	.108	.679	29.70	+0.4	100.4	100.4	99.2	94.0	87.2	86.8
7637	53 5 12.24918		238 14	-21 42	.009	.509	31.36	-1.7	98.2	98.2	98.3	85.3	80.6	80.6
7664	53 5 13.16918		206 23	+0 46	.113	.791	18.28	+1.1	89.8	89.8	88.0	84.1	77.7	77.7
7666	53 5 13.18491		258 5	+57 14	-.410	.440	14.55	+0.3	84.9	84.9	84.6	82.6	81.1	80.4
7726	53 6 4.20432		261 7	-23 31	.071	.360	30.76	+1.2	96.9	96.9	96.8	92.1	89.1	89.1
7734	53 6 4.24505		213 13	-6 42	.411	.721	15.19	+1.9	81.1	80.1	79.0	78.0	73.4	73.4
7742	53 6 5.17470		299 7	+44 56	-.298	.382	42.39	+0.9	107.9	107.6	107.5	99.0	96.4	95.4
7744	53 6 5.17704		235 12	-12 51	.110	.625	19.76	+1.4	85.9	85.9	85.2	78.1	74.1	73.7
7750	53 6 5.21477		223 33	-12 56	.183	.701	16.83	+1.7	87.2	87.2	85.9	81.3	77.9	77.9
7754	53 6 5.25789		249 10	-7 11	.432	.757	22.01	+0.1	90.4	89.6	88.7	82.6	78.5	77.8
7758	53 6 5.28705		309 43	+4 2	.141	.461	61.82	-0.3	111.1	110.4	113.2	100.9	95.7	95.5
7787	53 6 8.28658		305 42	+41 5	.370	.736	45.68	+1.0	108.0	107.4	106.5	95.6	91.4	90.1
7820	53 6 9.23606		234 32	+43 25	-.255	.982	18.92	-0.4	95.9	94.5	96.3	79.4	74.6	74.6
7838	53 6 9.34633		241 1	+35 48	-.212	.880	16.25	+0.5	85.4	85.4	85.3	79.6	76.7	74.8
7841	53 6 9.38816		343 13	-8 17	.106	.426	70.57	-0.2	112.7	111.7	113.9	102.4	98.1	97.9
7871	53 6 13.35828		271 45	-27 35	-.274	.485	26.06	+0.6	99.8	99.0	98.3	88.6	85.6	85.6
7873	53 6 13.36281		322 11	+11 6	-.238	.764	63.03	-0.4	111.1	110.2	117.0	95.8	91.0	90.9
7882	53 6 13.41612		246 19	+28 56	.125	.650	19.62	+1.0	91.5	91.5	90.0	83.4	78.5	78.1
7902	53 6 16.35285		317 35	-4 35	.004	.661	60.17	-0.2	110.8	110.0	111.8	98.9	95.9	95.7
7929	53 6 20.39857		340 16	-4 57	.015	.639	69.42	-1.8	112.9	111.8	113.0	91.7	90.9	90.3
7944	53 7 6.30795		274 9	-8 2	.414	.736	22.20	+0.5	99.2	99.1	100.8	87.5	80.1	79.8
7946	53 7 6.31827		261 51	+26 37	.798	.894	18.49	-0.7	88.1	87.7	88.2	64.0	49.3	49.3
8012	53 7 15.25842		295 1	+2 58	.087	.837	30.09	-0.6	102.8	102.4	102.5	81.5	79.1	79.1
8017	53 7 15.26933		282 18	-23 6	.186	.565	21.77	+1.6	96.2	94.9	93.7	88.8	85.3	84.9
8054	53 7 16.28712		22 29	+60 18	.198	.451	54.13	-1.5	111.5	110.5	112.3	104.1	96.5	96.1
8068	53 7 16.38349		50 6	+3 14	.218	.104	65.67	+0.5	109.86	109.7		107.2	104.2	103.9
8075	53 7 16.41267	20	321 58	-3 59	.399	.780	37.57	-0.3	97.6	97.2	97.4	86.0	80.6	80.6
8083	53 7 16.43128		357 39	+5 45	.103	.864	65.99	-0.9	113.5	110.8	112.5	94.5	91.7	91.7
8089	53 7 20.36831		283 38	+50 45	.099	.825	31.38	-0.9	105.6	104.8	103.5	94.5	83.1	83.1
8106	53 7 21.39199		324 25	-17 15	.321	.637	29.91	+1.5	98.1	98.1	97.8	89.3	84.6	84.6
8108	53 7 21.40291		335 26	+67 0	.350	.824	44.11	-0.4	106.7	104.9	106.2	95.0	86.8	86.8
8110	53 7 21.41963	3	312 9	-12 11	.325	.594	31.05	+1.4	99.4	99.4	98.4	89.2	85.6	85.6
8113	53 7 23.42250		30 35	+22 9	.401	.760	70.85	-2.2	117.8	117.0	118.5	102.2	94.8	94.8
8127	53 8 3.19528		301 19	+15 54	.228	.832	26.80	+1.8	97.6	97.6	96.4	90.5	86.5	86.5
8143	53 8 4.21589		284 12	+38 58	.726	.994	23.67	-0.4	98.6	98.6	96.7	86.6	82.3	82.3
8147	53 8 4.22409	1	315 26	-7 8	.150	.664	27.52	+1.7	101.5	101.5	100.8	97.9	96.1	96.1
8149	53 8 4.25930	1	310 0	-6 21	.223	.763	24.91	+1.1	98.5	97.9	97.2	91.1	87.8	86.3
8153	53 8 4.29693	7	36 53	+56 0	-.280	.492	60.10	-1.3	111.9	111.9	114.1	99.8	96.4	96.4
8168	53 8 5.24897	50	340 2	-1 13	-.232	.598	42.99	-1.1	99.7		98.2	89.0		84.3
8187	53 8 5.33668	5	343 39	-14 17	-.036	.654	41.61	+0.3	102.5	102.5	101.8	94.8	89.9	89.5
8189	53 8 5.34042		299 8	+5 31	.542	.778	21.65	+2.2	94.1	92.9	89.1	86.8	82.4	82.4
8192	53 8 5.35035		344 0	-13 51	.169	.675	25.48	+1.0	90.6G	90.6		89.1	83.6	83.5
8215	53 8 5.43212		55 24	+82 15	-.277	.601	43.62	+1.3	100.8	100.8	101.7	93.8	86.2	85.9
8224	53 8 5.45574	7	36 42	+56 38	.411	.866	59.70	-0.2	109.3		110.1	100.3		94.8

TABLE 1.1.—Basic physical data for 413 Super-Schmidt meteors: Trajectories.—Continued

Trail No.	L_A °	L_B °	D	n_A	n_B	ΔM	Vis.A	Vis.B	C.I.	ϵ_m	$m_{=2}$	$m_{=1}$	log σ	χ	W	B	Rem.
7607	6.7	7.1	.44	24	25	2.6	+2.5	+3	-2.4	-.732	0.1194	-.01850	-10.82	+.14	0	0	A
7635	5.6	8.4	.69	34	37	2.7	+1	+2	-1.1	-.557	0.2195	-.03400	-11.15	+.11	0	0	
7637	8.8	10.7	1.10	66	47	5.4		0	-1.9	+.368	1.5618	-.24190	-11.04	+.03	3	0	
7664	4.3	6.6	.89	53	42	2.4	+1	+2	+0.0	-.814	0.5772	-.08940	-10.97	-.17	0.30	0	
7666	4.8	4.2	.62	37	36	3.6	+2	+3	-2.0	-.699	1.3688	-.21200	-10.95	+.80	2	3	
7726	8.7	11.1	.70	37	42	1.6		+3	-1.4	-.730	0.1298	-.02010	-11.12	+.46	0	0	
7734	6.1	5.2	.71	39	30	2.0	+1	+3	-0.4	-1.146	0.4197	-.06500	-10.54	+.28	2	0	
7742	15.3	14.8	.78	41	40	1.9		+1	-0.1	-.638	0.0620	-.00960	-11.26	+.34	0.3	1	
7744	5.7	8.3	1.02	57	52	1.9		+2	-0.6	-.759	0.4778	-.07400	-11.25	+.33	0	0	
7750	3.5	5.9	.80	42	44	2.0		+4	+2.8	-1.106	0.3480	-.05390	-10.89	+.30	0	0	
7754	4.4	6.1	.77	40	40	3.4	+1.5	+1	-1.3	-.370	0.8264	-.12800	-10.94	+.11	2	0	
7758	15.8	15.7	.55	26	32	2.4	-1	+2	-0.6	-.282	0.0646	-.00890	-11.13	+.85	0	0	
7787	8.0	9.8	.53	29	27	1.7	+1.5	+3	-1.2	-.461	0.0297	-.00460	-11.38	+.15	0	0	
7820	7.1	3.4	1.17	61	67	4.0	+2	+1	-2.1	-.164	2.1952	-.34000	-11.16	+.17	0.3	0	
7838	4.7	3.9	.79	35	39	3.0	+2.5	+1.5	-2.6	-.561	1.3443	-.20820	-11.25	+.49	0.5	1.5	A
7841	11.1	15.0	.49	25	27	2.5		+0.5	-0.5	-.382	0.0239	-.00370	-11.37	+.47	0.3	0	
7871	12.2	17.0	1.14	50	61	2.0	+2	+0.5	-0.7	-.494	0.3758	-.05820	-11.25	+.39	1	0	
7873	10.2	11.8	.42	25	26	2.0	C	0	-0.2	-.341	0.0368	-.00570	-10.93	+.45	0	0	
7882	7.3	9.1	1.10	41	62	2.3	+2	+2	-1.1	-.576	0.7044	-.10910	-11.10	+.26	1.0	0	
7902	8.2	10.7	.38	20	22	2.3	+1	+1	-1.0	-.473	0.0316	-.00490	-11.29	+.42	0	0	
7929	14.4	16.8	.51	27	29	4.3	-1	-1	-0.7	+.076	0.0717	-.01110	-11.53	+.25	0	0	
7944	8.1	10.0	1.21	52	63	3.1	0	+1	-0.1	-.362	0.8006	-.12400	-11.17	+.15	2	0	
7946	19.7	13.5	2.55	103	147	5.0	-3	0	-1.6	+.517	11.8413	1.83400	-11.47	+.08	4	0	F
8012	10.3	13.1	.97	57	54	3.9	0	0	-0.9	-.002	0.7916	-.12260	-11.55	+.06	1	0	
8017	5.1	9.4	.94	44	48	1.6	+3	+3	-1.5	-.778	0.3422	-.05300	-11.24	+.21	0.0	0	
8054	14.7	7.80	.60	35	16	3.8	0		-0.8	+.100	0.1569	-.02430	-10.07	+.30	0.5	0	
8068	21.46	12.00	.810	44	21	1.7	+1	0	+0.3	-.265	0.0387	-.00600	-11.25	-.01	0	0	
8075	8.2	10.2	.59	31	36	3.3	C	0	-0.4	-.396	0.1530	-.02370	-11.73	+.36	1	1	
8083	5.1	7.6	.35	21	18	3.6	+1	+1	-1.8	-.392	0.0284	-.00440	-11.12	+.02	0	0	
8089	11.8	9.4	.88	50	49	3.7			-1.3	+.030	0.7031	-.10890	-11.06	-.07	2.3	0	
8106	9.4	11.2	.72	41	39	1.3	+4		-2.5	-.776	0.1291	-.02000	-11.29	+.13	0	0	
8108	7.6	4.1	.55	31	31	3.4	0	+0.5	-0.7	-.314	0.1136	-.01760	-11.02	+.02	1	0	
8110	10.4	11.9	.76	39	43	1.3	+4	+1	-1.1	-.743	0.1240	-.01920	-11.31	+.23	0	0	
8113	7.8	7.4	.43	26	21	4.4	0	0	-1.6	+.015	0.0594	-.00920	-11.43	+.04	0.7	0	
8127	5.7	5.4	.50	31	25	1.4	+2.8	+2	-0.7	-1.061	0.0917	-.01420	-11.10	+.40	0	0	
8143	4.1	3.1	.70	42	37	3.7	+3	+1.5	-2.7	-.329	0.7231	-.11200	-11.01	+.52	2.3	0	
8147	1.9	2.9	.30	18	16	1.1	+3		-1.0	-1.214	0.0588	-.00910	-11.26	+.78	0.0	0.0	
8149	2.3	3.0	.65	31	25	1.8		+3	-1.8	-.858	0.1840	-.02850	-10.79	+.37	0.0	0	
8153	13.3	15.4	.52	25	32	3.5	0	0	-1.1	+.089	0.1130	-.01750	-10.93	+.54	0.3	0	
8168	9.1	10.2	.62	36	27	3.9	+1.5	+1	-2.4		0.1433	-.02220			1	2	
8187	8.4	7.6	.48	28	26	2.5	+2		-1.5	-.702	0.0568	-.00880	-11.39	+.31	0	1	
8189	4.9	4.1	.71	37	34	1.8	+3	+3	-1.0	-1.178	0.1440	-.02230	-11.17	+.04	0	0	
8192	4.2	5.1	.41	23	22	2.3	+3		-2.0	-.854	0.1743	-.02700	-10.56	+.33	0	1	
8215	11.2	10.3	.58	32	30	1.5	+2	+1	-0.3	-.781	0.0403	-.00624	-10.90	-.85	0.5	1.3	
8224	5.8	5.4	.28	14	15	2.5	+2		-2.0		0.0194	-.00300			0	0	

TABLE 1.1.—Basic physical data for 413 Super-Schmidt meteors: Trajectories.—Continued

Trail No.	Date	Sh.No.	Apparent radiant α , δ	sin Q	cos Z _R	v _c	M _{pm}	H _B	H _{BD}	H _{2.5}	H _{ML}	H _{ED}	H _E
8238	53 8 6.21211	5	343 19 -14 43	.088	.279	41.26	+0.5	103.7	103.7	104.6	96.0	92.5	92.5
8240	53 8 6.22121		298 19 +35 48	.670	.986	28.77	-0.8	102.0	102.0	101.4	85.6	81.0	81.0
8244	53 8 6.24351		264 18 +25 52	.061	.885	16.50	+1.8	89.2	87.9	87.4	80.0	72.6	72.6
8254	53 8 6.29543	5	342 5 -13 31	.087	.598	41.72	+1.6	102.4	102.4	100.4	95.9	92.0	92.0
8294	53 8 7.39845		271 40 +22 5	.183	.330	13.73	+0.5	83.4	83.3	83.3	82.9	82.0	80.6
8307	53 8 8.19278	3	333 58 -13 37	-.093	-.343	36.06	+0.8	101.3	101.0	100.7	92.9	88.8	88.8
8344	53 8 8.39184	5	348 18 -13 15	-.407	-.697	41.23	+0.7	101.3	101.3	100.7	94.3	88.4	88.4
8368	53 8 9.21638	10	319 7 -0 39	.004	.719	27.99	+0.5	100.9	100.9	100.1	88.7	86.9	86.9
8394	53 8 10.22697		272 37 +0 31	-.497	-.794	14.52	+1.0	80.7	80.7	76.7	72.8	69.4	69.3
8401	53 8 10.24674	7	42 51 +58 47	-.266	-.365	59.93	-1.6	115.7	115.3	116.5	98.0	96.2	96.0
8413	53 8 10.30711		279 45 +64 29	.082	.753	26.29	+1.6	102.8	102.8	99.7	88.4	86.8	86.8
8415	53 8 10.30810		274 38 -8 33	.403	.479	14.12	+1.5	80.7	80.6	80.6	80.2	75.0	75.0
8417	53 8 10.32681		338 32 +3 11	-.207	-.861	29.18	-1.1	88.2	88.2	88.3	87.7	81.2	81.2
8447	53 8 11.42992		287 48 +32 51	-.095	-.418	20.83	+1.2	96.1	96.1	93.9	85.9	83.6	83.5
8463	53 8 13.45529	7	45 46 +58 3	-.219	-.155	60.52	-0.1	113.0	112.8	114.2	109.4	107.5	106.9
8469	53 8 13.24211	7	48 36 +58 4	-.269	-.326	60.59	-2.6	117.5	117.5	119.1	95.6	91.4	91.4
8476	53 8 13.28005	120	280 15 +47 55	-.069	-.861	22.19	-0.1	97.9	97.9	95.3	84.1	82.0	82.0
8510	53 8 13.42525		289 19 +31 3	-.138	-.421	17.74	-1.5	84.2	84.0	83.9	80.2	78.1	77.4
8546	53 8 14.29511		307 7 -22 18	-.385	-.551	18.79	+0.8	90.0	89.7	88.2	83.7	71.0	70.8
8572	53 8 14.43341		23 50 +1 0	-.255	-.834	64.21	-0.4	112.8		112.4	102.2		95.6
8576	53 8 14.43670		34 14 -35 11	.041	.333	52.79	+0.5	112.8	112.8	115.0	105.4	102.1	102.1
8609	53 8 17.32828		30 25 +48 24	.310	.733	61.91	-1.2	107.8	107.0	108.5	97.9	91.2	91.2
8640	53 12 14.43091		152 29 -42 16	.086	.219	55.74	-1.6	111.2G	110.7		100.5	96.8	96.8
8645	53 12 13.34920	4	112 46 +32 21	-.148	-.984	36.20	-3.5	102.7	102.2	108.1	88.6	84.1	84.1
8648	53 12 15.48317	16	130 41 +1 21	-.061	-.804	58.59	-0.8	112.7	111.5	114.9	93.5	91.9	91.9
8658	53 8 10.44060	7	46 50 +56 56	-.560	-.820	60.46	-0.9	113.7	112.9	113.7	100.6	93.9	93.9
8668	53 8 10.45569	1	314 57 -3 32	-.260	-.377	22.78	+1.2	98.3	98.3	97.8	92.0	92.5	90.3
8679	53 8 11.46806	7	46 10 +57 14	.501	-.866	60.80	-2.5	119.7	118.9	118.2	90.1	83.3	81.8
8719	53 8 14.19444	7	49 36 +57 57	-.270	-.204	60.13	-2.0	99.4G	99.2		98.4	94.4	94.4
8726	53 8 14.29057	7	47 28 +56 45	-.223	-.471	61.10	-3.6	118.2	118.2	119.9	93.6	90.9	90.9
8766	53 9 30.19335		6 23 -2 59	-.224	-.662	24.01	-0.4	101.6	101.1	100.0	87.4	81.5	81.3
8793	53 10 2.28006		345 3 +38 34	.028	.956	26.59	+1.2	101.8	101.0	97.9	86.8	84.0	83.6
8817	53 10 2.35018		119 12 +36 36	-.287	-.329	68.89	+0.7	113.4	113.4	119.5	105.4	103.0	102.3
8819	53 10 2.35251		24 53 +44 26	-.202	-.975	45.45	+0.3	101.9	101.9	101.1	90.8	84.2	84.2
8881	53 10 6.24826		269 51 +33 32	-.132	-.330	17.02	+0.0	96.5	96.5	93.7	81.1	79.2	79.2
8891	53 10 6.29615		309 59 +72 3	-.152	-.623	32.72	-0.2	104.7	103.7	105.2	89.7	87.7	87.7
8917	53 10 7.39307		13 5 +3 8	-.424	-.699	20.63	+0.6	87.5	87.5	84.0	78.9	76.4	76.4
8943	53 10 9.19222	9	278 23 +48 33	-.087	-.669	20.20	+0.1	103.8	103.5	102.8	96.3	95.9	90.6
8945	53 10 9.19547	2	32 4 +9 52	-.206	-.615	31.06	+1.7	102.2	102.2	98.2	90.9	85.2	85.2
8951	53 10 9.23348	9	279 13 +49 42	-.063	-.546	20.11	+0.1	103.5	103.5	102.5	97.0	98.8	91.3
8974	53 10 9.31756		24 13 -1 20	-.326	-.831	25.66	-1.9	88.1	88.0	87.5	84.1	79.4	79.4
8976	53 10 9.31647		121 26 +66 35	-.745	-.454	57.96	+0.6	112.4	112.0	115.0	103.8	102.5	102.5
8990	53 10 9.47638	20	39 1 +12 13	-.221	-.713	26.95	+1.6	100.2	99.2	97.7	93.2	83.3	83.3
9015	53 10 10.29028	2	32 37 +8 14	-.084	-.878	30.88	-0.1	103.5	102.7	100.8	82.5	75.8	75.8
9030	53 10 10.39572		19 11 +13 38	-.349	-.797	24.07	+1.2	99.6	96.9	95.9	88.1	79.1	79.1

TABLE 1.1.—Basic physical data for 413 Super-Schmidt meteors: Trajectories.—Continued

Trail No.	L_A °	L_B °	D	n_A	n_B	ΔM	Vis. A	Vis. B	C. I.	ϵ_∞	m_{-2}	m_{-1}	log σ	χ	W	B	Rem.
8238	17.7	15.8	.95	53	40	2.5	+2	+1	-0.9	-.392	0.1162	-.01800	-11.18	+.69	0.3	0.5	
8240	3.1	5.8	.75	26	44	3.7	+1	+2	-2.4	-.150	0.6224	-.09640	-11.20	+.15	0.5	0	
8244	2.9	3.8	1.17	31	54	1.5	+3		-1.1	-.746	0.8716	-.13500	-11.08	+.14	0.0	0	
8254	6.0	6.0	.42	23	17	1.4				-1.145	0.0200	-.00310	-11.44	+1.02	0	0.0	
8294	4.7	5.9	.64	20	0	3.1	+4		-3.0	-.711	2.2598	-.35000	-11.25	+.21	0.5	4	A
8307	16.2	18.8	1.02	50	50	2.4	+2	+1	-0.8	-.485	0.1433	-.02220	-11.20	-.13	1	0	
8344	5.2	6.6	.46	26	25	2.3	+1.5	+2	-1.0	-.919	0.0349	-.00540	-11.32	+.36	0	1	
8368	7.6	9.2	.70	42	40	2.1	+1	+2	-1.0	-.673	0.2008	-.03110	-11.20	+.37	0.3	0	
8394	7.3	3.9G	1.03	58	30	2.8	0	+1	+0.0	-.628	1.7058	-.26420	-10.90	+.18	2	0.5	U
8401	27.5	26.7	.90	53	53	3.8	0	0	-1.4	+.403	0.2370	-.03670	-11.32	+.57	0.5	0	
8413	2.9G	8.4	.82	13	43	1.6	+3	+3	-1.5	-.830	0.1672	-.02590	-11.08	+.35	1.0	0	
8415	6.4	6.4	.85	46	45	1.9	+2	+2	-0.6	-.888	0.9620	-.14900	-10.56	+.49	1	0	
8417	2.4G	3.4	.28	13	17	4.3	+1.5			-.626	0.2002	-.03100	-10.90	-.08	0	1.0	A
8447	16.7	14.8G	1.50	89	60	1.9	+2	+1	-0.4	-.466	0.8071	-.12500	-11.22	+.46	1	0	
8463	15.8	18.3	.65	30	35	1.8	+1	+1	-0.7	-.346	0.0407	-.00630	-11.19	+.41	0	0.3	
8469	41.3	40.3	1.33	79	78	4.5		+1	-3.5	+.834	0.6179	-.09570	-11.49	+.04	2	0	
8476	9.0	5.5	.85	52	31	3.2	+2	+1	-1.5	-.556	0.5398	-.08360	-11.18	+.29	0.5	0	
8510	10.2	10.3	.93	49	47	5.0	C	0	-1.6	+.065	4.2484	-.65800	-10.98	+.75	4	2.5	
8546	13.8	16.9	1.85	110	104	2.7		+0.5	+0.0	-.292	1.6658	-.25800	-11.22	+.15	1.0	0	
8572	3.7	5.9	.32	19	18	3.0	+2	+1	-1.7		0.0200	-.00310			0	0	
8576	11.7	12.9	.60	35	30	1.7				-.561	0.0378	-.00585	-10.87	+.78	0	0	
8609	9.5	10.3	.37	20	21	3.6	+1	+2	-2.5	-.182	0.0567	-.00878	-11.65	+.09	0.3	0	
8640	34.0G	31.6G	1.18G	67	68	4.1	-1	-1.5	-0.2	+.571	0.4358	-.06750	-11.42	+.02	2	0	
8645	9.4	15.2	1.10	41	63	5.9	0	-2	-2.0	+1.007	4.4034	-.68200	-11.59	+.15	4	0	
8648	6.7	6.2	.43	24	20	2.9	0	+2	-1.1	-.296	0.0510	-.00790	-11.56	+.11	0	0	
8658	6.4	5.3	.40	23	23	4.0	0	0	-0.9	-.222	0.0549	-.00850	-11.06	+.19	0.7	0	
8668	11.8	12.3	.97	42	37	1.9		+2	-0.9	-.555	0.5146	-.07970	-11.43	+.31	2	3	
8679	13.3	6.7	.72	41	29	5.3				+.478	0.2705	-.04190	-11.32	-.28	3	0	
8719	12.4G	7.7G	.40G	24	15	4.4	0		-1.8						1	0	
8726	26.4	24.0	.96	59	49	5.6	-2	-1	-1.8	+1.147	1.2913	-.20000	-11.55	+.55	3	0	
8766	5.0	8.1G	1.30	74	59	3.8	+3	+1	-1.6	-.010	1.4882	-.23050	-11.25	+.22	2	0	
8793	5.8	4.1	.73	36	39	2.1	+3	+2	-1.2	-.883	0.1453	-.02250	-11.32	+.01	0.5	0	
8817	13.3	14.9	.49	26	21	1.2	+2	+2	-1.0	-.461	0.0213	-.00330	-11.36	+1.73	0	0.0	
8819	6.2	4.4	.38	24	23	2.0		+1	-0.8	-.645	0.0491	-.00760	-11.08	+.15	1.0	0.0	
8881	30.7G	32.5G	3.48G	173	130	3.2	+1	+1	-1.1	+.170	7.4379	1.15200	-11.39	+.12	2.5	0.0	
8891	13.2	13.1	.85	47	48	2.6	+1.5	+1	-1.2	-.188	0.3803	-.05890	-11.15	-.01	0.3	0	
8917	8.8	7.3	.78	48	39	2.9		+1	-0.6	-.626	0.5740	-.08890	-11.14	+.34	2	1	
8943	10.3	8.5	1.10	26	0	1.6	+1		-0.8	-.318	1.8724	-.29000	-14.09	+1.32	0	4	
8945	5.1	5.9	.90	49	18	1.6	+2		-0.3	-.885	0.0910	-.01410	-11.45	+.09	0	0	
8951	11.6	10.6	1.33	19	25	1.7	+1		-0.8	-.264	2.1307	-.33000	-15.67	+2.46	0	4	
8974	4.4	4.5	.42	24	22	5.4		+2	-3.8	-.238	0.7186	-.11130	-10.69	-.01	1	0	S
8976	10.9	10.9	.38	22	20	1.7	+2	+1	-0.6	-.743	0.0187	-.00290	-11.23	+.62	0	0	
8990	5.5	8.4	.90	46	44	1.4	+3	+3	-0.9	-.852	0.1524	-.02360	-11.40	+.03	0.0	0	
9015	5.8	13.6	1.05	60	58	3.6		+1.5	-1.8	-.176	0.4662	-.07220	-11.50	+.20	0.5	0	
9030	10.0	9.3	1.09	54	53	2.0	+1	+2	-0.5	-.591	0.3893	-.06030	-11.26	+.00	0	0	

TABLE 1.1.—Basic physical data for 418 Super-Schmidt meteors: Trajectories.—Continued

Trail No.	Date	Sh.No.	Apparent radiant α , δ ,	sin Q	cos Z_R	V_m	M_{Pm}	H_B	H_{ED}	$H_{2.5}$	H_{ML}	H_{ED}	H_E
9062	53 10 12.44075		140 20 +2 30	.186	.342	62.23	+0.2	112.6	111.9	116.0	104.0	101.9	101.5
9087	53 10 16.46267		36 45 -19 26	.328	.357	19.80	+0.2	85.8	88.8	88.7	88.5	86.3	84.9
9104	53 10 20.47562	2	43 40 +12 10	.225	.651	30.30	-0.1	100.9	100.3	102.3	84.2	82.7	82.4
9130	53 11 2.12048		285 30 +32 44	.258	.776	17.98	+1.4	92.5	92.5	90.0	85.2	81.7	81.3
9147	53 11 2.29009		91 16 +43 49	.321	.743	58.79	-0.1	111.0	110.2	113.8	97.1	90.7	90.7
9149	53 11 2.30611		68 10 +50 26	.516	.907	48.46	-1.9	95.5	94.6	94.7	87.2	78.6	78.6
9170	53 11 3.20197		58 26 -19 56	.095	.322	33.83	+1.3	105.0	105.0	104.4	97.3	94.3	94.3
9172	53 11 3.21307		20 54 +22 42	.265	.976	25.10	-1.7	102.9	102.9	102.2	82.9	77.1	77.1
9238	53 11 7.37403	2	55 17 +14 10	.472	.906	28.35	+0.2	100.6	100.6	99.4	87.2	82.6	82.6
9240	53 11 7.37850	2	52 43 +13 37	.460	.881	26.20	+0.3	98.0	97.9	98.3	84.6	81.0	80.3
9246	53 11 7.43475	2	55 45 +15 39	.568	.765	29.34	+1.1	102.7	98.7	100.9	86.1	84.7	84.7
9252	53 11 7.46139		37 14 +16 5	.357	.448	19.84	+1.7	86.2	86.2	84.6	81.2	79.1	79.1
9257	53 11 7.48135	17	55 58 +22 26	.289	.632	30.60	-1.2	103.7	103.7	103.8	79.9	75.9	75.6
9265	53 11 9.25547	17	54 23 +22 50	.387	.933	30.53	+1.0	100.0	99.9	98.7	88.0	84.1	84.1
9284	53 11 10.36421		60 3 -16 9	.003	.639	26.34	-1.2	92.3	91.4	93.0	80.5	74.7	74.7
9331	53 11 13.35062	17	62 14 +23 46	.097	.978	30.75	-1.9	105.3	104.9	105.2	84.3	78.2	78.2
9335	53 11 13.35944		101 47 -1 44	.149	.734	58.52	-1.5	109.9	109.2	112.6	92.0	88.5	88.5
9375	53 11 26.17665		54 57 +14 26	.230	.823	21.96	+1.0	88.5	88.1	87.9	85.5	79.8	74.4
9379	53 12 1.13503		22 46 +47 5	.429	.957	19.63	-0.3	99.9	99.9	76.6	89.6	83.6	82.1
9411	53 12 4.44648	16	122 2 +2 55	.066	.866	60.39	-0.9	111.4	111.4	115.5	93.2	85.5	85.5
9416	53 12 7.39528	20	80 1 +16 0	.085	.841	25.61	-0.4	100.2	98.3	101.8	82.9	76.2	76.2
9418	53 12 7.40209	4	105 57 +32 6	.205	.993	36.30	-0.9	98.1	98.1	100.2	83.3	78.0	77.4
9451	53 12 9.37006	4	109 11 +33 8	.234	.997	35.23	+0.0	101.5	101.5	102.7	86.9	83.2	82.1
9507	53 12 11.39574	4	111 46 +33 12	.293	.999	35.39	-0.4	98.6	98.5	99.9	90.3	82.0	81.6
9547	53 12 12.35211	4	111 25 +32 37	.189	.987	36.26	-1.0	100.5	99.5	101.4	83.0	80.7	80.7
9611	53 12 13.31978	4	111 38 +32 17	.351	.950	36.92	-0.8	100.2	100.2	100.2	89.7	83.9	80.9
9627	53 12 13.36039	4	112 29 +31 54	.171	.993	36.61	-0.8	101.0	99.8	100.7	88.9	84.7	83.6
9631	53 12 13.36283	4	112 39 +32 26	.232	.994	36.27	-0.2	98.4	98.4	99.6	84.0	80.5	79.4
9656	53 12 13.43186	4	113 25 +32 25	.315	.969	36.04	-1.3	102.9	102.9	105.8	85.6	83.5	80.9
9660	53 12 13.43706	16	128 43 +1 52	.036	.859	58.66	-0.5	111.5	109.0	110.5	92.1	89.6	88.9
9709	53 12 13.52675	4	114 13 +32 59	.154	.743	35.89	-0.2	99.5	98.8	98.4	90.3	86.4	84.7
9719	53 12 14.34826	4	113 22 +31 46	.355	.984	36.43	+0.9	101.3	100.3	100.2	87.0	84.9	83.6
9725	53 12 14.37895	4	114 12 +32 19	.336	1.000	36.10	-2.4	92.2	92.2	92.2	70.4	59.4	59.4
9742	53 12 14.40185	4	113 41 +32 8	.405	.995	36.76	-1.0	98.0	96.8	101.7	81.2	79.5	78.5
9749	53 12 14.40912	4	114 6 +32 23	.271	.991	36.23	-2.5	100.3	100.3	100.5	84.1	70.6	70.6
9804	54 3 9.47776		252 50 -15 42	.072	.612	72.78	-3.8	117.5	112.5	117.7	97.0	93.3	93.3
9815	54 3 8.29651		241 49 +16 51	.234	.345	59.73	-2.3	103.8	103.5		100.1	96.2	96.2
9833	53 12 29.24403		94 18 -2 38	.176	.785	24.94	-0.2	88.6	88.4	88.6	86.7	78.9	78.9
9880	54 1 1.31854		107 56 -40 57	.039	.285	25.97	-0.1	93.3	93.3	93.9	86.9	80.7	78.7
9888	54 1 1.44056		36 16 +74 59	.171	.423	18.93	+0.5	96.5	96.2	96.2	85.1	77.5	77.0
9900	54 1 2.27567		94 39 +80 32	.255	.669	23.87	+0.2	93.8	93.8	92.5	82.6	76.3	76.2
9917	54 1 3.21446		80 28 +4 23	.173	.874	16.44	+1.8	90.9	89.7	87.7	77.8	75.1	75.1
9925	54 1 3.32581		126 17 -6 53	.058	.750	44.57	-1.2	106.3	104.2	107.3	98.5	91.0	91.0
9945	54 1 3.42157	10	232 57 +49 18	.262	.450	41.45	+0.4	101.8	101.8	102.4	95.8	93.7	93.7
9951	54 1 3.45117		166 55 +28 21	.249	.989	60.40	+0.0	108.5	108.5	112.4	95.5	91.5	91.5

TABLE 1.1.—Basic physical data for 413 Super-Schmidt meteors: Trajectories.—Continued

Trail No.	L_A S	L_B S	D	n_A	n_B	ΔM	Vis. A	Vis. B	C. I.	ϵ_m	$m_{=2}$	$m_{=1}$	log σ	x	W	B	Rem.
9062	8.5	16.3	.52	C	28	1.5	+2	+1	-0.8	-4.43	0.0303	-0.0470	-11.17	+1.4	0	0	
9087	6.8	5.1	.61	22	22	3.0	+3	+3.5	-3.2	-7.20	0.5101	-0.0900	-11.00	+6.4	0.3	3	A
9104	10.8	13.9	.96	38	55	2.3		+1	-1.2	-2.06	0.4746	-0.7350	-11.32	-1.28	0	0	
9130	8.2	6.2	.88	49	42	2.1	+2	+1.5	-0.6	-8.18	0.5920	-0.8550	-10.96	+1.9	2	0Q	
9147	11.5	12.0	.47	28	25	2.8	+1	+1	-1.0	-4.44	0.0355	-0.0550	-11.30	+0.3	0	0	
9149	5.6	4.7	.39	19	23	4.8	+1	+0.5	-2.6	-0.009	0.1756	-0.2720	-11.41	+6.0	3	0	S
9170	12.2	14.0	.86	52	47	1.3	+4		-2.3	-6.31	0.1241	-0.1922	-11.25	-1.0	0	0	
9172	7.4	6.3G	1.07	65	42	5.0	C	+1	-2.2	+3.74	3.0410	-4.7100	-11.01	+2.7	3	0	F
9238	6.3	5.4	.72	41	28	2.2	+3.5	+1.5	-2.4	-6.27	0.2189	-0.0390	-11.26	-0.9	0	0	
9240	7.8	7.2	.79	41	33	2.6	+3	+1	-1.9	-4.48	0.4223	-0.0650	-11.33	+0.8	0	0	
9246	6.1	4.3	.81	25	36	1.8	+3	+2	-1.5	-6.54	0.1821	-0.2820	-11.34	+3.9	0Q	0	
9252	7.4	5.9	.81	44	35	1.9	+3	+2	-1.0	-9.23	0.3209	-0.6970	-11.04	+2.5	1	1	
9257	19.7	14.0	1.51	84	85	4.3	0	0	-1.5	+3.57	1.7381	-2.6920	-11.55	-0.5	0.3	0	
9265	4.8	6.5	.57	34	34	2.1	+2.5	+2	-1.3	-7.96	0.1162	-0.1800	-11.38	+1.0	0	0	
9284	8.7	8.5	1.05	60	52	3.9	+1	+1.5		+1.91	1.7362	-2.6890	-11.03	+1.6	2.5	0	
9331	7.6	7.8	.92	54	48	4.8		0	-1.4	+3.68	1.6690	-2.5850	-11.32	-0.8	2	0	
9335	10.6	12.3	.50	30	27	4.1		+0.5	-1.8	+0.46	0.1130	-0.1750	-11.49	+1.1	1	0	
9375	5.1	4.1	.81	28	20	2.3	+2		-1.0	-5.67	0.5527	-0.0850	-11.17	+1.4	0.3	2	A
9379	6.9	6.2	.93	52	42	3.9	+1.5		-1.7	-2.67	1.4773	-2.2880	-10.68	-0.1	2Q	3	
9411	8.4	8.4	.50	27	27	2.1	+1.5	+1	-1.1	-1.46	0.0659	-0.1020	-11.44	+0.3	0	0	
9416	4.6	6.1	1.05	51	61	2.6	+2.5	+3	-2.0	-2.16	0.7851	-1.2160	-11.36	-1.4	0	0	
9418	5.0	5.6	.58	29	30	3.0	+1	+2	-1.4	-0.70	0.3603	-0.5580	-11.10	-0.7	1	0	
9451	6.7	5.2	.56	28	26	2.6		+2	-1.3	-5.57	0.1298	-0.2010	-11.34	+2.9	1	0	
9507	5.3	5.1	.48	27	26	3.0	+1		-0.6	-4.02	0.1788	-0.2770	-10.50	-0.6	0.3	0	
9547	7.4	7.2	.55	28	30	3.0	+1.5	+1	-1.7	-2.08	0.2615	-0.4050	-11.18	+1.6	1	0	
9611	8.0	7.6	.55	29	28	3.6	+1.5	0	-1.3	-2.95	0.2034	-0.3150	-10.89	+2.3	2	1	
9627	6.0	4.1	.48	26	18	3.6	+1.5	+1	-1.4	-4.24	0.1537	-0.2380	-11.30	+0.9	1.5	0.5Q	
9631	6.2	6.4	.51	30	30	2.4		+1	-0.3	-4.06	0.1711	-0.2650	-11.20	+0.7	0.5	0	
9656	5.5	5.3	.63	33	33	3.4	+1	+0.5	-1.2	+0.17	0.4455	-0.6900	-10.80	+4.7	2	1.5	
9660	6.8	7.8	.45	23	20	3.2	+1	+1.5	-1.5	-4.24	0.0374	-0.0580	-11.37	-0.2	1	0	
9709	5.8	3.5	.58	29	27	3.3	+2.5		-2.6	-5.08	0.1382	-0.2140	-11.53	+4.5	1	2	
9719	5.6	5.7	.50	25	27	2.2	+2	+1.5	-0.8	-8.14	0.0646	-0.1000	-10.86	+2.5	1	0.5	
9725	12.1	13.1	.95G	54	57	4.9	0	-1	-1.8	+7.90	2.7569	-4.2700	-11.90	+1.8	2Q	0	
9742	5.4	5.5	.54	28	29	3.7	+1	+2	-2.1	-1.43	0.2989	-0.4630	-11.41	+1.6	2	0	
9749	5.0	8.5	.84	50	48	4.9	0	0	-1.7	+5.83	1.6400	-2.5400	-11.37	+1.5	3	0	
9804	12.9	9.6	.54	27	20	6.1	-1	+0.5	-2.9	+7.76	0.3151	-0.4880	-11.16	-0.6	2.5	0	
9815	10.9G	11.2G	.38G	22	20	4.7	-1	+1	-1.9	+3.37	0.2034	-0.3150	-11.11	+2.9	2	0	
9833	4.4	5.0	.50	29	25	3.4	+1.5	+3	-2.2	-6.98	0.2712	-0.4200	-11.33	0	0	0.3	A
9880	19.0	16.7G	1.99	100	74	2.5	+2	-1.1		+0.59	1.3798	-2.1370	-11.12	-0.8	2	3	
9888	23.2G	24.9G	2.57G	105	143	2.7	+1		-0.6	-0.33	2.9700	-4.6000	-11.29	-0.8	10	0	
9900	14.1	11.4G	1.14	61	57	2.8	+1.5	+1	-0.9	-3.17	0.7496	-1.1610	-11.14	-0.6	1	0	
9917	6.3	7.2	1.17	66	57	1.9	+3.5	+3	-1.6	-7.88	0.8710	-1.3490	-11.18	-0.9	0	0	
9925	5.1	7.8	.46	23	21	3.9	+1.5		-2.4	-2.06	0.1427	-0.2210	-11.13	+3.6	1	1.5	
9945	5.8	8.8	.45	28	21	1.9	+3	+2	-1.8	-6.30	0.0671	-0.1040	-11.43	+4.4	0	1	
9951	5.4	5.0	.29	14	16	2.1	+2	+2	-1.2	-6.86	0.0187	-0.0290	-11.65	+2.7	0	0Q	

TABLE 1.1.—Basic physical data for 413 Super-Schmidt meteors: Trajectories.—Continued

Trail No.	Date	Sh.No.	Apparent radiant		sin Q	cos Z _R	v _∞	M _{pm}	H _B	H _{BD}	H _{2.5}	H _{ML}	H _{ED}	H _E	
			α	δ											
9953	54 1	3.45659	10	228 11	+48 35	.299	.611	43.15	+0.4	100.6	100.6	102.1	95.4	90.8	89.9
9955	54 1	3.45699	10	224 10	+51 13	.228	.651	43.25	+0.7	104.0	104.0	104.0	100.5	94.2	94.2
9974	54 1	3.48882	10	228 48	+48 38	.224	.706	43.14	-1.0	104.8	103.9	104.3	91.7	86.7	86.3
9983	54 1	3.49569	10	229 19	+48 28	.230	.722	43.07	-1.3	102.4	101.7	103.7	89.2	87.2	87.2
9985	54 1	3.50371	10	231 10	+48 53	.167	.730	42.40	-0.4	101.1	101.1	102.1	91.6	87.5	87.5
9997	54 1	3.52012	10	227 57	+48 56	.353	.797	43.72	+1.1	100.6	100.6	100.2	94.0	88.7	88.7
10006	54 1	4.45827	10	230 2	+48 8	.277	.608	43.30	+0.4	103.0	103.0	104.0	96.5	90.6	90.2
10012	54 1	4.53118		176 15	+23 50	-.984	.972	64.63	-1.0	114.6	114.4	114.0	101.7	91.4	91.4
10064	54 1	9.42393		118 46	+8 19	-.356	.758	29.01	-0.6	91.8	91.8	91.8	89.6	79.6	79.1
10070	54 1	11.37924		114 53	+14 8	-.365	.872	26.03	+0.2	103.1	103.1	100.4	79.3	71.5	71.4
10094	54 4	10.47485		317 55	+32 11	-.174	.689	49.31	-2.6	112.0	109.3	112.4	85.5	81.8	81.3
10098	54 4	6.23252		230 58	+16 12	.256	.553	45.71	-2.9	95.7G	94.5	97.9	85.0	78.3	77.9
10106	54 4	1.37265		190 48	-22 55	.253	.490	30.71	-0.2	97.4	96.5	96.0	84.7	81.3	79.9
10127	54 4	28.45642		240 49	-1 52	-.198	.693	37.55	-1.8	89.3	89.3	89.5	87.0	81.9	81.9
10173	54 2	27.16305		139 36	+23 32	-.395	.875	17.07	+1.4	82.9	82.7	81.7	80.6	72.8	72.8
10218	54 3	5.30805		168 53	+7 11	.234	.903	27.44	+0.4	101.8	100.5	100.6	89.8	85.9	85.9
10222	54 3	5.33948		227 57	-9 1	.108	.450	67.90	-0.3	115.5	115.5	118.5	104.1	101.1	101.1
10240	54 3	5.45765		178 2	-20 14	.311	.397	39.51	+0.9	106.2	105.9	106.2	95.5	89.9	89.9
10247	54 3	6.42134	110	182 13	-1 18	.117	.744	34.49	+0.1	90.6	90.6	92.6	84.4	79.0	78.7
10252	54 3	6.48481		251 5	+28 19	-.134	.954	55.28	-1.6	109.1	108.8	112.0	91.9	89.7	89.7
10255	54 3	6.49676		329 38	+35 57	.259	.269	20.66	-0.6	89.3	89.2	89.5	87.2	85.5	84.8
10273	54 3	6.37011		250 58	+48 55	-.173	.674	37.10	-0.2	99.0	100.0	91.5	81.5	84.6	84.6
10279	54 3	8.44085		186 21	-0 39	-.357	.716	20.56	+2.4	88.1	87.4	84.5	81.5	74.9	74.2
10281	54 3	8.47246		166 19	-1 20	.474	.376	26.47	+0.3	94.3	93.9	93.7	88.5	85.4	85.3
10342	54 3	26.27791		155 0	+65 29	.612	.815	13.15	+1.3	78.5	78.3	77.7	69.9	68.4	68.3
10358	54 4	1.30207		198 21	+4 26	.024	.875	29.43	+1.1	103.2	99.7	100.9	88.9	81.8	81.4
10365	54 4	1.34746		178 56	-23 30	.270	.465	25.04	+1.3	99.0	98.1	98.8	92.5	86.3	85.4
10380	54 4	2.34276		210 55	-19 23	.030	.615	45.93	-0.2	94.6	94.6	95.3	89.3	85.3	84.9
10384	54 4	2.37276		207 15	-15 21	.020	.658	33.38	-0.1	107.2	104.6	112.6	86.3	78.3	78.3
10394	54 4	2.42132		164 23	+38 43	.004	.554	15.11	+1.4	90.5	90.5	87.6	84.2	80.5	80.1
10414	54 4	5.19665		143 54	-20 15	-.234	.585	17.03	-0.9	95.2	95.2	93.9	72.9	61.4	61.4
10439	54 4	5.38519		207 54	-13 57	.014	.653	34.71	-0.5	104.9	104.9	105.6	84.8	81.6	81.6
10447	54 4	5.41316		202 28	-19 27	.133	.491	33.85	-0.4	100.9	100.9	101.4	89.7	85.3	85.3
10478	54 4	6.26447		177 21	-24 13	-.209	.545	23.71	-1.7	91.1	90.8	90.5	86.7	83.5	83.4
10480	54 4	6.29420		165 25	-38 51	-.205	.249	22.70	+1.9	99.3	98.5	98.4	95.6	92.8	92.4
10531	54 4	7.46231	60	267 22	+30 58	.333	.982	51.07	-0.9	108.9	108.1	109.4	99.5	85.0	85.0
10555	54 4	12.42529		197 43	+77 21	.249	.646	18.02	-0.2	83.2	83.1	83.2	79.8	78.0	76.6
10566	54 6	30.25718		252 28	+53 40	.337	.923	26.18	-3.2	109.5	108.0	107.0	84.1	82.7	78.1
10583	54 6	4.39391		3 0	+0 45	-.161	.215	68.98	-1.2	117.2	116.5	119.8	107.3	103.6	103.4
10587	54 6	4.39369		298 31	+65 24	.419	.833	36.63	-2.0	107.9	107.9	107.3	91.7	87.7	87.5
11816	54 5	3.15099		156 7	-47 30	-.156	-.161	19.87	+1.1	93.4	92.8	93.2	89.8	88.0	86.6
11818	54 5	3.17971		116 45	+35 33	-.175	-.639	15.58	-0.1	93.9	93.9	91.6	82.5	73.1	73.1
11825	54 5	3.23657		209 42	-14 43	.004	.665	22.96	+0.3	99.2	99.2	98.2	88.1	83.7	83.7
11856	54 5	3.43132		214 17	-11 24	.474	.369	20.73	+1.0	90.8	89.5	89.0	82.1	80.9	80.5
11862	54 5	3.45107	19	335 20	-1 33	-.127	.420	66.76	-0.7	115.6	115.6	119.6	102.1	100.7	99.7

TABLE 1.1.—Basic physical data for 413 Super-Schmidt meteors: Trajectories.—Continued

Traill No.	L _A o	L _B o	D	n _A	n _B	ΔM	Vis.A	Vis.B	C.I.	ε _∞	m _{∞2}	m _{∞1}	log σ	x	W	B	Rem.
9953	6.4	7.0	.42	15	20	2.4	+1	+3	-1.4	-.659	0.0568	.00880	-11.71	+.61	0.5	1	
9955	6.5	6.6	.36	20	21	1.6	+3	+3	-1.5	-.733	0.0486	.00753	-11.85	+.55	0	0	
9974	13.0	10.3	.62	34	31	3.5	+1	0	-0.9	-.142	0.1795	.02780	-11.06	+.40	1.5	1	
9983	10.4	5.2G	.50	29	16	3.7	+0.5	+2	-2.0	-.095	0.2014	.03120	-11.28	+.35	1.5	1	
9985	8.2	5.9	.45	27	21	2.6	+2	0	-0.6	-.503	0.0826	.01280	-11.49	+.39	0.5	0.5	
9997	6.8	6.0	.35	21	19	1.8	+2		-0.9	-1.019	0.0240	.00371	-11.65	+.16	0	0.5	
10006	11.4	9.7	.50	30	23	2.2		+1	-0.3	-.657	0.0549	.00850	-11.12	-.04	0	1	
10012	2.1	2.8	.37	21	23	4.3	+1	0	-1.1	-.514	0.0228	.00353	-11.05	-.04	00	0	
10064	5.4	5.3	.58	32	32	3.5	+1	+2	-1.6	-.487	0.2718	.04210	-10.68	-.32	0	00	A
10070	3.9	6.5	1.46	78	73	2.7	+2.5	+1	-1.4	-.116	0.9330	.14450	-11.64	+.12	00	0	
10094	21.5	17.7	.92	56	50	4.8	-0.5	-1	-1.2	+.578	0.6457	.10000	-11.53	-.15	1	0	
10098	15.5G	19.0G	.71G	36	38	5.7	-0.5	-1	-2.0	+.654	0.9814	.15200	-11.33	-.04	3.5	0	
10106	15.8	16.5	1.15	59	57	3.2	+2	0	-0.9	-.243	0.3997	.06190	-11.10	+.61	10	3	F
10127	3.0	3.4	.29	18	16	4.9		+0.5	-1.8	-.112	0.2970	.04600	-11.05	+.17	2	0	S
10173	5.1	6.3	.68	35	35	2.1	+2.5	+3	-1.4	-.890	0.5340	.08270	-10.72	+.83	1	0	
10218	4.5	5.1	.65	35	33	2.7	+1.5	+3	-1.3	-.685	0.2085	.03230	-11.23	+.29	0.50	1	
10222	13.9	12.1	.47	27	25	1.9	+2		-1.4	0.0245	.00380		-11.33	0	0		
10240	16.0	15.5	1.04	62	58	1.8	+1	+2	-0.4	-.469	0.1117	.01730	-11.38	+.04	0	0	
10247	4.3	5.0	.47	27	28	3.0				-.612	0.1233	.01910	-11.43	+.18	0	0.5	A
10252	7.5	6.9	.37	0	23	3.8		+1	-1.3	-.067	0.1040	.01610	-11.40	+.07	1	0	
10255	6.5	5.1	.91	43	32	3.1	+3	+2.5	-2.6	-.087	2.1242	.32900	-11.24	+.22	1	2.5	A
10273	9.1	6.5	.59	36	29	2.4	+3	+2	-1.8	0.1711	.02650		-11.33	0	0		
10279	7.2	6.5	.97	53	38	1.4	+4		-1.8	-1.044	0.2169	.03360	-11.06	+.27	00	0	F
10281	5.6	5.0	.90	48	44	2.7	+2.5	+1	-0.5	-.672	0.2344	.03630	-11.34	+.12	1	0	
10342	5.2	3.0	.98	57	51	2.9	+0.5	+1	+0.1	-.732	1.7497	.27100	-10.87	+.37	1.5	0.50	
10358	8.7	9.6	.86	42	40	2.4	+1.5		-0.6	-.638	0.1814	.02810	-11.20	+.26	0.5	0	
10365	9.6	8.6	1.17	60	44	1.8	+2.5	+2	-0.7	-.584	0.3377	.05230	-10.86	+.49	00	0	
10380	5.5	5.6	.34	20	18	2.4	+1	-1	+0.4	-.574	0.0575	.00890	-11.83	+.37	1	0.5	
10384	11.4	13.6	1.34	68	73	2.1		+2.5	-1.5	+.040	0.6101	.09450	-11.54	-.23	0	0	
10394	4.5	2.7	1.29	47	55	2.4	+3		-1.3	-.870	0.9265	.14350	-10.88	-.04	20	0	
10414	28.5	31.8	3.84	131	158	4.1	+1	+2.5	-2.3	+.602	20.7255	3.21000	-11.45	-.10	1.5	0	F
10439	8.4	10.4	1.04	50	59	2.8		+2	-1.7	-.058	0.4500	.06970	-11.58	-.04	0	0	
10447	11.2	10.9	.94	54	51	2.9	+1.5	+2	-1.5	-.176	0.3525	.05460	-11.14	-.20	0.5	0	
10478	3.5G	7.9	.61	15	35	4.6		+3	-4.0	-.191	1.0330	.16000	-11.12	+.12	1.7	0.7	
10480	8.9	7.8	1.22	31	31	1.2	+4	+2	-0.6	-.708	0.3667	.05680	-11.40	+.71	00	2	
10531	8.0	8.2	.48	29	27	3.0	+2	+2.5	-2.7	-.126	0.1123	.01740	-11.51	+.08	0	0	
10555	3.3	2.7	.60	23	26	3.0		+2	-1.5	-.477	1.2390	.19190	-10.93	+.16	1	2	
10566	7.1	8.0	1.30	53	64	5.8	0		-2.8	+.849	7.8415	1.21450	-10.71	-.05	30	2.5	
10583	26.6	20.1	1.00	50	47	3.0	0	+1	-0.8	+.048	0.0678	.01050	-11.16	+.25	0.5	0	
10587	8.0	7.5	.67	33	40	5.2	+1.5	0	-2.3	+.105	0.5217	.08080	-11.09	+.40	3.5	0	
11816	23.3	15.1	2.16	72	38	1.0	+3	+3	-1.6	-.261	1.4327	.22190	-10.91	+.93	30	00	
11818	8.3	4.2	2.19	117	0	3.4	+2	+1	-1.2	+.339	6.5728	1.01800	-11.07	-.17	00	0	F
11825	8.2	10.7	1.03	59	58	2.9	0	+2	-0.5	-.421	0.6521	.10100	-11.01	+.10	2	0	
11856	8.7	6.9	1.32	65	64	2.2	+2.5	+2.5	-1.2	-.521	0.6850	.10610	-10.82	+.48	1.5	0	
11862	14.4	14.0	.58	33	34	2.4	0	0	+0.3	-.202	0.0420	.00650	-11.01	+.09	0	0	

TABLE 1.1.—Basic physical data for 413 Super-Schmidt meteors: Trajectories.—Continued

Trail No.	Date	Sh.No.	Apparent radiant		sin Q	cos Z _R	v _∞	M _{pm}	H _B	H _{BD}	H _{2.5}	H _{ML}	H _{ED}	H _E
			α	δ										
11973	54 5 6.29583		267 8	+25 13	.266	.779	44.93	-0.8	109.4	108.1	108.8	93.1	86.9	86.1
12342	54 5 31.35359		242 16	-15 14	.264	.587	23.04	+1.1	92.6	92.6	92.0	89.0	81.3	81.3
12361	54 6 1.18112		222 20	-35 39	.088	.349	22.62	+0.5	97.1	97.1	96.4	88.4	86.0	86.0
12363	54 6 1.18437		103 20	+48 11	.044	.252	18.93	+0.2	94.8	94.2	95.6	85.1	84.0	83.6
12399	54 6 2.23660		236 24	+35 30	.449	.992	20.07	+0.4	93.9	93.9	92.4	79.9	78.0	78.0
12504	54 6 5.26538		115 20	+65 47	.121	.284	19.32	-0.5	98.2	98.2	95.9	89.0	82.5	82.5
12577	54 6 11.41127		271 45	-12 30	.152	.606	29.65	-0.6	101.5	101.5	102.5	84.6	82.8	82.8
12714	54 6 25.26276		276 58	-0 21	.211	.806	25.92	+0.1	100.0	100.0	99.2	90.0	83.6	83.4

Trail No.	L _A	L _B	D	n _A	n _B	ΔM	Vis.A	Vis.B	C.I.	ε _∞	m _{∞2}	m _{∞1}	log σ	χ	W	B	Rem.
11973	13.2	14.0	.67	38	34	3.3	+1	+1	-1.4	-.177	0.1498	.02320	-11.31	-.01	0	0	
12342	5.5	8.7	.85	50	43	2.2	+2	+1.5	-0.4	-.736	0.3022	.04680	-11.24	+.73	3	0	
12361	18.2	16.6	1.44	80	74	2.7	+1.5	+2	-1.1	-.370	0.7942	.12300	-10.91	-.01	3	0	
12363	12.6	9.6	2.34	90	120	2.3	+1.5	+3	-1.0	+.067	3.8810	.59800	-11.06	-.06	0	1	
12399	5.2	5.6	.84	47	48	2.9	+2	+3	-2.1	-.448	0.9665	.14970	-11.31	+.19	0	0	
12504	25.2	26.6	2.95	169	172	3.9		+1	-1.3	+.261	5.4170	.83900	-10.97	+.06	3	0	F
12577	11.7	11.9	1.06	60	62	3.2	+1	+0.5	-0.6	-.109	0.6211	.09620	-11.35	+.20	1	0	
12714	6.1	8.2	.81	47	47	2.9	+3.5	+2.5	-2.8	-.389	0.4907	.07600	-10.86	-.28	2	1	

Notes on Table 1.1

Meteor No.

- 3053 No v.t.* Estimated time error ± 1 minute.
- 3072 No v.t. Estimated time error ± 1.3 minutes.
- 3076 No v.t. Estimated time error ± 20 s.
- 3288 No v.t. Common point and ratio of velocities insensitive to time. Possible error ± 5 minutes. Heights could be greatly in error.
- 3334 No v.t. Estimated time error ± 0.9 minutes.
- 3355 No v.t. Time from equalization of velocities.
- 3636 On Super-Schmidt film 28 segments in the middle of the trail are lost in the shutter hole.
- 3640 Four fragments became successively detached from the main body and can be followed on the photographs for short lengths of time.
- 3643 No v.t. Time computed from maximum-light segments.

*v.t. = visual time, i.e., time from visual observation.

Meteor No.

- 4141 Visual time given only to ± 1 minute.
- 4181 No v.t. Time from good common point.
- 4199 No v.t. Time from good common point.
- 4388 Possible error of ± 1 minute in timing.
- 4394 Possible error of ± 1 minute in timing.
- 4464 A fragment became detached near the end of the trajectory and remained visible for 0.1.
- 4507 No v.t. No good common point. Time error could amount to several minutes.
- 4596 Trails intersect at 0°26 angle. Solution by direct triangulation, poor because of uncertainty in common point.
- 4701 No v.t. Time from one good common point.
- 4952 No v.t. Time from two common points; estimated error ± 30 s.
- 5273 No v.t. Time from equalization of velocities, rather uncertain.
- 5450 No v.t. Time from end flare, good.

Meteor No.		Meteor No.	
6093	Shutter flutter nearly masks deceleration on both films.	8719	Only the end section of meteor trail was photographed. Persistent train; the meteor was reduced for the train program.
6398	A fragment became detached near the end of the trajectory.	8943	Most of the trail is completely blended.
6961	Shutter breaks completely obliterated by blending in the last one-third of the trail.	8951	Most of the trail is completely blended.
7046	No v.t. Time from a common point, could be somewhat in error.	9172	A fragment became detached toward the end of the trajectory and could be followed for 0°3.
7184	Trails intersect at 0°34 angle. Solution by direct triangulation.	9284	Trails intersect at 0°14 angle. Solution by direct triangulation, using a good common point.
7272	No v.t. Time from a good common point.	9815	Persistent train; meteor reduced for the train program.
7592	The last two-thirds of the trail appears completely blended.	10106	A fragment became detached in the second part of the trajectory and could be followed for 0°2.
7637	Trails intersect at 0°5 angle. Solution by direct triangulation.	10222	Large shutter flutter masks deceleration and makes even velocity uncertain.
8089	No v.t. Time from a good common point.	10247	No v.t. Time from a good common point.
8168	Owing to shutter flutter and terminal blending, no significant deceleration can be derived for this meteor.	10394	Large shutter flutter on both cameras.
8224	Large shutter flutter makes even velocity somewhat uncertain; no decelerations were derived.	10414	A fragment became detached in the second half of the trajectory and could be followed for 0°3. Another fragment is doubtful.
8254	No v.t. Time from one good common point.	11816	Meteor trail runs through shutter hole on one film.
8294	The second half of the trail appears completely blended.	11818	A fragment became detached in the second half of the trajectory and could be followed for 0°3.
8576	No v.t. Time from one common point, rather uncertain.	12504	A fragment became detached in the second half of the trajectory and possibly subfragmented; it could be followed for 0°70.
8679	No v.t. Time from one fairly good common point.		

TABLE 1.2.—Basic physical data for 413 Super-Schmidt meteors: Accelerations

Trail No.	H	v	\dot{v}	p.e.	n	m_1	s	log σ	log ρ_{obs}	$\Delta \log \rho_{\text{obs}}$	$\Delta \log \rho_{\text{corr}}$	p
2961	86.45	30.845	-1.900	.169	31	.17600	+.02		-8.28	-.07	-.07	5.6
	85.89	30.719	-2.077	.129	22	.15800	+.12		-8.26	-.09	-.14	5.9
	85.92	30.661	-2.664	.205	29	.16000	+.12		-8.14	+.03	-.01	5.3
	86.38	30.618	-1.675	.069	40	.17400	+.04	-11.07	-8.33	-.12	-.14	6.9
	88.61	30.702	-0.490	.045	29	.24400	-.28	-10.66	-8.82	-.43	-.33	6.5
80.61	29.589	-12.790	.710	11	.02800	+1.09	-11.53	-7.68	+.08	-.32	2.5	
3000	101.02	49.503	-2.090	.100	22	.00780	-.11	-11.17	-9.10	+.28	+.26	7.5
	101.34	49.466	-1.570	.150	22	.00810	-.16	-11.07	-9.22	+.19	+.18	6.2
3024	108.03	68.529	-2.002	.125	35	.00146	-.01	-11.71	-9.65	+.24	+.19	6.4
	106.44	68.498	-1.557	.226	33	.00103	+.26	-11.31	-9.81	-.03	-.18	3.0
3037	109.45	59.912	-0.162	.008	40	.00459	+.05	-10.64	-10.46	-.48	-.67	6.2
3053	89.14	15.983	-0.267	.024	60	.98000	-1.20	-11.21	-8.31	+.12	+.11	7.8
	79.80	15.296	-0.881	.044	39	.37200	+.25	-10.60	-7.90	-.20	-.19	5.4
	74.73	13.833	-7.800	.280	13	.03000	+1.52	-10.79	-7.23	+.12	+.15	1.7
	89.30	15.941	-0.102	.026	52	.98000	-1.20	-10.78	-8.73	-.28	-.30	1.9
	80.83	15.431	-0.873	.030	41	.50300	+.02	-10.70	-7.87	-.10	-.09	6.3
	75.36	14.244	-5.240	.140	23	.05800	+1.22	-10.97	-7.73	+.06	+.09	2.4
3072	92.13	38.758	-1.436	.153	20	.01440	-.53	-11.26	-8.96	-.28	-.02	6.2
	92.09	38.786	-1.692	.157	22	.01430	-.52	-11.32	-8.89	-.21	+.04	7.0
3074	94.09	55.146	-1.140	.044	31	.00760	-.14	-11.12	-9.46	-.62	-.65	7.6
	93.76	55.243	-2.002	.070	29	.00710	-.11	-11.31	-9.23	-.41	-.45	7.5
3076	86.30	16.638	-0.623	.041	39	.22900	-.49	-11.10	-8.19	+.01	+.17	7.8
	80.70	15.633	-3.680	.320	17	.11000	+.24	-11.33	-7.47	+.29	+.27	4.8
	77.94	14.095	-9.160	.640	14	.03100	+.92	-11.28	-7.17	+.39	+.20	2.9
	87.39	16.709	-0.582	.072	37	.25600	-.75	-11.30	-8.21	+.08	+.30	5.5
	82.74	16.145	-2.100	.260	21	.15900	-.06	-11.31	-7.69	+.23	+.28	4.4
	79.75	15.219	-6.300	1.090	11	.08300	+.44	-11.42	-7.26	+.43	+.36	2.1
	77.78	13.828	-9.320	1.730	11	.02700	+1.01	-11.27	-7.17	+.38	+.16	0.9
	3088	94.35	25.688	-0.791	.050	39	.03440	-.38	-11.26	-8.74	+.12	+.16
87.49		24.874	-4.910	.360	19	.00780	+.72	-11.27	-8.13	+.17	+.12	3.6
94.55		25.681	-0.656	.037	41	.03500	-.41	-11.18	-8.82	+.06	+.09	7.6
87.41		24.901	-5.090	.500	16	.00750	+.74	-11.28	-8.12	+.17	+.13	2.7
3217	98.68	47.914	-2.510	.380	16	.00398	+.18	-11.00	-9.09	+.11	+.02	3.2
	99.61	47.947	-1.150	.390	17	.00493	+.01	-10.73	-9.40	-.12	-.18	0.7
3228	96.76	40.612	-2.451	.140	25	.00244	+.05	-11.24	-9.03	+.03	-.04	6.2
	97.61	40.528	-1.706	.119	27	.00278	-.06	-11.16	-9.17	-.05	-.08	6.6
3234	83.63	28.478	-2.568	.134	25	.01080	+.20	-11.13	-8.49	-.50	-.45	5.6
	83.97	28.554	-2.674	.209	24	.01170	+.14	-11.14	-8.46	-.44	-.40	5.2
3250	95.36	29.075	-1.448	.083	32	.01590	-.46	-11.34	-8.70	+.24	+.16	7.8
	88.06	28.080	-6.330	.470	14	.00327	+.75	-11.24	-8.25	+.10	+.16	3.1
	93.01	28.885	-1.851	.085	32	.01240	-.13	-11.22	-8.62	+.13	+.09	7.6

TABLE 1.2.—Basic physical data for 413 Super-Schmidt meteors: Accelerations.—Continued

Traill No.	H	v	\dot{v}	p.e.	n	m_1	s	log σ	log ρ_{obs}	Δ log ρ_{obs}	Δ log ρ_{corr}	P
3265	100.06	41.215	-1.848	.056	32	.00782	-.10	-11.35	-9.00	+.31	+.30	7.5
3271	95.10	47.214	-1.226	.079	28	.01960	-.20	-11.10	-9.16	-.24	-.30	7.0
	95.02	47.236	-1.129	.059	29	.01940	+.19	-11.06	-9.20	-.28	-.32	5.6
3277	100.41	50.449	-3.270	.070	25	.00771	-.20	-11.47	-8.93	+.41	+.36	7.8
	99.46	50.120	-3.120	.320	22	.00663	-.05	-11.33	-8.96	+.30	+.25	5.1
3286					0							
3288	81.27	20.755	-0.196	.004	63	.04550	-.15	-10.44	-9.12	-1.31	-1.13	7.7
	81.70	21.060	-0.255	.007	50	.04820	-.21	-10.57	-9.01	-1.17	-.94	7.9
3295	95.29	32.005	-1.442	.201	28	.00742	-.25	-11.15	-8.89	+.05	+.10	4.0
	94.69	31.986	-1.596	.184	28	.00680	-.15	-11.16	-8.86	+.03	+.08	5.4
3299	93.28	28.718	-2.310	.110	26	.00992	-.05	-11.13	-8.55	+.23	+.28	6.5
	93.70	28.730	-1.280	.130	29	.01082	-.14	-10.98	-8.79	+.02	+.07	5.3
3303	80.47	17.164	-2.650	.110	27	.02330	+.04	-11.21	-7.92	-.17	-.13	6.9
	82.14	17.310	-0.078	.080	14	.03070						0.0
3307	88.11	19.007	-1.076	.089	29	.06050	-.20	-11.22	-8.26	+.09	+.17	6.3
	82.07	17.684	-10.270	.880	13	.01690	+.70	-11.37	-7.41	+.46	+.23	3.3
	88.62	19.071	-1.001	.053	33	.06320	-.24	-11.11	-8.29	+.10	+.19	7.2
	82.13	17.693	-7.230	1.040	13	.01740	+.68	-11.20	-7.55	+.32	+.10	7.1
3312	84.35	15.852	-2.623	.053	38	.04780	-.05	-11.37	-7.75	+.30	+.33	7.3
	85.65	16.002	-1.970	.080	46	.05530	-.19	-11.41	-7.86	+.29	+.37	7.8
3327	97.06	35.709	-2.160	.320	24	.00338	-.08	-11.15	-8.93	+.15	+.17	3.7
	96.96	35.719	-2.230	.270	18	.00328	-.05	-11.15	-8.92	+.15	+.16	4.4
3332	87.24	24.265	-1.188	.049	35	.03910	-.52	-11.22	-8.49	-.21	-.35	8.8
	78.65	23.513	-3.420	.300	18	.01090	+.57	-10.92	-8.19	-.58	-.40	3.7
	84.73	24.098	-1.668	.131	30	.03010	-.16	-11.18	-8.37	-.29	-.33	6.7
	79.20	23.376	-4.090	.540	19	.00870	+.69	-10.96	-8.14	-.49	-.27	7.5
3334	102.18	53.381	-2.131	.093	24	.00526	-.18	-11.23	-9.22	+.25	+.21	7.8
3340	96.69	62.738	-1.006	.117	24	.00588	-.53	-11.36	-9.67	-.67	-.45	6.2
	95.87	62.609	-1.715	.185	25	.00542	-.40	-11.47	-9.44	-.65	-.34	5.9
3342	81.62	19.459	-0.251	.010	60	.44960	-.73	-10.97	-8.62	-.79	-.33	9.2
	79.28	19.344	-0.602	.014	51	.36710	-.34	-11.10	-8.27	-.61	-.40	8.3
	76.71	19.000	-1.789	.054	31	.20720	+.20	-10.99	-7.86	-.38	-.43	6.2
	74.72	16.790	-45.696	3.290	7	.00840	+1.79	-11.29	-6.81	+.54	-.26	1.1
	81.84	19.471	-0.226	.010	59	.45620	-.77	-10.96	-8.67	-.67	-.41	9.2
	79.23	19.344	-0.605	.022	41	.36500	-.34	-11.12	-8.27	-.61	-.40	8.3
	76.40	18.934	-1.932	.060	27	.17640	+.31	-10.91	-7.85	-.19	-.49	5.7
3344	88.21	18.603	-2.430	.540	21	.00810	+.29	-10.88	-8.18	+.16	+.27	1.7
	89.42	18.729	-1.566	.096	28	.01240	-.03	-10.81	-8.32	+.14	+.14	6.5

TABLE 1.2.—Basic physical data for 418 Super-Schmidt meteors: Accelerations.—Continued

Traill No.	H	v	\dot{v}	p.e.	n	m_1	s	log σ	log ρ_{obs}	Δ log ρ_{obs}	Δ log ρ_{corr}	p
1355	86.19	33.470	-9.890	.420	20	.00460	-.36	-11.70	-8.16	+.03	+.14	8.3
	86.58	33.593	-7.980	.430	16	.00530	-.61	-11.60	-8.24	-.02	+.15	8.1
1360	88.59	43.136	-18.200	1.300	14	.00410	+.24	-11.74	-8.13	+.26	+.17	5.4
	88.73	43.110	-17.900	1.200	13	.00440	+.19	-11.74	-8.13	+.27	+.20	5.6
1377	102.88	65.212	-1.320	.110	23	.00353	-.23	-11.13	-9.66	-.14	-.12	6.3
	102.84	65.270	-1.540	.120	21	.00357	-.22	-11.20	-9.59	-.07	-.05	6.3
1379	92.14	24.659	-2.030	.180	28	.01520	+.01	-10.95	-8.41	+.27	+.29	5.6
	91.96	24.561	-1.300	.830	17	.01430	+.07	-10.74	-8.61	+.06	+.05	0.0
1386	89.63	24.362	-2.127	.186	27	.01320	-.26	-11.05	-8.40	+.08	+.15	6.4
	89.49	24.487	-1.910	.621	18	.01280	-.22	-10.98	-8.46	+.00	+.07	0.8
1393	92.72	35.877	-2.022	.119	24	.00730	-.11	-11.19	-8.85	-.12	-.12	6.8
	91.94	35.769	-3.266	.122	25	.00640	+.01	-11.32	-8.65	+.02	+.04	7.0
1399	93.11	42.701	-3.160	.420	18	.00468	-.21	-11.25	-8.87	-.11	-.07	3.9
	91.34	42.375	-7.190	.180	25	.00259	+.27	-11.51	-8.59	+.03	-.09	5.9
	91.78	42.608	-6.810	.410	15	.00302	+.17	-11.50	-8.60	+.05	-.03	5.7
1405	91.19	26.037	-0.395	.020	40	.45800	-.86	-11.07	-8.68	-.08	+.22	8.4
	82.96	24.880	-8.020	.340	16	.09900	+.63	-11.37	-7.55	+.39	+.22	4.4
	91.01	26.057	-0.374	.048	28	.45300	-.83	-11.03	-8.70	-.11	+.18	5.6
	84.89	25.547	-3.320	.270	13	.20200	+.18	-11.26	-7.86	+.23	+.21	5.0
	81.80	24.227	-14.920	1.700	9	.04200	+.06	-11.29	-7.38	+.47	+.17	2.0
1407	89.80	34.874	-2.840	.370	16	.00500	+.43	-10.84	-8.73	-.24	-.33	3.1
1411	90.90	23.708	-4.190	.460	20	.00844	-.06	-11.24	-8.15	+.43	+.48	5.1
	88.16	24.150	-1.430	1.800	9							0.0
1416	90.18	25.400	+0.000	.000	8	.00670						0.0
	92.21	25.168	-1.518	.112	26	.01500	+.05	-10.87	-8.56	+.13	+.13	5.5
1424	95.37	43.114	-0.599	.035	29	.03460	-.31	-11.00	-9.31	-.36	-.20	7.4
	95.30	43.197	-0.936	.056	25	.03430	-.29	-11.19	-9.12	-.18	-.03	7.3
1450	93.29	42.584	-2.340	.330	17	.00860	-.24	-11.24	-8.91	-.13	+.06	4.0
	91.87	42.270	-13.000	.450	14	.00490	+.25		-8.24	+.42	+.25	6.0
1463	96.59	43.380	-0.662	.066	26	.01130	-.48	-11.05	-9.43	-.39	-.16	6.1
	95.52	43.282	-1.400	.169	23	.01010	-.31	-11.24	-9.12	-.16	-.03	4.9
1487	92.65	41.471	-4.940	.230	21	.00476	-.17	-11.41	-8.65	+.07	+.16	7.7
	92.24	41.233	-7.230	.440	17	.00416	-.06	-11.53	-8.49	+.20	+.25	6.6
1497	89.83	27.995	-1.750	.140	23	.00806	+.17	-10.91	-8.68	-.19	-.26	5.1
1567	93.24	26.774	-0.631	.032	38	.03600	-.38	-10.90	-8.87	-.10	+.10	7.6
	92.90	26.764	-0.919	.044	34	.03440	-.32	-10.99	-8.71	+.03	+.20	8.2

TABLE 1.2.—Basic physical data for 413 Super-Schmidt meteors: Accelerations.—Continued

Trail No.	H	v	v	p.e.	n	m_1	s	log σ	log ρ_{obs}	Δ log ρ_{obs}	Δ log ρ_{corr}	p
1573	90.60	36.710	-0.549	.039	37	.0628C	-.71	-10.94	-9.12	-.56	-.32	8.2
	90.66	36.783	-0.632	.035	36	.06300	-.72	-11.00	-9.06	-.50	-.25	8.2
1604	98.46	30.903	-1.189	.084	23	.0256C	-.17	-10.94	-8.77	+.47	+.40	7.0
	98.55	30.836	-1.045	.108	21	.0259C	-.18	-10.89	-8.82	+.37	+.36	5.4
1610	92.31	41.184	-6.900	.170	24	.00507	-.34	-11.65	-8.49	+.21	+.28	8.3
	91.83	40.861	-7.140	.250	20	.00461	-.22	-11.58	-8.48	+.18	+.23	7.9
1612	103.73	58.616	-1.118	.067	24	.00362	-.20	-11.14	-9.63	-.05	-.03	7.0
1629	94.42	33.686	-2.092	.102	30	.00562	-.02	-11.25	-8.81	+.06	+.10	6.4
	93.62	33.560	-2.170	.35C	25	.00474	+.12	-11.19	-8.87	-.02	+.05	2.6
1633	92.50	23.837	-0.721	.063	31	.03450	-.64	-11.17	-8.71	+.00	+.05	7.2
	86.98	23.462	-2.591	.075	25	.020CC	+.05	-11.23	-8.22	+.04	+.05	6.9
	91.27	23.706	-0.813	.052	36	.0319C	-.48	-11.07	-8.67	-.06	-.02	7.8
	86.19	23.297	-2.870	.180	25	.01660	+.19	-11.01	-8.20	-.01	-.00	5.6
3636	91.61	23.301	-0.523	.012	59	.185CC	-.71	-11.29	-8.59	+.05	+.14	9.1
	84.70	22.764	-2.408	.032	39	.114CC	-.03	-11.43	-7.98	+.09	+.12	7.2
	79.37	20.940	-11.440	.220	21	.03050	+.80	-11.53	-7.42	+.25	+.19	1.7
	88.78	23.198	-1.069	.018	36	.16200	-.44	-11.44	-8.30	+.10	+.17	8.6
	79.47	20.983	-9.120	.520	18	.0319C	+.77	-11.46	-7.51	+.16	+.11	3.4
3640	81.5C	15.484	-0.299	.004	71	4.55000	-.85	-10.96	-8.02	-.19	-.05	9.4
	74.43	14.937	-1.823	.030	31	2.37000	+.08	-11.04	-7.29	+.04	-.02	6.7
	71.06	14.059	-4.510	.174	21	1.01000	+.62	-11.34	-6.97	+.15	-.02	4.4
	68.08	11.492	-8.256	.139	19	.11800	+.63	-11.00	-6.84	+.10	-.27	1.5
	79.24	15.402	-0.524	.013	61	3.96000	-.51	-11.01	-7.79	-.13	-.06	8.7
	73.97	14.814	-1.823	.045	31	2.11000	+.16	-11.01	-7.30	-.00	-.07	6.4
	69.69	13.135	-8.650	.141	21	.53000	+.94	-11.24	-6.72	+.32	+.08	3.2
3643	94.14	26.818	-1.133	.105	37	.01160	-.12	-11.04	-8.78	+.07	+.14	6.0
	93.86	26.836	-1.487	.155	28	.01110	-.07	-11.13	-8.67	+.15	+.20	5.1
3651	86.37	25.095	-0.385	.023	35	.01970	+.00	-10.34	-9.11	-.90	-.90	6.4
	85.44	25.052	-0.733	.063	29	.01590	+.17	-10.61	-8.86	-.73	-.87	5.1
3655	92.57	26.532	-0.837	.032	45	.0418C	-.56	-11.28	-8.72	-.00	-.06	8.9
	85.51	25.900	-4.610	.240	21	.01520	+.40	-11.29	-8.10	+.04	-.01	4.8
	91.56	26.483	-1.197	.056	41	.03950	-.46	-11.36	-8.57	+.06	+.01	8.6
	85.87	25.920	-3.700	.220	21	.01680	+.34	-11.24	-8.18	-.01	-.06	5.0
3657	102.21	55.667	-2.640	.100	17	.00279	-.27	-11.36	-9.25	+.22	+.27	8.1
	101.68	55.535	-4.580	.670	14	.00253	-.16	-11.54	-9.02	+.41	+.42	3.8
3663	94.39	30.153	-0.868	.020	41	.0306C	-.39	-11.33	-8.86	+.01	+.13	8.4
	88.30	29.527	-5.180	.140	22	.01430	+.30	-11.46	-8.17	+.20	+.19	5.8
	94.85	30.232	-0.931	.062	30	.03170	-.45	-11.38	-8.82	+.08	+.21	7.7
	88.14	29.419	-5.190	.160	22	.01350	+.34	-11.44	-8.18	+.17	+.16	5.6

TABLE 1.2.—Basic physical data for 413 Super-Schmidt meteors: Accelerations.—Continued

Trail No.	H	v	\dot{v}	p.e.	n	m_1	s	log σ	log ρ_{obs}	$\Delta \log \rho_{\text{obs}}$	$\Delta \log \rho_{\text{corr}}$	p
1784	92.95	37.349	-2.150	.210	18	.01280	-.13	-10.99	-8.77	-.02	+.05	5.3
	92.72	37.290	-3.840	.170	17	.01170	-.05	-11.20	-8.53	+.20	+.23	7.3
1786	84.60	21.103	-1.336	.030	39	.05340	+.03	-10.58	-8.28	-.21	-.17	6.9
	84.61	21.073	-1.545	.032	39	.05360	+.02	-10.64	-8.21	-.14	-.10	7.0
1813	93.90	22.597	-0.819	.023	66	.02430	+.10	-10.88	-8.66	+.17	+.20	6.7
	94.17	22.611	-0.676	.039	63	.02650	+.03	-10.85	-8.73	+.12	+.15	6.3
1847	92.19	58.480	-16.640	1.020	10	.00106	-.13	-11.75	-8.64	+.05	+.05	6.8
	92.37	58.690	-26.410	1.400	11	.00110	-.17	-11.97	-8.43	+.27	+.29	7.0
1861	98.90	52.165	-1.086	.044	30	.03230	-.39	-11.32	-9.23	-.01	+.06	8.4
	98.40	52.149	-1.014	.035	28	.03140	-.35	-11.24	-9.26	-.08	-.02	8.3
1877	92.24	25.683	-1.252	.030	46	.02210	-.25	-11.27	-8.60	+.09	+.16	8.0
	88.68	25.470	-2.048	.059	35	.01680	+.02	-11.20	-8.42	-.02	+.03	7.0
1886	94.83	28.976	-0.749	.024	43	.04060	-.48	-11.45	-8.84	+.06	+.06	8.7
	90.32	28.622	-1.848	.079	24	.02740	-.01	-11.40	-8.50	+.03	+.08	7.1
	86.04	27.840	-4.385	.182	20	.00970	+.66	-11.28	-8.25	-.07	+.05	4.2
	95.58	28.930	-0.606	.027	41	.04200	-.54	-11.40	-8.93	+.03	+.07	8.8
	90.60	28.608	-1.497	.043	31	.02840	-.05	-11.34	-8.58	-.02	+.02	7.3
	85.97	27.799	-4.320	.245	19	.00940	+.68	-11.75	-8.26	-.08	+.04	4.2
4103	87.39	18.703	-1.690	.320	26	.01280	-.14	-10.97	-8.28	+.01	+.11	2.3
	86.93	18.649	-2.550	.260	24	.01150	-.04	-11.08	-8.11	+.14	+.21	5.1
4111	82.69	16.798	-0.165	.043	33	.86500	-1.37	-11.26	-8.59	-.67	-.17	2.0
	78.01	16.583	-1.010	.130	20	.63300	-.37	-11.07	-7.83	-.26	-.09	5.0
	75.27	16.158	-3.260	.390	14	.29200	+.32	-11.02	-7.41	-.03	-.08	3.4
	73.48	15.389	-15.790	2.240	9	.03400	+.140	-11.17	-7.00	+.27	+.15	1.0
	81.75	16.738	-0.186	.062	27	.85000	-1.20	-11.11	-8.53	-.69	-.24	1.0
	77.99	16.600	-0.856	.110	19	.63100	-.37	-11.00	-7.91	-.34	-.17	5.0
	75.26	16.177	-2.330	.260	15	.29000	+.32	-10.88	-7.56	-.18	-.23	4.0
	73.32	15.046	-17.730	1.320	10	.02500	+.152	-11.12	-6.97	+.29	-.17	1.4
4125	80.66	18.317	-0.603	.136	18	.04340	-.31	-10.60	-8.53	-.77	-.60	1.6
	76.32	17.624	-7.510	.480	11	.01120	+.68	-11.11	-7.60	-.15	-.47	3.7
	81.13	18.348	-0.724	.140	20	.04650	-.40	-10.71	-8.44	-.64	-.43	2.5
	76.48	17.631	-5.850	.440	13	.01230	+.62	-10.97	-7.69	-.23	-.52	1.5
	79.11	18.217	-1.508	.034	29	.03230	+.01	-10.87	-9.17	-.52	-.51	7.0
79.28	18.206	-1.450	.042	33	.03350	-.03	-10.86	-8.18	-.52	-.49	7.2	
4136	99.19	53.427	-2.754	.087	21	.00920	-.41	-11.55	-9.03	+.21	+.27	8.5
	98.80	53.061	-1.900	.230	22	.00890	-.36	-11.35	-9.19	+.02	+.02	5.0
4138	104.52	68.527	-3.050	.260	24	.00183	-.04	-11.47	-9.43	+.21	+.16	5.8
	105.44	68.566	-2.890	.340	18	.00207	-.17	-11.54	-9.44	+.26	+.24	5.4
4141	81.31	16.741	-1.039	.083	22	.15300	-.63	-11.04	-8.03	-.22	+.11	7.2
	77.62	15.783	-7.780	1.080	9	.04700	+.48	-11.44	-7.28	+.26	+.10	2.5
	80.10	16.603	-2.039	.037	31	.12100	-.25	-10.94	-7.77	-.05	+.11	8.0

TABLE 1.2.—Basic physical data for 413 Super-Schmidt meteors: Accelerations.—Continued

Trail No.	R	v	\dot{v}	p.e.	n	m_1	s	log σ	log ρ_{Obs}	Δ log ρ_{Obs}	Δ log ρ_{Corr}	P
	81.04	16.815	-1.133	.187	19	.14800	-.58	-11.21	-8.00	-.21	+.09	3.6
	77.86	16.018	-7.370	1.500	10	.05100	+.44	-11.40	-7.30	+.26	+.11	1.5
	79.92	16.689	-2.124	.072	29	.11500	-.20	-10.91	-7.76	-.05	+.08	7.8
4143	92.98	29.824	-0.996	.020	38	.01006	-.10	-11.10	-8.95	-.20	-.15	7.5
	91.41	29.533	-1.927	.048	29	.00766	+.13	-11.19	-8.69	-.07	-.18	6.5
4147	81.66	22.656	-0.108	.030	37	.84300	-1.06		-9.03	-1.19	-.90	1.0
	74.94	22.288	-3.030	.230	17	.29700	+.32	-11.30	-7.72	-.36	-.38	4.6
	71.82	20.772	-19.460	2.300	10	.05600	+.19	-11.22	-7.09	+.07	-.15	1.5
	81.99	22.668	-0.460	.036	31	.85400	-1.12	-11.25	-8.40	-.54	-.23	7.7
	75.96	22.383	-1.870	.210	17	.38400	+.14	-11.06	-7.90	-.47	-.45	4.5
	72.43	21.444	-8.910	.510	13	.11900	+.83	-11.27	-7.35	-.15	-.29	3.2
	75.89	22.348	-1.190	.250	28	.37700			-8.09	-.67		0.0
	78.41	22.600	-0.718		64	.64000			-8.25	-.65		0.0
	78.48	22.554	-0.638		63	.64700			-8.29	-.69		0.0
4151	103.24	70.875	-1.174	.104	28	.00355	-.11	-11.28	-9.78	-.23	-.23	6.0
4153	90.66	20.496	-0.447	.052	22	.12500	-.55	-11.02	-8.60	-.04	+.21	5.3
	85.48	19.767	-5.360	.260	15	.03370	+.57	-11.18	-7.68	+.46	+.22	4.6
	90.90	20.523	-0.521	.051	32	.12200	-.49	-11.06	-8.54	+.04	+.26	6.1
	85.46	19.728	-5.880	.420	15	.03340	+.57	-11.21	-7.64	+.49	+.26	4.1
	89.47	20.412	-0.801	.013	37	.10900			-8.37	+.09		0.0
	89.14	20.429	-1.018	.016	47	.10500			-8.27	+.16		0.0
4181	95.55	30.463	-0.241	.028	35	.14200	-.75	-10.80	-9.20	-.24	+.04	5.5
	93.81	30.433	-0.601	.010	46	.12300	-.42	-11.03	-8.82	-.00	+.13	8.5
	87.99	29.616	-7.310	.570	11	.03220	+.62	-11.28	-7.91	+.43	+.11	3.5
	94.33	30.353	-0.513	.038	29	.12800	-.49	-11.00	-8.88	-.02	+.15	7.0
	92.57	30.288	-0.896	.014	40	.10900	-.27	-11.10	-8.66	+.06	+.13	8.1
	88.00	29.626	-6.990	.580	11	.03220	+.62	-11.26	-7.93	+.41	+.09	3.5
4199	91.67	31.787	-2.936	.087	27	.00563	-.05	-11.49	-8.62	+.02	+.08	7.3
	92.50	31.690	-1.665	.044	34	.00635	-.17	-11.29	-8.84	-.13	-.06	7.7
	88.69	31.061	-5.860	.520	16	.00255	+.50	-11.32	-8.41	-.01	-.02	3.9
4216	102.65	60.355	-1.730	.120	25	.00230	-.19	-11.31	-9.53	-.03	-.05	7.0
	101.72	60.266	-1.670	.160	21	.00198	-.04	-11.23	-9.57	-.14	-.18	5.8
4229	97.63	33.848	-1.311	.054	40	.00940	-.12	-11.16	-8.95	+.17	+.13	7.5
	98.37	33.854	-0.980	.065	38	.01050	-.24	-11.25	-9.06	+.12	+.08	7.2
4289	85.29	18.299	-1.513	.034	38	.12700	-.32	-11.13	-7.97	+.15	+.07	8.2
	79.03	16.973	-5.330	.160	21	.02250	+.87	-11.15	-7.61	+.03	+.08	3.4
	85.33	18.295	-1.653	.073	35	.12800	-.33	-11.17	-7.94	+.18	+.10	8.3
4311	84.17	19.523	-3.773	.175	23	.03400	+.54	-10.79	-7.82	+.21	+.22	4.7
	84.10	19.456	-3.950	.220	20	.03110	+.59	-10.82	-7.81	+.22	+.22	4.1
4313	79.95	15.150	-0.569	.032	43	.12200	-.25	-10.95	-8.24	-.53	-.44	7.2
	76.57	14.775	-1.777	.152	23	.07600	+.17	-11.00	-7.79	-.32	-.33	5.1
	74.78	14.313	-2.830	.200	21	.03600	+.63	-10.90	-7.67	-.32	-.44	3.9

TABLE 1.2.—Basic physical data for 413 Super-Schmidt meteors: Accelerations.—Continued

Trail No.	H	v	\dot{v}	p.e.	n	m_1	s	log σ	log ρ_{obs}	$\Delta \log \rho_{\text{obs}}$	$\Delta \log \rho_{\text{corr}}$	P
	79.86	15.130	-0.667	.036	44	.12200	-.25	-11.02	-8.17	-.47	-.38	7.2
	76.51	14.740	-2.145	.156	23	.07400	+.19	-11.07	-7.71	-.25	-.26	5.6
	74.74	14.255	-3.009	.128	25	.03490	+.65	-10.93	-7.65	-.30	-.43	4.3
4320	85.89	25.659	-1.136	.046	33	.04380	-.58	-11.17	-8.55	-.38	-.37	8.9
	81.67	25.283	-2.790	.140	25	.02550	+.07	-11.21	-8.22	-.38	-.44	6.1
	85.31	25.613	-1.074	.066	31	.04140	-.48	-11.09	-8.58	-.46	-.46	7.8
	81.83	25.336	-3.210	.160	24	.02630	+.04	-11.28	-8.16	-.31	-.36	6.2
4330	106.05	64.163	-0.398	.035	32	.01540	+.18	-10.55	-9.95	-.14	-.27	5.0
	107.25	64.122	-0.115	.035	31	.01690	+.11	-10.02	-10.47	-.64	-.73	0.7
4340	92.37	22.525	-0.737	.038	42	.15800	-.63	-11.27	-8.43	+.27	+.41	8.1
	86.99	21.942	-3.400	.100	21	.08740	+.09	-11.37	-7.83	+.43	+.46	6.7
	84.36	21.091	-7.630	.290	17	.04100	+.57	-11.37	-7.56	+.49	+.45	4.6
	91.85	22.496	-1.021	.060	38	.15300	-.56	-11.37	-8.30	+.36	+.49	8.0
	87.01	21.924	-3.660	.230	21	.08790	+.08	-11.40	-7.80	+.46	+.49	6.1
	84.42	21.126	-6.920	.360	19	.04170	+.56	-11.35	-7.60	+.45	+.41	4.2
4351	88.24	24.723	-0.983	.079	25	.04320	-.63	-11.23	-8.58	-.22	-.16	7.2
	83.45	24.182	-3.250	.170	22	.01450	+.43	-11.06	-8.20	-.22	-.18	4.7
	85.65	24.500	-1.991	.071	34	.03200	-.18	-11.21	-8.31	-.16	-.11	7.8
4360	90.94	45.162	-5.260	.190	21	.00465	-.23	-11.61	-8.70	-.12	-.01	7.9
	90.29	44.927	-7.410	.290	19	.00397	-.06	-11.64	-8.57	-.04	-.05	7.3
4369	93.65	26.553	-0.890	.050	38	.01990	-.37	-11.24	-8.80	+.01	-.00	7.5
	87.12	26.010	-3.940	.250	21	.00960	+.29	-11.35	-8.24	+.03	+.00	5.2
	91.01	26.448	-1.504	.077	36	.01630	-.13	-11.25	-8.59	-.00	-.02	6.8
4388	79.87	15.507	-1.234	.042	41	.12400	-.43	-11.11	-7.92	-.22	-.28	8.5
	76.32	14.995	-1.722	.089	27	.06360	+.22	-11.01	-7.85	-.40	-.42	5.5
	74.09	14.431	-4.170	.155	25	.02330	+.80	-11.01	-7.57	-.27	-.24	3.7
	78.74	15.372	-1.350	.041	35	.10400	-.20	-11.04	-7.90	-.28	-.33	7.8
	75.91	14.904	-1.873	.109	25	.05690	+.30	-10.94	-7.82	-.40	-.41	5.2
	74.36	14.527	-3.727	.190	21	.02710	+.72	-11.00	-7.60	-.28	-.26	3.6
4394	90.15	33.805	-0.924	.071	26	.00650	-.16	-10.88	-9.15	-.63	-.53	6.2
	90.18	33.705	-0.879	.130	25	.00653	-.16	-10.86	-9.17	-.65	-.55	3.8
4454	106.30				0							0.0
	106.20				0							0.0
4464	94.08	21.813	-0.153	.012	59	.82300	-1.42	-11.44	-8.85	-.01	+.14	7.9
	85.45	21.549	-1.119	.040	28	.65100	-.51	-11.58	-8.01	+.12	+.21	8.7
	80.72	20.781	-2.218	.060	19	.44400	-.03	-11.50	-7.74	+.03	+.08	7.2
	77.39	19.648	-6.128	.121	17	.24600	+.39	-11.61	-7.33	+.20	+.22	5.4
	74.76	17.137	-15.890	.530	14	.03150	+1.42	-11.23	-7.10	+.25	+.20	1.9
	93.43	21.825	-0.209	.013	57	.81700	-1.34	-11.52	-8.72	+.07	+.21	8.8
	84.24	21.382	-1.268	.032	31	.60900	-.40	-11.59	-7.96	+.08	+.15	8.5
	79.04	20.355	-3.763	.068	23	.34800	+.16	-11.61	-7.52	+.12	+.16	6.4
	75.48	18.109	-11.343	.165	19	.07890	+.99	-11.31	-7.16	+.24	+.22	3.0

TABLE 1.2.—Basic physical data for 413 Super-Schmidt meteors: Accelerations.—Continued

Trail No.	H	v	\dot{v}	p.e.	n	m_1	s	log σ	log ρ_{obs}	Δ log ρ_{obs}	Δ log ρ_{corr}	P
4472	95.46	23.404	-0.459	.024	41	.04370	-.39	-10.89	-8.86	+.09	+.13	7.6
	94.17	23.357	-0.814	.014	51	.0382C	-.22	-11.00	-8.63	+.22	+.22	7.9
	90.12	22.831	-4.130	.14C	21	.0115C	+.64	-11.03	-8.08	+.44	+.74	4.3
	95.36	23.447	-0.642	.028	43	.04330	-.38	-11.03	-8.72	+.22	+.26	8.4
	94.19	23.383	-0.844	.019	52	.03830	-.22	-11.07	-8.61	+.24	+.24	7.9
	90.45	22.910	-3.030	.250	23	.0136C	+.55	-10.95	-8.19	+.35	+.18	3.8
4505	94.81	25.254	-1.885	.078	34	.01180	-.11	-11.31	-8.50	+.40	+.38	7.5
	94.43	25.218	-2.255	.111	31	.01120	-.06	-11.34	-8.43	+.44	+.41	6.6
4507	92.67	28.812	-1.925	.089	31	.00482	-.09	-11.12	-8.74	-.01	+.07	7.4
	92.23	28.774	-2.371	.113	27	.00443	-.01	-11.17	-8.68	+.03	+.08	7.1
4513	89.35	18.902	-0.836	.069	33	.131CC	-.17	-11.12	-8.26	+.19	+.30	6.2
	89.46	18.882	-0.788	.114	29	.136CC	-.21	-11.08	-8.27	+.19	+.31	3.9
4534	97.24	31.705	-0.332	.012	43	.19500	-1.02	-11.32	-9.05	+.04	+.13	9.6
	91.52	31.424	-1.562	.044	25	.138CC	-.26	-11.24	-8.42	+.21	+.20	8.0
	87.53	30.879	-5.410	.18C	17	.04900	+.52	-11.23	-8.01	+.29	+.17	4.8
	97.76	31.722	-0.325	.013	40	.19800	-1.09	-11.37	-9.06	+.07	+.16	9.6
	91.74	31.492	-1.527	.036	25	.14200	-.29	-11.27	-8.43	+.22	+.21	8.1
	87.77	30.961	-4.250	.180	19	.055CC	+.46	-11.19	-8.10	+.22	+.11	5.1
4542	92.43	23.639	-1.490	.049	35	.02020	-.41	-11.20	-8.47	+.24	+.41	8.5
	91.46	23.538	-2.171	.083	29	.01770	-.23	-11.23	-8.32	+.31	+.42	7.9
4574	95.22	28.418	-1.292	.028	41	.00818	-.07	-11.11	-8.82	+.11	+.18	7.3
	95.13	28.351	-0.900	.130	36	.00807	-.03	-10.94	-8.98	-.05	+.00	3.6
4596	88.44	21.719	-1.579	.027	50	.0281C	-.12	-11.30	-8.32	+.06	+.10	7.5
	87.29	22.010	-1.697	.028	49	.02420	+.07	-11.27	-8.32	-.04	+.01	7.0
4618	91.39	20.394	-0.963	.030	46	.01990	-.11	-11.18	-8.53	+.09	+.21	7.5
	87.27	19.661	-7.660	.410	16	.00672	+.63	-11.17	-7.76	+.52	+.19	3.9
	91.73	20.368	-0.757	.035	39	.02070	-.15	-10.92	-8.63	+.02	+.16	7.7
	88.82	20.328	-2.520	.340	20	.01290	+.24	-11.05	-8.16	+.25	+.15	3.6
4622	109.79	67.813	-1.053	.275	21	.00112	-.05	-11.05	-9.96	+.05	+.03	1.5
	110.24	67.781	-0.830	.230	22	.00128	-.19	-11.04	-10.04	-.00	+.07	1.6
4624	88.88	18.353	-0.951	.016	53	.0764C	-.32	-10.96	-8.25	+.16	+.16	8.2
	84.78	17.809	-3.655	.173	19	.0208C	+.65	-10.88	-7.83	+.25	+.24	4.3
	88.24	18.301	-1.530	.033	46	.06910	-.20	-11.04	-8.06	+.30	+.30	7.8
	85.30	17.893	-2.680	.167	22	.02660	+.51	-10.85	-7.93	+.19	+.18	4.4
4645	101.09	58.699	-1.574	.113	23	.00679	-.23	-11.27	-9.19	-.00	+.03	7.1
	100.69	58.795	-2.034	.109	22	.00648	-.18	-11.34	-9.29	+.07	+.08	7.0
4657	94.69	23.589	-0.379	.009	50	.1386C	-.66	-11.30	-8.78	+.11	+.06	9.1
	87.29	22.915	-1.583	.023	40	.0583C	+.28	-11.27	-8.26	+.02	+.02	5.9
	84.64	22.127	-4.031	.079	27	.01930	+.89	-11.21	-7.99	+.08	+.10	3.4
	95.68	23.606	-0.326	.015	35	.14510	-.78	-11.33	-8.84	+.13	+.07	9.3
	89.07	23.176	-1.020	.021	40	.08320	+.01	-11.24	-8.41	+.07	+.00	7.0

TABLE 1.2.—Basic physical data for 413 Super-Schmidt meteors: Accelerations.—Continued

Trail No.	H	v	\dot{v}	p.e.	n	m_{\perp}	s	log σ	log ρ_{obs}	$\Delta \log \rho_{\text{obs}}$	$\Delta \log \rho_{\text{corr}}$	P
	85.26	22.369	-3.130	.066	30	.02820	+.70	-11.21	-8.05	+.07	+.08	4.1
4659	83.92	18.082	-0.723	.011	44	.12100	-.53	-11.00	-8.29	-.28	+.33	8.8
	83.90	18.069	-0.688	.011	47	.12100	-.52	-10.98	-8.31	-.30	+.30	8.8
4677	100.31	41.036	-0.652	.016	49	.02220	-.23	-11.24	-9.29	+.04	+.02	7.9
	99.68	40.996	-0.572	.020	47	.02110	-.17	-11.10	-9.36	-.08	-.11	7.7
4679	92.22	17.403	-0.217	.029	56	.35800	-1.05	-11.14	-8.62	+.07	+.15	4.8
	86.68	17.080	-1.021	.061	31	.21400	-.09	-11.07	-8.01	+.22	+.18	6.7
	83.84	16.237	-4.410	.440	17	.02000	+1.27	-7.67	-7.67	+.34	+.13	1.6
	91.29	17.363	-0.288	.018	56	.34400	-.87	-11.13	-8.50	+.11	+.17	8.4
	86.19	16.978	-1.190	.059	27	.19100	+.02	-11.02	-7.95	+.24	+.19	6.3
	83.66	16.016	-5.930	.360	15	.01300	+1.46	-7.60	-7.60	+.39	+.17	1.6
4683	105.88	67.159	-0.577	.054	22	.00523	-.38	-10.81	-9.98	-.24	-.15	6.7
	104.80	67.080	-0.344	.145	20	.00448						0.0
4701	90.88	29.623	-1.773	.058	45	.01180	-.10	-11.35	-8.67	-.09	-.04	7.5
	91.44	29.644	-1.499	.029	54	.01260	-.17	-11.37	-8.73	-.10	-.05	7.7
	87.38	29.043	-4.230	.210	27	.00588	+.42	-11.40	-8.37	-.08	-.05	4.7
4702	93.67	31.613	-0.117	.027	29	.25300	-.75	-10.40	-9.46	-.65	+.07	1.8
	89.53	31.537	-1.362	.114	19	.17100	-.11	-11.03	-8.45	+.02	+.12	6.0
	85.44	30.796	-13.290	1.500	9	.06800	+.51	-11.61	-7.57	+.56	+.06	3.4
	89.12	31.570	-2.142	.154	14	.16100	-.07	-11.02	-8.26	+.17	+.24	6.6
	88.29	31.200	-5.070	.730	16	.13900	+.05		-7.90	+.46	+.41	3.4
4952	74.10	11.164	-1.283	.048	32	.18300	-.45	-10.99	-7.56	-.25	-.17	8.6
	73.21	11.019	-1.796	.028	39	.15700	-.24	-10.89	-7.43	-.18	-.11	8.0
	71.26	10.484	-3.210	.240	16	.06940	+.41	-10.92	-7.25	-.12	-.10	4.2
	74.23	11.107	-1.100	.042	35	.18700	-.49	-10.93	-7.62	-.31	-.22	8.7
	73.35	10.995	-1.370	.022	42	.17800	-.41	-10.87	-7.53	-.27	-.19	8.5
	71.55	10.626	-2.117	.032	20	.07830	+.34	-10.76	-7.43	-.28	-.26	5.6
4962	92.14	21.269	-0.839	.107	23	.11550	-.69	-11.18	-8.37	+.31	+.03	5.5
	84.69	20.658	-0.388	.405	17	.03270	+.53					0.0
	92.45	21.449	-0.910	.079	25	.11750	-.72	-11.25	-8.34	+.37	+.07	7.3
	84.59	20.856	-2.100	.275	18	.03240	+.53	-10.85	-8.14	-.08	+.05	2.9
4964	88.83	15.751	-0.950	.062	34	.10000	-.49	-10.98	-8.08	+.33	+.42	7.8
	84.88	15.029	-5.380	.770	14	.02560	+.61	-11.15	-7.49	+.60	+.43	2.2
	89.02	15.762	-0.627	.045	39	.09330	-.39	-10.84	-8.27	+.15	+.22	7.6
	84.40	14.853	-4.930	.550	14	.01850	+.79	-11.05	-7.56	+.49	+.28	2.6
4966	94.03	26.143	-0.965	.042	41	.01650	-.24	-11.06	-8.77	+.07	+.21	8.0
	92.19	26.113	-0.684	.057	26	.01280	+.01	-10.70	-8.96	-.27	-.23	5.6
4974	109.08	66.968	-0.618	.018	41	.00540	-.06	-11.20	-9.95	+.01	+.00	7.3
	108.79	66.957	-0.699	.033	43	.00520	-.01	-11.24	-9.90	+.04	-.00	7.1
006	107.43	68.128	-1.330	.190	21	.00155	-.04	-11.03	-9.81	+.04	+.01	3.6
	107.18	67.933	-1.040	.470	19	.00148	+.01	-10.90	-9.92	-.09	-.14	0.0

TABLE 1.2.—Basic physical data for 413 Super-Schmidt meteors: Accelerations.—Continued

Trail No.	H	v	\dot{v}	p.e.	n	m_1	s	log σ	log ρ_{obs}	Δ log ρ_{obs}	Δ log ρ_{corr}	P
.022	94.51	29.993	-0.661	.C78	27	.11700	-.83	-11.32	-8.78	+.10	+.05	5.6
	85.70	29.448	-3.544	.174	15	.05700	+.14	-11.44	-8.13	+.07	+.09	5.8
	80.02	27.812	-15.060	.800	11	.00810	+1.20	-11.33	-7.74	-.03	+.17	7.2
	94.25	29.967	-0.852	.092	27	.11600	-.79	-11.44	-8.67	+.19	+.14	6.5
	85.44	29.356	-2.906	.192	15	.05600	+.15	-11.35	-8.22	-.09	-.02	5.8
80.53	28.308	-10.460	.840	9	.01310	+.39	-11.28	-7.84	-.09	+.08	2.4	
.C45	94.56	42.381	-1.786	.C45	24	.C174C	-.42	-11.08	-8.92	-.04	+.16	8.5
	93.41	42.117	-3.259	.139	21	.01180	+.01	-11.12	-8.71	+.08	+.02	7.0
.047	83.13	16.055	-1.656	.038	37	.07250	-.27	-10.70	-7.90	+.05	+.15	8.1
	83.04	15.977	-1.610	.C44	32	.06980	-.21	-10.53	-7.92	+.02	+.11	7.9
.063	113.36	70.666	-0.810	.045	28	.00169	-.11	-11.24	-10.04	+.19	+.20	6.8
	112.65	70.463	-0.472	.081	32	.00150	+.00	-10.95	-10.29	-.10	-.15	2.8
5073	93.89	20.231	-0.193	.C11	59	.72900	-1.37	-11.37	-8.70	+.13	+.15	8.8
	83.39	19.900	-0.775	.070	29	.32900	+.12	-11.37	-8.20	-.23	-.24	5.3
	78.33	18.304	-12.630	.470	16	.02730	+1.43	-11.14	-7.28	+.31	+.28	1.9
	94.55	20.208	-0.123	.C13	63	.73500	-1.47	-11.25	-8.90	-.02	+.00	6.9
	83.32	19.841	-1.300	.C63	30	.32400	+.13	-11.02	-7.97	-.01	-.01	6.5
78.37	18.395	-11.630	.540	13	.02780	+1.42	-11.11	-7.31	+.28	+.25	1.9	
5079	111.22	67.928	-1.821	.646	17	.00369	-.21	-11.33	-9.55	+.55	+.63	0.8
	110.51	67.746	-0.860	.180	23	.00330	-.11	-10.92	-9.89	+.16	+.18	2.3
5083	107.15	67.254	-1.105	.060	26	.00950	+.08	-10.87	-9.62	+.21	+.13	6.1
	106.34	67.083	-2.328	.C71	25	.00790	+.21	-11.12	-9.32	+.45	+.33	6.2
5101	107.23	67.305	-0.727	.276	20	.00173	+.35	-10.71	-10.05	-.22	-.43	0.6
	107.11	67.436	-0.796	.252	20	.00170	+.35	-10.75	-10.01	-.19	-.40	0.6
5112	103.36	67.303	-2.240	.200	22	.00980	-.45	-11.59	-9.31	+.24	+.26	6.9
	102.53	67.255	-4.170	.140	24	.00930	-.36	-11.80	-9.04	+.45	+.45	8.3
5124	95.37	27.533	-0.713	.C40	45	.C9900	-.69	-11.54	-8.69	+.26	+.04	8.2
	86.70	26.848	-2.021	.C79	25	.04680	+.19	-11.36	-8.33	-.10	-.04	6.3
	82.05	25.635	-6.620	.340	15	.01310	+.91	-11.45	-7.96	-.09	+.19	3.0
	95.70	27.529	-0.697	.028	44	.10000	-.69	-11.42	-8.70	+.27	+.06	9.1
	87.25	26.925	-1.788	.C61	22	.05100	+.11	-11.35	-8.37	-.09	-.06	6.6
5176	94.51	30.352	-0.647	.057	31	.09200	-.67	-11.33	-8.83	+.05	+.08	7.3
	85.78	29.634	-4.350	.310	13	.04090	+.24	-11.17	-8.10	+.06	+.11	5.4
	81.56	28.210	-14.500	2.100	8	.00340	+1.49	-11.28	-7.89	-.06	+.07	0.9
	96.23	30.277	-0.435	.107	29	.09720	-.83	-11.31	-8.99	+.02	+.06	1.9
	87.04	29.875	-2.970	.180	15	.05220	+.05	-11.37	-8.24	+.02	+.07	6.2
	82.38	28.731	-5.320	2.780	9	.C0730	+1.14	-10.89	-8.23	-.34	-.26	0.0
5180	86.06	31.804	-0.788	.067	25	.02950	-.49	-11.15	-8.95	-.77	-.39	7.0
	86.96	31.832	-0.497	.074	30	.03120	-.60	-11.06	-9.14	-.86	-.44	4.5
5195	95.97	28.694	-0.780	.C53	32	.C3090	-.34	-11.14	-8.86	+.13	+.19	7.5
	88.63	27.700	-5.340	.580	13	.00750	+.69	-11.37	-8.20	+.19	+.23	2.9

TABLE 1.2.—Basic physical data for 413 Super-Schmidt meteors: Accelerations.—Continued

Trail No.	H	v	\dot{v}	p.e.	n	m_1	s	log σ	log ρ_{obs}	Δ log ρ_{obs}	Δ log ρ_{corr}	P
	96.52	28.722	-0.728	.057	39	.0378C	-.42	-11.16	-8.88	+16	+21	6.8
	88.73	27.678	-4.750	.540	16	.00780	+68	-11.29	-8.24	+16	+20	2.9
231	107.68	67.727	-0.535	.043	31	.00403	-.17	-10.96	-10.06	-.20	-.18	6.2
	108.05	67.841	-0.554	.053	27	.00421	-.11	-11.00	-10.04	-.15	-.15	5.3
237	95.34	28.493	-0.597	.059	37	.02190	-.42	-11.05	-9.02	-.08	-.06	6.0
	93.46	28.431	-1.077	.027	46	.0189C	-.23	-11.16	-8.78	+01	-.00	7.9
	86.71	27.307	-6.860	1.02C	9	.00324	+91	-11.12	-8.20	+04	-.17	1.7
	94.53	28.513	-0.717	.059	33	.02070	-.34	-11.07	-8.95	-.07	-.06	6.6
	92.85	28.446	-1.228	.026	42	.01770	-.16	-11.17	-8.73	+01	-.01	7.7
	86.81	27.517	-10.990	1.150	9	.0035C	+88	-11.36	-7.99	+25	+05	2.4
257	92.34	32.807	-0.458	.034	33	.13500	-.67	-11.12	-8.99	-.29	-.07	7.3
	89.82	32.751	-0.954	.013	43	.12200	-.45	-11.28	-8.69	-.20	-.03	8.6
	81.11	31.596	-11.810	1.140	10	.0245C	+76	-11.31	-7.79	+01	-.14	2.7
	92.03	32.832	-0.345	.025	41	.13400	-.67	-10.97	-9.12	-.45	-.22	7.3
273	109.37	62.973	-2.628	.458	15	.00375	-.11	-11.42	-9.32	+66	+69	3.0
	108.84	62.896	-2.330	.281	20	.00326	+01	-11.29	-9.39	+55	+50	4.2
289	104.62	63.242	-1.990	.190	21	.00156	+01	-11.34	-9.57	+08	+02	5.6
	104.32	63.272	-2.550	.330	19	.00148	+07	-11.42	-9.47	+15	+06	4.1
332	87.03	22.799	-1.096	.044	36	.03960	-.39	-11.22	-8.47	-.21	-.20	8.4
	85.07	22.635	-1.773	.026	49	.03250	-.15	-11.26	-8.29	-.19	-.18	7.7
	86.68	22.737	-1.320	.048	32	.03840	-.35	-11.27	-8.39	-.16	-.14	8.3
	84.87	22.574	-1.966	.020	44	.0317C	-.12	-11.28	-8.24	-.15	-.14	7.5
	80.46	21.698	-5.690	.170	20	.00980	+67	-11.31	-7.92	-.17	-.17	4.2
346	95.53	28.629	-0.819	.053	36	.0242C	-.64	-11.37	-8.87	+09	+17	8.1
	92.91	28.510	-1.325	.022	49	.0206C	-.35	-11.34	-8.68	+07	+13	8.3
	86.97	27.744	-6.200	.320	18	.00654	+55	-11.23	-8.15	+11	+13	4.2
	95.01	28.591	-0.798	.046	35	.0236C	-.59	-11.28	-8.88	+04	+12	8.0
	92.75	28.491	-1.401	.029	44	.0203C	-.33	-11.35	-8.65	+08	+15	8.3
	87.56	27.840	-5.620	.32C	18	.00838	+40	-11.26	-8.16	+14	+17	4.8
5370	71.34	15.291	-1.616	.050	37	.04900	-.01	-10.92	-7.93	-.80	-.84	7.1
	71.28	15.287	-1.724	.032	37	.0483C	+00	-10.95	-7.90	-.77	-.82	7.1
5450	106.00	71.820	-0.178	.016	35	.03640	-.64	-10.71	-10.27	-.52	-.34	7.2
	103.79	71.548	-0.408	.039	32	.03300	-.45	-10.95	-9.92	-.33	-.22	6.0
5472	96.39	46.607	-1.115	.139	26	.0195C	-.40	-11.19	-9.19	-.16	-.15	5.1
	97.25	46.620	-1.232	.104	26	.02100	-.53	-11.31	-9.14	-.05	-.01	7.0
5511	95.49	30.876	-0.576	.016	44	.0575C	-.57	-11.25	-8.96	-.00	-.11	8.9
	90.38	30.643	-1.632	.036	30	.0465C	-.09	-11.38	-8.55	-.01	-.07	7.4
	85.04	29.986	-4.489	.085	23	.01850	+47	-11.42	-8.21	-.11	-.11	5.0
	95.81	30.934	-0.767	.038	39	.05750	-.57	-11.37	-8.84	+14	+03	8.0
	90.09	30.614	-1.703	.078	28	.0395C	-.07	-11.39	-8.54	-.03	-.08	7.3
	84.08	29.723	-7.800	.28C	17	.0145C	+61	-11.58	-8.00	+02	+04	4.4

TABLE 1.2.—Basic physical data for 413 Super-Schmidt meteors: Accelerations.—Continued

Traill No.	H	v	\dot{v}	p.e.	n	m_1	s	log σ	log ρ_{obs}	Δ log ρ_{obs}	Δ log ρ_{corr}	P
5551	106.36	60.652	-1.569	.192	21	.00117	-.06	-11.21	-9.68	+.09	+.07	4.4
	106.14	60.615	-1.245	.436	20	.00112	-.02	-11.07	-9.78	-.02	-.07	0.7
5557	91.33	22.563	-0.428	.018	52	.25100	-.88	-11.19	-8.61	+.01	+.15	9.4
	83.86	22.039	-2.867	.174	21	.12860	+.08	-11.29	-7.86	+.15	+.08	6.1
	80.94	21.067	-9.679	.190	17	.05100	+.66	-11.39	-7.42	+.36	+.17	4.2
	89.84	22.534	-0.625	.027	42	.23600	-.61	-11.73	-8.45	+.04	+.13	9.0
	84.65	22.160	-2.596	.077	25	.14800	-.04	-11.32	-7.88	+.19	+.15	7.2
	81.14	21.140	-8.377	.228	17	.05620	+.61	-11.39	-7.47	+.33	+.14	4.4
5572	87.35	16.857	-0.840	.039	43	.09310	-.56	-11.33	-8.20	+.09	+.07	8.9
	82.75	16.410	-1.860	.149	26	.05380	+.08	-11.08	-7.91	+.01	-.01	5.4
	79.88	15.662	-5.165	.263	21	.01930	+.71	-11.05	-7.58	+.12	+.11	1.6
	87.22	16.863	-0.825	.054	42	.09230	-.54	-11.20	-8.21	+.07	+.05	7.9
	82.86	16.425	-2.008	.140	23	.05490	+.07	-11.13	-7.88	+.05	+.03	6.1
	79.80	15.700	-4.630	.217	19	.01810	+.75	-10.86	-7.64	+.06	+.04	7.9
601	94.70	36.554	-0.544	.058	34	.00948	-.21	-10.71	-9.39	-.50	-.43	5.5
	94.10	36.540	-0.982	.080	31	.00840	-.09	-10.85	-9.16	-.52	-.26	5.9
605	91.29	36.112	-0.285	.009	50	.44600	-.84	-11.07	-9.10	-.49	-.17	9.3
	81.72	35.683	-2.560	.110	21	.19300	+.22	-11.34	-8.27	-.43	-.40	6.1
	77.82	34.964	-7.050	.210	17	.06230	+.86	-11.27	-7.97	-.41	-.43	3.5
	90.66	36.177	-0.305	.014	51	.43500	-.76	-11.08	-9.08	-.52	-.41	9.2
	81.85	35.735	-2.624	.091	23	.19700	+.20	-11.36	-8.25	-.40	-.36	6.2
	77.36	34.876	-9.570	.410	16	.05180	+.95	-11.46	-7.86	-.34	-.36	3.2
640	94.52	36.849	-2.690	.300	20	.00334	+.00	-11.25	-8.86	+.02	+.07	4.9
	94.54	36.869	-4.200	.360	18	.00335	+.00	-11.45	-8.67	+.21	+.26	5.7
644	91.43	35.509	-0.668	.023	33	.01700	-.23	-10.97	-9.20	-.58	-.38	7.9
	91.86	35.473	-0.668	.044	32	.01780	-.29	-10.99	-9.19	-.53	-.30	7.3
648	93.20	36.062	-0.814	.037	42	.03410	-.43	-11.06	-9.02	-.25	-.23	8.5
	93.00	36.024	-0.839	.042	38	.03350	-.40	-11.04	-9.01	-.26	-.24	7.6
688	99.18	68.612	-0.136	.005	55	.74000	-1.20	-11.19	-9.91	-.67	-.44	9.7
	81.53	66.483	-18.820	.590	13	.09500	+.86	-11.87	-8.04	-.21	-.46	3.5
	99.80	68.647	-0.130	.005	52	.74400	-1.20	-11.24	-9.93	-.64	-.41	9.7
	83.03	67.021	-12.280	.740	13	.18600	+.50	-11.90	-8.14	-.20	-.36	4.4
759	96.39	36.277	-0.992	.074	37	.00580	-.17	-11.17	-9.20	-.17	-.05	6.2
	95.61	36.120	-1.470	.136	33	.00494	-.02	-11.24	-9.05	-.09	-.03	5.7
6062	82.34	15.066	-1.884	.047	34	.06050	-.17	-11.09	-7.82	+.07	+.26	7.7
	82.25	15.005	-2.263	.058	33	.05870	-.14	-11.15	-7.74	+.14	+.31	7.6
6093	105.21	43.438	-0.296	.102	29	.00306	+.12	-10.36	-9.97	-.28	-.46	0.7
	105.22	43.510	-0.428	.098	27	.00308	+.12	-10.52	-9.81	-.12	-.30	1.3
6095	88.69	29.510	-1.283	.027	40	.02690	-.02	-10.87	-8.69	-.29	-.24	7.2
	88.22	29.467	-1.426	.041	39	.02370	+.09	-10.92	-8.66	-.30	-.26	6.7

TABLE 1.2.—Basic physical data for 413 Super-Schmidt meteors: Accelerations.—Continued

Trail No.	H	v	\dot{v}	p.e.	n	m_{\perp}	s	log σ	log ρ_{obs}	Δ log ρ_{obs}	Δ log ρ_{corr}	P
6105	92.61	43.103	-4.810	.080	32	.00324	+22	-11.75	-8.75	-.03	+.01	6.1
	92.83	43.171	-4.840	.080	35	.00337	+19	-11.75	-8.74	-.00	+.04	6.3
6218	105.41	72.773	-0.586	.104	24	.00402	-46	-11.07	-10.09	-.39	-.27	3.4
	106.26	72.696	-0.727	.087	24	.00426	-56	-11.30	-9.98	-.22	-.06	5.3
6275	104.64	61.211	-2.120	.071	34	.00548	-07	-11.30	-9.33	+.32	+.26	7.3
6329	89.90	22.390	-2.295	.050	38	.01770	-15	-11.28	-8.25	+.25	+.34	7.7
	90.13	22.355	-1.836	.083	34	.01830	-18	-11.20	-8.34	+.18	+.28	7.8
6376	95.29	31.509	-0.755	.036	44	.03465	-17	-11.02	-8.94	-.00	+.04	7.7
	95.58	31.533	-0.755	.029	45	.03634	-23	-11.06	-8.93	+.03	+.09	7.9
6398	91.98	27.299	-0.240	.010	54	1.35700	-109	-11.13	-8.78	-.11	-.08	9.6
	77.33	26.319	-5.902	.098	21	.72900	+01	-11.69	-7.45	+.07	+.02	7.0
	71.94	24.008	-18.260	.260	17	1.16500	+90	-11.43	-7.09	+.08	-.03	3.3
	90.80	27.285	-0.408	.020	49	1.32600	-97	-11.30	-8.55	+.02	+.04	8.6
	76.83	26.177	-6.370	.150	20	.68200	+06	-11.68	-7.42	+.07	+.01	6.8
	71.08	23.159	-22.390	.740	11	.09100	+118	-11.53	-7.06	+.06	-.07	2.5
	6429	85.49	35.230	-1.983	.046	30	.01010	-13	-11.12	-8.79	-.65	-.54
	85.94	35.258	-1.719	.058	30	.01120	-25	-11.23	-8.84	-.67	-.50	8.0
6433	101.74	65.830	-2.520	.140	23	.00300	-22	-11.51	-7.41	+.03	-.03	7.9
6437					0							
6491	84.57	22.506	-1.005	.084	30	.07960	-43	-11.14	-8.40	-.34	-.33	6.8
	79.93	22.066	-3.270	.170	21	.04500	+16	-11.28	-7.95	-.24	-.27	5.8
	77.02	21.511	-4.420	.480	15	.02170	+61	-11.27	-7.91	-.41	-.46	3.1
	85.26	22.455	-0.668	.108	30	.08390	-52	-11.00	-8.57	-.45	-.44	3.5
	80.27	22.095	-2.560	.230	20	.04800	+11	-11.17	-8.05	-.32	-.34	5.3
	77.03	21.476	-5.780	.350	19	.02170	+61	-11.39	-7.79	-.29	-.34	4.0
6546	99.63	64.268	-1.590	.220	21	.00267	-23	-11.31	-9.60	-.32	-.35	4.0
	99.57	64.250	-2.520	.190	22	.00265	-22	-11.51	-9.40	-.13	-.15	6.3
6795	84.00	16.931	-5.400	.250	18	.04420	-03	-10.85	-7.51	+.51	+.53	7.2
	83.93	16.838	-4.550	.290	17	.04410	-03	-10.72	-7.58	+.43	+.46	6.5
6802	104.33	54.723	-1.560	.210	23	.00130	-06	-11.24	-9.57	+.05	+.04	4.4
	103.86	54.670	-1.360	.520	20	.00120	+02	-11.16	-9.65	-.06	-.12	0.7
6811	96.33	60.922	-6.530	.730	22	.00098	+06	-11.84	-9.09	-.07	-.07	5.1
	95.86	60.338	-10.790	.890	20	.00088	+03	-12.09	-8.88	+.10	+.03	5.6
6842					0							
6882	74.66	12.389	-0.790	.036	41	.11010	-35	-10.90	-7.94	-.60	-.50	8.3
	72.65	12.169	-1.377	.015	64	.08140	-02	-11.06	-7.72	-.51	-.45	7.2
	69.43	11.464	-2.755	.203	26	.04480	+41	-11.13	-7.46	-.44	-.45	5.3
	74.40	12.376	-1.035	.049	37	.10690	-31	-10.99	-7.82	-.49	-.40	8.2

TABLE 1.2.—Basic physical data for 413 Super-Schmidt meteors: Accelerations.—Continued

Trail No.	H	v	\dot{v}	p.e.	n	m_1	s	log c	log ρ_{obs}	Δ log ρ_{obs}	Δ log ρ_{corr}	P
	72.49	12.146	-1.425	.016	59	.07950	+0.00	-11.07	-7.71	-.51	-.46	7.1
	69.37	11.448	-2.834	.111	26	.04330	+0.43	-11.12	-7.45	-.43	-.45	5.2
6904	104.14	59.672	-1.682	.239	28	.00130	+0.16	-11.42	-9.61	+0.00	-.16	3.2
	105.21	59.688	-1.413	.112	31	.00170	-.02	-11.42	-9.66	+0.03	-.01	5.7
6915	87.47	20.184	-1.520	.150	22	.01110	-.05	-10.86	-8.41	-.11	-.13	5.1
	87.54	20.200	-1.870	.130	27	.01130	-.04	-10.95	-8.32	-.02	-.04	6.5
6932	93.56	31.604	-1.528	.068	30	.01480	-.11	-11.06	-8.75	+0.05	+0.03	7.5
	93.50	31.622	-1.366	.044	33	.01460	-.10	-11.00	-8.81	-.02	-.03	7.5
6949	91.10	26.987	-0.285	.008	57	.14290	-.81	-11.15	-9.02	-.42	-.30	9.3
	88.40	26.936	-0.586	.004	74	.12990	-.57	-11.26	-8.72	-.35	-.25	8.9
	83.50	26.675	-1.726	.059	27	.07920	+0.03	-11.16	-8.31	-.33	-.30	6.9
	79.76	26.025	-6.352	.102	19	.03180	+0.62	-11.35	-7.86	-.16	-.21	4.4
	91.68	27.012	-0.288	.009	53	.14520	-.87	-11.18	-9.01	-.37	-.23	9.4
	88.63	26.950	-0.590	.003	72	.13120	-.59	-11.29	-8.71	-.32	-.22	8.9
	84.00	26.691	-1.671	.039	30	.08570	-.04	-11.19	-8.32	-.30	-.27	7.2
	79.92	26.024	-5.405	.141	21	.03370	+0.59	-11.32	-7.92	-.21	-.25	4.5
6959	102.24	48.649	-1.100	.076	33	.01450	-.51	-11.49	-9.28	+0.19	+0.18	7.9
	100.13	48.539	-1.633	.037	43	.01220	-.24	-11.43	-9.13	+0.18	+0.15	8.0
	94.32	47.662	-7.761	.415	17	.00340	+0.67	-11.57	-8.62	+0.24	+0.14	3.8
	101.62	48.518	-0.897	.032	33	.01390	-.42	-11.34	-9.37	+0.06	+0.04	8.5
	99.71	48.430	-1.617	.021	42	.01160	-.19	-11.45	-9.14	+0.14	+0.11	7.8
	94.86	47.804	-6.254	.240	19	.00420	+0.56	-11.53	-8.69	+0.21	+0.13	4.6
6961	91.97	20.027	-0.458	.013	50	.29600	-.79	-11.34	-8.45	+0.22	+1.07	9.3
	92.04	19.998	-0.368	.012	68	.29800	-.81	-11.27	-8.54	+0.13	+1.00	9.3
6971	82.20	21.195	-2.887	.381	21	.01010	-.17	-11.10	-8.19	-.31	-.30	4.6
	82.18	21.201	-1.692	.348	20	.01000	-.15	-10.87	-8.42	-.54	-.53	2.3
6992	91.53	24.375	-1.344	.058	35	.01290	-.36	-11.32	-8.61	+0.02	-.01	8.3
	90.05	24.247	-1.974	.042	44	.01120	-.19	-11.36	-8.45	+0.06	+0.02	7.8
	85.98	23.520	-4.885	.384	21	.00530	+0.39	-11.42	-8.14	+0.04	-.03	4.3
	92.36	24.470	-1.294	.042	36	.01370	-.46	-11.36	-8.62	+0.08	+0.05	8.6
	90.86	24.358	-1.799	.032	44	.01220	-.29	-11.40	-8.49	+0.09	+0.05	8.1
	87.06	23.792	-4.981	.259	22	.00690	+0.22	-11.40	-8.11	+0.15	+0.10	5.5
998	97.32	29.779	-1.416	.042	45	.01270	-.10	-11.26	-8.76	+0.34	+0.28	7.5
	97.31	29.798	-1.338	.034	55	.01270	-.10	-11.23	-8.78	+0.32	+0.26	7.5
7002	83.31	31.031	-4.365	.157	22	.00450	+0.04	-11.30	-8.46	-.50	-.46	6.4
	83.16	30.802	-1.689	.179	24	.00430	+0.08	-10.86	-8.87	-.92	-.89	4.7
7022	95.31	27.064	-1.082	.058	32	.01740	-.24	-11.02	-8.75	+0.19	+0.12	7.2
	93.99	26.962	-1.649	.038	41	.01360	+0.01	-11.11	-8.60	+0.23	+0.18	7.0
	90.38	26.350	-4.116	.536	17	.00470	+0.69	-11.13	-8.34	+0.20	+0.20	2.5
	95.78	27.090	-1.069	.036	34	.01870	-.33	-11.09	-8.74	+0.24	+0.16	8.3
	94.45	26.992	-1.466	.029	42	.01490	-.07	-11.04	-8.64	+0.23	+0.18	7.3
	90.52	26.384	-3.019	.378	16	.00495	+0.66	-11.02	-8.46	+0.09	+0.09	2.5

TABLE 1.2.—Basic physical data for 418 Super-Schmidt meteors: Accelerations.—Continued

Trail No.	H	v	\dot{v}	p.e.	n	m_1	s	log σ	log ρ_{obs}	$\Delta \log \rho_{\text{obs}}$	$\Delta \log \rho_{\text{corr}}$	P
7026	92.40	39.428	-4.671	.231	27	.00205	+.22	-11.39	-8.75	-.05	-.11	5.5
	91.75	39.589	-5.495	.232	28	.00180	+.31	-11.45	-8.70	-.05	-.12	5.7
7040	84.61	21.517	-3.368	.070	28	.02370	-.18	-11.04	-8.01	+.06	+.09	7.8
	84.64	21.498	-2.996	.125	25	.02400	-.20	-11.00	-8.06	+.01	+.04	7.8
7044	100.39	44.869	-1.470	.110	22	.00853	-.40	-11.22	-9.16	+.17	+.35	6.8
	100.82	44.858	-1.630	.140	22	.00884	-.46	-11.31	-9.11	+.26	+.47	6.9
7046	88.89	18.522	-0.955	.024	50	.05110	-.14	-11.05	-8.32	+.09	+.17	7.6
	89.55	18.541	-0.807	.017	53	.05540	-.23	-11.04	-8.38	+.09	+.21	7.9
7052	104.98	54.075	-6.246	.398	15	.00200	-.26	-11.55	-8.70	+.77	+.77	7.2
	104.46	53.967	-4.185	.584	16	.00180	-.12	-11.22	-9.09	+.54	+.52	3.8
7067	81.56	18.444	-0.890	.061	37	.01830	+.52	-10.47	-8.49	-.66	-.76	4.3
	82.05	18.459	-0.687	.058	30	.02190	+.41	-10.36	-8.58	-.71	-.79	4.2
7069	86.04	27.550	-1.495	.118	30	.03985	-.79	-11.64	-8.50	-.32	+.74	7.4
	85.87	27.509	-1.733	.052	30	.03951	-.76	-11.67	-8.44	-.27	+.74	9.2
7073	91.06	34.119	-0.083	.107	33	.00432	+.06		-10.27	-1.68		0.0
7075	82.10	17.896	-1.293	.076	26	.02850	-.32	-10.90	-8.24	-.37	-.13	8.2
	81.45	17.838	-2.251	.078	31	.02500	-.16	-11.08	-8.01	-.19	-.07	7.7
	79.01	17.071	-12.763	1.051	13	.01040	+.49	-11.34	-7.35	+.29	-.12	4.0
	81.75	17.839	-1.638	.060	31	.02660	-.23	-10.98	-8.14	-.30	-.13	7.9
7097	96.31	32.587	-0.620	.047	31	.01870	-.35	-10.98	-9.14	-.12	+.02	6.7
	90.11	32.074	-7.130	.570	14	.00410	+.75	-11.29	-8.29	+.23	+.09	3.1
	95.20	32.558	-1.029	.038	36	.01660	-.20	-10.95	-8.94	-.01	+.09	7.8
	96.33	32.660	-0.761	.045	32	.01870	-.35	-11.07	-9.05	-.03	+.11	7.5
	89.67	31.911	-8.960	.530	14	.00330	+.86	-11.29	-8.21	+.27	+.10	3.1
7158	84.86	22.942	-1.698	.046	25	.05460	-.09	-10.78	-8.24	-.15	-.09	7.4
	84.78	22.904	-2.166	.070	25	.05260	-.05	-10.87	-8.14	-.06	-.01	7.3
7161	105.25	49.109	-0.280	.010	59	.07460	-.79	-11.37	-7.64	+.05	-.01	9.3
	102.74	49.049	-0.448	.005	78	.06620	-.51	-11.37	-9.45	+.06	+.00	8.7
	101.57	49.009	-0.663	.033	37	.06140	-.38	-11.47	-7.29	+.13	+.08	8.4
	96.64	48.675	-1.438	.044	31	.03500	+.17	-11.44	-9.03	+.02	-.03	6.4
	105.78	49.116	-0.243	.011	59	.07610	-.85	-11.34	-7.70	+.03	-.03	9.4
	102.31	49.037	-0.499	.004	86	.06450	-.46	-11.39	-9.41	+.07	+.01	8.6
	100.90	48.981	-0.682	.015	44	.05830	-.31	-11.42	-7.29	+.08	+.03	8.2
7169	94.79	48.417	-2.481	.045	29	.02310	+.44	-11.38	-8.85	+.05	+.00	5.2
	83.86	17.812	-0.894	.016	45	.04400	-.01	-10.75	-8.33	-.32	-.30	7.1
82.44	82.44	17.463	-2.580	.140	20	.01570	+.65	-10.79	-8.00	-.10	-.32	4.3
	83.81	17.840	-0.981	.022	47	.04300	+.01	-10.80	-8.30	-.30	-.29	7.0
	82.33	17.434	-3.340	.230	21	.01410	+.71	-10.88	-7.91	-.02	-.26	3.6

TABLE 1.2.—Basic physical data for 413 Super-Schmidt meteors: Accelerations.—Continued

Traill No.	H	v	v̄	p.e.	n	m ₁	s	log σ	log ρ _{obs}	Δ log ρ _{obs}	Δ log ρ _{corr}	P	
184	82.41	22.857	-1.734	.042	38	.02020	+.09	-10.97	-8.37	-.48	-.44	6.7	
	81.76	22.786	-1.831	.043	33	.01710	+.21	-10.91	-8.37	-.53	-.51	6.2	
188	98.74	38.715	-3.090	.200	23	.0195C	-.13	-11.16	-8.59	+.67	+.59	7.6	
	98.88	38.697	-2.470	.170	22	.02020	-.17	-11.08	-8.68	+.54	+.51	7.7	
190	94.43	29.438	-0.357	.022	41	.13110	-.80	-11.07	-9.01	-.14	-.01	9.3	
	92.00	29.398	-0.718	.011	51	.1192C	-.56	-11.17	-8.72	-.05	+.03	8.9	
	84.52	28.833	-5.120	.183	21	.05740	+.22	-11.42	-7.95	+.11	+.01	6.1	
210	76.13	13.402	-1.051	.023	48	.11400	-.17	-10.77	-7.88	-.44	-.37	7.7	
	76.22	13.364	-1.203	.020	48	.116CC	-.19	-10.84	-7.81	-.37	-.29	7.8	
216	98.13	31.816	-0.217	.005	69	.29890	-.94	-11.18	-9.17	-.01	-.00	9.5	
	94.70	31.740	-0.512	.002	97	.25820	-.54	-11.28	-8.82	+.07	+.05	8.8	
	90.31	31.473	-1.452	.022	39	.1754C	-.05	-11.33	-8.42	+.11	+.06	7.3	
	86.47	30.822	-4.028	.065	27	.05770	+.68	-11.36	-8.12	+.10	+.01	4.2	
	97.02	31.810	-0.302	.004	69	.28760	-.80	-11.24	-9.04	+.04	+.03	9.3	
	93.93	31.718	-0.628	.002	94	.2463C	-.45	-11.32	-8.74	+.09	+.07	8.6	
	91.35	31.561	-1.144	.016	41	.1985C	-.17	-11.39	-8.50	+.12	+.08	7.7	
	85.31	30.416	-6.142	.132	23	.03490	+.93	-11.41	-7.99	+.13	+.03	3.2	
	7240	82.74	21.641	-2.173	.062	26	.0454C	+.12	-10.77	-8.11	-.19	-.18	6.6
		82.85	21.707	-2.547	.083	24	.0476C	+.08	-10.86	-8.04	-.11	-.09	6.7
7272	95.83	30.841	-0.458	.023	40	.09440	-.82	-11.22	-8.99	-.01	+.08	8.4	
	92.48	30.753	-1.011	.011	56	.0814C	-.48	-11.36	-8.66	+.05	+.12	8.7	
	89.56	30.594	-1.863	.041	31	.0663C	-.20	-11.40	-8.42	+.05	+.10	7.8	
	84.22	29.790	-7.962	.385	17	.0265C	+.49	-11.49	-7.90	+.14	+.13	4.9	
	95.81	30.832	-0.519	.022	41	.09440	-.82	-11.28	-8.93	+.05	+.14	9.3	
	92.47	30.743	-1.013	.009	57	.0814C	-.48	-11.36	-8.66	+.05	+.12	8.7	
	89.56	30.579	-1.760	.030	31	.0663C	-.20	-11.38	-8.45	+.02	+.07	7.8	
	84.23	29.799	-7.809	.226	17	.02660	+.49	-11.48	-7.91	+.13	+.12	4.9	
	7277	103.19	60.648	-0.671	.036	30	.004CC	-.28	-11.13	-9.87	-.33	-.16	7.3
102.37		60.609	-0.705	.041	28	.0037C	-.17	-11.06	-9.86	-.38	-.30	7.0	
7331	81.65	25.343	-2.498	.190	24	.01670	-.27	-11.20	-8.33	-.49	-.41	6.5	
	81.03	25.235	-4.197	.122	28	.0148C	-.14	-11.32	-8.12	-.33	-.29	7.6	
7333	97.39	31.244	-1.414	.081	38	.00860	-.16	-11.17	-8.86	+.24	+.23	6.9	
	96.83	31.052	-1.790	.078	36	.00790	-.08	-11.20	-8.76	+.30	+.29	7.4	
7339	105.06	44.592	-1.205	.188	20	.0022C	+.06	-11.05	-9.44	+.24	+.14	3.4	
	105.20	44.425	-1.296	.212	24	.00220	+.02	-11.10	-9.39	+.30	+.23	2.8	
7367	89.49	21.689	-1.261	.013	46	.0331C	-.24	-11.15	-8.39	+.07	+.08	8.0	
	86.29	21.062	-4.606	.132	19	.0116C	+.55	-11.10	-7.96	+.24	+.05	4.7	
	89.41	21.711	-1.370	.028	46	.03270	-.21	-11.19	-8.36	+.10	+.10	7.9	
	86.88	21.256	-4.203	.152	23	.01600	+.36	-11.16	-7.97	+.78	+.14	5.5	
7372	91.19	21.104	-1.251	.163	23	.0341C	-.06	-10.89	-8.37	+.23	+.35	4.4	
	91.13	21.013	-0.665	.056	30	.03360	-.04	-10.60	-8.64	-.04	+.05	5.8	

TABLE 1.2.—Basic physical data for 413 Super-Schmidt meteors: Accelerations.—Continued

Trail No.	H	v	\dot{v}	p.e.	n	m_1	s	log σ	log ρ_{obs}	$\Delta \log \rho_{\text{obs}}$	$\Delta \log \rho_{\text{corr}}$	p
7388	83.84	23.177	-3.638	.145	21	.0284C	+1.10	-11.30	-8.01	-0.00	-0.02	6.7
	83.96	23.240	-2.167	.071	20	.03070	+0.04	-11.09	-8.23	-0.22	-0.19	6.9
7392	88.11	27.303	-2.283	.061	29	.0308C	-0.31	-11.18	-8.35	+0.00	+0.09	8.2
	87.85	27.211	-2.210	.040	35	.0288C	-0.23	-11.11	-8.37	-0.04	+0.03	7.9
7454	94.84	47.083	-1.007	.131	31	.00810	-0.25	-11.36	-9.37	-0.47	-0.33	8.0
	93.94	47.007	-2.161	.083	37	.0071C	-0.11	-11.64	-9.05	-0.22	-0.19	7.5
	91.03	46.005	-12.413	1.194	14	.0029C	+0.53	-11.82	-8.41	+0.18	-0.26	4.3
	92.16	46.598	-7.391	.234	25	.0048C	+0.21	-11.85	-8.57	+0.11	-0.09	6.2
	90.28	44.833	-20.518	2.379	10	.00170	+0.81	-11.83	-8.25	+0.28	-0.37	2.6
7474	97.58	36.518	-1.462	.038	37	.0079C	-0.02	-11.15	-8.99	+0.13	+0.10	7.2
	97.86	36.542	-2.149	.062	36	.00833	-0.07	-11.34	-8.82	+0.32	+0.30	7.3
7476	96.77	33.525	-0.831	.022	47	.0288C	-0.41	-11.29	-8.97	+0.09	+0.12	8.5
	94.93	33.457	-1.548	.016	58	.0249C	-0.22	-11.41	-8.72	+0.19	+0.23	7.9
7478	97.00	31.678	-1.262	.053	42	.0121C	-0.12	-11.28	-8.87	+0.20	+0.27	7.5
	96.93	31.677	-0.985	.077	39	.012CC	-0.11	-11.17	-8.98	+0.09	+0.15	6.0
7480	89.22	18.724	-0.888	.016	55	.06660	-0.23	-11.12	-8.32	+0.12	+0.22	7.9
	85.64	18.203	-3.448	.191	23	.02980	+0.41	-10.96	-7.82	+0.33	+0.22	5.3
	88.12	18.631	-1.323	.022	46	.0588C	-0.10	-11.16	-8.16	+0.19	+0.24	7.5
	85.28	18.099	-4.392	.157	20	.0243C	+0.53	-11.04	-7.74	+0.38	+0.23	4.8
7494	85.56	21.163	-1.379	.059	37	.02220	-0.06	-10.91	-8.39	-0.25	-0.19	7.3
	86.02	21.185	-1.194	.057	28	.0245C	-0.16	-10.94	-8.44	-0.26	-0.19	7.7
7496	79.60	13.213	-3.130	.220	21	.07130	-0.05	-10.92	-7.46	+0.22	+0.29	6.5
	79.56	13.248	-3.100	.270	21	.07080	-0.04	-10.91	-7.47	+0.21	+0.28	5.8
7499	91.74	27.775	-1.762	.067	38	.0159C	-0.14	-11.32	-8.57	+0.08	+0.12	7.6
	92.77	27.757	-1.413	.023	39	.01760	-0.25	-11.34	-8.65	+0.08	+0.12	8.0
7520	87.05	17.825	-1.052	.041	42	.062CC	-0.49	-11.16	-8.21	+0.05	+0.08	8.7
	85.65	17.710	-1.521	.029	53	.0533C	-0.27	-11.13	-8.07	+0.08	+0.10	8.1
	82.28	17.169	-3.915	.172	27	.02340	+0.40	-11.08	-7.75	+0.13	+0.14	5.3
	86.75	17.837	-1.327	.034	39	.06020	-0.44	-11.22	-8.12	+0.12	+0.14	8.6
	84.98	17.643	-1.598	.023	52	.0482C	-0.15	-11.15	-7.96	+0.14	+0.15	7.7
7522	80.82	16.639	-5.237	.234	20	.01270	+0.74	-11.22	-7.69	+0.08	+0.08	3.9
	79.62	20.838	-1.940	.031	35	.0964C	-0.31	-11.14	-8.02	-0.33	-0.06	8.2
7524	79.80	20.841	-1.792	.036	37	.0994C	-0.35	-11.15	-8.05	-0.35	-0.04	8.3
	100.89	35.970	-0.739	.045	31	.06740	-0.39	-10.84	-8.96	+0.41	+0.35	7.6
7524	99.31	35.911	-1.321	.030	38	.05000	-0.05	-10.89	-8.75	+0.50	+0.45	7.3
7534	88.66	34.609	-4.448	.212	19	.00724	-0.52	-11.68	-8.47	-0.07	+0.09	8.8
	86.85	34.074	-10.068	.113	27	.00536	-0.12	-11.85	-8.15	+0.10	+0.12	7.5
	83.96	31.594	-33.017	1.489	12	.00282	+0.37	-12.36	-7.66	+0.35	+0.21	5.5
	88.39	34.402	-6.489	.321	17	.00698	-0.45	-11.79	-8.31	+0.06	+0.21	7.7
	86.76	33.795	-10.343	.286	25	.00526	-0.10	-11.87	-8.13	+0.11	+0.13	7.5

TABLE 1.2.—Basic physical data for 413 Super-Schmidt meteors: Accelerations.—Continued

Trail No.	H	v	\dot{v}	p.e.	n	m_1	s	log σ	log ρ_{obs}	Δ log ρ_{obs}	Δ log ρ_{corr}	p
	84.40	31.901	-19.599	1.616	13	.00311	+ .31	-12.12	-7.87	+ .18	+ .06	4.6
/560	98.28	37.495	-1.926	.082	27	.00819	- .20	-11.16	-8.89	+ .28	+ .26	7.8
	97.96	37.474	-2.540	.069	28	.00777	- .15	-11.25	-8.78	+ .37	+ .34	7.7
	94.05	36.935	-8.130	.490	13	.00247	+ .64	-11.34	-8.42	+ .42	+ .30	3.9
562	89.63	26.096	-2.339	.052	37	.01900	- .03	-11.37	-8.37	+ .11	+ .06	7.2
	92.02	26.149	-1.189	.030	39	.02420	- .28	-11.25	-8.63	+ .04	+ .02	8.1
	90.23	26.027	-1.881	.016	49	.02040	- .09	-11.36	-8.45	+ .08	+ .03	7.4
	84.95	25.074	-7.380	.140	21	.00740	+ .60	-11.45	-7.97	+ .12	+ .02	4.5
/592					0							
/607	88.20	31.384	-1.978	.113	24	.00682	+ .23	-10.87	-8.75	- .39	- .47	5.5
	88.06	31.351	-1.858	.075	25	.00642	+ .27	-10.82	-8.79	- .44	- .53	5.9
/635	93.98	29.480	-1.537	.028	34	.02110	- .21	-11.10	-8.64	+ .19	+ .20	7.9
	93.01	29.298	-2.231	.035	37	.01740	- .02	-11.18	-8.50	+ .25	+ .24	7.2
/637	91.95	31.321	-0.352	.019	46	.22020	-1.01	-11.31	-8.99	- .32	- .27	8.6
	89.26	31.241	-0.583	.007	66	.18900	- .55	-11.07	-8.79	- .35	- .31	8.8
	81.84	30.654	-3.920	.157	23	.03480	+ .77	-11.06	-8.20	- .35	- .35	3.8
	87.95	31.176	-0.788	.021	37	.16050	- .29	-11.00	-8.69	- .35	- .32	8.1
	86.60	31.094	-1.358	.014	47	.12630	- .04	-11.09	-8.48	- .25	- .23	7.2
	82.89	30.492	-5.040	.147	19	.02350	+ .97	-10.96	-8.14	- .21	- .22	3.1
/64	85.30	17.688	-1.523	.042	38	.06800	- .50	-11.13	-8.03	+ .09	+ .03	8.7
	83.56	17.465	-2.063	.023	53	.04640	- .03	-10.93	-7.94	+ .04	+ .06	7.2
	80.49	16.845	-3.391	.123	27	.01420	+ .72	-11.06	-7.87	- .12	+ .03	4.0
	82.95	17.301	-2.170	.028	42	.03750	+ .14	-10.88	-7.95	- .01	+ .03	6.5
/666	82.91	14.411	-1.302	.059	37	.14650	- .35	-10.94	-7.81	+ .12	+ .45	8.3
	83.73	14.519	-0.510	.130	22	.18040	- .76	-10.77	-8.19	- .19	+ .46	1.8
	82.98	14.420	-1.342	.048	36	.14980	- .38	-10.96	-7.80	+ .14	+ .49	8.4
/726	92.91	30.593	-0.964	.039	37	.01090	- .07	-11.06	-8.97	- .27	- .16	7.3
	93.00	30.558	-1.047	.037	42	.01110	- .09	-11.12	-8.93	- .18	- .10	7.4
/734	76.89	15.018	-1.022	.037	39	.03150	+ .03	-10.60	-8.18	- .69	- .65	6.9
	76.77	14.983	-0.770	.100	30	.03030	+ .06	-10.46	-8.30	- .82	- .78	4.1
/742	101.95	42.232	-1.028	.046	41	.00590	- .20	-11.22	-9.31	+ .14	+ .16	7.8
	102.05	42.214	-0.949	.072	40	.00601	- .22	-11.19	-9.34	+ .12	+ .15	6.3
7744	80.77	19.456	-1.057	.026	50	.04530	- .20	-11.14	-8.33	- .56	- .44	7.8
	78.33	19.143	-2.439	.083	32	.03290	+ .10	-11.00	-8.00	- .41	- .39	6.7
	76.16	18.488	-4.910	.230	21	.01650	+ .54	-11.31	-7.77	- .33	- .46	4.7
	79.85	19.363	-1.490	.020	57	.04010	- .07	-11.23	-8.20	- .50	- .42	7.3
	80.17	19.439	-1.221	.020	52	.04200	- .12	-11.15	-8.28	- .55	- .46	7.5
7750	81.96	16.577	-1.400	.031	42	.03150	- .15	-11.05	-8.12	- .26	- .17	7.7
	79.75	16.115	-4.218	.244	21	.01120	+ .58	-11.00	-7.77	- .08	- .20	4.1
	82.42	16.616	-1.182	.017	44	.03360	- .22	-11.18	-8.19	- .29	- .18	7.9

TABLE 1.2.—Basic physical data for 413 Super-Schmidt meteors: Accelerations.—Continued

Trail No.	H	v	\dot{v}	p.e.	n	m_1	s	log σ	log ρ_{obs}	$\Delta \log \rho_{\text{obs}}$	$\Delta \log \rho_{\text{corr}}$	p
	79.71	16.060	-4.896	.193	21	.01090	+.59	-11.06	-7.71	-.02	-.15	4.5
7754	84.07	21.788	-1.195	.029	40	.07720	-.18	-10.96	-8.30	-.28	-.21	7.8
	84.11	21.767	-1.011	.016	40	.07870	-.20	-10.90	-8.37	-.34	-.27	7.8
7758	103.69	61.991	-0.297	.072	26	.00440	-.25	-10.74	-10.23	-.65	-.49	1.6
	103.01	61.763	-0.776	.041	32	.00400	-.15	-11.08	-9.82	-.29	-.21	6.9
7787	99.49	45.568	-1.587	.098	29	.00270	-.18	-11.27	-9.30	-.03	-.06	7.0
	98.75	45.247	-2.880	.123	27	.00250	-.09	-11.47	-9.05	+.16	+.17	7.4
7820	86.06	18.834	-0.588	.015	46	.28600	-.72	-11.12	-8.29	-.11	+.03	9.2
	82.39	18.648	-1.404	.043	31	.22770	-.31	-11.25	-7.94	-.05	+.02	8.2
	77.60	17.889	-5.832	.129	21	.08850	+.45	-11.24	-7.42	+.12	+.06	5.1
	86.49	18.783	-0.479	.016	53	.29160	-.78	-11.08	-8.38	-.16	-.01	9.3
	82.20	18.580	-1.485	.067	31	.22420	-.29	-11.26	-7.91	-.03	+.04	8.1
	77.71	17.878	-4.392	.177	23	.09140	+.44	-11.13	-7.54	+.01	-.05	5.2
7938	81.02	16.010	-1.126	.049	35	.14310	-.34	-11.04	-7.97	-.18	+.04	8.3
	80.97	15.976	-1.685	.040	39	.14220	-.33	-11.20	-7.79	-.01	+.21	8.3
7941	104.48	70.430	-2.030	.106	25	.00200	-.06	-11.46	-9.62	+.02	-.01	7.3
	104.83	70.447	-0.892	.102	27	.00210	-.11	-11.13	-9.97	-.31	-.31	4.5
7971	91.89	25.887	-0.870	.018	50	.03490	-.18	-11.32	-8.70	-.04	+.08	7.8
	88.37	25.356	-3.640	.210	21	.01580	+.43	-11.19	-8.18	+.19	+.07	4.7
	93.32	25.946	-0.514	.022	52	.03910	-.31	-11.12	-8.92	-.14	+.03	8.2
	92.18	25.888	-0.801	.012	61	.03580	-.20	-11.33	-8.73	-.04	+.08	7.8
	87.56	25.054	-5.080	.230	19	.01120	+.62	-11.47	-8.07	+.23	+.04	4.4
7973	100.60	62.995	-0.525	.168	25	.00340	-.17	-10.87	-10.03	-.68	-.65	0.8
7982	83.90	19.385	-1.869	.034	41	.05880	-.07	-11.09	-8.04	-.03	-.05	7.3
	86.68	19.309	-0.620	.028	44	.08390	-.52	-11.14	-8.47	-.24	-.14	8.8
	83.16	18.958	-2.037	.079	30	.04830	+.10	-11.02	-8.02	-.07	-.13	6.7
	80.75	18.261	-5.545	.137	25	.01780	+.71	-11.18	-7.69	+.08	-.15	4.0
7992	102.86	60.132	-1.103	.207	20	.00300	-.21	-11.25	-9.69	-.17	-.13	2.4
	103.13	60.047	-0.938	.191	22	.00310	-.23	-11.19	-9.75	-.21	-.17	2.4
7929	101.32	69.365	-1.135	.054	27	.00870	-.57	-11.43	-9.64	-.24	-.14	8.9
	101.13	69.307	-1.141	.029	29	.00860	-.54	-11.42	-9.64	-.25	-.16	8.8
7944	89.10	21.937	-0.740	.006	52	.08600	-.35	-11.13	-8.50	-.07	-.04	8.3
	83.53	21.257	-4.310	.075	21	.03140	+.47	-11.28	-7.85	+.13	+.04	5.0
	88.65	21.889	-1.130	.016	63	.08300	-.30	-11.23	-8.32	+.07	+.10	8.2
	83.19	21.138	-4.590	.130	24	.02770	+.54	-11.26	-7.84	+.11	+.01	4.7
7946	76.44	18.373	-0.304	.043	54	1.64500	-.94	-11.16	-8.30	-.84	-.72	9.5
	65.69	17.933	-1.102	.018	37	1.13300	-.21	-11.38	-7.78	-.97	-.90	7.9
	59.40	17.214	-2.837	.024	31	.72100	+.20	-11.52	-7.40	-.91	-.88	6.2
	55.56	16.169	-5.750	.044	23	.44800	+.49	-11.59	-7.10	-.81	-.80	4.9
	51.51	13.724	-16.000	.150	19	.12600	+1.13	-11.38	-6.67	-.60	-.64	2.6

TABLE 1.2.—Basic physical data for 413 Super-Schmidt meteors: Accelerations.—Continued

Trail No.	H	v	v̇	p.e.	n	m ₁	s	log σ	log ρ _{obs}	Δ log ρ _{obs}	Δ log ρ _{corr}	p
	77.49	18.400	-0.232	.009	72	1.68300	-1.05	-11.10	-8.42	-.89	-.76	9.6
	65.78	17.964	-1.094	.012	59	1.14000	-.22	-11.38	-7.78	-.96	-.90	7.9
	58.94	17.148	-3.151	.020	45	.69100	+.22	-11.55	-7.35	-.89	-.86	6.1
	55.21	16.027	-6.375	.033	35	.42500	+.52	-11.68	-7.06	-.79	-.76	4.8
	51.05	12.578	-18.620	.150	23	.09060	+1.28	-11.51	-6.61	-.56	-.67	2.2
1012	93.62	29.973	-0.825	.015	42	.10640	-.82	-11.44	-8.69	+.11	+.11	9.3
	88.21	29.661	-2.335	.033	31	.07630	-.22	-11.48	-8.28	+.08	+.04	7.9
	82.51	28.464	-10.862	.245	19	.02980	+.49	-11.62	-7.71	+.19	+.11	6.9
	92.89	29.884	-0.905	.015	41	.10340	-.73	-11.40	-8.65	+.09	+.09	9.2
	86.68	29.400	-3.633	.038	25	.06530	-.06	-11.58	-8.10	+.13	+.09	7.3
	82.64	28.375	-10.282	.169	19	.03090	+.47	-11.61	-7.73	+.18	+.10	5.0
1017	90.84	21.523	-1.412	.041	34	.03640	-.34	-11.25	-8.33	+.25	+.30	8.3
	89.83	21.392	-1.752	.032	44	.03070	-.14	-11.19	-8.25	+.24	+.25	7.6
	87.44	20.860	-3.462	.180	21	.01590	+.37	-11.27	-8.03	+.27	+.17	6.9
	91.04	21.530	-1.025	.062	39	.03730	-.38	-11.13	-8.46	+.13	+.19	7.6
	90.02	21.420	-1.606	.039	48	.03180	-.18	-11.19	-8.27	+.22	+.24	7.8
	87.21	20.738	-5.145	.309	20	.01470	+.42	-11.43	-7.86	+.42	+.31	4.7
1054	103.50	54.120	-0.110	.018	35	.01260	-.03	-10.06	-10.39	-.82	-.87	2.9
	107.59	54.245			16	.02270	-1.15					0.0
1068	106.99	65.377	-0.596	.049	44	.00269	+.09	-11.16	-10.04	-.22	-.27	5.4
	105.41	64.939	-2.220	.450	21	.00125	+.58	-11.48	-9.58	+.12	+.08	1.4
075	90.68	37.561	-0.320	.120	25	.01810	-.51	-10.64	-9.55	-.99	-.75	0.9
	83.22	34.373	-5.400	9.700	6	.00230	+.97	-11.35	-8.55	-.59	-.89	0.0
	91.08	37.455	-0.597	.071	26	.01880	-.58	-10.96	-9.28	-.68	-.43	5.3
	82.54	33.998	-18.260	.520	10	.00190	+1.06	-11.98	-8.04	-.14	-.47	2.8
1083	101.14	65.897	-1.130	.278	21	.00290	-.27	-11.12	-9.76	-.37	-.41	1.6
	102.06	66.352	-0.561	.276	18	.00310	-.38	-10.90	-10.06	-.60	-.64	0.0
1089	96.19	31.207	-0.696	.021	40	.08320	-.51	-10.95	-8.84	+.17	+.09	8.7
	93.40	31.112	-1.199	.019	50	.05910	-.07	-10.99	-8.65	+.14	+.08	7.3
	90.19	30.916	-2.192	.080	28	.03230	+.37	-11.05	-8.47	+.05	+.03	5.5
	85.97	30.272	-8.840	.770	14	.00670	+1.18	-11.40	-8.07	+.11	+.14	2.0
	94.00	31.273	-1.010	.023	49	.06440	-.16	-10.95	-8.71	+.13	+.06	7.7
106	91.23	29.569	-1.789	.041	41	.01020	-.02	-11.29	-8.68	-.07	-.02	7.2
	91.84	29.610	-1.473	.030	39	.01100	-.09	-11.29	-8.76	-.10	-.04	7.4
108	95.85	43.985	-1.233	.052	31	.01178	-.31	-11.09	-9.17	-.19	-.23	8.2
	95.78	43.976	-0.856	.082	31	.01167	-.29	-10.92	-9.33	-.35	-.40	5.7
110	93.46	30.852	-1.102	.055	32	.01177	-.20	-11.22	-8.91	-.12	-.06	7.8
	92.38	30.777	-1.506	.043	39	.01032	-.07	-11.28	-8.79	-.09	-.06	7.3
	88.58	30.190	-4.800	.460	18	.00442	+.52	-11.32	-8.19	-.00	-.11	3.4
	93.94	30.880	-0.855	.049	34	.01237	-.26	-11.15	-9.01	-.18	-.11	7.2
	92.41	30.786	-1.512	.030	43	.01037	-.07	-11.28	-8.79	-.09	-.06	7.3
	88.50	30.167	-5.550	.260	20	.00429	+.54	-11.38	-8.33	+.05	-.06	4.7

TABLE 1.2.—Basic physical data for 413 Super-Schmidt meteors: Accelerations.—Continued

Trail No.	H	v	\dot{v}	p.e.	n	m_1	s	log σ	log ρ_{obs}	Δ log ρ_{obs}	Δ log ρ_{corr}	p
113	105.79	70.620	-2.860	.14C	26	.00509	-.09	-11.39	-9.34	+.39	+.34	7.4
	106.31	70.549	-3.190	.150	21	.00549	-.17	-11.47	-9.28	+.49	+.44	7.7
127	92.03	26.655	-1.675	.095	31	.0081C	-.12	-11.07	-8.65	+.02	+.12	6.8
	91.05	26.511	-2.222	.121	25	.00672	+.05	-11.10	-8.55	+.04	+.07	6.2
143	90.37	23.625	-0.671	.017	42	.08380	-.47	-10.82	-8.61	-.07	+.12	8.6
	90.11	23.574	-0.751	.022	37	.0813C	-.42	-10.83	-8.56	-.04	+.12	8.5
147	98.79	27.344	-3.070	.23C	18	.00502	-.09	-11.20	-8.48	+.73	+.83	5.9
	98.68	27.372	-0.960	.400	16	.00486	-.06	-10.68	-8.99	+.21	+.29	0.0
149	92.77	24.791	-0.970	.140	31	.0163C	-.13	-10.81	-8.73	+.00	+.07	3.8
	92.82	24.819	-0.750	.160	25	.01640	-.13	-10.70	-8.84	-.10	-.03	2.3
153	104.58	60.078	-0.260	.140	25	.01096	-.22	-10.65	-10.13	-.49	-.42	0.0
	104.14	60.055	-0.450	.051	32	.01039	-.16	-10.86	-9.90	-.29	-.25	5.4
168					0							
187	96.18	41.475	-1.870	.12C	28	.00582	-.29	-11.27	-9.04	-.03	+.02	7.3
	95.80	41.296	-2.940	.200	26	.00546	-.21	-11.38	-8.85	+.13	+.16	7.1
189	87.60	21.059	-2.700	.050	37	.0114C	-.02	-11.20	-8.19	+.12	+.10	7.2
	85.42	20.565	-5.070	.19C	22	.00570	+.46	-11.14	-8.00	+.13	+.09	5.1
	87.30	21.001	-2.810	.080	34	.01070	+.04	-11.18	-8.18	+.10	+.08	6.9
192	87.42	25.422	-1.130	.210	23	.0084C	+.35	-10.65	-8.78	-.49	-.55	1.7
	86.90	25.244	-1.380	.240	22	.00685	+.47	-10.69	-8.72	-.47	-.57	2.0
215	94.50	43.572	-0.204	.088	30	.00360	-.13	-10.49	-10.11	-1.23	-1.39	0.0
	94.29	43.581	-0.176	.111	25	.00352	-.11	-10.41	-10.18	-1.32	-1.47	0.0
	94.06	43.586	-0.346	.040	37	.00342	-.08	-10.67	-9.89	-1.05	-1.17	4.4
	93.20	43.604	-1.009	.032	30	.00306	+.02	-11.07	-9.44	-.67	-.70	7.0
224					0							
238	99.01	41.198	-0.389	.011	53	.01127	-.22	-10.97	-9.62	-.39	-.26	7.9
	97.22	41.166	-1.297	.059	40	.00818	+.08	-11.31	-9.14	-.05	-.13	6.7
240	87.66	28.485	-2.960	.130	26	.05040	-.04	-11.35	-8.20	+.11	+.07	7.2
	93.02	28.678	-0.630	.023	37	.07980	-.68	-11.11	-8.81	-.06	-.00	9.1
	84.61	27.984	-6.310	.310	17	.0229C	+.51	-11.18	-7.97	+.10	-.03	4.4
	91.38	28.635	-0.967	.015	44	.0728C	-.49	-11.19	-8.64	-.02	+.00	8.7
244	84.04	16.176	-0.820	.210	31	.09510	-.38	-11.04	-8.18	-.16	-.10	1.7
	81.99	16.228	-1.068	.049	40	.0778C	-.13	-11.07	-8.09	-.23	-.20	7.6
	75.35	15.066	-5.140	.260	21	.03030	+.54	-7.48	-7.48	-.09	-.16	4.3
	79.98	16.040	-1.667	.019	54	.06030	+.09	-11.11	-7.93	-.22	-.23	6.7
254	96.90	41.691	-2.582	.197	23	.00168	-.07	-11.38	-9.08	-.01	+.01	5.9
	96.04	41.474	-2.813	.216	17	.00147	+.04		-9.06	-.06	-.15	5.5

TABLE 1.2.—Basic physical data for 413 Super-Schmidt meteors: Accelerations.—Continued

Trail No.	H	v	v	p.e.	n	m ₁	s	log σ	log ρ _{obs}	Δ log ρ _{obs}	Δ log ρ _{corr}	P
294	82.65	12.301	-3.293	.214	20	.214CC	-.20	-11.22	-7.22	+.69	+.79	7.0
307	94.93	35.687	-0.806	.024	50	.C1340	-.18	-11.21	-9.15	-.24	-.31	7.8
	96.07	35.804	-0.791	.029	36	.01540	-.35	-11.34	-9.15	-.15	-.24	8.3
	91.76	35.381	-1.818	.097	28	.00590	+.44	-11.15	-8.91	-.26	-.25	4.6
344	94.70	41.012	-2.830	.180	26	.00299	-.09	-11.25	-8.95	-.06	-.02	6.7
	95.11	41.005	-2.550	.120	25	.00324	-.18	-11.32	-8.98	-.06	+.02	7.8
368	93.8C	27.840	-0.997	.C16	42	.02040	-.28	-11.11	-8.78	+.04	+.16	8.1
	93.43	27.826	-1.163	.035	40	.01960	-.23	-11.15	-8.72	+.07	+.18	7.9
394	76.18	14.312	-0.720	.020	45	.2327C	-.87	-11.01	-7.99	-.55	-.34	9.4
	73.74	14.078	-1.309	.025	33	.1539C	-.14	-10.85	-7.78	-.50	-.42	7.6
	71.35	13.630	-3.488	.107	23	.06630	+.47	-10.93	-7.45	-.32	-.35	5.0
	71.94	13.769	-2.952	.090	30	.08630	+.31	-10.99	-7.49	-.32	-.33	5.7
401	105.73	59.892	-0.256	.012	53	.C235C	-.25	-10.91	-10.02	-.29	-.20	8.0
	98.39	59.364	-7.609	.766	13	.00470	+.83	-11.53	-8.77	+.41	-.11	2.5
	105.57	59.892	-0.387	.011	53	.02320	-.24	-11.09	-9.84	-.13	-.04	8.0
	98.92	59.385	-5.157	.271	15	.00618	+.69	-11.48	-8.90	+.32	-.12	3.7
413	89.06	25.561	-6.410	.770	14	.00471	+.65	-11.39	-8.11	+.32	+.10	2.6
	94.72	26.153	-0.823	.015	43	.01510	-.15	-10.96	-8.86	+.03	+.10	7.7
415	77.76	13.928	-0.689	.021	46	.0639C	+.12	-10.59	-8.18	-.63	-.64	6.6
	77.78	13.944	-0.740	.023	45	.06450	+.12	-10.63	-8.15	-.60	-.61	6.6
417	85.25	28.860	-2.556	.394	13	.00748	+.49	-10.83	-8.55	-.43	-.34	2.0
	84.70	28.707	-3.005	.387	17	.00584	+.64	-10.87	-8.51	-.44	-.34	2.6
447	91.03	20.729	-0.373	.006	70	.09490	-.50	-11.05	-8.73	-.14	+.04	8.7
	89.68	20.655	-0.644	.004	89	.0849C	-.33	-11.20	-8.51	-.03	+.07	8.3
	85.55	19.882	-3.590	.056	31	.C3360	+.43	-11.26	-7.86	+.28	+.03	5.2
	90.50	20.681	-0.416	.006	60	.09100	-.43	-11.11	-8.69	-.14	+.01	8.5
463	110.17	60.322	-0.710	.130	30	.CC378	-.18	-11.03	-9.85	+.18	+.21	3.1
	110.18	60.464	-0.850	.140	35	.00381	-.19	-11.22	-9.77	+.26	+.29	3.9
469	104.33	60.525	-0.366	.003	79	.07100	-.46	-11.42	-9.71	-.09	-.12	8.6
	97.86	60.243	-1.574	.024	41	.0440C	+.07	-11.48	-9.15	-.01	-.06	6.8
	94.95	59.900	-2.839	.118	23	.02080	+.56	-11.35	-8.99	-.08	-.15	4.6
	103.94	60.483	-0.388	.002	78	.06980	-.43	-11.44	-9.69	-.09	-.13	8.5
	97.77	60.212	-1.613	.017	41	.04340	+.08	-11.48	-9.13	+.00	-.05	6.7
476	89.85	22.016	-0.902	.C15	52	.06170	-.45	-11.18	-8.46	+.03	+.15	8.6
	85.02	21.540	-3.775	.148	21	.0333C	+.18	-11.18	-7.91	+.19	+.12	6.3
	90.76	22.084	-0.617	.060	31	.06540	-.56	-11.08	-8.62	-.05	+.09	6.2
510	81.02	17.639	-0.795	.017	49	.42900	-.27	-10.78	-8.05	-.26	-.01	8.1
	81.21	17.632	-0.717	.010	47	.45200	-.34	-10.81	-8.08	-.28	+.03	8.3

TABLE 1.2.—Basic physical data for 413 Super-Schmidt meteors: Accelerations.—Continued

Trail No.	H	v	\dot{v}	p.e.	n	m_1	s	log σ	log ρ_{obs}	Δ log ρ_{obs}	Δ log ρ_{corr}	p
546	83.58	18.652	-0.384	.008	70	.2082C	-.62	-10.82	-8.51	-.52	-.42	9.0
	80.14	18.445	-0.892	.002	110	.14470	-.11	-11.17	-8.19	-.47	-.44	7.5
	79.28	18.357	-1.189	.015	51	.13190	-.02	-11.32	-8.08	-.42	-.40	7.2
	75.60	17.691	-2.456	.040	31	.0685C	+.46	-11.32	-7.82	-.42	-.47	5.2
	73.20	16.730	-5.485	.078	27	.0285C	+.91	-11.06	-7.55	-.30	-.43	3.3
	82.97	18.605	-0.425	.004	65	.19530	-.49	-10.88	-8.48	-.54	-.46	8.7
	79.63	18.388	-0.996	.002	1C3	.13690	-.05	-11.21	-8.15	-.46	-.46	7.3
	78.63	18.241	-1.415	.012	45	.1190C	+.07	-11.30	-8.01	-.40	-.39	6.8
	75.38	17.631	-2.757	.020	35	.06540	+.47	-11.38	-7.78	-.39	-.45	5.0
	72.70	16.409	-6.950	.120	25	.01830	+1.12	-11.15	-7.50	-.28	-.44	2.7
572					0							
576	107.58	52.724	-0.381	.046	35	.00337	-.13	-10.83	-10.02	-.16	-.11	4.5
	106.68	52.760	-0.566	.040	30	.00282	+.03	-10.84	-9.87	-.08	-.15	6.3
609	99.14	61.555	-4.840	.170	20	.00495	-.11	-11.61	-8.99	+.25	+.21	7.5
	98.56	61.315	-6.640	.180	21	.00447	-.02	-11.69	-8.87	+.33	+.28	7.2
640	106.14	55.596	-0.557	.016	45	.0460C	-.33	-11.49	-9.52	+.24	+.19	8.3
	101.44	55.216	-1.480	.085	26	.02220	+.31	-11.41	-9.20	+.21	+.16	5.2
	99.23	54.816	-2.860	.140	22	.00920	+.80	-11.36	-9.03	+.22	+.15	3.7
	105.65	55.502	-0.521	.023	46	.04420	-.28	-11.42	-9.55	+.17	+.13	8.1
	101.05	55.114	-1.468	.118	26	.0210C	+.35	-11.35	-9.21	+.17	+.12	4.4
	98.88	54.719	-3.520	.240	22	.00780	+.88	-11.40	-8.96	+.26	+.19	3.1
	102.53	55.757	-1.570	.480	23	.02990	+.10	-11.58	-9.14	+.35	+.30	0.7
645	89.50	36.159	-0.193	.018	41	.63200	-1.10	-11.07	-9.23	-.77	-.55	6.7
	86.00	36.175	-0.405	.012	50	.58500	-.78	-11.11	-8.92	-.74	-.57	9.3
	73.10	35.389	-5.890	.170	19	.22700	+.30	-11.66	-7.87	-.63	-.62	5.8
	70.00	32.241	-37.570	.770	13	.01800	+1.57	-11.59	-7.35	-.30	-.48	1.6
648	101.66	58.353	-2.210	.160	24	.00559	-.38	-11.61	-9.27	+.16	+.15	7.6
	99.87	58.426	-2.160	.310	20	.00483	-.20	-11.41	-9.30	-.00	-.03	3.9
658	103.41	60.306	-1.310	.110	23	.00522	-.20	-11.14	-9.54	+.02	+.01	6.3
	103.13	60.445	-0.831	.098	23	.00504	-.16	-10.92	-9.74	-.20	-.22	4.6
668	95.37	22.519	-0.815	.032	42	.0620C	-.55	-11.28	-8.53	+.42	+.60	8.8
	95.25	22.506	-0.938	.053	37	.0612C	-.57	-11.32	-8.47	+.47	+.84	7.9
679	100.94	60.646	-0.774	.026	41	.03570	-.76	-11.51	-9.49	-.11	-.38	9.2
	101.84	60.892	-0.228	.046	29	.0366C						0.0
719	96.79	60.036	-1.929	.058	24	.00940		-11.22	-9.28	-.22		0.0
	95.99	59.720	-5.120	.210	15	.00560		-11.46	-8.92	+.08		0.0
9726	105.88	61.075	-0.212	.005	53	.1555C	-.54	-10.97	-9.85	-.11	+.13	8.8
	104.45	61.064	-0.340	.004	59	.14470	-.41	-11.12	-9.65	-.02	+.16	8.5
	94.57	60.263	-8.604	.566	17	.03840	+.63	-11.70	-8.43	+.45	+.05	3.9
	105.71	61.089	-0.132	.006	49	.1544C	-.52	-10.76	-10.05	-.33	-.09	8.8

TABLE 1.2.—Basic physical data for 413 Super-Schmidt meteors: Accelerations.—Continued

Trail No.	H	v	\dot{v}	p.e.	n	m_1	s	log σ	log ρ_{obs}	Δ log ρ_{obs}	Δ log ρ_{corr}	p
766	93.93	23.909	-0.323	.014	54	.20180	-.85	-11.10	-8.81	+.02	+.26	9.4
	91.14	23.832	-0.727	.005	74	.17340	-.48	-11.17	-8.48	+.12	+.28	8.7
	86.79	23.454	-2.613	.099	27	.09670	+.14	-11.26	-7.99	+.25	+.27	6.5
	83.96	22.605	-7.609	.187	20	.03730	+.71	-11.32	-7.63	+.38	+.28	3.6
	91.08	23.891	-0.702	.014	45	.17260	-.47	-11.15	-8.49	+.11	+.26	8.6
	89.22	23.785	-1.265	.007	59	.14440	-.22	-11.21	-8.26	+.18	+.28	7.9
	84.26	22.850	-6.352	.141	21	.04390	+.63	-11.30	-7.70	+.34	+.25	4.4
.793	91.08	26.077	-2.333	.038	36	.01200	-.06	-11.36	-8.43	+.17	+.12	7.3
	87.57	25.574	-5.626	.137	19	.00630	+.41	-11.28	-8.13	+.18	+.12	4.8
	92.60	26.397	-1.669	.043	39	.01400	-.22	-11.27	-8.57	+.15	+.10	7.9
	88.43	25.936	-4.162	.253	21	.00800	+.26	-11.28	-8.24	+.14	+.08	5.4
817	108.40	68.775	-0.870	.280	26	.00153	+.06	-11.34	-10.00	-.09	-.24	0.7
	107.54	68.779	-2.310	.230	21	.00137	+.15	-11.69	-9.59	+.26	-.04	4.5
819	92.66	45.338	-1.160	.240	24	.00467	-.20	-10.98	-9.36	-.63	-.65	2.3
	92.61	45.348	-1.660	.280	23	.00464	-.20	-11.13	-9.20	-.48	-.50	3.1
881	91.87	16.879	-0.190	.010	61	1.08900	-1.24	-11.43	-8.49	+.17	+.28	9.7
	90.53	16.819	-0.304	.003	90	1.05000	-1.01	-11.45	-8.29	+.26	+.35	9.5
	88.61	16.684	-0.486	.014	50	.97500	-.74	-11.51	-8.09	+.30	+.35	9.2
	85.40	16.296	-1.028	.017	39	.76600	-.30	-11.44	-7.78	+.35	+.35	8.2
	82.79	15.659	-1.610	.019	40	.50400	+.11	-11.42	-7.61	+.31	+.26	6.6
	80.47	14.652	-2.796	.038	34	.24000	+.58	-11.33	-7.42	+.33	+.22	4.6
	93.24	16.909	-0.107	.010	48	1.11500	-1.48	-11.41	-8.74	+.03	+.17	7.9
	91.38	16.859	-0.207	.003	69	1.07600	-1.15	-11.40	-8.46	+.16	+.26	9.7
	88.62	16.716	-0.471	.011	27	.97500	-.74	-11.52	-8.11	+.28	+.33	9.2
	86.10	16.416	-0.820	.015	24	.82400	-.40	-11.43	-7.87	+.32	+.33	8.5
	83.73	15.915	-1.393	.019	34	.59700	-.03	-11.40	-7.67	+.33	+.29	7.2
	81.46	15.179	-2.033	.031	33	.37140	+.32	-11.25	-7.53	+.29	+.22	5.7
891	95.73	32.591	-0.682	.018	47	.03660	-.22	-10.95	-9.00	-.03	-.08	7.9
	91.36	32.305	-2.010	.130	21	.01670	+.40	-11.06	-8.64	-.02	-.07	4.8
	97.31	32.635	-0.601	.018	38	.04380	-.46	-11.00	-9.03	+.07	+.01	8.6
	95.64	32.574	-0.887	.012	48	.03620	-.20	-11.07	-8.89	+.08	+.03	7.8
	90.98	32.160	-3.070	.140	21	.01480	+.47	-11.17	-8.47	+.12	+.07	5.0
917	81.86	20.413	-1.137	.015	48	.05860	-.29	-11.03	-8.31	-.46	-.31	8.1
	81.44	20.370	-1.356	.019	39	.05510	-.21	-11.12	-8.24	-.42	-.30	7.9
943	100.80	19.894	-2.430	.310	26	.28000	-1.45	-12.51	-7.73	+.164	+.351	5.9
945	95.45	30.807	-0.993	.055	38	.00985	-.37	-11.29	-8.78	-.03	+.06	7.5
	93.58	30.684	-1.625	.029	49	.00837	-.16	-11.55	-8.79	+.01	+.07	7.7
	88.53	29.848	-5.920	.140	22	.00352	+.48	-11.46	-8.33	+.05	+.06	5.0
	91.68	30.513	-2.710	.240	18	.00691	+.02	-11.50	-8.59	+.05	+.10	5.6
951	100.57	19.641	-4.250	.380	19	.31600	-1.36	-12.83	-7.45	+.190	+.521	7.8
	101.06	19.696	-3.460	.290	25	.31800	-1.42	-12.83	-7.55	+.184	+.530	7.9
974	83.44	25.240	-4.316	.132	24	.03390	+.36	-10.67	-7.99	-.02	+.04	5.5
	84.30	25.312	-2.836	.149	22	.07290	-.28	-10.71	-8.06	-.02	+.03	7.3

TABLE 1.2.—Basic physical data for 413 Super-Schmidt meteors: Accelerations.—Continued

Trail No.	H	v	\dot{v}	p.e.	n	m_1	s	log σ	log ρ_{obs}	Δ log ρ_{obs}	Δ log ρ_{corr}	p
4976	107.03	57.736	-1.501	.382	22	.00120	+.13	-11.18	-9.65	+.17	+.04	1.3
	107.29	57.899	-1.953	.302	20	.00130	+.09	-11.32	-9.53	+.31	+.20	3.3
8990	94.05	26.760	-1.054	.071	32	.01720	-.43	-11.27	-8.75	+.09	+.15	7.7
	91.35	26.563	-1.794	.028	46	.01300	-.09	-11.37	-8.55	+.07	+.12	7.4
	86.51	25.695	-5.456	.499	16	.00570	+.50	-11.53	-8.16	+.06	+.09	3.9
	92.23	26.632	-1.243	.059	35	.01430	-.19	-11.24	-8.70	-.01	+.05	7.8
	90.50	26.489	-2.057	.036	44	.01180	+.00	-11.34	-8.51	+.04	+.09	7.1
	86.31	25.668	-6.732	.388	18	.00540	+.53	-11.59	-8.08	+.12	+.16	4.3
1015	92.75	30.786	-0.410	.012	45	.05940	-.67	-11.14	-9.10	-.37	-.18	9.1
	89.14	30.714	-1.049	.011	60	.05020	-.36	-11.27	-8.72	-.29	-.16	8.3
	84.67	30.402	-2.944	.071	24	.03330	+.07	-11.43	-8.32	-.25	-.21	6.8
	78.99	28.578	-21.400	.910	15	.00770	+.92	-11.59	-7.62	+.02	-.11	3.3
	91.85	30.850	-0.529	.015	43	.05740	-.59	-11.20	-9.00	-.34	-.17	8.9
	88.25	30.747	-1.265	.011	58	.04730	-.28	-11.28	-8.65	-.29	-.18	8.1
	84.22	30.431	-3.046	.079	25	.03150	+.11	-11.41	-8.31	-.27	-.25	6.6
79.00	28.844	-16.930	.490	16	.00790	+.86	-11.51	-7.71	-.07	-.19	3.5	
1030	90.01	23.826	-0.971	.035	41	.03750	-.22	-11.12	-8.57	-.06	-.01	7.9
	86.86	23.589	-1.933	.083	29	.02500	+.38	-11.19	-8.32	-.07	-.02	5.4
	82.23	22.654	-6.824	.163	20	.00822	+.80	-11.28	-7.90	-.02	+.03	3.7
	89.64	23.810	-1.142	.024	41	.03620	-.18	-11.15	-8.51	-.03	+.02	7.8
	87.78	23.669	-1.758	.013	53	.02870	+.04	-11.19	-8.35	-.03	+.02	6.9
	82.24	22.598	-6.259	.153	23	.00822	+.80	-11.24	-7.94	-.06	-.01	3.7
1062	106.87	62.069	-0.943	.155	28	.00220	+.04	-11.17	-9.83	-.02	-.08	2.8
	87.47	19.557	-2.510	.200	22	.03750	+.04	-11.05	-7.99	+.31	+.33	5.5
87.57	19.475	-2.030	.240	22	.04000	-.01	-10.96	-8.07	+.24	+.29	4.3	
1104	93.06	29.937	-1.224	.042	38	.05340	-.42	-11.47	-8.62	+.14	+.07	8.5
	93.45	29.992	-0.921	.042	42	.05450	-.46	-11.37	-8.74	+.05	-.03	8.6
	89.59	29.737	-1.597	.080	26	.03910	-.06	-11.28	-8.54	-.07	-.03	6.6
	86.09	29.316	-3.285	.155	23	.02100	+.40	-11.31	-8.31	-.12	+.04	5.3
1130	87.00	17.707	-1.010	.030	49	.05480	-.25	-11.01	-8.24	+.02	+.02	8.0
	84.36	17.383	-2.810	.080	26	.02740	+.33	-10.97	-7.88	+.17	+.05	5.6
	86.77	17.722	-1.260	.035	42	.05310	-.21	-11.08	-8.15	+.09	+.08	7.9
	84.12	17.295	-3.000	.165	19	.02420	+.40	-10.96	-7.87	+.16	+.03	4.8
1147	100.50	58.608	-1.956	.057	28	.00307	-.10	-11.34	-9.41	-.07	-.11	7.5
	99.71	58.587	-1.895	.072	25	.00277	-.01	-11.26	-9.44	-.16	-.21	7.1
1149	85.73	48.377	-2.383	.129	19	.01900	-.37	-11.28	-8.90	-.74	-.57	7.5
	86.52	48.260	-1.380	.147	23	.02110	-.54	-11.09	-9.12	-.90	-.63	6.2
1170	99.86	33.570	-0.810	.052	42	.01070	-.10	-11.17	-9.13	+.16	+.10	6.7
	98.95	33.490	-1.078	.033	52	.00920	+.04	-11.26	-9.03	+.20	+.15	6.9
	96.42	33.105	-1.933	.236	24	.00450	+.51	-11.30	-8.87	+.16	+.16	2.9
	100.38	33.631	-0.858	.048	47	.01170	-.19	-11.22	-9.09	+.24	+.17	7.0

TABLE 1.2.—Basic physical data for 413 Super-Schmidt meteors: Accelerations.—Continued

Trail No.	H	v	\dot{v}	p.e.	n	m_1	s	log σ	log ρ_{obs}	$\Delta \log \rho_{obs}$	$\Delta \log \rho_{corr}$	P
1172	91.05	25.084	-0.133	.004	59	.35000	-.46	-10.31	-9.16	-.57	-.49	8.6
	79.70	24.205	-10.432	.382	15	.0427C	+1.00	-11.20	-7.54	+1.15	-.17	3.0
	89.98	25.088	-0.251	.004	65	.32300	-.34	-10.59	-8.89	-.39	-.34	8.3
	94.48	25.095	-0.116	.016	42	.42000	-.92	-10.49	-9.19	-.32	-.12	6.6
1238	91.49	27.970	-1.823	.047	41	.0219C	-.26	-11.27	-8.51	+1.12	+1.15	8.0
	90.38	27.901	-2.450	.130	28	.01920	-.12	-11.29	-8.40	+1.14	+1.18	6.8
1240	89.29	25.955	-1.681	.028	41	.0432C	-.29	-11.29	-8.39	+1.06	+1.13	8.1
	88.18	25.592	-2.418	.065	33	.03820	-.15	-11.34	-8.24	+1.12	+1.18	7.7
1246	90.84	29.028	-2.577	.103	29	.01340	+0.04	-11.38	-8.47	+1.11	+1.14	6.9
	91.64	29.060	-1.803	.050	36	.0149C	-.05	-11.30	-8.61	+1.03	+1.10	7.3
1252	82.91	19.490	-1.338	.079	44	.02900	-.15	-11.07	-8.30	-.37	-.28	6.9
	82.93	19.529	-1.040	.037	35	.02920	-.15	-10.96	-8.41	-.48	-.39	7.7
1257	94.68	30.249	-0.428	.013	52	.2473C	-1.05	-11.79	-8.86	+1.03	+1.02	9.6
	86.08	29.826	-1.823	.048	31	.1681C	-.22	-11.51	-8.28	-.10	-.06	7.9
	81.70	29.127	-4.464	.095	23	.09570	+1.26	-11.55	-7.95	-.11	-.05	6.0
	78.36	27.486	-16.417	.379	19	.0278C	+1.94	-11.53	-7.51	+1.08	+1.17	3.2
	93.93	30.244	-0.596	.019	58	.2418C	-.95	-11.81	-8.72	+1.11	+1.10	9.5
	86.01	29.762	-1.684	.076	31	.1638C	-.19	-11.48	-8.31	-.13	-.10	7.8
	81.67	29.085	-4.923	.135	23	.09170	+1.29	-11.57	-7.91	-.07	-.02	5.8
	78.67	27.717	-13.595	.401	17	.0307C	+1.89	-11.51	-7.59	+1.03	+1.11	3.4
1265	91.58	30.123	-2.180	.058	32	.01112	-.21	-11.31	-8.60	+1.04	+1.09	7.9
	91.84	30.308	-2.591	.081	32	.01144	-.24	-11.42	-8.53	+1.13	+1.19	8.0
1284	84.95	26.285	-0.387	.013	46	.2311C	-.79	-11.14	-8.79	-.70	-.53	9.3
	82.98	26.228	-0.658	.006	60	.20100	-.47	-11.01	-8.58	-.64	-.53	8.6
	77.68	25.733	-3.395	.109	23	.0595C	+1.55	-11.17	-8.03	-.48	-.53	4.7
	82.20	26.159	-0.745	.015	52	.1829C	-.33	-10.91	-8.54	-.66	-.57	8.3
1331	94.80	30.728	-0.479	.016	41	.22490	-.33	-11.17	-8.84	+1.06	+1.04	9.3
	91.53	30.651	-1.051	.007	54	.1969C	-.50	-11.35	-8.52	+1.11	+1.12	8.7
	87.04	30.396	-2.916	.089	24	.14650	-.12	-11.48	-8.11	+1.15	+1.19	7.5
	81.89	29.476	-8.557	.401	15	.0417C	+1.72	-11.26	-7.80	+1.05	+1.16	4.0
	92.79	30.523	-0.753	.022	38	.20850	-.62	-11.26	-8.65	+1.09	+1.09	9.0
	90.32	30.438	-0.957	.017	48	.18500	+1.40	-11.26	-8.56	-.03	-.01	8.5
82.94	29.826	-3.826	.208	21	.0632C	+1.49	-11.02	-8.10	-.16	-.08	4.5	
1335	98.77	58.320	-1.788	.034	30	.01130	-.26	-11.47	-9.26	-.05	-.07	8.0
	98.75	58.432	-1.810	.044	27	.01130	-.26	-11.47	-9.25	-.04	-.06	8.0
1375	83.97	21.717	-1.002	.089	28	.0632C	-.45	-11.12	-8.40	-.38	-.27	6.9
	84.51	21.783	-1.047	.179	20	.06660	-.55	-11.13	-8.38	-.32	-.19	3.5
1379	91.68	19.477	-0.639	.021	52	.1781C	-.55	-10.72	-8.35	+1.29	+1.24	8.8
	90.06	19.428	-0.952	.031	42	.1330C	-.14	-10.65	-8.22	+1.29	+1.24	7.6
1411	99.61	60.299	-1.042	.120	27	.00720	-.38	-11.32	-9.59	-.31	-.35	5.0
	97.50	60.183	-2.177	.080	27	.0062C	-.20	-11.51	-9.29	-.18	-.22	7.8

TABLE 1.2.—Basic physical data for 413 Super-Schmidt meteors: Accelerations.—Continued

Trail No.	H	v	\dot{v}	p.e.	n	m_1	s	log σ	log ρ_{obs}	Δ log ρ_{obs}	Δ log ρ_{corr}	p
1416	89.07	25.368	-1.083	.020	51	.08990	-.45	-11.36	-8.45	-.02	-.03	8.6
	83.91	24.901	-2.355	.148	23	.05690	+.06	-11.22	-8.17	-.16	-.10	6.1
	90.43	25.417	-0.819	.054	40	.09560	-.57	-11.44	-8.57	-.03	-.06	8.0
	86.66	25.221	-1.603	.016	61	.07660	-.23	-11.36	-8.30	-.07	-.05	7.9
	84.00	24.959	-2.898	.169	25	.05780	+.04	-11.35	-8.07	-.05	+.00	6.2
	79.49	23.969	-6.646	.247	21	.01170	+.98	-11.19	-7.91	-.23	-.05	3.1
1418	89.41	36.183	-0.841	.085	29	.04410	-.58	-11.12	-8.97	-.51	-.50	6.2
	86.84	36.071	-1.559	.056	30	.03500	-.23	-11.14	-8.74	-.49	-.46	7.9
1451	92.40	35.158	-1.058	.062	28	.01540	-.51	-11.33	-9.00	-.30	-.10	7.0
	90.47	35.067	-1.121	.103	26	.01360	-.33	-11.17	-8.99	-.44	-.30	5.8
1507	89.98	35.341	-0.240	.116	27	.01440	-.04	-10.11	-9.66	-1.16	-1.11	0.0
	90.24	35.336	-0.585	.133	26	.01520	-.08	-10.49	-9.27	-.74	-.70	1.5
1547	90.19	36.132	-0.781	.054	28	.02930	-.42	-11.06	-9.06	-.54	-.42	7.7
	90.05	36.174	-1.132	.042	30	.02900	-.40	-11.21	-8.91	-.40	-.29	8.5
1611	92.06	36.857	-0.632	.052	29	.02010	-.25	-10.79	-9.23	-.55	-.45	6.4
	91.68	36.822	-0.970	.052	28	.01930	-.20	-10.92	-9.05	-.41	-.31	7.0
1627	92.18	36.434	-1.612	.129	26	.01760	-.45	-11.27	-8.83	-.14	-.05	6.9
	89.92	36.510	-1.042	.469	18	.01320	-.09	-10.70	-9.06	-.56	-.50	0.0
1631	89.40	36.132	-0.935	.073	30	.01680	-.24	-11.17	-9.07	-.61	-.55	6.4
	89.08	36.158	-1.097	.057	30	.01640	-.21	-11.22	-9.00	-.57	-.51	7.1
1656	92.84	35.972	-0.260	.048	33	.04530	-.28	-10.57	-9.47	-.73	-.55	3.2
	93.22	36.057	-0.402	.052	33	.04660	-.32	-10.77	-9.28	-.51	-.31	4.9
1660	99.25	58.535	-1.400	.133	23	.00390	-.31	-11.34	-9.52	-.27	-.33	5.7
	99.06	58.424	-1.888	.301	20	.00380	-.29	-11.46	-9.39	-.16	-.21	3.3
1709	92.52	35.726	-1.984	.050	29	.01540	-.41	-11.31	-8.74	-.03	+.21	8.5
	92.25	35.620	-3.250	.112	27	.01490	-.36	-11.47	-8.53	+.16	+.37	8.3
1719	92.39	36.378	-0.906	.076	25	.00540	-.06	-10.86	-9.25	-.55	-.48	5.8
	92.53	36.334	-0.838	.064	27	.00550	-.08	-10.83	-9.28	-.57	-.50	5.9
1725	78.85	35.813	-1.449	.028	37	.29100	-.33	-11.50	-8.46	-.83	-.72	8.3
	69.38	34.834	-7.940	.090	23	.15000	+.27	-11.85	-7.79	-.77	-.77	5.9
	63.46	32.015	-31.500	.770	18	.05700	+.81	-12.14	-7.26	-.57	-.66	3.7
	80.11	35.929	-1.259	.024	40	.30700	-.41	-11.51	-8.51	-.79	-.67	8.5
	71.19	35.195	-5.860	.050	31	.18100	+.13	-11.81	-7.90	-.78	-.75	6.5
	63.51	32.081	-30.400	.530	18	.05770	+.81	-12.13	-7.27	-.57	-.67	3.7
1742	87.60	36.525	-1.571	.135	28	.03140	-.32	-11.32	-8.76	-.45	-.35	6.6
	88.20	36.616	-1.757	.103	29	.03270	-.38	-11.42	-8.71	-.35	-.24	7.6
1749	87.70	36.157	-0.473	.014	42	.20750	-.65	-10.97	-9.00	-.68	-.54	9.0
	85.31	36.124	-0.974	.009	50	.17440	-.34	-11.02	-8.71	-.59	-.49	8.3
	76.40	35.347	-8.859	.143	21	.05530	+.56	-11.64	-7.90	-.44	-.48	4.6

TABLE 1.2.—Basic physical data for 413 Super-Schmidt meteors: Accelerations.—Continued

Trail No.	H	v	\dot{v}	p.e.	n	m_L	s	log σ	log ρ_{obs}	Δ log ρ_{obs}	Δ log ρ_{corr}	p
	87.51	36.160	-0.629	.026	38	.20510	-.62	-11.07	-8.88	-.58	-.44	9.0
	84.52	36.090	-1.185	.010	48	.16110	-.24	-11.04	-8.63	-.57	-.48	8.0
	75.64	35.112	-10.127	.218	19	.0464C	+.65	-11.61	-7.86	-.45	-.50	4.3
7804	102.85	72.414	-3.215	.083	27	.03260	-.30	-11.31	-9.04	+.48	+.41	8.2
	100.93	72.577	-2.473	.070	20	.02710	-.10	-11.03	-9.18	+.20	+.14	6.7
9815	99.62	59.203	-7.290	.154	22	.00570	+.65	-11.38	-8.76	+.52	+.28	4.3
	100.08	59.539	-3.059	.115	20	.00830	+.45	-11.09	-9.09	+.22	+.04	5.1
9833	83.57	24.810	-1.311	.087	29	.0109C	+.45	-10.36	-8.65	-.67	-.79	4.6
	84.13	24.841	-0.938	.084	25	.0125C	+.37	-10.66	-8.78	-.75	-.85	4.4
9880	88.93	25.767	-0.342	.009	68	.17310	-.63	-11.18	-8.87	-.45	-.45	9.0
	86.93	25.650	-0.526	.005	100	.1326C	-.21	-10.95	-8.72	-.47	-.43	7.9
	83.85	25.328	-0.896	.027	53	.0686C	+.33	-11.16	-8.57	-.56	-.49	5.6
	85.76	25.570	-0.733	.011	74	.10260	+.03	-11.06	-8.61	-.45	-.40	6.9
	83.61	25.293	-1.091	.061	40	.06500	+.36	-11.24	-8.49	-.50	-.42	5.5
7888	88.39	18.598	-0.493	.012	55	.32800	-.40	-11.22	-8.34	+.03	-.05	8.5
	84.91	18.233	-1.285	.014	48	.22000	+.04	-11.20	-7.96	+.13	+.08	6.9
	82.40	17.723	-1.670	.033	38	.13800	+.28	-11.30	-7.89	+.00	-.02	5.9
	80.21	17.169	-2.067	.043	34	.0835C	+.65	-11.33	-7.84	-.11	-.11	4.3
	90.89	18.740	-0.311	.006	77	.3720C	-.63	-11.19	-8.53	+.05	-.05	9.0
	86.29	18.428	-0.935	.015	50	.27100	-.16	-11.32	-8.08	+.12	+.06	7.7
	83.73	18.021	-1.547	.028	40	.17600	+.21	-11.32	-7.90	+.10	+.06	6.2
	81.37	17.477	-1.845	.030	37	.109CC	+.51	-11.23	-7.87	-.05	-.06	4.9
	79.21	16.791	-3.095	.059	31	.06650	+.77	-11.50	-7.68	-.07	-.01	3.8
9900	88.10	23.754	-0.569	.027	37	.09730	-.71	-11.26	-8.66	-.31	-.35	9.1
	84.98	23.592	-1.074	.009	61	.0776C	-.30	-11.25	-8.41	-.31	-.33	8.2
	80.08	22.990	-2.795	.067	31	.02810	+.50	-11.07	-8.12	-.40	-.37	4.9
	85.85	23.584	-0.806	.020	42	.08380	-.41	-11.15	-8.53	-.36	-.38	8.5
	83.75	23.444	-1.335	.010	57	.06880	-.16	-11.23	-8.33	-.33	-.34	7.7
	79.63	22.863	-3.240	.09C	26	.02380	+.59	-11.12	-8.08	-.39	-.35	4.5
9917	85.18	16.038	-1.299	.027	39	.09910	-.44	-11.32	-7.96	+.15	+.16	8.6
	81.04	15.518	-2.097	.037	33	.06630	+.01	-11.22	-7.78	+.01	+.06	7.0
	77.51	14.705	-4.640	.153	25	.02770	+.59	-11.05	-7.52	+.01	+.12	4.5
	82.06	15.693	-1.907	.010	66	.07560	-.11	-11.28	-7.81	+.06	+.10	7.5
	84.25	15.878	-1.012	.037	38	.09740	-.34	-11.17	-8.07	-.03	-.01	8.3
	80.12	15.408	-2.404	.068	28	.05720	+.13	-11.18	-7.74	-.02	+.04	6.5
	77.25	14.685	-4.590	.187	20	.02460	+.65	-11.04	-7.54	-.02	+.08	4.3
	81.94	15.657	-1.711	.015	57	.07450	-.09	-11.22	-7.86	-.00	+.04	7.4
9925	97.15	44.339	-4.150	.125	23	.00740	+.30	-11.20	-8.72	+.37	+.21	5.8
	98.30	44.351	-3.188	.135	21	.01070	+.03	-11.16	-8.78	+.40	+.33	6.9
9945	97.73	41.172	-2.155	.093	28	.00590	-.12	-11.35	-8.97	+.16	+.21	7.5
	97.89	41.278	-2.401	.271	21	.00610	-.16	-11.42	-8.92	+.22	+.29	5.4
9951	100.05	60.317	-5.558	.403	14	.00173	-.17	-11.73	-9.07	+.24	+.23	7.0
	98.82	59.827	-4.254	.539	16	.0015C	-.03	-11.52	-9.20	+.02	-.03	4.3

TABLE 1.2.—Basic physical data for 413 Super-Schmidt meteors: Accelerations.—Continued

Trail No.	H	v	\dot{v}	p.e.	n	m_{\perp}	s	log σ	log ρ_{obs}	$\Delta \log \rho_{\text{obs}}$	$\Delta \log \rho_{\text{corr}}$	p
9953	94.14	42.654	-7.607	.273	15	.00450	-.02	-11.79	-8.49	+36	+38	7.2
	96.23	42.987	-0.680	.229	20	.00650	-.44	-11.07	-9.38	-.37	-.09	1.7
9955	98.65	42.895	-4.471	.242	20	.00491	-.27	-11.81	-8.71	+49	+63	7.3
	99.35	42.937	-2.912	.288	21	.00531	-.38	-11.61	-8.89	+37	+56	5.9
9974	95.28	43.089	-0.633	.027	34	.01660	-.17	-11.00	-9.39	-.45	-.32	7.7
	95.30	43.098	-0.485	.017	31	.01670	-.18	-10.89	-9.51	-.57	-.43	7.8
9983	94.37	42.931	-1.511	.061	29	.02100	-.31	-11.22	-8.98	-.12	-.01	8.2
	91.43	42.804	-3.940	.036	16	.01230	+19	-11.31	-8.63	-.01	-.07	5.0
9985	94.18	42.223	-3.140	.090	27	.00862	-.32	-11.51	-8.77	+08	+20	8.2
	93.89	42.114	-2.420	.170	21	.00824	-.26	-11.30	-8.89	-06	+03	7.2
9997	94.52	43.018	-7.703	.374	21	.00192	-.03	-11.67	-8.62	+26	+23	7.2
	94.39	43.082	-7.093	.337	19	.00187	-.01	-11.62	-8.66	+21	+18	7.1
10006	96.75	42.983	-2.035	.059	30	.00500	-.15	-11.25	-9.05	+00	-.02	7.7
	95.97	43.035	-1.509	.152	23	.00420	+01	-11.00	-9.21	-.22	-.23	4.9
10012	102.25	64.461	-2.260	.284	21	.00180	-.02	-10.98	-9.51	-.04	-.09	4.3
	102.84	64.450	-2.585	.184	23	.00205	-.14	-11.13	-9.43	+09	+03	6.9
10064	85.74	28.820	-0.816	.077	32	.00960	+53	-10.56	-9.01	-.85	-.63	3.3
	85.43	28.807	-0.604	.111	32	.00880	+58	-10.46	-9.15	-1.07	-.78	1.8
10070	91.74	25.937	-0.401	.014	59	.12220	-.74	-11.15	-8.86	-.21	-.08	9.2
	84.21	25.607	-2.048	.047	40	.08660	-.17	-11.53	-8.19	-.16	-.09	7.7
	78.70	24.632	-6.969	.108	30	.04750	+31	-11.67	-7.71	-.09	-.09	5.7
	73.94	21.160	-26.692	.930	19	.01000	+13	-11.61	-7.22	+08	-.02	2.4
	89.76	25.911	-0.721	.025	53	.11400	-.57	-11.35	-8.61	-.12	-.01	8.9
	83.35	25.467	-2.403	.083	35	.08120	-.11	-11.54	-8.12	-.15	-.10	7.5
	79.30	24.773	-5.611	.178	25	.05230	+25	-11.63	-7.80	-.14	-.13	6.0
	75.76	23.177	-16.340	.529	17	.02400	+70	-11.78	-7.39	+02	-.02	3.7
10094	99.58	49.218	-0.567	.032	35	.08550	-.77	-11.53	-9.32	-.05	-.21	8.3
	91.00	48.878	-2.387	.085	23	.05330	-.06	-11.61	-8.75	-.16	-.22	7.3
	85.52	48.180	-7.660	.370	15	.01930	+62	-11.37	-8.38	-.24	-.20	4.4
10098	85.40	45.342	-1.872	.032	36	.10010	-.29	-11.32	-8.70	-.57	-.63	8.1
	86.46	45.457	-1.385	.013	38	.11570	-.50	-11.38	-8.82	-.60	-.67	8.7
10106	88.89	30.697	-0.479	.016	57	.04330	-.37	-10.92	-9.08	-.67	-.47	8.4
10127	85.47	37.240	-5.610	.270	18	.01470	+33	-11.16	-9.33	-.19	-.26	5.6
	86.08	37.161	-3.040	.380	16	.02030	+10	-10.94	-8.55	-.37	-.39	4.0
10173	77.84	16.966	-0.573	.027	35	.04670	-.11	-10.56	-8.47	-.91	-.77	7.5
	77.03	16.965	-1.107	.032	35	.04000	+03	-10.83	-8.21	-.71	-.68	6.9
10218	93.08	27.175	-1.690	.036	35	.01890	-.15	-11.13	-8.55	+21	+27	7.7
	93.67	27.264	-1.879	.044	33	.02040	-.23	-11.25	-8.49	+32	+40	7.9

TABLE 1.2.—Basic physical data for 413 Super-Schmidt meteors: Accelerations.—Continued

Traill No.	H	v	\dot{v}	p.e.	n	m_1	s	log c	log ρ_{obs}	$\Delta \log \rho_{obs}$	$\Delta \log \rho_{corr}$	P
10222					0							
10240	97.76	39.246	-1.261	.013	62	.00920	-.05	-11.35	-9.10	+0.03	-.01	7.3
	99.25	39.330	-0.774	.019	45	.0111C	-.25	-11.24	-9.28	-.03	-.07	8.0
	97.56	39.220	-1.246	.014	58	.0089C	-.03	-11.33	-9.10	+0.02	-.03	7.2
	93.03	38.486	-4.182	.215	23	.00290	+0.70	-11.41	-8.73	+0.03	-.05	3.7
10247	84.45	34.122	-2.974	.096	27	.0085C	+0.09	-11.09	-8.61	-.56	-.53	6.7
	84.83	34.221	-3.053	.090	28	.0096C	+0.00	-11.18	-8.59	-.51	-.47	7.1
10252	99.20	55.090	-2.280	.140	23	.01010	-.23	-11.39	-9.12	+0.12	+0.09	7.1
10255	87.28	20.063	-2.589	.027	43	.20700	-.23	-11.23	-7.75	+0.53	+0.63	7.9
	87.86	20.231	-1.104	.092	32	.26800	-.64	-11.10	-8.09	+0.24	+0.43	7.2
10273					0							
10279	81.05	20.270	-1.204	.016	53	.01560	+0.06	-11.00	-8.47	-.68	-.65	6.8
	81.62	20.348	-1.530	.043	38	.0172C	-.02	-11.12	-8.35	-.52	-.46	7.2
10281	89.74	26.349	-0.730	.022	48	.02300	-.24	-11.13	-8.85	-.37	-.12	8.0
	89.42	26.375	-0.740	.022	44	.02200	-.19	-11.12	-8.86	-.40	-.22	7.8
10342	73.22	12.896	-0.910	.012	57	.1633C	-.18	-10.79	-7.85	-.60	-.48	7.8
	73.23	12.894	-1.017	.019	51	.1638C	-.18	-10.84	-7.81	-.56	-.44	7.8
10358	91.49	29.369	-0.911	.022	38	.01580	-.11	-11.00	-8.91	-.28	-.29	7.5
	90.62	29.339	-1.310	.028	42	.0143C	-.02	-11.10	-8.76	-.20	-.23	7.2
	85.93	28.877	-6.120	.220	20	.00605	+0.56	-11.32	-8.20	-.03	-.21	4.6
	90.90	29.101	-1.598	.027	40	.01480	-.05	-11.20	-8.66	-.08	-.10	7.3
	86.71	28.590	-4.350	.170	21	.00734	+0.45	-11.31	-8.31	-.07	-.22	5.1
10365	93.06	24.942	-0.495	.038	44	.0300C	-.13	-10.81	-8.94	-.18	-.11	6.1
10380	89.51	45.062	-11.293	.224	20	.00500	-.09	-11.82	-8.35	+0.12	+0.10	7.4
	89.28	45.199	-11.694	.368	18	.0046C	-.03	-11.80	-8.35	+0.10	+0.06	7.2
10384	95.76	33.272	-0.831	.016	49	.07120	-.49	-11.52	-8.84	+0.14	+0.07	8.7
	92.29	33.107	-1.190	.012	68	.0598C	-.24	-11.43	-8.70	-.01	-.01	8.0
	85.25	32.372	-3.330	.100	29	.0293C	+0.35	-11.50	-8.34	-.22	-.09	5.6
	95.35	33.134	-0.666	.021	50	.0702C	-.46	-11.40	-8.93	+0.01	-.04	8.6
	87.69	32.660	-2.394	.045	35	.04030	+0.13	-11.53	-8.44	-.12	-.04	6.5
	81.65	31.244	-10.210	.190	21	.01340	+0.78	-11.68	-7.93	-.09	+0.14	3.8
	91.14	32.956	-1.442	.010	73	.0549C	-.14	-11.45	-8.63	-.03	-.01	7.6
10394	84.84	14.361	-1.484	.030	47	.07310	-.02	-10.86	-7.85	+0.23	+0.25	7.2
	85.39	14.443	-1.219	.021	55	.08660	-.18	-10.92	-7.92	+0.21	+0.22	7.8
10414	86.62	16.798	-0.271	.022	36	3.0670C	-1.33	-11.45	-8.19	+0.04	-.06	7.8
	76.47	16.047	-1.345	.020	25	2.09100	-.27	-11.55	-7.51	-.05	-.04	8.1
	69.26	14.404	-2.962	.027	24	.9000C	+0.41	-11.31	-7.19	-.18	-.10	5.3
	63.58	11.039	-6.212	.021	46	.1720C	+1.25	-11.29	-6.88	-.18	-.07	7.3
	88.46	16.829	-0.203	.007	40	3.13800	-1.64	-11.46	-8.31	+0.07	-.06	9.9

TABLE 1.2.—Basic physical data for 413 Super-Schmidt meteors: Accelerations.—Continued

Trail No.	H	v	\dot{v}	p.e.	n	m_{\perp}	s	log σ	log ρ_{obs}	Δ log ρ_{obs}	Δ log ρ_{corr}	P
	77.04	16.145	-1.228	.008	30	2.1670C	-.32	-11.54	-7.55	-.05	-.05	8.2
	69.39	14.455	-2.964	.016	45	.9320C	+.39	-11.30	-7.18	-.16	-.09	5.4
	63.80	11.271	-6.098	.027	43	.19500	+1.19	-11.30	-6.89	-.18	-.02	2.5
10439	93.73	34.577	-1.465	.065	35	.0523C	-.48	-11.63	-8.67	+.14	+.13	8.7
	90.90	34.322	-2.520	.034	50	.0431C	-.21	-11.63	-8.46	+.12	+.12	7.9
	85.53	33.194	-6.560	.340	23	.01840	+.45	-11.51	-8.13	+.01	+.03	4.6
	96.14	34.532	-0.688	.019	43	.05800	-.70	-11.46	-8.98	+.03	+.00	9.1
	93.09	34.413	-1.249	.011	59	.05040	-.42	-11.52	-8.74	+.02	+.01	8.5
	85.57	33.418	-6.710	.260	23	.01880	+.43	-11.54	-8.13	+.01	+.04	5.2
10447	94.80	33.631	-0.729	.022	42	.03860	-.38	-11.22	-8.99	-.09	-.22	8.4
	93.12	33.548	-0.919	.012	54	.03340	-.20	-11.30	-8.91	-.15	-.24	7.8
	89.29	33.218	-1.805	.068	29	.01510	+.42	-10.90	-8.72	-.27	-.24	5.2
	93.86	33.635	-0.746	.038	45	.03560	-.27	-11.24	-9.99	-.17	-.27	7.3
	92.60	33.573	-0.938	.028	51	.03180	-.14	-11.29	-8.91	-.19	-.27	7.6
	89.14	33.286	-1.886	.101	26	.0143C	+.45	-10.92	-8.71	-.28	-.24	4.6
10478	87.14	23.246	-2.455	.051	35	.10500	-.29	-11.10	-8.00	+.27	+.31	8.1
10480	95.57	22.343	-1.507	.063	31	.0324C	-.12	-11.35	-8.35	+.61	+.73	7.5
	95.80	22.319	-1.093	.184	31	.0343C	-.18	-11.24	-8.48	+.50	+.66	3.1
10531	96.58	50.847	-2.129	.057	29	.00940	-.07	-11.47	-9.09	-.05	-.09	7.3
	95.77	50.850	-2.706	.050	27	.0088C	-.01	-11.55	-9.00	-.02	-.07	7.1
10555	80.10	17.534	-2.744	.104	23	.10130	-.05	-10.89	-7.71	+.01	+.00	7.3
	80.65	17.641	-2.217	.105	26	.13030	-.33	-10.93	-7.77	-.01	+.03	8.3
10566	95.28	26.118	-0.236	.016	64	1.1505C	-1.25	-10.79	-8.77	+.17	+.06	8.8
10583	109.46	68.892	-0.622	.022	50	.00581	-.09	-11.16	-9.96	+.03	-.00	7.4
	105.86	68.460	-3.090	.390	19	.00088	+1.04	-11.26	-9.53	+.20	-.11	1.7
	110.48	68.810	-0.344	.032	47	.00700	-.30	-11.05	-10.19	-.14	-.11	6.5
10587	96.65	36.566	-0.993	.021	33	.05240	-.27	-10.97	-8.89	+.16	+.21	8.1
	97.72	36.536	-0.728	.016	40	.0590C	-.43	-10.98	-9.00	+.13	+.25	8.5
11816	90.38	19.777	-0.267	.007	72	.13150	+.16	-10.79	-8.79	-.25	-.05	7.7
	89.61	19.662	-0.621	.043	38	.10110	+.08	-10.96	-8.46	+.01	-.01	6.1
11818	87.27	15.377	-0.710	.013	54	.91990	-.97	-11.53	-7.87	+.41	+.20	9.5
	83.00	15.123	-0.811	.011	51	.62550	-.20	-10.92	-7.85	+.09	+.01	7.8
	78.99	14.534	-2.193	.021	39	.31460	+.35	-11.31	-7.48	+.16	+.17	5.6
	76.70	13.885	-2.930	.051	29	.1634C	+.72	-11.20	-7.41	+.07	+.14	4.0
	74.39	12.712	-5.715	.229	21	.03911	+1.40	-11.11	-7.25	+.07	+.26	2.0
11825	92.41	22.847	-0.614	.024	48	.07880	-.56	-11.08	-8.63	+.07	+.14	8.9
	91.01	22.780	-0.960	.014	59	.0695C	-.35	-11.14	-8.45	+.14	+.19	8.3
	86.36	22.181	-4.378	.155	23	.02020	+.60	-11.09	-7.95	+.26	+.21	4.5
	92.65	22.807	-0.542	.015	45	.08020	-.59	-11.05	-8.68	+.04	+.12	8.9
	91.00	22.735	-0.828	.008	58	.06950	-.35	-11.08	-8.51	+.08	+.13	8.3
	86.37	22.224	-3.134	.112	23	.0202C	+.60	-10.95	-8.09	+.12	+.07	4.5

TABLE 1.2.—Basic physical data for 413 Super-Schmidt meteors: Accelerations.—Continued

Trail No.	H	v	\dot{v}	p.e.	n	m_1	s	log σ	log ρ_{obs}	$\Delta \log \rho_{\text{obs}}$	$\Delta \log \rho_{\text{corr}}$	P
11856	85.70	20.611	-0.404	.010	56	.06070	-.13	-10.69	-8.76	-.61	-.49	7.6
	85.12	20.576	-0.553	.009	65	.05300	+.00	-10.78	-8.64	-.53	-.48	7.1
	82.80	20.289	-1.856	.084	30	.02218	+.58	-11.04	-8.23	-.31	-.53	4.6
	86.00	20.621	-0.340	.020	49	.06470	-.19	-10.63	-8.82	-.64	-.50	7.0
	85.03	20.569	-0.576	.012	64	.05190	+.02	-10.79	-8.62	-.52	-.48	7.0
	82.53	20.223	-2.619	.102	27	.01917	+.66	-11.03	-8.10	-.20	-.46	4.2
11862	108.16	66.686	-0.456	.067	33	.00400	-.19	-11.00	-10.12	-.22	-.26	3.9
11973	98.83	44.820	-0.929	.029	33	.01790	-.53	-11.34	-9.25	-.03	-.09	8.8
	97.38	44.776	-1.303	.018	38	.01640	-.38	-11.38	-9.11	-.01	-.06	8.4
	90.80	44.206	-6.381	.169	15	.00489	+.57	-11.42	-8.59	-.02	-.06	4.6
	98.30	44.813	-0.897	.031	29	.01740	-.47	-11.29	-9.27	-.09	-.15	8.6
	96.84	44.768	-1.276	.018	34	.01570	-.32	-11.31	-9.13	-.07	-.12	8.2
	91.04	44.321	-5.045	.182	14	.00528	+.53	-11.34	-8.68	-.09	-.13	4.8
12342	87.67	22.884	-0.643	.020	43	.02460	-.04	-10.77	-8.78	-.47	-.44	7.2
	86.88	22.842	-0.960	.014	50	.02130	+.08	-10.97	-8.62	-.37	-.43	6.7
	83.22	22.169	-5.711	.207	19	.00944	+.60	-11.42	-7.94	+.02	-.42	4.5
	87.91	22.997	-0.885	.068	33	.02560	-.08	-10.99	-8.64	-.31	-.25	5.9
	86.56	22.866	-1.734	.026	43	.02010	+.12	-11.22	-8.37	-.15	-.23	6.6
	84.35	22.360	-4.546	.120	23	.01340	+.40	-11.48	-8.00	+.05	-.25	5.3
12361	93.13	22.385	-0.508	.012	54	.09580	-.54	-11.15	-8.66	+.10	+.05	8.8
	90.40	22.127	-1.003	.019	43	.05980	+.03	-11.02	-8.43	+.11	+.06	6.9
	87.85	21.557	-3.660	.088	27	.00960	+1.07	-10.75	-8.18	+.15	+.11	2.8
	91.43	22.240	-0.831	.006	80	.07530	-.19	-11.09	-8.48	+.14	+.09	7.8
	92.53	22.340	-0.641	.016	54	.08940	-.42	-11.16	-8.57	+.14	+.09	8.5
	90.22	22.080	-1.083	.026	40	.05680	+.07	-11.01	-8.40	+.12	+.07	6.8
	88.08	21.639	-2.269	.117	27	.01380	+.90	-10.62	-8.27	+.08	+.04	3.0
	91.12	22.205	-0.897	.008	74	.07070	-.13	-11.10	-8.45	+.15	+.10	7.6
12363	89.04	18.350	-0.506	.017	56	.35370	-.16	-11.09	-8.30	+.13	+.11	7.7
	87.44	18.143	-0.763	.023	44	.26540	+.10	-11.10	-8.16	+.14	+.14	6.7
	85.48	17.685	-1.480	.057	35	.11690	+.61	-10.85	-7.97	+.17	+.20	4.4
	87.68	18.171	-0.776	.006	90	.27980	+.06	-11.14	-8.14	+.17	+.17	6.8
	91.19	18.620	-0.410	.014	66	.45720	-.51	-11.25	-8.37	+.23	+.20	8.7
	87.63	18.191	-0.832	.024	50	.27700	+.06	-11.17	-8.12	+.19	+.19	6.8
	85.52	17.708	-1.371	.052	37	.12030	+.60	-10.84	-8.00	+.14	+.17	4.5
12399	87.84	19.831	-1.144	.051	31	.12410	-.69	-11.23	-8.17	+.16	+.30	9.1
	85.24	19.616	-2.307	.021	47	.09740	-.27	-11.30	-7.89	+.23	+.29	8.1
	80.51	18.393	-9.815	.291	19	.03080	+.59	-11.23	-7.37	+.38	+.28	4.5
	88.33	19.897	-1.060	.034	33	.12760	-.76	-11.28	-8.20	+.17	+.32	9.2
	85.86	19.718	-2.059	.014	48	.10450	-.36	-11.30	-7.93	+.24	+.32	8.3
	81.53	18.817	-7.786	.137	21	.04760	+.33	-11.40	-7.43	+.40	+.35	5.6
12504	93.28	19.201	-0.147	.005	90	.76300	-1.00	-10.96	-8.77	+.01	+.06	9.5
	89.69	19.006	-0.542	.009	71	.54300	-.26	-10.97	-8.24	+.24	+.25	8.0
	86.60	18.564	-1.000	.011	61	.20900	+.48	-11.02	-8.09	+.14	+.10	5.0
	83.79	17.575	-3.514	.043	33	.03140	+1.41	-11.22	-7.77	+.23	+.14	1.9
	89.73	19.007	-0.477	.001	169	.54800	-.27	-10.93	-8.30	+.18	+.19	0.0
	94.06	19.228	-0.155	.005	87	.79100	-1.22	-11.17	-8.74	+.10	+.17	9.7

TABLE 1.2.—Basic physical data for 413 Super-Schmidt meteors: Accelerations.—Continued

Trail No.	H	v	\dot{v}	p.e.	n	m_{\perp}	s	log σ	log ρ_{obs}	$\Delta \log \rho_{\text{obs}}$	$\Delta \log \rho_{\text{corr}}$	P
90.39	19.043	-0.469	.006	71	.60500	-.41	-11.14	-8.29	+0.25	+0.27	8.5	
87.26	18.682	-0.786	.008	71	.26100	+0.35	-10.92	-8.17	+0.11	+0.08	5.6	
83.99	17.673	-3.984	.096	35	.03640	+1.34	-11.29	-7.71	+0.31	+0.22	2.1	
90.16	19.035	-0.425	.001	172	.58800	-.37	-11.04	-8.34	+0.18	+0.20	0.0	
12577	94.47	29.537	-0.459	.025	41	.07650	-.59	-11.21	-8.98	-.11	+0.06	8.0
89.70	29.293	-1.677	.038	29	.05400	-.11	-11.37	-8.46	+0.02	+0.09	7.5	
85.58	28.587	-5.589	.124	19	.02180	+0.53	-11.41	-8.05	+0.09	+0.04	4.8	
91.63	29.429	-0.968	.007	60	.06490	-.32	-11.34	-8.68	-.04	+0.07	8.2	
94.62	29.576	-0.457	.024	44	.07700	-.60	-11.22	-8.98	-.09	+0.08	8.0	
89.54	29.294	-1.643	.080	27	.05260	-.08	-11.34	-8.47	-.00	+0.06	7.4	
85.42	28.536	-7.124	.274	19	.02060	+0.56	-11.50	-7.95	+0.18	+0.12	4.6	
91.92	29.477	-0.946	.009	62	.06620	-.34	-11.35	-8.69	+0.03	+0.09	8.3	
12714	93.53	25.697	-0.843	.024	35	.05720	-.48	-11.04	-8.64	+0.16	+0.07	8.7
91.46	25.597	-1.132	.019	47	.04290	-.11	-10.86	-8.55	+0.08	+0.10	7.5	
88.03	25.344	-1.804	.081	27	.01460	+0.62	-10.62	-8.49	-.15	+0.08	4.4	
91.89	25.588	-1.163	.022	47	.04630	-.19	-10.92	-8.53	+0.13	+0.13	7.8	

TABLE 2.1.—Correlation between mass and velocity for Super-Schmidt and small-camera meteors (In the table for small-camera meteors only those were included for which log σ was determined.)

Super-Schmidt Meteors			Small-Camera Meteors		
Mean $v_{\infty} \pm$ s.d. (km/s)	Mean $m_{\infty} \pm$ s.d. (g)	No. obs.	Mean $v_{\infty} \pm$ s.d. (km/s)	Mean $m_{\infty} \pm$ s.d. (g)	No. obs.
13.5 \pm 0.3	1.42 \pm 0.15	9	16.2 \pm 0.9	125 \pm 45	9
17.7 \pm 0.2	2.65 \pm 0.71	57	25.9 \pm 0.6	176 \pm 85	27
22.4 \pm 0.2	0.88 \pm 0.14	65	34.4 \pm 0.5	97 \pm 41	36
27.4 \pm 0.2	0.70 \pm 0.20	63	45.5 \pm 2.1	12 \pm 5	4
31.9 \pm 0.2	0.51 \pm 0.09	48	55.5 \pm 1.9	47 \pm 25	5
36.7 \pm 0.2	0.48 \pm 0.15	39	61.6 \pm 0.9	7 \pm 4	7
42.8 \pm 0.2	0.09 \pm 0.01	34	All	110 \pm 31	88
47.3 \pm 0.4	0.24 \pm 0.08	14			
53.0 \pm 0.5	0.10 \pm 0.03	9			
58.2 \pm 0.4	0.09 \pm 0.03	18			
61.8 \pm 0.3	0.13 \pm 0.05	25			
67.7 \pm 0.2	0.27 \pm 0.23	22			
71.4 \pm 0.3	0.10 \pm 0.04	8			
All	0.80 \pm 0.11	411			

TABLE 2.2.—Correlation of velocity, mass, and brightness with the zenith angle for Super-Schmidt meteors for which σ was determined

Range of $\cos Z_R$	Mean $\cos Z_R$	Mean $v_{\infty} \pm$ s.d. (km/s)	Mean $m_{\infty} \pm$ s.d. (g)	Mean $\epsilon_{\infty} \pm$ s.d.	No. obs.
0.1 - 0.2	0.14	48.7 \pm 14.5	0.5 \pm 0.5	-0.29 \pm 0.03	3
0.2 - 0.3	0.25	43.3 \pm 7.4	1.3 \pm 0.7	-0.14 \pm 0.15	9
0.3 - 0.4	0.35	40.3 \pm 3.3	0.6 \pm 0.3	-0.36 \pm 0.09	28
0.4 - 0.5	0.46	44.5 \pm 3.4	0.8 \pm 0.2	-0.21 \pm 0.10	32
0.5 - 0.6	0.55	33.7 \pm 2.4	1.4 \pm 0.7	-0.43 \pm 0.09	29
0.6 - 0.7	0.65	33.8 \pm 1.7	1.2 \pm 0.5	-0.40 \pm 0.06	76
0.7 - 0.8	0.75	32.0 \pm 1.6	0.4 \pm 0.1	-0.53 \pm 0.05	70
0.8 - 0.9	0.84	31.7 \pm 1.9	0.6 \pm 0.2	-0.52 \pm 0.06	61
0.9 - 1.0	0.97	33.7 \pm 1.8	1.1 \pm 0.3	-0.28 \pm 0.09	40

TABLE 3

Identification of coefficients for tables 3.1 through 3.17. c_0 to c_5 are coefficients of an equation of the type: $\log \rho = c_0 + \sum_{i=1}^k c_i(x_i - \bar{x}_i)$, where $k=2, 3, 4, 5$ and $x_1 = \log \cos Z_R$, $x_2 = \log v_\infty$, $x_3 = \log m_\infty$, $x_4 = \log \sigma$, $x_5 = \chi$, $\bar{x}_1 = -0.2$, $\bar{x}_2 = 6.4771$, $\bar{x}_3 = -0.5229$, $\bar{x}_4 = -11.20$, $\bar{x}_5 = 0.25$.

TABLE 3.1.—Solutions for the totality of Super-Schmidt meteors

	H_B	$H_{2.5}$	H_{ML}	H_E
c_0	-9.20 ± 0.02	-9.16 ± 0.02	-8.43 ± 0.02	-8.07 ± 0.02
c_1	0.07 ± 0.11	0.19 ± 0.11	1.01 ± 0.11	1.36 ± 0.10
c_2	-2.97 ± 0.09	-3.37 ± 0.09	-2.41 ± 0.09	-2.23 ± 0.09
	(403)	(402)	(412)	(411)
c_0	-9.21 ± 0.02	-9.17 ± 0.02	-8.42 ± 0.02	-8.05 ± 0.01
c_1	0.02 ± 0.11	0.14 ± 0.11	1.10 ± 0.09	1.42 ± 0.09
c_2	-3.59 ± 0.13	-4.09 ± 0.12	-1.43 ± 0.11	-1.17 ± 0.11
c_3	-0.25 ± 0.04	-0.30 ± 0.04	0.41 ± 0.03	0.45 ± 0.03
	(402)	(402)	(411)	(409)
c_0	-9.21 ± 0.02	-9.17 ± 0.02	-8.41 ± 0.01	-8.05 ± 0.01
c_1	0.05 ± 0.12	0.19 ± 0.11	1.13 ± 0.10	1.46 ± 0.09
c_2	-3.49 ± 0.14	-4.02 ± 0.13	-1.50 ± 0.12	-1.21 ± 0.11
c_3	-0.24 ± 0.04	-0.29 ± 0.04	0.39 ± 0.03	0.44 ± 0.03
c_4	0.13 ± 0.06	0.09 ± 0.06	-0.19 ± 0.06	-0.15 ± 0.05
	(387)	(387)	(396)	(394)
c_0	-9.22 ± 0.02	-9.17 ± 0.02	-8.41 ± 0.01	-8.05 ± 0.01
c_1	0.15 ± 0.12	0.23 ± 0.12	1.09 ± 0.10	1.36 ± 0.09
c_2	-3.44 ± 0.14	-4.00 ± 0.13	-1.52 ± 0.12	-1.25 ± 0.11
c_3	-0.22 ± 0.04	-0.28 ± 0.04	0.38 ± 0.03	0.42 ± 0.03
c_4	0.15 ± 0.06	0.09 ± 0.06	-0.19 ± 0.06	-0.16 ± 0.05
c_5	0.16 ± 0.06	0.07 ± 0.05	-0.07 ± 0.05	-0.16 ± 0.04
	(387)	(387)	(396)	(394)

TABLE 3.2.—All Super-Schmidt meteors (D meteors excluded)

	H_B	$H_{2.5}$	H_{ML}	H_E
c_0	-9.22 ± 0.02	-9.18 ± 0.02	-8.43 ± 0.02	-8.08 ± 0.02
c_1	0.04 ± 0.12	0.16 ± 0.12	1.01 ± 0.11	1.34 ± 0.11
c_2	-2.88 ± 0.09	-3.29 ± 0.09	-2.35 ± 0.09	-2.15 ± 0.09
	(382)	(381)	(390)	(389)
c_0	-9.23 ± 0.02	-9.18 ± 0.02	-8.42 ± 0.02	-8.07 ± 0.01
c_1	-0.00 ± 0.11	0.12 ± 0.11	1.09 ± 0.09	1.40 ± 0.09
c_2	-3.48 ± 0.13	-3.99 ± 0.12	-1.35 ± 0.11	-1.08 ± 0.11
c_3	-0.24 ± 0.04	-0.29 ± 0.04	0.41 ± 0.03	0.45 ± 0.03
	(381)	(381)	(389)	(387)
c_0	-9.23 ± 0.02	-9.18 ± 0.02	-8.42 ± 0.01	-8.06 ± 0.01
c_1	0.03 ± 0.12	0.16 ± 0.12	1.12 ± 0.10	1.44 ± 0.09
c_2	-3.40 ± 0.14	-3.94 ± 0.13	-1.42 ± 0.12	-1.12 ± 0.11
c_3	-0.24 ± 0.04	-0.28 ± 0.04	0.40 ± 0.03	0.44 ± 0.03
c_4	0.11 ± 0.07	0.06 ± 0.07	-0.20 ± 0.06	-0.19 ± 0.05
	(367)	(367)	(375)	(373)
c_0	-9.23 ± 0.02	-9.18 ± 0.02	-8.42 ± 0.01	-8.06 ± 0.01
c_1	0.10 ± 0.12	0.19 ± 0.12	1.07 ± 0.10	1.33 ± 0.09
c_2	-3.37 ± 0.14	-3.93 ± 0.13	-1.44 ± 0.12	-1.17 ± 0.11
c_3	-0.22 ± 0.04	-0.28 ± 0.04	0.39 ± 0.03	0.42 ± 0.03
c_4	0.12 ± 0.07	0.06 ± 0.07	-0.21 ± 0.06	-0.20 ± 0.05
c_5	0.13 ± 0.06	0.03 ± 0.05	-0.10 ± 0.05	-0.19 ± 0.04
	(367)	(367)	(375)	(373)

TABLE 3.3.—Sporadic Super-Schmidt meteors

	H_B	$H_{2.5}$	H_{ML}	H_E
c_0	-9.19 ± 0.02	-9.14 ± 0.02	-8.43 ± 0.02	-8.08 ± 0.02
c_1	0.07 ± 0.14	0.24 ± 0.14	0.82 ± 0.12	1.13 ± 0.12
c_2	-3.01 ± 0.11	-3.41 ± 0.11	-2.51 ± 0.10	-2.35 ± 0.09
	(282)	(283)	(289)	(288)
c_0	-9.20 ± 0.02	-9.15 ± 0.02	-8.42 ± 0.02	-8.06 ± 0.02
c_1	0.04 ± 0.14	0.13 ± 0.13	0.95 ± 0.10	1.24 ± 0.10
c_2	-3.71 ± 0.16	-4.16 ± 0.15	-1.58 ± 0.13	-1.35 ± 0.13
c_3	-0.27 ± 0.05	-0.30 ± 0.05	0.36 ± 0.04	0.40 ± 0.04
	(281)	(283)	(289)	(287)
c_0	-9.20 ± 0.02	-9.16 ± 0.02	-8.40 ± 0.02	-8.05 ± 0.02
c_1	0.01 ± 0.15	0.20 ± 0.14	0.96 ± 0.10	1.27 ± 0.10
c_2	-3.62 ± 0.18	-4.11 ± 0.17	-1.82 ± 0.13	-1.48 ± 0.13
c_3	-0.26 ± 0.05	-0.29 ± 0.05	0.34 ± 0.04	0.39 ± 0.04
c_4	0.11 ± 0.09	0.05 ± 0.09	-0.39 ± 0.07	-0.28 ± 0.07
	(271)	(273)	(279)	(277)
c_0	-9.20 ± 0.02	-9.16 ± 0.02	-8.40 ± 0.02	-8.05 ± 0.02
c_1	0.19 ± 0.15	0.31 ± 0.15	1.02 ± 0.11	1.24 ± 0.11
c_2	-3.52 ± 0.17	-4.07 ± 0.17	-1.79 ± 0.13	-1.50 ± 0.13
c_3	-0.22 ± 0.05	-0.27 ± 0.05	0.36 ± 0.04	0.39 ± 0.04
c_4	0.10 ± 0.09	0.03 ± 0.09	-0.40 ± 0.07	-0.28 ± 0.07
c_5	0.28 ± 0.07	0.13 ± 0.06	0.09 ± 0.05	-0.04 ± 0.05
	(271)	(273)	(279)	(277)

TABLE 3.4.—Sporadic Super-Schmidt meteors (D meteors excluded)

	H_B	$H_{2.5}$	H_{ML}	H_E
c_0	-9.21 ± 0.02	-9.16 ± 0.02	-8.43 ± 0.02	-8.09 ± 0.02
c_1	0.01 ± 0.15	0.18 ± 0.15	0.79 ± 0.12	1.08 ± 0.12
c_2	-2.92 ± 0.11	-3.32 ± 0.11	-2.45 ± 0.10	-2.27 ± 0.09
	(261)	(262)	(267)	(266)
c_0	-9.22 ± 0.02	-9.17 ± 0.02	-8.42 ± 0.02	-8.07 ± 0.02
c_1	-0.10 ± 0.14	0.08 ± 0.14	0.92 ± 0.11	1.18 ± 0.10
c_2	-3.61 ± 0.17	-4.06 ± 0.16	-1.50 ± 0.13	-1.26 ± 0.12
c_3	-0.26 ± 0.05	-0.29 ± 0.05	0.37 ± 0.04	0.40 ± 0.04
	(260)	(262)	(267)	(265)
c_0	-9.22 ± 0.02	-9.17 ± 0.02	-8.41 ± 0.02	-8.06 ± 0.01
c_1	-0.04 ± 0.16	0.15 ± 0.15	0.91 ± 0.10	1.19 ± 0.10
c_2	-3.54 ± 0.18	-4.04 ± 0.17	-1.77 ± 0.13	-1.45 ± 0.12
c_3	-0.25 ± 0.05	-0.28 ± 0.05	0.35 ± 0.04	0.40 ± 0.04
c_4	0.06 ± 0.10	-0.02 ± 0.10	-0.48 ± 0.07	-0.40 ± 0.07
	(251)	(253)	(258)	(256)
c_0	-9.22 ± 0.02	-9.17 ± 0.02	-8.41 ± 0.02	-8.06 ± 0.01
c_1	0.10 ± 0.16	0.23 ± 0.16	0.96 ± 0.11	1.15 ± 0.10
c_2	-3.48 ± 0.18	-4.02 ± 0.17	-1.76 ± 0.13	-1.46 ± 0.12
c_3	-0.22 ± 0.05	-0.27 ± 0.05	0.30 ± 0.04	0.39 ± 0.04
c_4	0.04 ± 0.10	-0.04 ± 0.10	-0.50 ± 0.08	-0.39 ± 0.07
c_5	0.26 ± 0.08	0.10 ± 0.07	0.08 ± 0.05	-0.06 ± 0.05
	(251)	(253)	(258)	(256)

TABLE 3.5.—*Sporadic Super-Schmidt meteors (A and S excluded)*

	H _B	H _{2.5}	H _{ML}	H _E
c ₀	-9.24 ± 0.02	-9.18 ± 0.02	-8.43 ± 0.02	-8.09 ± 0.02
c ₁	-0.03 ± 0.14	0.14 ± 0.14	0.82 ± 0.12	1.10 ± 0.12
c ₂	-2.93 ± 0.11	-3.36 ± 0.11	-2.51 ± 0.10	-2.36 ± 0.10
	(253)	(254)	(260)	(259)
c ₀	-9.24 ± 0.02	-9.19 ± 0.02	-8.42 ± 0.02	-8.07 ± 0.02
c ₁	-0.13 ± 0.13	0.04 ± 0.13	0.95 ± 0.11	1.20 ± 0.10
c ₂	-3.60 ± 0.15	-4.10 ± 0.15	-1.57 ± 0.14	-1.34 ± 0.13
c ₃	-0.26 ± 0.05	-0.29 ± 0.04	0.37 ± 0.04	0.41 ± 0.04
	(252)	(254)	(260)	(258)
c ₀	-9.25 ± 0.02	-9.19 ± 0.02	-8.41 ± 0.02	-8.06 ± 0.02
c ₁	-0.08 ± 0.14	0.10 ± 0.14	0.94 ± 0.11	1.22 ± 0.10
c ₂	-3.58 ± 0.17	-4.10 ± 0.16	-1.80 ± 0.14	-1.49 ± 0.13
c ₃	-0.25 ± 0.05	-0.29 ± 0.04	0.35 ± 0.04	0.40 ± 0.04
c ₄	0.00 ± 0.09	-0.05 ± 0.09	-0.43 ± 0.07	-0.35 ± 0.07
	(243)	(245)	(251)	(249)
c ₀	-9.24 ± 0.02	-9.19 ± 0.02	-8.41 ± 0.02	-8.06 ± 0.02
c ₁	0.12 ± 0.15	0.22 ± 0.15	1.00 ± 0.12	1.19 ± 0.11
c ₂	-3.48 ± 0.16	-4.07 ± 0.16	-1.78 ± 0.14	-1.50 ± 0.13
c ₃	-0.21 ± 0.05	-0.26 ± 0.05	0.36 ± 0.04	0.39 ± 0.04
c ₄	-0.02 ± 0.09	-0.07 ± 0.09	-0.44 ± 0.08	-0.35 ± 0.07
c ₅	0.29 ± 0.07	0.14 ± 0.06	0.09 ± 0.05	-0.04 ± 0.05
	(243)	(245)	(251)	(249)

TABLE 3.6.—*Sporadic Super-Schmidt meteors (A, S, and D excluded)*

	H _B	H _{2.5}	H _{ML}	H _E
c ₀	-9.25 ± 0.02	-9.20 ± 0.02	-8.44 ± 0.02	-8.10 ± 0.02
c ₁	-0.09 ± 0.14	0.09 ± 0.14	0.75 ± 0.13	1.03 ± 0.12
c ₂	-2.88 ± 0.10	-3.31 ± 0.10	-2.47 ± 0.10	-2.30 ± 0.10
	(240)	(241)	(246)	(245)
c ₀	-9.26 ± 0.02	-9.21 ± 0.02	-8.43 ± 0.02	-8.08 ± 0.02
c ₁	-0.19 ± 0.13	-0.01 ± 0.13	0.89 ± 0.11	1.12 ± 0.10
c ₂	-3.56 ± 0.15	-4.04 ± 0.15	-1.51 ± 0.13	-1.28 ± 0.13
c ₃	-0.26 ± 0.05	-0.28 ± 0.04	0.37 ± 0.04	0.40 ± 0.04
	(239)	(241)	(246)	(244)
c ₀	-9.26 ± 0.02	-9.21 ± 0.02	-8.42 ± 0.02	-8.07 ± 0.01
c ₁	-0.16 ± 0.15	0.03 ± 0.14	0.86 ± 0.11	1.13 ± 0.10
c ₂	-3.56 ± 0.17	-4.08 ± 0.16	-1.79 ± 0.14	-1.47 ± 0.12
c ₃	-0.25 ± 0.05	-0.28 ± 0.04	0.35 ± 0.04	0.40 ± 0.03
c ₄	-0.05 ± 0.10	-0.12 ± 0.10	-0.51 ± 0.08	-0.44 ± 0.07
	(230)	(232)	(237)	(235)
c ₀	-9.26 ± 0.02	-9.21 ± 0.02	-8.42 ± 0.02	-8.07 ± 0.01
c ₁	-0.00 ± 0.15	0.11 ± 0.15	0.92 ± 0.11	1.08 ± 0.10
c ₂	-3.49 ± 0.17	-4.06 ± 0.16	-1.77 ± 0.14	-1.49 ± 0.12
c ₃	-0.21 ± 0.05	-0.27 ± 0.05	0.36 ± 0.04	0.39 ± 0.04
c ₄	-0.07 ± 0.10	-0.14 ± 0.10	-0.53 ± 0.08	-0.43 ± 0.07
c ₅	0.26 ± 0.07	0.10 ± 0.06	0.08 ± 0.05	-0.06 ± 0.05
	(230)	(232)	(237)	(235)

TABLE 3.7.—*Sporadic Super-Schmidt meteors (A, S, and D excluded) with log σ < -11.4*

	H _B	H _{2.5}	H _{ML}	H _E
c ₀	-9.42 ± 0.09	-9.40 ± 0.10	-8.03 ± 0.10	-7.64 ± 0.07
c ₁	0.03 ± 0.40	0.11 ± 0.51	0.63 ± 0.37	1.03 ± 0.25
c ₂	-1.75 ± 0.39	-2.05 ± 0.43	-3.21 ± 0.41	-3.46 ± 0.28
	(35)	(34)	(37)	(36)
c ₀	-9.28 ± 0.09	-9.25 ± 0.10	-8.21 ± 0.08	-7.74 ± 0.07
c ₁	-0.10 ± 0.34	-0.12 ± 0.44	0.87 ± 0.27	1.13 ± 0.24
c ₂	-3.07 ± 0.48	-3.42 ± 0.54	-1.47 ± 0.43	-2.43 ± 0.47
c ₃	-0.34 ± 0.09	-0.35 ± 0.10	0.45 ± 0.08	0.24 ± 0.09
	(35)	(34)	(37)	(36)
c ₀	-9.66 ± 0.11	-9.64 ± 0.14	-8.51 ± 0.11	-8.08 ± 0.12
c ₁	0.04 ± 0.27	0.05 ± 0.38	0.94 ± 0.24	1.22 ± 0.21
c ₂	-3.06 ± 0.38	-3.41 ± 0.46	-1.42 ± 0.38	-1.89 ± 0.45
c ₃	-0.33 ± 0.07	-0.34 ± 0.09	0.46 ± 0.07	0.36 ± 0.09
c ₄	-1.08 ± 0.26	-1.10 ± 0.31	-0.85 ± 0.25	-0.83 ± 0.26
	(35)	(34)	(37)	(36)
c ₀	-9.64 ± 0.12	-9.66 ± 0.15	-8.48 ± 0.12	-8.11 ± 0.13
c ₁	0.11 ± 0.32	-0.06 ± 0.46	1.02 ± 0.27	1.12 ± 0.24
c ₂	-3.04 ± 0.39	-3.43 ± 0.47	-1.39 ± 0.38	-1.95 ± 0.45
c ₃	-0.31 ± 0.08	-0.36 ± 0.10	0.48 ± 0.08	0.33 ± 0.10
c ₄	-1.04 ± 0.28	-1.15 ± 0.33	-0.79 ± 0.27	-0.90 ± 0.27
c ₅	0.08 ± 0.17	-0.09 ± 0.21	0.10 ± 0.16	-0.12 ± 0.14
	(35)	(34)	(37)	(36)

TABLE 3.8.—*Sporadic Super-Schmidt meteors (A, S, and D excluded) with -11.4 ≤ log σ ≤ -11.0*

	H _B	H _{2.5}	H _{ML}	H _E
c ₀	-9.29 ± 0.02	-9.23 ± 0.02	-8.47 ± 0.02	-8.13 ± 0.02
c ₁	-0.01 ± 0.18	0.19 ± 0.18	0.72 ± 0.15	0.97 ± 0.16
c ₂	-2.92 ± 0.13	-3.33 ± 0.13	-2.62 ± 0.12	-2.45 ± 0.13
	(150)	(152)	(154)	(153)
c ₀	-9.30 ± 0.02	-9.24 ± 0.02	-8.45 ± 0.02	-8.11 ± 0.02
c ₁	-0.09 ± 0.18	0.08 ± 0.18	0.90 ± 0.13	1.18 ± 0.12
c ₂	-3.32 ± 0.21	-3.88 ± 0.20	-1.67 ± 0.16	-1.29 ± 0.15
c ₃	-0.15 ± 0.06	-0.20 ± 0.06	0.35 ± 0.05	0.43 ± 0.04
	(150)	(152)	(154)	(153)
c ₀	-9.30 ± 0.02	-9.24 ± 0.02	-8.45 ± 0.02	-8.10 ± 0.02
c ₁	-0.04 ± 0.18	0.11 ± 0.18	0.89 ± 0.13	1.17 ± 0.12
c ₂	-3.24 ± 0.21	-3.81 ± 0.20	-1.70 ± 0.17	-1.31 ± 0.15
c ₃	-0.15 ± 0.06	-0.20 ± 0.06	0.35 ± 0.05	0.43 ± 0.04
c ₄	0.57 ± 0.23	0.39 ± 0.23	-0.17 ± 0.19	-0.08 ± 0.18
	(150)	(152)	(154)	(153)
c ₀	-9.29 ± 0.02	-9.23 ± 0.02	-8.45 ± 0.02	-8.11 ± 0.02
c ₁	0.05 ± 0.18	0.16 ± 0.18	0.91 ± 0.14	1.15 ± 0.12
c ₂	-3.19 ± 0.21	-3.79 ± 0.20	-1.69 ± 0.17	-1.32 ± 0.15
c ₃	-0.11 ± 0.06	-0.18 ± 0.06	0.36 ± 0.05	0.42 ± 0.04
c ₄	0.52 ± 0.23	0.36 ± 0.23	-0.19 ± 0.19	-0.06 ± 0.18
c ₅	0.27 ± 0.09	0.15 ± 0.09	0.08 ± 0.08	-0.11 ± 0.07
	(150)	(152)	(154)	(153)

TABLE 3.9.—*Sporadic Super-Schmidt meteors (A, S, and D excluded), with log $\sigma > -11.0$*

	H_B	$H_{2.5}$	H_{ML}	H_E
c_0	-9.25 ± 0.06	-9.22 ± 0.06	-8.56 ± 0.05	-8.17 ± 0.05
c_1	-0.01 ± 0.34	0.17 ± 0.29	0.80 ± 0.26	0.93 ± 0.24
c_2	-3.46 ± 0.30	-3.89 ± 0.27	-2.79 ± 0.25	-2.39 ± 0.22
	(45)	(46)	(46)	(46)
c_0	-9.24 ± 0.06	-9.22 ± 0.05	-8.56 ± 0.05	-8.17 ± 0.04
c_1	-0.13 ± 0.31	0.09 ± 0.27	0.82 ± 0.27	0.99 ± 0.23
c_2	-4.26 ± 0.38	-4.66 ± 0.35	-2.55 ± 0.35	-1.93 ± 0.30
c_3	-0.38 ± 0.13	-0.36 ± 0.12	0.11 ± 0.12	0.21 ± 0.10
	(45)	(46)	(46)	(46)
c_0	-9.24 ± 0.21	-9.18 ± 0.19	-8.24 ± 0.18	-7.90 ± 0.15
c_1	-0.09 ± 0.33	0.13 ± 0.27	0.80 ± 0.27	1.01 ± 0.22
c_2	-4.24 ± 0.40	-4.59 ± 0.36	-2.37 ± 0.35	-1.75 ± 0.29
c_3	-0.36 ± 0.13	-0.33 ± 0.12	0.14 ± 0.12	0.26 ± 0.10
c_4	-0.03 ± 0.58	-0.14 ± 0.51	-0.92 ± 0.50	-0.78 ± 0.41
	(45)	(46)	(46)	(46)
c_0	-9.22 ± 0.21	-9.17 ± 0.19	-8.21 ± 0.19	-7.93 ± 0.16
c_1	0.01 ± 0.35	0.15 ± 0.32	0.95 ± 0.31	0.88 ± 0.26
c_2	-4.21 ± 0.40	-4.59 ± 0.37	-2.36 ± 0.35	-1.76 ± 0.29
c_3	-0.35 ± 0.13	-0.32 ± 0.12	0.16 ± 0.12	0.25 ± 0.10
c_4	-0.09 ± 0.59	-0.16 ± 0.54	-1.04 ± 0.52	-0.67 ± 0.43
c_5	0.13 ± 0.15	0.01 ± 0.11	0.10 ± 0.11	-0.09 ± 0.09
	(45)	(46)	(46)	(46)

TABLE 3.10.—*Sporadic Super-Schmidt meteors (A, S, and D excluded) with $|\chi| \leq 0.8$*

	H_B	$H_{2.5}$	H_{ML}	H_E
c_0	-9.35 ± 0.03	-9.28 ± 0.03	-8.43 ± 0.03	-8.04 ± 0.03
c_1	0.29 ± 0.21	0.49 ± 0.22	0.74 ± 0.19	0.91 ± 0.17
c_2	-2.86 ± 0.15	-3.25 ± 0.15	-2.38 ± 0.15	-2.16 ± 0.14
	(117)	(118)	(120)	(119)
c_0	-9.33 ± 0.03	-9.25 ± 0.03	-8.46 ± 0.02	-8.07 ± 0.02
c_1	-0.01 ± 0.21	0.16 ± 0.20	1.08 ± 0.16	1.27 ± 0.14
c_2	-3.60 ± 0.21	-4.03 ± 0.20	-1.34 ± 0.19	-1.07 ± 0.16
c_3	-0.29 ± 0.06	-0.32 ± 0.06	0.42 ± 0.06	0.44 ± 0.05
	(117)	(118)	(120)	(119)
c_0	-9.33 ± 0.03	-9.25 ± 0.03	-8.46 ± 0.02	-8.07 ± 0.02
c_1	0.02 ± 0.20	0.18 ± 0.20	1.02 ± 0.15	1.22 ± 0.13
c_2	-3.39 ± 0.23	-3.86 ± 0.22	-1.76 ± 0.20	-1.36 ± 0.17
c_3	-0.27 ± 0.06	-0.30 ± 0.06	0.37 ± 0.05	0.41 ± 0.04
c_4	0.25 ± 0.15	0.22 ± 0.15	-0.59 ± 0.13	-0.40 ± 0.11
	(116)	(117)	(119)	(118)
c_0	-9.17 ± 0.06	-9.14 ± 0.06	-8.36 ± 0.06	-8.06 ± 0.05
c_1	-0.05 ± 0.20	0.14 ± 0.20	0.99 ± 0.15	1.22 ± 0.13
c_2	-3.33 ± 0.22	-3.82 ± 0.22	-1.73 ± 0.20	-1.35 ± 0.17
c_3	-0.26 ± 0.06	-0.29 ± 0.06	0.38 ± 0.05	0.41 ± 0.05
c_4	0.30 ± 0.14	0.25 ± 0.15	-0.56 ± 0.13	-0.40 ± 0.11
c_5	0.78 ± 0.27	0.51 ± 0.27	0.46 ± 0.24	0.06 ± 0.21
	(116)	(117)	(119)	(118)

TABLE 3.11.—*Sporadic Super-Schmidt meteors (A, S, and D excluded) with $\chi > 0.8$*

	H_B	$H_{2.5}$	H_{ML}	H_E
c_0	-9.16 ± 0.03	-9.13 ± 0.03	-8.44 ± 0.03	-8.15 ± 0.03
c_1	-0.17 ± 0.21	0.05 ± 0.21	0.83 ± 0.21	1.06 ± 0.18
c_2	-3.06 ± 0.15	-3.45 ± 0.15	-2.46 ± 0.15	-2.35 ± 0.14
	(109)	(110)	(113)	(112)
c_0	-9.17 ± 0.03	-9.15 ± 0.03	-8.40 ± 0.03	-8.12 ± 0.03
c_1	-0.18 ± 0.21	0.03 ± 0.20	0.88 ± 0.18	1.10 ± 0.16
c_2	-3.32 ± 0.23	-3.85 ± 0.22	-1.54 ± 0.20	-1.47 ± 0.20
c_3	-0.11 ± 0.07	-0.16 ± 0.07	0.37 ± 0.06	0.35 ± 0.06
	(109)	(110)	(113)	(112)
c_0	-9.15 ± 0.03	-9.12 ± 0.03	-8.38 ± 0.03	-8.09 ± 0.02
c_1	-0.23 ± 0.21	-0.10 ± 0.20	0.78 ± 0.16	1.00 ± 0.15
c_2	-3.48 ± 0.23	-4.05 ± 0.22	-1.79 ± 0.19	-1.57 ± 0.19
c_3	-0.10 ± 0.07	-0.16 ± 0.06	0.38 ± 0.06	0.40 ± 0.06
c_4	-0.37 ± 0.13	-0.45 ± 0.12	-0.54 ± 0.10	-0.48 ± 0.10
	(109)	(110)	(113)	(112)
c_0	-9.18 ± 0.04	-9.11 ± 0.04	-8.37 ± 0.03	-8.08 ± 0.03
c_1	-0.15 ± 0.22	-0.15 ± 0.22	0.75 ± 0.18	0.96 ± 0.17
c_2	-3.45 ± 0.23	-4.06 ± 0.22	-1.79 ± 0.19	-1.58 ± 0.19
c_3	-0.08 ± 0.07	-0.16 ± 0.07	0.38 ± 0.06	0.40 ± 0.06
c_4	-0.38 ± 0.13	-0.44 ± 0.13	-0.53 ± 0.11	-0.47 ± 0.10
c_5	0.13 ± 0.13	-0.05 ± 0.10	-0.03 ± 0.08	-0.04 ± 0.08
	(109)	(110)	(113)	(112)

TABLE 3.12.—*Sporadic Super-Schmidt meteors (A, S, and D excluded) with $\chi > 0.4$*

	H_B	$H_{2.5}$	H_{ML}	H_E
c_0	-9.09 ± 0.05	-9.09 ± 0.05	-8.47 ± 0.05	-8.18 ± 0.05
c_1	0.18 ± 0.28	0.29 ± 0.28	0.78 ± 0.28	0.99 ± 0.27
c_2	-2.98 ± 0.20	-3.46 ± 0.21	-2.55 ± 0.21	-2.42 ± 0.20
	(50)	(51)	(52)	(52)
c_0	-9.09 ± 0.05	-9.11 ± 0.05	-8.43 ± 0.05	-8.12 ± 0.05
c_1	0.18 ± 0.29	0.24 ± 0.28	0.87 ± 0.27	1.10 ± 0.25
c_2	-3.07 ± 0.40	-3.86 ± 0.40	-1.77 ± 0.39	-1.43 ± 0.37
c_3	-0.03 ± 0.12	-0.14 ± 0.12	0.28 ± 0.12	0.36 ± 0.11
	(50)	(51)	(52)	(52)
c_0	-9.02 ± 0.05	-9.05 ± 0.05	-8.36 ± 0.05	-8.06 ± 0.05
c_1	0.19 ± 0.27	0.19 ± 0.26	0.84 ± 0.24	1.08 ± 0.23
c_2	-3.09 ± 0.37	-3.85 ± 0.38	-1.78 ± 0.35	-1.43 ± 0.33
c_3	0.05 ± 0.12	-0.06 ± 0.12	0.37 ± 0.11	0.44 ± 0.11
c_4	-0.52 ± 0.18	-0.48 ± 0.18	-0.54 ± 0.16	-0.50 ± 0.15
	(50)	(51)	(52)	(52)
c_0	-8.99 ± 0.08	-9.01 ± 0.07	-8.33 ± 0.06	-8.02 ± 0.06
c_1	0.14 ± 0.29	0.06 ± 0.29	0.73 ± 0.27	0.96 ± 0.25
c_2	-3.13 ± 0.38	-3.87 ± 0.38	-1.80 ± 0.35	-1.46 ± 0.33
c_3	0.05 ± 0.12	-0.07 ± 0.12	0.36 ± 0.11	0.43 ± 0.11
c_4	-0.54 ± 0.18	-0.45 ± 0.18	-0.51 ± 0.16	-0.47 ± 0.15
c_5	-0.09 ± 0.17	-0.11 ± 0.11	-0.10 ± 0.11	-0.10 ± 0.10
	(50)	(51)	(52)	(52)

TABLE 3.13.—*Super-Schmidt meteors with abrupt beginning*

	H _B	H _{2.5}	H _{ML}	H _E
c ₀	-8.91 ± 0.06	-8.91 ± 0.06	-8.50 ± 0.06	-8.00 ± 0.04
c ₁	0.75 ± 0.33	0.86 ± 0.33	1.36 ± 0.33	1.78 ± 0.23
c ₂	-3.95 ± 0.29	-4.17 ± 0.30	-3.14 ± 0.30	-2.63 ± 0.20
	(26)	(26)	(26)	(26)
c ₀	-8.92 ± 0.05	-8.92 ± 0.05	-8.49 ± 0.06	-8.00 ± 0.04
c ₁	0.44 ± 0.27	0.54 ± 0.27	1.49 ± 0.34	1.78 ± 0.24
c ₂	-5.16 ± 0.39	-5.40 ± 0.39	-2.63 ± 0.49	-2.63 ± 0.34
c ₃	-0.63 ± 0.16	-0.65 ± 0.16	0.27 ± 0.20	0.00 ± 0.14
	(26)	(26)	(26)	(26)
c ₀	-8.88 ± 0.05	-8.87 ± 0.05	-8.38 ± 0.05	-7.95 ± 0.04
c ₁	0.42 ± 0.27	0.55 ± 0.27	1.55 ± 0.28	1.79 ± 0.22
c ₂	-5.14 ± 0.44	-5.47 ± 0.43	-2.96 ± 0.44	-2.71 ± 0.35
c ₃	-0.69 ± 0.17	-0.73 ± 0.17	0.10 ± 0.17	-0.09 ± 0.13
c ₄	-0.08 ± 0.19	-0.15 ± 0.18	-0.45 ± 0.19	-0.18 ± 0.15
	(24)	(24)	(24)	(24)
c ₀	-8.88 ± 0.05	-8.87 ± 0.05	-8.38 ± 0.06	-7.95 ± 0.04
c ₁	0.41 ± 0.28	0.52 ± 0.27	1.54 ± 0.29	1.76 ± 0.22
c ₂	-5.22 ± 0.46	-5.56 ± 0.45	-2.98 ± 0.47	-2.81 ± 0.36
c ₃	-0.70 ± 0.17	-0.74 ± 0.17	0.09 ± 0.18	-0.10 ± 0.13
c ₄	-0.12 ± 0.20	-0.20 ± 0.19	-0.46 ± 0.20	-0.23 ± 0.15
c ₅	-0.14 ± 0.20	-0.17 ± 0.20	-0.03 ± 0.21	-0.17 ± 0.16
	(24)	(24)	(24)	(24)

TABLE 3.14.—*Sporadic Super-Schmidt meteors with Q ≤ 6 a.u.*

	H _B	H _{2.5}	H _{ML}	H _E
c ₀	-9.16 ± 0.04	-9.10 ± 0.04	-8.43 ± 0.03	-8.04 ± 0.03
c ₁	0.20 ± 0.19	0.31 ± 0.18	0.80 ± 0.15	0.99 ± 0.16
c ₂	-3.20 ± 0.24	-3.49 ± 0.23	-2.59 ± 0.19	-2.12 ± 0.20
	(164)	(164)	(165)	(166)
c ₀	-9.18 ± 0.04	-9.14 ± 0.04	-8.38 ± 0.03	-7.99 ± 0.03
c ₁	0.05 ± 0.19	0.13 ± 0.18	1.06 ± 0.13	1.26 ± 0.13
c ₂	-3.77 ± 0.31	-4.27 ± 0.29	-1.46 ± 0.21	-0.84 ± 0.21
c ₃	-0.19 ± 0.08	-0.28 ± 0.07	0.40 ± 0.05	0.48 ± 0.05
	(163)	(164)	(165)	(165)
c ₀	-9.21 ± 0.04	-9.16 ± 0.04	-8.39 ± 0.03	-8.00 ± 0.03
c ₁	0.28 ± 0.20	0.35 ± 0.19	1.18 ± 0.15	1.39 ± 0.14
c ₂	-3.25 ± 0.33	-3.83 ± 0.31	-1.57 ± 0.24	-0.88 ± 0.24
c ₃	-0.10 ± 0.08	-0.20 ± 0.07	0.40 ± 0.05	0.50 ± 0.05
c ₄	0.59 ± 0.13	0.50 ± 0.13	-0.08 ± 0.10	-0.02 ± 0.10
	(157)	(158)	(159)	(159)
c ₀	-9.20 ± 0.04	-9.15 ± 0.04	-8.39 ± 0.03	-8.00 ± 0.03
c ₁	0.44 ± 0.21	0.48 ± 0.20	1.25 ± 0.15	1.39 ± 0.15
c ₂	-3.10 ± 0.33	-3.72 ± 0.32	-1.51 ± 0.24	-0.88 ± 0.24
c ₃	-0.06 ± 0.08	-0.17 ± 0.07	0.42 ± 0.05	0.50 ± 0.05
c ₄	0.57 ± 0.13	0.48 ± 0.13	-0.09 ± 0.10	-0.02 ± 0.10
c ₅	0.24 ± 0.10	0.18 ± 0.10	0.10 ± 0.08	-0.01 ± 0.07
	(157)	(158)	(159)	(159)

TABLE 3.15.—*Sporadic Super-Schmidt meteors with Q > 6 a.u.*

	H _B	H _{2.5}	H _{ML}	H _E
c ₀	-9.37 ± 0.04	-9.31 ± 0.04	-8.49 ± 0.04	-8.11 ± 0.04
c ₁	0.10 ± 0.20	0.32 ± 0.20	0.91 ± 0.19	1.31 ± 0.17
c ₂	-2.29 ± 0.17	-2.76 ± 0.17	-2.26 ± 0.19	-2.26 ± 0.17
	(118)	(119)	(124)	(122)
c ₀	-9.35 ± 0.04	-9.29 ± 0.04	-8.52 ± 0.04	-8.14 ± 0.04
c ₁	0.11 ± 0.18	0.31 ± 0.19	0.96 ± 0.17	1.33 ± 0.15
c ₂	-3.13 ± 0.23	-3.54 ± 0.24	-1.18 ± 0.24	-1.27 ± 0.23
c ₃	-0.30 ± 0.06	-0.27 ± 0.06	0.38 ± 0.06	0.34 ± 0.06
	(118)	(119)	(124)	(122)
c ₀	-9.34 ± 0.04	-9.28 ± 0.04	-8.50 ± 0.03	-8.12 ± 0.03
c ₁	0.10 ± 0.18	0.24 ± 0.18	0.92 ± 0.14	1.29 ± 0.14
c ₂	-3.24 ± 0.23	-3.67 ± 0.23	-1.43 ± 0.21	-1.36 ± 0.21
c ₃	-0.30 ± 0.06	-0.28 ± 0.06	0.38 ± 0.05	0.37 ± 0.06
c ₄	-0.32 ± 0.10	-0.35 ± 0.10	-0.67 ± 0.09	-0.48 ± 0.09
	(114)	(115)	(120)	(118)
c ₀	-9.33 ± 0.03	-9.28 ± 0.04	-8.50 ± 0.03	-8.13 ± 0.04
c ₁	0.20 ± 0.18	0.29 ± 0.20	0.96 ± 0.15	1.25 ± 0.14
c ₂	-3.21 ± 0.22	-3.66 ± 0.23	-1.42 ± 0.21	-1.37 ± 0.21
c ₃	-0.26 ± 0.06	-0.27 ± 0.06	0.39 ± 0.05	0.35 ± 0.06
c ₄	-0.30 ± 0.10	-0.36 ± 0.10	-0.68 ± 0.09	-0.47 ± 0.09
c ₅	0.22 ± 0.09	0.06 ± 0.08	0.07 ± 0.07	-0.07 ± 0.06
	(114)	(115)	(120)	(118)

TABLE 3.16.—*All small-camera meteors*

	H _B	H _{ML}	H _E
c ₀	-8.79 ± 0.04	-7.75 ± 0.05	-7.33 ± 0.05
c ₁	0.26 ± 0.22	0.94 ± 0.23	0.97 ± 0.29
c ₂	-3.28 ± 0.18	-2.99 ± 0.22	-3.05 ± 0.24
	(209)	(210)	(208)
c ₀	-8.73 ± 0.08	-8.57 ± 0.08	-8.31 ± 0.08
c ₁	0.39 ± 0.26	1.77 ± 0.26	1.90 ± 0.25
c ₂	-3.44 ± 0.22	-1.48 ± 0.22	-1.17 ± 0.23
c ₃	-0.05 ± 0.04	0.48 ± 0.04	0.58 ± 0.04
	(205)	(206)	(204)
c ₀	-8.81 ± 0.15	-8.42 ± 0.12	-8.13 ± 0.11
c ₁	0.14 ± 0.51	1.24 ± 0.38	1.28 ± 0.35
c ₂	-4.41 ± 0.50	-2.60 ± 0.39	-2.23 ± 0.37
c ₃	-0.12 ± 0.09	0.31 ± 0.07	0.41 ± 0.06
c ₄	-0.57 ± 0.25	-0.93 ± 0.19	-0.99 ± 0.18
	(87)	(88)	(86)
c ₀	-8.69 ± 0.17	-8.25 ± 0.17	-8.04 ± 0.12
c ₁	0.30 ± 0.46	1.20 ± 0.43	1.30 ± 0.30
c ₂	-4.83 ± 0.48	-2.40 ± 0.47	-1.86 ± 0.35
c ₃	-0.10 ± 0.09	0.29 ± 0.09	0.43 ± 0.06
c ₄	-0.79 ± 0.24	-0.94 ± 0.24	-1.06 ± 0.17
c ₅	1.13 ± 0.28	0.24 ± 0.30	0.21 ± 0.21
	(50)	(51)	(49)

TABLE 3.17.—Sporadic small-camera meteors

	H _B	H _{ML}	H _E
c ₀	-8.71 ± 0.06	-7.74 ± 0.07	-7.36 ± 0.07
c ₁	0.47 ± 0.32	0.72 ± 0.38	0.70 ± 0.40
c ₂	-3.25 ± 0.25	-3.00 ± 0.29	-3.07 ± 0.32
	(88)	(88)	(88)
c ₀	-8.79 ± 0.14	-8.63 ± 0.13	-8.40 ± 0.13
c ₁	0.95 ± 0.43	1.90 ± 0.39	1.97 ± 0.40
c ₂	-3.21 ± 0.36	-1.21 ± 0.34	-0.92 ± 0.35
c ₃	0.02 ± 0.08	0.53 ± 0.07	0.63 ± 0.07
	(84)	(84)	(84)
c ₀	-8.99 ± 0.28	-8.69 ± 0.19	-8.36 ± 0.20
c ₁	1.04 ± 0.90	1.86 ± 0.57	1.74 ± 0.59
c ₂	-4.18 ± 0.75	-2.00 ± 0.52	-1.87 ± 0.56
c ₃	-0.01 ± 0.16	0.49 ± 0.11	0.55 ± 0.12
c ₄	-0.66 ± 0.37	-0.77 ± 0.26	-0.81 ± 0.27
	(40)	(41)	(40)
c ₀	-8.79 ± 0.28	-8.60 ± 0.19	-8.23 ± 0.18
c ₁	0.50 ± 0.78	2.13 ± 0.47	1.96 ± 0.45
c ₂	-4.98 ± 0.69	-1.79 ± 0.46	-1.70 ± 0.45
c ₃	-0.03 ± 0.15	0.48 ± 0.10	0.54 ± 0.09
c ₄	-0.96 ± 0.34	-0.75 ± 0.23	-0.84 ± 0.21
c ₅	1.50 ± 0.39	-0.13 ± 0.30	0.05 ± 0.28
	(25)	(26)	(25)

TABLE 4.—Coefficients of the equation: $\log \rho = c_0 + c_1 (\log \cos Z_R + 0.2) + c_2 (\log v_\infty - 6.477) + c_3 (\log m_\infty + 0.523) + c_4 (\log \sigma + 11.20) + c_5 (\chi - 0.25)$ for four sets of heights, from a critical evaluation of the solutions of table 3

	H _B		H _{2.5}		H _{ML}		H _E	
	Theory	Observations	Theory	Observations	Theory	Observations	Theory	Observations
H ₀ *	104.8	99.0 ± 0.3	104.3	98.5 ± 0.3	90.1	88.9 ± 0.2	83.3	84.5 ± 0.2
c ₀	-9.66	-9.23 ± 0.02	-9.62	-9.19 ± 0.02	-8.51	-8.41 ± 0.02	-7.96	-8.06 ± 0.02
c ₁	0	0.0 ± 0.1	0	0.1 ± 0.1	1	1.0 ± 0.1	1	1.2 ± 0.1
c ₂	≈ -5	-3.5 ± 0.15	-6	-4.0 ± 0.15	≈ -2	-1.7 ± 0.1	≈ -2	-1.4 ± 0.1
c ₃	$\frac{2}{3}$	-0.25 ± 0.05	$\frac{2}{3}$	-0.28 ± 0.05	$\frac{1}{3}$	0.37 ± 0.04	$\frac{1}{3}$	0.40 ± 0.04
c ₄	-1	0.0 ± 0.1	-1	0.0 ± 0.1	-1	-0.5 ± 0.1	-1	-0.4 ± 0.1
c ₅	—	0.2 ± 0.1	—	0.1 ± 0.1	—	0.0 ± 0.1	—	-0.1 ± 0.1

*H₀ is the height corresponding to $\log \rho = c_0$ in the U.S. Standard Atmosphere 1962.

TABLE 5.1.1.—Heights of the standard meteor when one parameter at a time is varied; all meteors, variable v_m

Velocity range (km/s)	Beginning						2.5				Maximum Light				End			
	Mean $\log v_m$ (km/s)	S.d. (km/s)	Mean $\log \rho$ (g/cm^3)	S.d. (g/cm^3)	Mean H (km)	No. obs.	Mean $\log \rho$ (g/cm^3)	S.d. (g/cm^3)	Mean H (km)	No. obs.	Mean $\log \rho$ (g/cm^3)	S.d. (g/cm^3)	Mean H (km)	No. obs.	Mean $\log \rho$ (g/cm^3)	S.d. (g/cm^3)	Mean H (km)	No. obs.
10-15	1.130	± 0.011	- 7.66	± 0.07	79.4	9	- 7.51	± 0.09	77.2	9	- 7.65	± 0.08	79.3	9	- 7.52	± 0.07	77.4	9
15-20	1.248	0.005	- 8.37	0.05	88.4	55	- 8.21	0.05	86.4	56	- 8.05	0.04	84.4	56	- 7.75	0.04	80.6	55
20-25	1.349	0.003	- 8.82	0.05	93.8	64	- 8.69	0.05	92.2	64	- 8.29	0.04	87.4	64	- 7.97	0.04	83.4	64
25-30	1.437	0.003	- 9.22	0.04	98.9	62	- 9.13	0.04	97.7	62	- 8.39	0.03	88.6	63	- 8.02	0.03	84.1	63
30-35	1.502	0.003	- 9.35	0.04	100.6	47	- 9.34	0.05	100.5	46	- 8.42	0.05	89.0	47	- 8.07	0.04	84.6	47
35-40	1.564	0.002	- 9.37	0.05	100.9	37	- 9.42	0.05	101.5	37	- 8.42	0.05	89.1	38	- 8.02	0.04	84.0	38
40-45	1.632	0.002	- 9.66	0.05	104.8	31	- 9.69	0.05	105.2	31	- 8.65	0.04	91.8	31	- 8.20	0.04	86.2	31
45-50	1.675	0.004	- 9.72	0.12	105.6	12	- 9.72	0.13	105.7	13	- 8.58	0.09	90.9	14	- 8.11	0.09	85.2	14
50-55	1.724	0.004	- 10.22	0.06	113.2	9	- 10.29	0.06	114.3	9	- 9.04	0.09	96.6	9	- 8.55	0.06	90.6	9
55-60	1.765	0.003	- 10.13	0.10	111.7	13	- 10.31	0.10	114.6	14	- 8.77	0.05	93.5	16	- 8.42	0.06	89.0	16
60-65	1.790	0.002	- 10.29	0.05	114.2	24	- 10.42	0.06	116.5	24	- 8.91	0.06	94.9	24	- 8.43	0.04	89.2	24
65-70	1.830	0.002	- 10.49	0.05	117.7	17	- 10.61	0.07	119.9	15	- 8.95	0.07	95.5	18	- 8.54	0.06	90.5	17
70-75	1.854	0.002	- 10.63	0.10	120.2	7	- 10.76	0.08	122.4	7	- 8.93	0.12	95.2	7	- 8.60	0.08	91.2	7
All	1.499	0.010	- 9.28	0.04	99.7	387	- 9.24	0.04	99.2	387	- 8.44	0.02	89.3	396	- 8.07	0.02	84.7	394

TABLE 5.1.2.—Heights of the standard meteor when one parameter at a time is varied; all meteors, variable m_m

Mass range (g)	Beginning						2.5				Maximum Light				End			
	Mean $\log m_m$ (g)	S.d. (g)	Mean $\log \rho$ (g/cm^3)	S.d. (g/cm^3)	Mean H (km)	No. obs.	Mean $\log \rho$ (g/cm^3)	S.d. (g/cm^3)	Mean H (km)	No. obs.	Mean $\log \rho$ (g/cm^3)	S.d. (g/cm^3)	Mean H (km)	No. obs.	Mean $\log \rho$ (g/cm^3)	S.d. (g/cm^3)	Mean H (km)	No. obs.
0.01-0.05	-1.52	± 0.02	- 8.95	± 0.04	95.5	56	- 8.88	± 0.04	94.5	55	- 8.78	± 0.04	93.3	57	- 8.46	± 0.04	89.5	57
0.05-0.10	-1.15	0.02	- 9.03	0.05	96.4	49	- 8.96	0.05	95.5	49	- 8.66	0.04	91.9	51	- 8.33	0.04	87.8	51
0.10-0.20	-0.84	0.01	- 9.18	0.04	98.4	71	- 9.10	0.04	97.4	71	- 8.56	0.03	90.7	72	- 8.19	0.03	86.1	72
0.20-0.40	-0.55	0.01	- 9.23	0.04	99.0	69	- 9.18	0.04	98.4	69	- 8.41	0.03	88.9	70	- 8.05	0.03	84.4	70
0.40-0.80	-0.23	0.01	- 9.29	0.04	100.0	59	- 9.28	0.04	99.7	58	- 8.26	0.04	87.0	60	- 7.92	0.03	82.8	60
0.80-1.60	0.04	0.01	- 9.32	0.05	100.2	42	- 9.30	0.05	100.0	43	- 8.18	0.04	86.1	43	- 7.82	0.04	81.6	43
1.6-5.0	0.37	0.03	- 9.39	0.08	101.1	29	- 9.41	0.07	101.3	29	- 8.10	0.09	85.1	30	- 7.67	0.08	79.6	29
5.0-34	0.92	0.07	- 9.52	0.14	102.8	12	- 9.52	0.12	102.9	13	- 7.83	0.09	81.6	13	- 7.38	0.11	75.3	12
All	-0.59	0.03	- 9.20	0.02	98.6	387	- 9.15	0.02	98.0	387	- 8.43	0.02	89.2	396	- 8.08	0.02	84.7	394

TABLE 5.1.3.—Heights of the standard meteor when one parameter at a time is varied; all meteors, variable Z_R

Range of $\cos Z_R$	Beginning						2.5				Maximum Light				End			
	Mean $\log \cos Z_R$	S.d.	Mean $\log \rho$ (g/cm^3)	S.d. (g/cm^3)	Mean H (km)	No. obs.	Mean $\log \rho$ (g/cm^3)	S.d. (g/cm^3)	Mean H (km)	No. obs.	Mean $\log \rho$ (g/cm^3)	S.d. (g/cm^3)	Mean H (km)	No. obs.	Mean $\log \rho$ (g/cm^3)	S.d. (g/cm^3)	Mean H (km)	No. obs.
0.1-0.2	-0.801	± 0.041	- 9.30	± 0.08	99.9	4	- 9.39	± 0.12	101.2	5	- 9.03	± 0.05	96.4	6	- 8.76	± 0.08	93.1	6
0.2-0.3	-0.596	0.016	- 9.26	0.10	99.5	9	- 9.27	0.10	99.6	8	- 8.88	0.07	94.6	10	- 8.62	0.09	91.4	10
0.3-0.4	-0.458	0.006	- 9.29	0.05	99.9	29	- 9.25	0.06	99.3	28	- 8.61	0.05	91.3	31	- 8.37	0.06	88.4	31
0.4-0.5	-0.335	0.004	- 9.23	0.05	99.0	37	- 9.22	0.05	98.9	37	- 8.57	0.05	90.8	37	- 8.27	0.05	87.1	35
0.5-0.6	-0.258	0.003	- 9.22	0.06	98.9	32	- 9.15	0.06	97.9	33	- 8.52	0.05	90.3	33	- 8.11	0.05	85.2	33
0.6-0.7	-0.187	0.002	- 9.15	0.04	98.0	84	- 9.12	0.04	97.6	85	- 8.41	0.03	88.8	86	- 8.04	0.03	84.3	86
0.7-0.8	-0.125	0.002	- 9.23	0.04	99.0	73	- 9.17	0.04	98.3	72	- 8.34	0.03	88.1	73	- 7.96	0.03	83.3	73
0.8-0.9	-0.075	0.002	- 9.21	0.04	98.7	74	- 9.13	0.04	97.8	74	- 8.24	0.03	86.8	74	- 7.86	0.03	82.0	74
0.9-1.0	-0.015	0.002	- 9.21	0.05	98.8	45	- 9.19	0.04	98.4	45	- 8.19	0.05	86.1	46	- 7.78	0.05	81.0	46
All	-0.195	0.006	- 9.21	0.02	98.8	387	- 9.17	0.02	98.2	387	- 8.40	0.02	88.8	396	- 8.04	0.02	84.3	394

TABLE 5.1.4.—Heights of the standard meteor when one parameter at a time is varied; all meteors, variable σ

Range of $\log \sigma$ ($\text{cm}^{-2} \text{g}^{-2}$)	Beginning				2.5				Maximum Light				End					
	Mean $\log \sigma$ ($\text{cm}^{-2} \text{g}^{-2}$)	S.d. ($\text{cm}^{-2} \text{g}^{-2}$)	Mean $\log \rho$ (g/cm^3)	S.d. (g/cm^3)	Mean H (km)	No. obs.	Mean $\log \rho$ (g/cm^3)	S.d. (g/cm^3)	Mean H (km)	No. obs.	Mean $\log \rho$ (g/cm^3)	S.d. (g/cm^3)	Mean H (km)	No. obs.	Mean $\log \rho$ (g/cm^3)	S.d. (g/cm^3)	Mean H (km)	No. obs.
-10.40- -11.00	-10.83	± 0.02	-9.12	± 0.04	97.6	86	-9.11	± 0.04	97.4	87	-8.48	± 0.03	89.8	88	-8.09	± 0.03	84.9	88
-11.00- -11.15	-11.09	0.01*	-9.17	0.04	98.2	92	-9.13	0.03	97.6	92	-8.43	0.03	89.1	92	-8.06	0.03	84.5	92
-11.15- -11.30	-11.23	0.01*	-9.29	0.03	99.8	99	-9.24	0.03	99.2	98	-8.45	0.02	89.4	102	-8.11	0.02	85.2	101
-11.30- -11.45	-11.37	0.01	-9.33	0.03	100.3	64	-9.25	0.03	99.3	65	-8.37	0.03	88.3	66	-8.04	0.03	84.3	66
-11.45- -12.05	-11.67	0.04	-9.12	0.06	97.6	46	-9.09	0.06	97.1	45	-8.21	0.06	86.4	48	-7.84	0.05	81.7	47
All	-11.19	0.01	-9.21	0.02	98.8	387	-9.17	0.02	98.2	387	-8.41	0.01	88.9	396	-8.05	0.01	84.4	394

* Actually 0.004

TABLE 5.2.1.—Heights of the standard meteor when one parameter at a time is varied; sporadic meteors minus (A+S+D), variable v_{∞}

Velocity range (km/s)	Beginning				2.5				Maximum Light				End					
	Mean $\log v_{\infty}$ (km/s)	S.d. (km/s)	Mean $\log \rho$ (g/cm^3)	S.d. (g/cm^3)	Mean H (km)	No. obs.	Mean $\log \rho$ (g/cm^3)	S.d. (g/cm^3)	Mean H (km)	No. obs.	Mean $\log \rho$ (g/cm^3)	S.d. (g/cm^3)	Mean H (km)	No. obs.	Mean $\log \rho$ (g/cm^3)	S.d. (g/cm^3)	Mean H (km)	No. obs.
10-15	1.124	± 0.016	-7.54	± 0.11	77.7	6	-7.34	± 0.12	74.7	6	-7.44	± 0.10	76.2	6	-7.35	± 0.07	74.7	6
15-20	1.250	0.005	-8.41	0.05	88.9	45	-8.25	0.05	86.9	46	-8.03	0.04	84.1	46	-7.74	0.03	80.6	45
20-25	1.349	0.004	-8.79	0.06	93.5	42	-8.66	0.05	91.9	42	-8.20	0.04	86.2	42	-7.90	0.03	82.5	42
25-30	1.436	0.004	-9.27	0.05	99.6	35	-9.16	0.04	98.2	35	-8.35	0.03	88.2	35	-8.01	0.03	83.9	35
30-35	1.505	0.003	-9.47	0.04	102.1	27	-9.48	0.05	102.2	27	-8.52	0.06	90.3	27	-8.18	0.05	86.1	27
35-40	1.571	0.006	-9.56	0.09	103.4	11	-9.56	0.09	103.4	11	-8.66	0.09	91.9	11	-8.20	0.07	86.2	11
40-45	1.634	0.005	-9.83	0.10	107.2	10	-9.84	0.09	107.5	10	-8.76	0.08	93.1	10	-8.29	0.09	87.4	10
45-50	1.673	0.005	-9.79	0.13	106.7	9	-9.78	0.14	106.6	10	-8.61	0.07	91.3	11	-8.17	0.08	85.9	11
50-55	1.724	0.005	-10.24	0.08	113.5	6	-10.29	0.08	114.3	6	-8.97	0.10	95.7	6	-8.58	0.03	91.0	6
55-60	1.762	0.004	-10.17	0.12	112.4	8	-10.39	0.13	116.0	9	-8.93	0.06	95.2	11	-8.53	0.08	90.4	11
60-65	1.794	0.003	-10.29	0.06	114.2	15	-10.42	0.07	116.4	15	-8.95	0.07	95.4	15	-8.47	0.06	89.7	15
65-70	1.830	0.003	-10.50	0.07	117.8	11	-10.57	0.09	119.2	10	-8.96	0.08	95.6	12	-8.58	0.05	90.9	11
70-75	1.855	0.003	-10.51	0.05	118.1	5	-10.68	0.09	121.1	5	-9.03	0.12	96.4	5	-8.66	0.06	92.9	5
All	1.484	0.013	-9.26	0.05	99.4	230	-9.21	0.06	98.7	232	-8.43	0.03	89.1	237	-8.08	0.02	84.8	235

TABLE 5.2.2.—Heights of the standard meteor when one parameter at a time is varied; sporadic meteors minus (A+S+D), variable m_{∞}

Mass range (g)	Beginning				2.5				Maximum Light				End					
	Mean $\log m_{\infty}$ (g)	S.d. (g)	Mean $\log \rho$ (g/cm^3)	S.d. (g/cm^3)	Mean H (km)	No. obs.	Mean $\log \rho$ (g/cm^3)	S.d. (g/cm^3)	Mean H (km)	No. obs.	Mean $\log \rho$ (g/cm^3)	S.d. (g/cm^3)	Mean H (km)	No. obs.	Mean $\log \rho$ (g/cm^3)	S.d. (g/cm^3)	Mean H (km)	No. obs.
0.01-0.05	-1.54	± 0.03	-9.00	± 0.04	96.0	37	-8.91	± 0.04	94.9	36	-8.73	± 0.04	92.7	38	-8.42	± 0.05	89.0	38
0.05-0.10	-1.14	0.02	-9.07	0.06	96.9	23	-9.02	0.07	96.3	24	-8.67	0.06	92.0	25	-8.33	0.05	87.9	25
0.10-0.20	-0.84	0.01	-9.29	0.04	99.9	39	-9.18	0.04	98.4	39	-8.58	0.03	91.0	39	-8.25	0.03	86.8	39
0.20-0.40	-0.52	0.01	-9.25	0.04	99.3	36	-9.20	0.04	98.6	36	-8.41	0.04	88.8	37	-8.05	0.04	84.4	37
0.40-0.80	-0.22	0.01	-9.33	0.05	100.3	38	-9.30	0.05	100.0	38	-8.29	0.04	87.3	39	-7.96	0.03	83.3	39
0.80-1.60	0.04	0.02	-9.35	0.06	100.6	30	-9.32	0.06	100.3	31	-8.23	0.05	86.6	31	-7.86	0.05	82.0	31
1.60-5.0	0.39	0.04	-9.40	0.10	101.3	16	-9.42	0.10	101.5	16	-8.07	0.07	84.7	16	-7.70	0.06	80.0	15
5.0 - 34	0.91	0.07	-9.56	0.13	103.4	11	-9.57	0.12	103.6	12	-7.92	0.07	82.7	12	-7.51	0.07	77.3	11
All	-0.55	0.04	-9.25	0.02	99.3	230	-9.20	0.02	98.6	232	-8.42	0.02	89.1	237	-8.08	0.02	84.8	235

TABLE 5.2.3.—Heights of the standard meteor when one parameter at a time is varied; sporadic meteors minus (A+S+D), variable Z_R

Range of $\cos Z_R$	Beginning						2.5				Maximum Light				End			
	Mean $\log \cos Z_R$	S.d.	Mean $\log \rho$ (g/cm^3)	S.d.	Mean H (km)	No. obs.	Mean $\log \rho$ (g/cm^3)	S.d.	Mean H (km)	No. obs.	Mean $\log \rho$ (g/cm^3)	S.d.	Mean H (km)	No. obs.	Mean $\log \rho$ (g/cm^3)	S.d.	Mean H (km)	No. obs.
0.1-0.2	-0.828	± 0.081	-9.40	--	101.2	1	-9.55	± 0.22	105.2	2	-8.95	± 0.03	95.4	3	-8.64	± 0.06	91.6	3
0.2-0.3	-0.605	0.021	-9.25	± 0.11	99.3	6	-9.25	0.10	99.3	5	-8.84	0.07	94.0	7	-8.58	0.11	90.9	7
0.3-0.4	-0.453	0.008	-9.33	0.07	100.3	18	-9.27	0.07	99.5	18	-8.62	0.06	91.3	20	-8.34	0.06	88.1	20
0.4-0.5	-0.336	0.005	-9.23	0.06	99.0	26	-9.19	0.06	98.5	26	-8.52	0.06	90.3	26	-8.20	0.06	86.2	24
0.5-0.6	-0.263	0.005	-9.25	0.06	99.3	18	-9.17	0.08	98.2	19	-8.51	0.05	90.1	19	-8.12	0.05	85.3	19
0.6-0.7	-0.188	0.003	-9.17	0.05	98.2	49	-9.15	0.05	98.0	50	-8.39	0.03	88.6	50	-8.05	0.03	84.3	50
0.7-0.8	-0.122	0.002	-9.28	0.04	99.7	45	-9.23	0.04	99.0	45	-8.40	0.04	88.8	45	-8.03	0.03	84.1	45
0.8-0.9	-0.076	0.002	-9.29	0.04	99.9	44	-9.20	0.04	98.6	44	-8.28	0.04	87.2	44	-7.93	0.03	82.8	44
0.9-1.0	-0.017	0.003	-9.29	0.07	99.9	23	-9.24	0.06	99.1	23	-8.24	0.06	86.8	23	-7.87	0.05	82.1	23
All	-0.203	0.010	-9.26	0.02	99.4	230	-9.20	0.02	98.7	232	-8.42	0.02	89.0	237	-8.07	0.02	84.7	235

TABLE 5.2.4.—Heights of the standard meteor when one parameter at a time is varied; sporadic meteors minus (A+S+D), variable σ

Range of $\log \sigma$ ($\text{cm}^{-2} \text{s}^2$)	Beginning						2.5				Maximum Light				End			
	Mean $\log \sigma$ ($\text{cm}^{-2} \text{s}^2$)	S.d.	Mean $\log \rho$ (g/cm^3)	S.d.	Mean H (km)	No. obs.	Mean $\log \rho$ (g/cm^3)	S.d.	Mean H (km)	No. obs.	Mean $\log \rho$ (g/cm^3)	S.d.	Mean H (km)	No. obs.	Mean $\log \rho$ (g/cm^3)	S.d.	Mean H (km)	No. obs.
-10.40- -11.00	-10.87	± 0.01	-9.20	± 0.05	98.7	47	-9.19	± 0.05	98.5	48	-8.55	± 0.05	90.6	48	-8.17	± 0.04	85.9	48
-11.00- -11.15	-11.09	0.01	-9.23	0.04	99.1	59	-9.18	0.04	98.4	59	-8.46	0.03	89.5	59	-8.11	0.03	85.1	59
-11.15- -11.30	-11.23	0.01*	-9.30	0.03	100.0	68	-9.26	0.03	99.4	69	-8.46	0.03	89.5	71	-8.11	0.02	85.1	70
-11.30- -11.45	-11.38	0.01	-9.36	0.04	100.7	34	-9.23	0.05	99.1	35	-8.34	0.04	88.1	36	-8.04	0.04	84.3	36
-11.45- -12.05	-11.63	0.03	-9.13	0.07	97.8	22	-9.09	0.09	97.2	21	-8.10	0.04	85.0	23	-7.79	0.04	81.2	22
All	-11.18	0.02	-9.26	0.02	99.4	230	-9.21	0.02	98.7	232	-8.43	0.02	89.1	237	-8.08	0.02	84.8	235

*Actually 0.0049

TABLE 5.3.1.—Heights of the standard meteor when one parameter at a time is varied; sporadic meteors with aphelion distance $Q \leq 6 \text{ a.u.}$, variable v_∞

Velocity range (km/s)	Beginning						2.5				Maximum Light				End			
	Mean $\log v_\infty$ (km/s)	S.d.	Mean $\log \rho$ (g/cm^3)	S.d.	Mean H (km)	No. obs.	Mean $\log \rho$ (g/cm^3)	S.d.	Mean H (km)	No. obs.	Mean $\log \rho$ (g/cm^3)	S.d.	Mean H (km)	No. obs.	Mean $\log \rho$ (g/cm^3)	S.d.	Mean H (km)	No. obs.
10-15	1.130	± 0.011	-7.89	± 0.07	82.4	9	-7.69	± 0.09	79.9	9	-7.70	± 0.08	80.0	9	-7.62	± 0.07	78.9	9
15-20	1.247	0.005	-8.50	0.05	90.1	47	-8.31	0.04	87.6	48	-8.05	0.03	84.3	48	-7.80	0.04	81.3	48
20-25	1.345	0.004	-8.78	0.05	93.3	44	-8.63	0.05	91.6	44	-8.20	0.04	86.3	44	-7.91	0.04	82.6	44
25-30	1.437	0.005	-9.15	0.07	98.0	31	-9.07	0.06	96.9	31	-8.35	0.04	88.2	32	-7.97	0.04	83.4	32
30-35	1.507	0.004	-9.39	0.06	101.1	17	-9.40	0.07	101.2	17	-8.41	0.08	88.9	17	-8.05	0.07	84.4	17
35-40	1.564	0.006	-9.07	0.19	96.9	7	-9.10	0.18	97.3	7	-8.36	0.08	88.3	7	-7.96	0.11	83.2	7
40-45	1.623	0.004	-9.57	0.33	103.5	2	-9.51	0.40	102.7	2	-8.61	0.10	91.2	2	-8.08	0.22	84.8	2
All	1.352	0.009	-8.61	0.04	93.7	157	-8.68	0.04	92.1	158	-8.19	0.02	86.1	159	-7.89	0.02	82.4	159

TABLE 5.3.2.—Heights of the standard meteor when one parameter at a time is varied; sporadic meteors with aphelion distance $Q \leq 6$ a.u., variable m_∞

Beginning				2.5				Maximum Light				End						
Mass range (g)	Mean log m_∞ (g)	S.d. (g)	Mean log ρ (g/cm^3)	S.d. (g/cm^3)	Mean H (km)	No. obs.	Mean log ρ (g/cm^3)	S.d. (g/cm^3)	Mean H (km)	No. obs.	Mean log ρ (g/cm^3)	S.d. (g/cm^3)	Mean H (km)	No. obs.	Mean log ρ (g/cm^3)	S.d. (g/cm^3)	Mean H (km)	No. obs.
0.01-0.05	-1.36	± 0.04	-8.92	± 0.22	95.0	2	-8.72	± 0.31	92.6	2	-8.69	± 0.08	92.3	2	-8.38	± 0.24	88.5	2
0.05-0.10	-1.12	0.03	-9.08	0.18	97.1	8	-8.99	0.18	95.9	8	-8.54	0.12	90.5	8	-8.27	0.12	87.1	8
0.10-0.20	-0.83	0.02	-9.26	0.08	99.5	25	-9.15	0.07	98.0	25	-8.54	0.05	90.5	26	-8.20	0.05	86.3	26
0.20-0.40	-0.53	0.01	-9.20	0.06	98.6	33	-9.14	0.06	97.8	33	-8.40	0.04	88.7	33	-7.96	0.04	83.2	33
0.40-0.80	-0.24	0.01	-9.26	0.05	99.4	37	-9.25	0.05	99.3	37	-8.25	0.04	86.9	37	-7.87	0.04	82.2	37
0.80-1.60	0.03	0.02	-9.24	0.06	99.2	29	-9.27	0.06	99.6	29	-8.15	0.05	85.7	29	-7.74	0.05	80.5	29
1.6-5.0	0.37	0.04	-9.22	0.09	98.9	15	-9.27	0.09	99.5	15	-8.00	0.07	83.8	15	-7.58	0.06	78.3	15
5.0-34	0.96	0.10	-9.34	0.16	100.5	8	-9.39	0.12	101.2	9	-7.75	0.10	80.6	9	-7.21	0.14	72.5	9
All	-0.28	0.04	-9.23	0.03	99.0	157	-9.21	0.03	98.7	158	-8.28	0.03	87.3	159	-7.88	0.03	82.3	159

TABLE 5.3.3.—Heights of the standard meteor when one parameter at a time is varied; sporadic meteors with aphelion distance $Q \leq 6$ a.u., variable Z_R

Beginning				2.5				Maximum Light				End						
Range of $\cos Z_R$	Mean log $\cos Z_R$	S.d.	Mean log ρ (g/cm^3)	S.d. (g/cm^3)	Mean H (km)	No. obs.	Mean log ρ (g/cm^3)	S.d. (g/cm^3)	Mean H (km)	No. obs.	Mean log ρ (g/cm^3)	S.d. (g/cm^3)	Mean H (km)	No. obs.	Mean log ρ (g/cm^3)	S.d. (g/cm^3)	Mean H (km)	No. obs.
0.1-0.2	-0.796	± 0.003	-9.54	± 0.11	103.1	2	-9.50	± 0.10	102.6	2	-9.19	± 0.12	98.5	2	-8.83	± 0.11	93.9	2
0.2-0.3	-0.573	0.012	-9.33	0.19	100.3	5	-9.31	0.16	100.1	5	-8.95	0.12	95.1	5	-8.59	0.15	91.0	5
0.3-0.4	-0.436	0.008	-9.25	0.07	99.3	11	-9.18	0.06	98.4	11	-8.90	0.09	90.0	11	-8.23	0.07	86.6	11
0.4-0.5	-0.332	0.007	-9.29	0.08	99.8	10	-9.25	0.08	99.4	10	-8.53	0.09	90.4	10	-8.15	0.08	85.7	10
0.5-0.6	-0.262	0.005	-9.25	0.05	99.3	16	-9.18	0.06	98.4	16	-8.51	0.05	90.2	16	-8.12	0.05	85.3	16
0.6-0.7	-0.182	0.003	-9.19	0.07	98.4	35	-9.17	0.07	98.2	36	-8.36	0.05	88.3	37	-8.00	0.04	83.8	37
0.7-0.8	-0.123	0.003	-9.23	0.06	99.0	30	-9.16	0.06	98.1	30	-8.33	0.04	87.9	30	-7.93	0.05	82.9	30
0.8-0.9	-0.075	0.003	-9.14	0.05	97.8	42	-9.07	0.05	96.9	42	-8.21	0.04	86.4	42	-7.80	0.04	81.2	42
0.9-1.0	-0.019	0.007	-9.08	0.19	97.1	6	-9.07	0.19	96.9	6	-8.06	0.13	84.5	6	-7.76	0.12	80.7	6
All	-0.192	0.012	-9.20	0.03	98.7	157	-9.15	0.03	98.0	158	-8.37	0.02	88.4	159	-7.99	0.03	83.7	159

TABLE 5.3.4.—Heights of the standard meteor when one parameter at a time is varied; sporadic meteors with aphelion distance $Q \leq 6$ a.u., variable σ

Beginning				2.5				Maximum Light				End						
Range of $\log \sigma$ ($cm^{-2} s^2$)	Mean log σ ($cm^{-2} s^2$)	S.d. ($cm^{-2} s^2$)	Mean log ρ (g/cm^3)	S.d. (g/cm^3)	Mean H (km)	No. obs.	Mean log ρ (g/cm^3)	S.d. (g/cm^3)	Mean H (km)	No. obs.	Mean log ρ (g/cm^3)	S.d. (g/cm^3)	Mean H (km)	No. obs.	Mean log ρ (g/cm^3)	S.d. (g/cm^3)	Mean H (km)	No. obs.
-10.40- -11.00	-10.84	± 0.02	-8.99	± 0.05	95.9	49	-8.97	± 0.04	95.7	49	-8.40	± 0.04	89.8	50	-7.99	± 0.03	83.7	50
-11.00- -11.15	-11.09	0.01	-9.09	0.05	97.2	47	-9.04	0.05	96.6	47	-8.35	0.04	88.2	47	-7.96	0.04	83.5	47
-11.15- -11.30	-11.23	0.01	-9.27	0.05	99.5	42	-9.23	0.05	99.0	43	-8.45	0.03	89.4	43	-8.06	0.03	84.5	43
-11.30- -11.45	-11.37	0.01	-9.50	0.03	102.5	12	-9.39	0.04	101.1	12	-8.43	0.07	89.1	12	-8.13	0.05	85.4	12
-11.45- -12.05	-11.62	0.07	-9.24	0.15	99.2	7	-9.20	0.18	98.6	7	-8.08	0.05	84.8	7	-7.66	0.10	79.5	7
All	-11.09	0.02	-9.14	0.03	97.9	157	-9.10	0.03	97.4	158	-8.39	0.02	88.6	159	-8.00	0.02	83.8	159

TABLE 5.4.1.—Heights of the standard meteor when one parameter at a time is varied; sporadic meteors with aphelion distance $Q > 6$ a.u., variable v_∞

Velocity range (km/s)	Beginning				2.5				Maximum Light				End					
	Mean $\log v_\infty$ (km/s)	S.d. (km/s)	Mean $\log \rho_3$ (g/cm^3)	S.d. (g/cm^3)	Mean H (km)	No. obs.	Mean $\log \rho_3$ (g/cm^3)	S.d. (g/cm^3)	Mean H (km)	No. obs.	Mean $\log \rho_3$ (g/cm^3)	S.d. (g/cm^3)	Mean H (km)	No. obs.	Mean $\log \rho_3$ (g/cm^3)	S.d. (g/cm^3)	Mean H (km)	No. obs.
15-20	1.247 ± 0.015		- 8.38 ± 0.19		88.5	7	- 8.28 ± 0.19		87.3	7	- 8.16 ± 0.14		85.7	7	- 7.75 ± 0.15		80.6	6
20-25	1.348	0.010	- 8.96	0.08	95.5	8	- 8.79	0.06	95.4	8	- 8.31	0.08	87.7	8	- 8.01	0.04	83.9	8
25-30	1.434	0.006	- 9.31	0.08	100.2	11	- 9.22	0.09	98.9	11	- 8.37	0.06	88.3	11	- 8.04	0.05	84.3	11
30-35	1.501	0.005	- 9.41	0.07	101.4	12	- 9.43	0.07	101.6	12	- 8.57	0.08	90.8	12	- 8.24	0.07	86.7	12
35-40	1.578	0.007	- 9.75	0.06	106.1	7	- 9.76	0.05	106.2	7	- 8.86	0.09	94.3	7	- 8.32	0.09	87.8	7
40-45	1.636	0.005	- 9.89	0.10	108.1	10	- 9.90	0.08	108.4	10	- 8.79	0.08	93.4	10	- 8.38	0.10	88.5	10
45-50	1.674	0.004	- 9.80	0.13	106.8	10	- 9.75	0.15	106.1	11	- 8.62	0.07	91.3	12	- 8.15	0.08	85.7	12
50-55	1.726	0.004	- 10.26	0.08	113.8	8	- 10.27	0.08	113.9	8	- 8.98	0.11	95.8	8	- 8.61	0.08	91.3	8
55-60	1.763	0.004	- 10.18	0.13	112.5	9	- 10.30	0.12	114.5	10	- 8.90	0.06	94.8	12	- 8.52	0.07	90.3	12
60-65	1.794	0.003	- 10.35	0.05	115.3	16	- 10.43	0.06	116.6	16	- 8.98	0.08	95.7	16	- 8.54	0.07	90.5	16
65-70	1.830	0.003	- 10.55	0.06	118.7	11	- 10.56	0.07	119.1	10	- 8.96	0.08	95.5	12	- 8.60	0.05	91.1	11
70-75	1.855	0.003	- 10.56	0.06	119.0	5	- 10.68	0.09	121.1	5	- 9.02	0.12	96.4	5	- 8.69	0.06	92.2	5
All	1.631	0.016	- 9.82	0.06	107.1	114	- 9.81	0.07	107.0	115	- 8.72	0.03	92.6	120	- 8.34	0.03	88.0	118

TABLE 5.4.2.—Heights of the standard meteor when one parameter at a time is varied; sporadic meteors with aphelion distance $Q > 6$ a.u., variable m_∞

Mass range (g)	Beginning				2.5				Maximum Light				End					
	Mean $\log m_\infty$ (g)	S.d. (g)	Mean $\log \rho_3$ (g/cm^3)	S.d. (g/cm^3)	Mean H (km)	No. obs.	Mean $\log \rho_3$ (g/cm^3)	S.d. (g/cm^3)	Mean H (km)	No. obs.	Mean $\log \rho_3$ (g/cm^3)	S.d. (g/cm^3)	Mean H (km)	No. obs.	Mean $\log \rho_3$ (g/cm^3)	S.d. (g/cm^3)	Mean H (km)	No. obs.
0.01-0.05	-1.55 ± 0.03		- 9.08 ± 0.04		97.1	39	- 9.02 ± 0.04		96.3	38	- 8.87 ± 0.05		94.5	40	- 8.47 ± 0.05		89.6	40
0.05-0.10	-1.14	0.02	- 9.14	0.07	97.9	16	- 9.12	0.07	97.6	17	- 8.82	0.07	93.7	18	- 8.39	0.06	88.6	18
0.10-0.20	-0.85	0.02	- 9.20	0.07	98.7	20	- 9.13	0.07	97.7	20	- 8.60	0.05	91.2	20	- 8.18	0.05	86.0	20
0.20-0.40	-0.55	0.02	- 9.28	0.05	99.7	12	- 9.23	0.07	99.0	12	- 8.53	0.09	90.3	13	- 8.21	0.07	86.3	13
0.40-0.80	-0.21	0.02	- 9.40	0.11	101.2	11	- 9.35	0.11	100.7	11	- 8.35	0.10	88.2	12	- 7.99	0.07	83.6	12
0.80-1.60	0.03	0.03	- 9.52	0.08	102.9	7	- 9.38	0.14	101.0	8	- 8.31	0.10	87.7	8	- 7.98	0.10	83.5	8
1.60-5.0	0.39	0.04	- 9.67	0.02	105.0	5	- 9.67	0.03	104.9	5	- 8.21	0.04	86.4	5	- 7.85	0.05	81.9	4
5.0-34	0.85	0.06	- 9.71	0.16	105.5	4	- 9.69	0.17	105.2	4	- 7.95	0.09	85.2	4	- 7.59	0.06	78.5	3
All	-0.86	0.06	- 9.24	0.03	99.2	114	- 9.18	0.03	98.4	115	- 8.63	0.03	91.6	120	- 8.25	0.03	86.9	118

TABLE 5.4.3.—Heights of the standard meteor when one parameter at a time is varied; sporadic meteors with aphelion distance $Q > 6$ a.u., variable Z_R

Range of $\cos Z_R$	Beginning				2.5				Maximum Light				End					
	Mean $\log \cos Z_R$	S.d.	Mean $\log \rho_3$ (g/cm^3)	S.d. (g/cm^3)	Mean H (km)	No. obs.	Mean $\log \rho_3$ (g/cm^3)	S.d. (g/cm^3)	Mean H (km)	No. obs.	Mean $\log \rho_3$ (g/cm^3)	S.d. (g/cm^3)	Mean H (km)	No. obs.	Mean $\log \rho_3$ (g/cm^3)	S.d. (g/cm^3)	Mean H (km)	No. obs.
0.1-0.2	-0.845 ± 0.138		--	--	--	--	- 9.66	--	104.7	1	- 9.01 ± 0.01		96.2	2	- 8.72 ± 0.13		92.6	2
0.2-0.3	-0.636	0.026	- 9.52 + 0.02		102.9	3	- 9.41 ± 0.04		101.3	2	- 9.00	0.07	96.0	4	- 8.78	0.04	93.3	4
0.3-0.4	-0.468	0.010	- 9.52	0.07	102.9	10	- 9.46	0.08	102.0	10	- 8.80	0.06	93.5	12	- 8.49	0.06	89.9	12
0.4-0.5	-0.338	0.006	- 9.33	0.06	100.3	21	- 9.29	0.06	99.8	21	- 8.64	0.06	91.6	21	- 8.30	0.07	87.5	19
0.5-0.6	-0.274	0.007	- 9.53	0.05	103.0	3	- 9.22	0.28	98.9	4	- 8.59	0.16	91.1	4	- 8.18	0.20	86.1	4
0.6-0.7	-0.193	0.004	- 9.19	0.06	98.5	21	- 9.13	0.06	97.7	21	- 8.41	0.05	88.9	21	- 8.06	0.05	84.5	21
0.7-0.8	-0.124	0.003	- 9.35	0.05	100.6	19	- 9.30	0.05	100.0	19	- 8.48	0.06	89.7	19	- 8.06	0.05	84.5	19
0.8-0.9	-0.079	0.003	- 9.37	0.08	100.8	17	- 9.27	0.08	99.6	17	- 8.41	0.08	88.8	17	- 7.98	0.06	83.5	17
0.9-1.0	-0.017	0.003	- 9.34	0.06	100.5	20	- 9.27	0.07	99.5	20	- 8.33	0.06	87.9	20	- 7.90	0.06	82.5	20
All	-0.218	0.017	- 9.34	0.03	100.5	114	- 9.27	0.03	99.6	115	- 8.52	0.03	90.3	120	- 8.14	0.03	85.5	118

TABLE 5.4.4.—Heights of the standard meteor when one parameter at a time is varied; sporadic meteors with aphelion distance $Q > 6$ a.u., variable σ

Range of log σ ($\text{cm}^{-2} \text{ s}^{-2}$)	Beginning				2.5				Maximum Light				End					
	Mean log σ ($\text{cm}^{-2} \text{ s}^{-2}$)	S.d. ($\text{cm}^{-2} \text{ s}^{-2}$)	Mean log ρ (g/cm^3)	S.d. (g/cm^3)	Mean H (km)	No. obs.	Mean log ρ (g/cm^3)	S.d. (g/cm^3)	Mean H (km)	No. obs.	Mean log ρ (g/cm^3)	S.d. (g/cm^3)	Mean H (km)	No. obs.	Mean log ρ (g/cm^3)	S.d. (g/cm^3)	Mean H (km)	No. obs.
-10.40- -11.00	-10.79 ± 0.05		-9.34 ± 0.09		100.5	17	-9.34 ± 0.08		100.5	18	-8.72 ± 0.09		92.6	18	-8.26 ± 0.08		87.0	18
-11.00- -11.15	-11.09	0.01	-9.38	0.04	100.9	21	-9.31	0.04	100.1	21	-8.60	0.05	91.1	21	-8.17	0.04	85.9	21
-11.15- -11.30	-11.23	0.01	-9.34	0.05	100.5	33	-9.29	0.05	99.9	33	-8.50	0.04	90.0	35	-8.15	0.04	85.6	34
-11.30- -11.45	-11.38	0.01	-9.42	0.04	101.5	25	-9.27	0.06	99.5	26	-8.42	0.05	89.0	27	-8.09	0.05	84.8	27
-11.45- -12.05	-11.64	0.03	-9.13	0.08	97.7	18	-9.06	0.10	96.8	17	-8.16	0.06	85.8	19	-7.84	0.06	81.8	18
All	-11.24	0.03	-9.33	0.03	100.4	114	-9.26	0.03	99.5	115	-8.48	0.03	89.7	120	-8.11	0.03	85.1	118

TABLE 5.5.1.—Heights of the standard meteor when one parameter at a time is varied; sporadic meteors minus $(A+S+D)$, with $|\chi| \leq 0.2$, variable v_∞

Velocity range (km/s)	Beginning				2.5				Maximum Light				End					
	Mean log v_∞ (km/s)	S.d. (km/s)	Mean log ρ (g/cm^3)	S.d. (g/cm^3)	Mean H (km)	No. obs.	Mean log ρ (g/cm^3)	S.d. (g/cm^3)	Mean H (km)	No. obs.	Mean log ρ (g/cm^3)	S.d. (g/cm^3)	Mean H (km)	No. obs.	Mean log ρ (g/cm^3)	S.d. (g/cm^3)	Mean H (km)	No. obs.
10-15	1.109 ± 0.029		-7.51 ± 0.07		77.2	3	-7.25 ± 0.05		73.1	3	-7.37 ± 0.07		75.1	3	-7.30 ± 0.05		74.0	3
15-20	1.250	0.007	-8.61	0.06	91.3	22	-8.42	0.06	89.0	22	-8.15	0.04	85.7	22	-7.80	0.05	81.3	21
20-25	1.352	0.005	-8.83	0.07	94.0	22	-8.69	0.06	92.2	22	-8.18	0.05	86.0	22	-7.86	0.04	82.0	22
25-30	1.440	0.005	-9.29	0.06	99.8	22	-9.19	0.05	98.4	22	-8.39	0.04	88.6	22	-8.02	0.04	84.0	22
30-35	1.507	0.005	-9.54	0.05	103.1	17	-9.51	0.05	102.7	17	-8.57	0.06	90.8	17	-8.21	0.04	86.4	17
35-40	1.580	0.009	-9.81	0.08	107.0	5	-9.81	0.07	107.0	5	-8.90	0.07	94.8	5	-8.26	0.12	87.1	5
40-45	1.649	0.004	-9.99	0.04	109.7	2	-9.98	0.04	109.6	2	-8.78	0.02	93.4	2	-8.18	0.04	86.0	2
45-50	1.674	0.006	-9.93	0.08	108.9	6	-9.81	0.16	106.9	7	-8.63	0.09	91.5	7	-8.15	0.10	85.6	7
50-55	1.721	0.008	-10.14	0.12	111.9	3	-10.21	0.12	113.0	3	-9.11	0.15	97.4	3	-8.58	0.06	91.0	3
55-60	1.754	0.006	-9.97	0.17	109.4	4	-10.16	0.20	112.3	4	-8.78	0.10	93.4	5	-8.37	0.13	88.4	5
60-65	1.799	0.004	-10.30	0.12	114.4	5	-10.40	0.12	116.1	5	-9.04	0.11	96.6	5	-8.50	0.09	90.0	5
65-70	1.824	0.005	-10.46	0.04	117.1	3	-10.54	0.01	118.7	3	-8.92	0.16	95.0	4	-8.45	0.08	89.4	4
70-75	1.856	0.006	-10.54	0.07	118.7	2	-10.59	0.11	119.6	2	-9.24	0.18	99.1	2	-8.78	0.02	93.3	2
All	1.468	0.017	-9.27	0.06	99.6	116	-9.19	0.07	98.5	117	-8.44	0.04	89.3	119	-8.06	0.03	84.5	118

TABLE 5.5.2.—Heights of the standard meteor when one parameter at a time is varied; sporadic meteors minus $(A+S+D)$, with $|\chi| \leq 0.2$, variable m_∞

Mass range (g)	Beginning				2.5				Maximum Light				End					
	Mean log m_∞ (g)	S.d. (g)	Mean log ρ (g/cm^3)	S.d. (g/cm^3)	Mean H (km)	No. obs.	Mean log ρ (g/cm^3)	S.d. (g/cm^3)	Mean H (km)	No. obs.	Mean log ρ (g/cm^3)	S.d. (g/cm^3)	Mean H (km)	No. obs.	Mean log ρ (g/cm^3)	S.d. (g/cm^3)	Mean H (km)	No. obs.
0.01-0.05	-1.51 ± 0.03		-9.01 ± 0.05		96.1	10	-8.92 ± 0.06		95.0	10	-8.72 ± 0.08		92.6	11	-8.32 ± 0.06		87.8	11
0.05-0.10	-1.13	0.03	-9.13	0.10	97.8	11	-9.07	0.10	96.9	11	-8.84	0.08	94.0	11	-8.45	0.07	89.4	11
0.10-0.20	-0.86	0.02	-9.35	0.05	100.6	24	-9.22	0.04	98.9	24	-8.64	0.04	91.6	24	-8.26	0.03	87.1	24
0.20-0.40	-0.52	0.02	-9.25	0.05	99.3	18	-9.20	0.05	98.6	18	-8.40	0.05	88.7	18	-8.02	0.04	84.1	18
0.40-0.80	-0.20	0.02	-9.45	0.05	101.9	19	-9.41	0.04	101.3	19	-8.32	0.06	87.8	20	-7.96	0.06	83.2	20
0.80-1.60	0.03	0.02	-9.37	0.09	100.9	17	-9.28	0.09	99.7	18	-8.19	0.06	86.2	18	-7.79	0.04	81.1	18
1.60-5.0	0.39	0.06	-9.52	0.13	102.9	9	-9.49	0.13	102.5	9	-8.21	0.07	85.1	9	-7.67	0.07	79.5	8
5.0-34	0.90	0.07	-9.85	0.07	107.5	8	-9.78	0.06	106.5	8	-8.02	0.07	84.1	8	-7.52	0.08	77.4	8
All	-0.43	0.06	-9.35	0.03	100.6	116	-9.28	0.03	99.6	117	-8.42	0.03	89.1	119	-8.03	0.03	84.2	118

TABLE 5.5.3.—Heights of the standard meteor when one parameter at a time is varied; sporadic meteors minus (A+S+D), with $|\chi| \leq 0.2$, variable Z_R

Range of $\cos Z_R$	Mean $\log \cos Z_R$	S.d.	Beginning				2.5				Maximum Light				End				
			Mean $\log \rho$ (g/cm^3)	S.d. (g/cm^3)	Mean H (km)	No. obs.	Mean $\log \rho$ (g/cm^3)	S.d. (g/cm^3)	Mean H (km)	No. obs.	Mean $\log \rho$ (g/cm^3)	S.d. (g/cm^3)	Mean H (km)	No. obs.	Mean $\log \rho$ (g/cm^3)	S.d. (g/cm^3)	Mean H (km)	No. obs.	
0.1-0.2	-0.985	--	--	--	--	--	--	--	--	--	--	--	--	--	--	--	--	--	--
0.2-0.3	-0.587	± 0.027	-9.24	± 0.21	99.1	3	-9.24	± 0.18	99.1	3	-8.88	± 0.15	94.5	4	-8.51	± 0.20	90.1	4	
0.3-0.4	-0.461	0.013	-9.47	0.03	102.1	7	-9.41	0.03	101.4	7	-8.73	0.04	92.7	7	-8.47	0.06	89.7	7	
0.4-0.5	-0.338	0.010	-9.34	0.12	100.5	8	-9.30	0.11	100.0	8	-8.69	0.10	92.3	8	-8.25	0.10	86.9	7	
0.5-0.6	-0.265	0.005	-9.27	0.08	99.6	10	-9.14	0.12	97.8	11	-8.53	0.07	90.3	11	-8.08	0.09	84.7	11	
0.6-0.7	-0.185	0.003	-9.27	0.05	99.5	24	-9.21	0.05	98.8	24	-8.41	0.05	88.9	24	-8.03	0.04	84.2	24	
0.7-0.8	-0.124	0.003	-9.37	0.05	100.8	28	-9.28	0.05	99.6	28	-8.43	0.05	89.2	28	-8.02	0.04	84.1	28	
0.8-0.9	-0.076	0.003	-9.33	0.06	100.3	22	-9.21	0.05	98.8	22	-8.30	0.06	87.5	22	-7.88	0.04	82.3	22	
0.9-1.0	-0.015	0.003	-9.34	0.08	100.5	14	-9.25	0.08	99.3	14	-8.23	0.07	86.7	14	-7.84	0.07	81.8	14	
All	-0.184	0.014	-9.33	0.03	100.3	116	-9.24	0.02	99.2	117	-8.44	0.05	89.3	119	-8.05	0.03	84.3	118	

TABLE 5.5.4.—Heights of the standard meteor when one parameter at a time is varied; sporadic meteors minus (A+S+D), with $|\chi| \leq 0.2$, variable σ

Range of $\log \sigma$ ($cm^{-2} s^{-2}$)	Mean $\log \sigma$ ($cm^{-2} s^{-2}$)	S.d. ($cm^{-2} s^{-2}$)	Beginning				2.5				Maximum Light				End				
			Mean $\log \rho$ (g/cm^3)	S.d. (g/cm^3)	Mean H (km)	No. obs.	Mean $\log \rho$ (g/cm^3)	S.d. (g/cm^3)	Mean H (km)	No. obs.	Mean $\log \rho$ (g/cm^3)	S.d. (g/cm^3)	Mean H (km)	No. obs.	Mean $\log \rho$ (g/cm^3)	S.d. (g/cm^3)	Mean H (km)	No. obs.	
-10.40- -11.00	-10.88	± 0.02	-9.23	± 0.09	99.1	18	-9.16	± 0.08	98.1	18	-8.65	± 0.07	91.7	18	-8.21	± 0.05	86.3	18	
-11.00- -11.15	-11.09	0.01	-9.24	0.05	99.2	29	-9.16	0.05	98.2	29	-8.48	0.05	89.8	29	-8.06	0.04	84.5	29	
-11.15- -11.30	-11.23	0.01	-9.38	0.04	101.0	34	-9.32	0.04	100.3	34	-8.49	0.04	89.9	35	-8.09	0.04	84.9	34	
-11.30- -11.45	-11.38	0.01	-9.43	0.04	101.7	23	-9.29	0.05	99.8	24	-8.37	0.04	88.3	25	-8.02	0.05	84.0	25	
-11.45- -12.05	-11.54	0.02	-9.33	0.05	100.3	12	-9.29	0.04	99.8	12	-8.19	0.05	86.1	12	-7.90	0.04	82.6	12	
All	-11.21	0.02	-9.33	0.03	100.3	116	-9.25	0.03	99.3	117	-8.46	0.02	89.5	119	-8.07	0.02	84.6	118	

TABLE 5.6.1.—Heights of the standard meteor when one parameter at a time is varied; sporadic meteors minus (A+S+D), with $\chi > 0.2$, variable v_∞

Velocity range (km/s)	Mean $\log v_\infty$ (km/s)	S.d. (km/s)	Beginning				2.5				Maximum Light				End				
			Mean $\log \rho$ (g/cm^3)	S.d. (g/cm^3)	Mean H (km)	No. obs.	Mean $\log \rho$ (g/cm^3)	S.d. (g/cm^3)	Mean H (km)	No. obs.	Mean $\log \rho$ (g/cm^3)	S.d. (g/cm^3)	Mean H (km)	No. obs.	Mean $\log \rho$ (g/cm^3)	S.d. (g/cm^3)	Mean H (km)	No. obs.	
10-15	1.140	± 0.013	-7.62	± 0.18	78.8	3	-7.49	± 0.19	77.0	3	-7.51	± 0.20	77.2	3	-7.41	± 0.16	75.7	3	
15-20	1.250	0.007	-8.29	0.07	87.4	23	-8.14	0.07	85.5	24	-7.93	0.05	82.9	24	-7.70	0.05	80.0	24	
20-25	1.344	0.006	-8.77	0.09	95.2	18	-8.64	0.09	91.6	18	-8.22	0.06	86.5	18	-7.95	0.05	83.2	18	
25-30	1.431	0.008	-9.24	0.11	99.1	12	-9.11	0.10	97.4	12	-8.31	0.06	87.6	12	-7.99	0.06	83.7	12	
30-35	1.500	0.005	-9.29	0.06	99.7	9	-9.27	0.09	99.6	9	-8.47	0.13	89.6	9	-8.14	0.12	85.5	9	
35-40	1.563	0.006	-9.32	0.10	100.2	6	-9.34	0.09	100.4	6	-8.46	0.09	89.5	6	-8.13	0.08	85.4	6	
40-45	1.629	0.006	-9.75	0.09	106.1	7	-9.79	0.10	106.6	7	-8.81	0.07	93.7	7	-8.42	0.09	89.0	7	
45-50	1.672	0.009	-9.46	0.27	102.0	3	-9.65	0.27	104.6	3	-8.60	0.14	91.2	4	-8.22	0.13	86.5	4	
50-55	1.727	0.006	-10.15	0.03	112.0	3	-10.23	0.06	113.3	3	-8.84	0.11	94.0	3	-8.59	0.05	91.1	3	
55-60	1.768	0.005	-10.22	0.07	113.2	4	-10.40	0.08	116.1	5	-9.02	0.03	96.3	6	-8.70	0.06	92.4	6	
60-65	1.791	0.003	-10.10	0.06	111.4	10	-10.30	0.08	114.4	10	-8.87	0.09	94.5	10	-8.47	0.08	89.6	10	
65-70	1.833	0.003	-10.42	0.05	116.5	8	-10.53	0.10	118.4	7	-8.98	0.09	95.7	8	-8.68	0.08	92.1	7	
70-75	1.854	0.004	-10.36	0.05	115.5	3	-10.64	0.12	120.5	3	-8.88	0.13	94.5	3	-8.59	0.05	91.1	3	
All	1.501	0.021	-9.22	0.08	98.9	109	-9.19	0.09	98.5	110	-8.42	0.04	89.0	113	-8.12	0.04	85.2	112	

TABLE 5.6.2.—Heights of the standard meteor when one parameter at a time is varied; sporadic meteors minus (A+S+D), with $\chi > 0.2$, variable m_{∞}

Mass range (g)	Beginning				2.5				Maximum Light				End					
	Mean $\log m_{\infty}$ (g)	S.d. (g)	Mean $\log \rho_3$ (g/cm ³)	S.d. (g/cm ³)	Mean H (km)	No. obs.	Mean $\log \rho_3$ (g/cm ³)	S.d. (g/cm ³)	Mean H (km)	No. obs.	Mean $\log \rho_3$ (g/cm ³)	S.d. (g/cm ³)	Mean H (km)	No. obs.	Mean $\log \rho_3$ (g/cm ³)	S.d. (g/cm ³)	Mean H (km)	No. obs.
0.01-0.05	-1.55	± 0.04	-9.00	± 0.04	96.0	27	-8.94	± 0.05	95.3	26	-8.75	± 0.05	92.9	27	-8.48	± 0.05	89.8	27
0.05-0.10	-1.14	0.02	-9.04	0.08	96.5	11	-8.99	0.08	96.0	12	-8.55	0.08	90.6	13	-8.28	0.06	87.2	13
0.10-0.20	-0.81	0.02	-9.19	0.09	98.6	15	-9.10	0.07	97.4	15	-8.52	0.06	90.2	15	-8.21	0.05	86.3	15
0.20-0.40	-0.53	0.02	-9.23	0.06	99.1	17	-9.18	0.06	98.3	17	-8.45	0.07	89.3	18	-8.10	0.07	85.0	18
0.40-0.80	-0.25	0.02	-9.13	0.09	97.7	17	-9.10	0.08	97.3	17	-8.22	0.07	86.6	17	-7.97	0.06	83.4	17
0.80-1.60	0.05	0.02	-9.30	0.11	100.0	12	-9.32	0.09	100.3	12	-8.23	0.07	86.6	12	-7.94	0.07	83.0	12
1.60-5.0	0.39	0.06	-9.23	0.17	99.0	7	-9.27	0.17	99.5	7	-7.99	0.14	83.7	7	-7.71	0.10	80.2	7
5.0-∞	0.94	0.19	-8.97	0.20	95.7	3	-9.15	0.22	97.9	4	-7.72	0.05	80.3	4	-7.39	0.06	75.4	3
All	-0.67	0.07	-9.13	0.03	97.8	109	-9.10	0.03	97.3	110	-8.43	0.03	89.1	113	-8.15	0.03	85.6	112

TABLE 5.6.3.—Heights of the standard meteor when one parameter at a time is varied; sporadic meteors minus (A+S+D), with $\chi > 0.2$, variable Z_R

Range of $\cos Z_R$	Beginning				2.5				Maximum Light				End					
	Mean $\log \cos Z_R$	S.d.	Mean $\log \rho_3$ (g/cm ³)	S.d. (g/cm ³)	Mean H (km)	No. obs.	Mean $\log \rho_3$ (g/cm ³)	S.d. (g/cm ³)	Mean H (km)	No. obs.	Mean $\log \rho_3$ (g/cm ³)	S.d. (g/cm ³)	Mean H (km)	No. obs.	Mean $\log \rho_3$ (g/cm ³)	S.d. (g/cm ³)	Mean H (km)	No. obs.
0.1-0.2	-0.750	± 0.043	-9.22	--	98.9	1	-9.24	± 0.01	99.2	2	-8.83	± 0.06	93.9	2	-8.65	± 0.03	91.8	2
0.2-0.3	-0.628	0.035	-9.17	± 0.04	98.3	3	-9.14	0.09	97.8	2	-8.79	0.07	93.5	3	-8.63	0.03	91.6	3
0.3-0.4	-0.449	0.010	-9.07	0.08	96.9	11	-9.07	0.09	96.9	11	-8.53	0.08	90.3	13	-8.29	0.08	87.3	13
0.4-0.5	-0.336	0.006	-9.09	0.07	97.3	18	-9.08	0.07	97.1	18	-8.43	0.07	89.1	18	-8.17	0.07	85.9	17
0.5-0.6	-0.261	0.008	-9.15	0.07	98.0	8	-9.12	0.07	97.6	8	-8.50	0.06	90.0	8	-8.18	0.05	86.0	8
0.6-0.7	-0.191	0.004	-9.08	0.08	97.0	23	-9.07	0.07	96.9	24	-8.39	0.05	88.6	24	-8.09	0.05	84.9	24
0.7-0.8	-0.119	0.004	-9.18	0.08	98.3	17	-9.16	0.07	98.1	17	-8.36	0.07	88.2	17	-8.03	0.06	84.1	17
0.8-0.9	-0.077	0.003	-9.24	0.07	99.2	20	-9.15	0.06	98.0	20	-8.27	0.06	87.1	20	-7.97	0.05	83.3	20
0.9-1.0	-0.019	0.006	-9.23	0.16	99.1	8	-9.19	0.14	98.5	8	-8.19	0.10	86.2	8	-7.87	0.08	82.2	8
All	-0.227	0.015	-9.15	0.03	97.9	109	-9.12	0.03	97.5	110	-8.40	0.03	88.7	113	-8.11	0.03	85.1	112

TABLE 5.6.4.—Heights of the standard meteor when one parameter at a time is varied; sporadic meteors minus (A+S+D), with $\chi > 0.2$, variable σ

Range of $\log \sigma$ (cm ⁻² s ²)	Beginning				2.5				Maximum Light				End					
	Mean $\log \sigma$ (cm ⁻² s ²)	S.d. (cm ⁻² s ²)	Mean $\log \rho_3$ (g/cm ³)	S.d. (g/cm ³)	Mean H (km)	No. obs.	Mean $\log \rho_3$ (g/cm ³)	S.d. (g/cm ³)	Mean H (km)	No. obs.	Mean $\log \rho_3$ (g/cm ³)	S.d. (g/cm ³)	Mean H (km)	No. obs.	Mean $\log \rho_3$ (g/cm ³)	S.d. (g/cm ³)	Mean H (km)	No. obs.
-10.40- -11.00	-10.85	± 0.02	-9.17	± 0.06	98.3	27	-9.18	± 0.06	98.4	28	-8.48	± 0.06	89.8	28	-8.17	± 0.05	85.9	28
-11.00- -11.15	-11.08	0.01	-9.22	0.05	98.9	29	-9.19	0.05	98.5	29	-8.46	0.04	89.5	29	-8.17	0.04	85.9	29
-11.15- -11.30	-11.23	0.01	-9.21	0.06	98.8	33	-9.19	0.05	98.5	34	-8.41	0.04	88.9	35	-8.11	0.03	85.2	35
-11.30- -11.45	-11.37	0.01	-9.19	0.10	98.6	11	-9.12	0.10	97.5	11	-8.32	0.09	87.7	11	-8.09	0.09	84.9	11
-11.45- -12.05	-11.75	0.05	-8.75	0.11	93.0	9	-8.68	0.13	92.1	8	-7.99	0.07	83.7	10	-7.69	0.08	79.8	9
All	-11.16	0.02	-9.16	0.03	98.2	109	-9.14	0.03	97.9	110	-8.40	0.03	88.7	113	-8.11	0.03	85.1	112

TABLE 6.1.—Mean observed heights of Super-Schmidt meteors for groups of different velocity

Velocity range (km/s)	Mean v_{∞} (km/s)	S.d. (km/s)	Mean H_B (km)	S.d. (km)	No. obs.	Mean $H_{2.5}$ (km)	S.d. (km)	No. obs.	Mean H_{ML} (km)	S.d. (km)	No. obs.	Mean H_E (km)	S.d. (km)	No. obs.
10 - 15	13.5	± 0.3	81.7	± 0.3	10	79.1	± 1.2	9	75.9	± 1.8	9	74.8	± 2.1	10
15 - 20	17.7	0.2	89.6	0.6	56	88.2	0.6	57	81.9	0.6	57	77.2	0.8	56
20 - 25	22.4	0.2	94.4	0.6	65	93.0	0.6	65	86.1	0.6	65	81.7	0.6	65
25 - 30	27.4	0.2	99.0	0.6	62	97.7	0.5	62	87.7	0.5	63	82.8	0.6	63
30 - 35	31.9	0.2	100.9	0.6	48	100.6	0.7	47	88.5	0.7	48	83.9	0.7	48
35 - 40	36.7	0.2	100.2	0.7	38	100.6	0.7	38	88.7	1.0	39	83.1	1.1	39
40 - 45	42.8	0.2	102.8	0.7	34	102.9	0.7	34	95.0	0.6	34	90.1	0.8	34
45 - 50	47.3	0.4	104.8	1.8	12	104.7	1.9	13	92.0	1.2	14	86.4	1.3	14
50 - 55	53.0	0.5	110.5	0.6	9	111.1	0.7	9	99.8	1.9	9	93.7	1.9	9
55 - 60	58.2	0.4	109.3	1.1	15	111.2	1.4	16	98.1	1.1	18	94.5	1.2	18
60 - 65	61.7	0.3	111.7	0.9	25	113.4	0.9	25	99.7	1.0	26	94.4	1.1	26
65 - 70	67.7	0.2	114.7	0.5	21	116.8	0.7	19	102.4	1.4	22	98.4	1.4	21
70 - 75	71.4	0.3	117.2	1.8	8	119.0	1.3	8	100.5	2.3	8	96.6	2.0	8
All	35.3	0.8	100.0	0.4	403	99.6	0.5	402	89.8	0.4	412	85.1	0.4	411

TABLE 6.2.—Mean observed heights of Super-Schmidt meteors for groups of different mass

Mass range (g)	Mean m (g)	S.d. (g)	Mean H_B (km)	S.d. (km)	No. obs.	Mean $H_{2.5}$ (km)	S.d. (km)	No. obs.	Mean H_{ML} (km)	S.d. (km)	No. obs.	Mean H_E (km)	S.d. (km)	No. obs.
0.01 - 0.05	0.031	± 0.001	109.2	± 0.8	65	110.3	± 0.9	64	100.1	± 0.7	66	95.4	± 0.8	66
0.05 - 0.10	0.072	0.002	104.4	1.0	51	104.2	1.1	51	94.9	0.7	53	90.3	0.7	53
0.10 - 0.20	0.146	0.003	100.2	0.7	73	99.4	0.8	73	90.8	0.6	74	85.8	0.5	74
0.20 - 0.40	0.290	0.007	98.8	1.0	70	98.1	1.0	70	88.7	0.6	71	83.9	0.6	71
0.40 - 0.80	0.596	0.014	95.4	1.1	60	94.6	1.2	59	85.0	0.6	61	80.7	0.6	61
0.80 - 1.60	1.11	0.03	93.2	1.3	42	92.5	1.4	43	83.3	0.8	43	79.0	0.7	43
1.60 - 5.0	2.51	0.17	95.0	1.5	29	94.5	1.7	29	82.4	1.3	30	77.1	1.3	29
5.0 - 34	10.15	2.27	97.3	2.5	12	95.6	2.5	13	78.1	1.8	13	70.9	2.4	12
All	0.80	0.12	100.0	0.4	402	99.6	0.5	402	89.8	0.4	411	85.1	0.4	409

TABLE 7.1.—The position of maximum light defined by the parameter $F = \frac{H_B - H_{ML}}{H_B - H_E}$, for Super-Schmidt meteors

Group	Mean F	S.d.	No. obs.
All meteors	0.65	± 0.01	400
A meteors	0.36	0.05	26
S meteors	0.48	0.05	12
Southern Taurids	0.69	0.04	17
Geminids	0.72	0.05	19
Draconids	0.55	0.02	2

TABLE 7.2.—The position of the maximum light defined by $F = \frac{H_B - H_{ML}}{H_B - H_E}$, as a function of velocity for Super-Schmidt meteors

Velocity range (km/s)	Mean v_{∞} (km/s)	Mean F	S.d.	No. obs.
10 - 20	17.2	0.59	± 0.03	64
20 - 25	22.4	0.63	0.02	65
25 - 30	27.4	0.66	0.03	62
30 - 40	34.0	0.68	0.02	86
40 - 60	48.2	0.64	0.02	70
60 - 73	65.5	0.70	0.02	53
All	35.1	0.65	0.01	400

TABLE 7.3.—The position of the maximum light, defined by $F = \frac{H_B - H_{ML}}{H_B - H_E}$, as a function of the ablation coefficient σ for Super-Schmidt meteors

Ablation coefficient range (cm ⁻² s ⁻²)	Mean log σ (cm ⁻² s ⁻²)	Mean F	S.d.	No. Obs.
-12.1 - -11.5	-11.65	0.64	± 0.03	35
-11.5 - -11.3	-11.37	0.73	0.01	79
-11.3 - -11.1	-11.19	0.67	0.01	139
-11.1 - -10.9	-11.01	0.64	0.02	78
-10.9 - -10.4	-10.75	0.53	0.03	52
All	-11.17	0.65	0.01	383

TABLE 7.4.—The position of the maximum light, defined by $F = \frac{H_B - H_{ML}}{H_B - H_E}$, as a function of the fragmentation index for Super-Schmidt meteors

Fragmentation index range	Mean χ	Mean F	S.d.	No. obs.
$\chi < 0$	-0.09	0.67	± 0.02	71
$0 \leq \chi < 0.1$	0.06	0.67	0.02	59
$0.1 \leq \chi < 0.2$	0.15	0.65	0.02	62
$0.2 \leq \chi < 0.3$	0.25	0.65	0.03	41
$0.3 \leq \chi < 0.5$	0.38	0.66	0.02	87
$\chi \geq 0.5$	0.73	0.60	0.02	67
All	0.26	0.65	0.01	387

TABLE 8.1.—The ratio $\frac{D_{obs}}{D_{th}}$ of observed and theoretical durations and the mean differences ΔH between observed and theoretical heights for Super-Schmidt meteors

Groups	No. obs.	Mean $\frac{D_{obs}}{D_{th}}$	S.d.	ΔH_B	S.d.	$\Delta H_{2.5}$	S.d.	ΔH_M	S.d.	ΔH_E	S.d.
				(km)	(km)	(km)	(km)	(km)	(km)		
All meteors	384	0.61	± 0.01	-8.9 ± 0.4		-6.8 ± 0.4		-1.5 ± 0.2		0.9 ± 0.2	
Sporadic meteors	273	0.60	0.01	-9.0	0.5	-6.7	0.5	-1.6	0.2	1.0	0.3
Shower meteors	111	0.65	0.02	-8.7	0.8	-7.0	0.8	-1.3	0.4	0.7	0.4
All - (A+S)	348	0.63	0.01	-8.3	0.4	-6.3	0.4	-1.4	0.2	1.1	0.2
Sporadic - (A+S)	245	0.62	0.01	-8.4	0.5	-6.2	0.5	-1.4	0.3	1.2	0.3
Sporadic - (A+S), with $Q \leq 6$ a.u.	138	0.63	0.01	-7.1	0.6	-4.4	0.5	-2.0	0.4	1.0	0.4
Sporadic - (A+S), with $Q > 6$ a.u.	107	0.62	0.01	-10.0	1.0	-8.6	1.0	-0.6	0.3	1.4	0.3
A	24	0.45	0.03	-14.3	1.1	-10.9	1.1	-3.0	0.8	-1.7	1.1
S	12	0.35	0.04	-15.5	2.7	-12.3	2.5	-1.7	1.3	0.5	1.5
F	11	0.74	0.04	-9.9	1.4	-6.1	1.1	-2.6	1.3	-1.0	1.8

TABLE 8.2.—The ratio $\frac{D_{\text{obs}}}{D_{\text{th}}}$ of observed and theoretical durations and the mean differences ΔH between observed and theoretical heights for all Super-Schmidt meteors minus ($A+S$), as functions of velocity

Velocity range (km/s)	Mean v_{∞} (km/s)	Mean $\frac{D_{\text{obs}}}{D_{\text{th}}}$	S.d.	ΔH_B	S.d.	$\Delta H_{2.5}$	S.d.	ΔH_{ML}	S.d.	ΔH_E	S.d.	No. obs.
10 - 20	17.3	0.58	± 0.02	-7.8 ± 0.8		-4.7 ± 0.6		-2.7 ± 0.6		0.9 ± 0.6		55
20 - 30	25.0	0.68	0.02	-4.9	0.6	-2.9	0.5	-0.5	0.3	2.2	0.4	113
30 - 40	33.9	0.68	0.02	-8.2	0.7	-5.7	0.7	-1.7	0.5	0.2	0.5	76
40 - 50	44.2	0.60	0.02	-9.2	1.1	-7.8	0.9	-0.6	0.5	0.9	0.6	39
50 - 60	56.1	0.59	0.03	-11.4	2.3	-10.9	2.5	-1.3	1.0	1.0	0.9	21
60 - 73	65.0	0.56	0.02	-15.4	1.9	-14.8	1.8	-2.0	0.6	0.1	0.5	44
All	35.0	0.63	0.01	-8.3	0.4	-6.3	0.4	-1.4	0.2	1.1	0.2	348

TABLE 8.3.—The ratio $\frac{D_{\text{obs}}}{D_{\text{th}}}$ of observed and theoretical durations and the mean differences ΔH between observed and theoretical heights for all Super-Schmidt meteors minus ($A+S$) as functions of mass

Mass range (g)	Mean m_{∞} (g)	Mean $\frac{D_{\text{obs}}}{D_{\text{th}}}$	S.d.	ΔH_B	S.d.	$\Delta H_{2.5}$	S.d.	ΔH_{ML}	S.d.	ΔH_E	S.d.	No. obs.
0.01 - 0.1	0.05	0.61	± 0.01	-8.5 ± 0.7		-7.2 ± 0.6		-1.0 ± 0.4		1.1 ± 0.4		98
0.1 - 0.2	0.15	0.67	0.02	-6.3	1.1	-4.8	1.1	-0.7	0.4	1.4	0.5	64
0.2 - 0.5	0.32	0.65	0.02	-8.9	1.2	-6.8	1.2	-2.1	0.4	0.4	0.5	76
0.5 - 2.0	1.29	0.63	0.02	-7.7	0.7	-5.3	0.7	-1.5	0.5	1.4	0.5	84
2.0 - 5.0	3.28	0.58	0.05	-11.2	1.9	-7.3	1.8	-1.9	1.3	1.2	1.3	13
5.0 - 34	10.15	0.66	0.05	-13.6	3.5	-9.6	3.0	-2.0	1.1	0.4	1.6	13
All	0.86	0.63	0.01	-8.3	0.4	-6.3	0.4	-1.4	0.2	1.1	0.2	348

TABLE 8.4.—The ratio $\frac{D_{\text{obs}}}{D_{\text{th}}}$ of observed and theoretical durations and the mean differences ΔH between observed and theoretical heights for all Super-Schmidt meteors minus ($A+S$), as functions of the ablation coefficient σ

Range of $\log \sigma$ ($\text{cm}^{-2} \text{s}^2$)	Mean $\log \sigma$ ($\text{cm}^{-2} \text{s}^2$)	Mean $\frac{D_{\text{obs}}}{D_{\text{th}}}$	S.d.	ΔH_B	S.d.	$\Delta H_{2.5}$	S.d.	ΔH_{ML}	S.d.	ΔH_E	S.d.	No. obs.
-12.05, -11.45	-11.60	0.70	± 0.03	-7.0 ± 1.3		-5.3 ± 1.2		0.0 ± 0.6		1.9 ± 0.6		42
-11.45, -11.30	-11.36	0.70	0.02	-5.1	0.8	-3.8	0.7	0.2	0.3	2.8	0.4	68
-11.30, -11.15	-11.22	0.65	0.01	-6.3	0.7	-4.4	0.7	-0.3	0.3	2.3	0.3	91
-11.15, -11.0	-11.08	0.60	0.02	-9.0	0.7	-6.8	0.6	-2.2	0.4	0.4	0.4	80
-11.0, -10.40	-10.83	0.55	0.02	-14.1	1.3	-11.6	1.3	-4.2	0.5	-2.1	0.5	67
All	-11.22	0.63	0.01	-8.3	0.4	-6.3	0.4	-1.4	0.2	1.1	0.2	348

TABLE 8.5.—*The ratio $\frac{D_{obs}}{D_{th}}$ of observed and theoretical durations and the mean differences ΔH between observed and theoretical heights for all Super-Schmidt meteors minus (A+S), as functions of the fragmentation index χ*

Range of χ	Mean χ	Mean $\frac{D_{obs}}{D_{th}}$	S.d.	ΔH_B	S.d.	$\Delta H_{2.5}$	S.d.	ΔH_{ML}	S.d.	ΔH_F	S.d.	No. obs.
$\chi < 0$	-0.11	0.72	± 0.02	-6.8	± 0.9	-5.2	± 0.9	-0.6	± 0.4	0.9	± 0.4	13
$0 < \chi < 0.2$	0.09	0.69	0.01	-6.9	0.6	-5.0	0.5	-0.9	0.4	1.2	0.4	110
$0.2 \leq \chi < 0.4$	0.30	0.62	0.02	-9.4	1.2	-7.1	1.1	-1.8	0.4	1.2	0.5	86
$0.4 \leq \chi < 0.6$	0.48	0.54	0.02	-10.8	1.3	-9.2	1.4	-2.2	0.6	0.9	0.6	45
$\chi \geq 0.6$	0.87	0.52	0.02	-9.2	1.1	-7.1	1.0	-2.0	0.7	1.0	0.8	44
All	0.24	0.63	0.01	-8.3	0.4	-6.3	0.4	-1.4	0.2	1.1	0.2	348

TABLE 8.6.—*The ratio $\frac{D_{obs}}{D_{th}}$ of observed and theoretical durations and the mean differences ΔH between observed and theoretical heights for all Super-Schmidt meteors minus (A+S), as functions of the brightness ϵ_m*

Brightness range	Mean ϵ_m	Mean $\frac{D_{obs}}{D_{th}}$	S.d.	ΔH_B	S.d.	$\Delta H_{2.5}$	S.d.	ΔH_{ML}	S.d.	ΔH_F	S.d.	No. obs.
-1.4, -1.0	-1.14	0.62	± 0.03	-4.8	± 1.1	-2.5	± 0.9	-2.1	± 0.9	1.2	± 1.0	23
-1.0, -0.75	-0.86	0.67	0.02	-4.3	0.6	-2.4	0.5	-1.0	0.5	1.0	0.5	13
-0.75, -0.50	-0.64	0.63	0.02	-6.0	0.6	-4.0	0.5	-0.9	0.4	1.7	0.4	94
-0.50, -0.25	-0.39	0.61	0.02	-9.0	0.7	-7.1	0.7	-1.3	0.4	0.8	0.5	17
-0.25, 0	-0.14	0.67	0.03	-9.0	1.0	-7.3	1.0	-1.3	0.5	1.0	0.5	52
0, 0.50	0.18	0.61	0.03	-12.9	1.4	-10.6	1.5	-1.9	0.6	0.5	0.7	40
0.50, 2.0	0.78	0.63	0.05	-21.8	3.9	-19.8	3.7	-3.1	1.0	-2.2	1.2	10
All	-0.41	0.63	0.01	-8.3	0.4	-6.3	0.4	-1.4	0.2	1.1	0.2	348

TABLE 9.— $\Delta \log \rho_{corr}$ as a function of aphelion distance Q (*=harmonic mean)

Range of Q (a.u.)	Mean Q (a.u.)	$\overline{\Delta \log \rho_{corr}}$	S.d.	No. obs.
0 - 3.5	2.9	-0.066	± 0.036	47
3.5 - 4.2	3.8	-0.054	0.034	44
4.2 - 4.8	4.6	-0.025	0.037	48
4.8 - 5.4	5.0	0.018	0.031	43
5.4 - 7.0	5.9	0.054	0.031	42
7.0 - 20	12	0.058	0.027	41
20 - 70	34	0.021	0.033	51
70 - ∞	312*	0.021	0.041	34
All	—	0.000	0.012	350

TABLE 10.1.— $\overline{\Delta \log \rho_{corr}^*}$ as a function of v_m , the velocity at the point where the mass of the meteor is reduced to half its original value

Mean v_m (km/s)	Mean $\overline{\Delta \log \rho_{corr}^*}$	S.d.	No. obs.
15.5	0.017	± 0.041	37
19.7	-0.008	0.037	47
23.3	0.001	0.042	35
26.2	0.028	0.032	34
30.0	0.016	0.025	50
34.3	-0.008	0.044	28
42.0	0.029	0.032	31
49.1	-0.028	0.055	27
60.4	-0.061	0.033	34
68.5	-0.022	0.047	27
All: 29.4	0.000	0.012	350

TABLE 10.2.— $\Delta \log \rho_{corr}^*$ as a function of the height H corresponding to individual decelerations

Height range (km)	Mean height (km)	Mean $\overline{\Delta \log \rho_{corr}^*}$	S.d.	No. obs.
50 - 75	72.6	-0.26	± 0.03	44
75 - 80	78.2	-0.18	0.03	88
80 - 84	82.3	-0.08	0.02	145
84 - 86	85.0	-0.03	0.02	110
86 - 88	87.0	0.02	0.02	105
88 - 90	89.0	0.04	0.02	99
90 - 92	91.1	0.05	0.02	125
92 - 95	93.5	0.07	0.01	165
95 - 99	96.7	0.04	0.02	118
99 - 114	103.2	0.03	0.02	150
All	90.1	0.00	0.01	1149

TABLE 10.3.— $\overline{\Delta \log \rho_{corr}^*}$ as a function of \overline{H} , the average for each meteor of the heights for which decelerations were determined

Height range (km)	Mean height \overline{H} (km)	Mean $\overline{\Delta \log \rho_{corr}^*}$	S.d.	No. obs.
72 - 80	76.9	-0.28	0.05	17
80 - 84	82.3	-0.04	0.04	32
84 - 86	84.8	-0.06	0.05	26
86 - 88	87.0	0.01	0.05	31
88 - 90	89.1	0.06	0.04	33
90 - 92	91.0	0.06	0.02	43
92 - 94	92.9	0.04	0.03	42
94 - 99	96.1	0.04	0.03	52
99 - 103	100.9	0.07	0.04	35
103 - 114	106.1	-0.01	0.03	39
All	91.0	0.00	0.01	350

TABLE 11.1.—Values obtained by least squares of the coefficients of the equation $M_{pm} = k_0 + k_1 (\log v_\infty - 6.477) + k_2 (\log m_\infty + 0.523) + k_3 (\log \cos Z_R + 0.2)$ for Super-Schmidt meteors

	All meteors	Sporadic meteors
k_0	0.07 ± 0.02	0.05 ± 0.03
k_1	-8.44 ± 0.16	-8.57 ± 0.21
k_2	-2.19 ± 0.05	-2.24 ± 0.06
k_3	-1.45 ± 0.13	-1.56 ± 0.17
No. obs.	411	289
All meteors minus (A + S + D)		
k_0	0.12 ± 0.02	0.12 ± 0.02
k_1	-8.68 ± 0.15	-8.84 ± 0.19
k_2	-2.22 ± 0.04	-2.31 ± 0.06
k_3	-1.52 ± 0.13	-1.55 ± 0.16
No. obs.	367	246

TABLE 11.2.—Values obtained by least squares of the coefficients of the equation: $M_{pm} = k_0 + k_1 (\log v_\infty - 6.477) + k_2 (\log m_\infty + 0.523) + k_3 (\log \cos Z_R + 0.2)$ for particular groups of Super-Schmidt meteors

	Sporadic meteors minus (A + S + D) with $\chi < 0.2$ (Mean $\chi = 0.05$)	Sporadic meteors minus (A + S + D) with $\chi > 0.2$ (Mean $\chi = 0.49$)
k_0	0.21 ± 0.04	0.02 ± 0.03
k_1	-9.01 ± 0.29	-8.85 ± 0.25
k_2	-2.30 ± 0.08	-2.41 ± 0.08
k_3	-1.81 ± 0.25	-1.40 ± 0.22
No. obs.	124	114

Sporadic meteors
minus (A + S + D)
with $\log \sigma < -11.40$
(Mean $\log \sigma = -11.55$)

	Sporadic meteors minus (A + S + D) with $\log \sigma < -11.40$ (Mean $\log \sigma = -11.55$)	Sporadic meteors minus (A + S + D) with $-11.40 \leq \log \sigma \leq -11.00$ (Mean $\log \sigma = -11.19$)
k_0	0.52 ± 0.08	0.15 ± 0.03
k_1	-10.19 ± 0.43	-9.46 ± 0.25
k_2	-2.22 ± 0.08	-2.41 ± 0.07
k_3	-2.02 ± 0.27	-1.67 ± 0.20
No. obs.	36	155

Sporadic meteors
minus (A + S + D)
with $\log \sigma > -11.00$
(Mean $\log \sigma = -10.86$)

k_0	0.01 ± 0.06
k_1	-8.71 ± 0.42
k_2	-2.59 ± 0.14
k_3	-1.64 ± 0.32
No. obs.	46

TABLE 11.3.—Values obtained by least squares of the coefficients of the equation: $M_{DM} = k_0 + k_1 (\log v_\infty - 6.477) + k_2 (\log m_\infty + 0.523) + k_3 (\log \cos Z_R + 0.2)$ for short- and long-period Super-Schmidt meteors

	Sporadic meteors minus (A + S + D) with $Q \leq 6$ a.u.	Sporadic meteors minus (A + S + D) with $Q > 6$ a.u.
k_0	0.20 ± 0.05	0.16 ± 0.03
k_1	-7.82 ± 0.43	-9.45 ± 0.21
k_2	-2.14 ± 0.10	-2.42 ± 0.05
k_3	-1.13 ± 0.28	-1.82 ± 0.15
No. obs.	133	113

TABLE 11.4.—Values obtained by least squares of the coefficients of the equation: $M_{DM} = k_0 + k_1 (\log v_\infty - 6.477) + k_2 (\log m_\infty + 0.523) + k_3 (\log \cos Z_R + 0.2)$ for small-camera meteors

	All meteors	Sporadic meteors
k_0	0.08 ± 0.14	-0.18 ± 0.21
k_1	-10.00 ± 0.37	-9.37 ± 0.55
k_2	-2.46 ± 0.07	-2.27 ± 0.12
k_3	-1.90 ± 0.43	-2.03 ± 0.63
No. obs.	207	85

	Meteors with flares	Meteors without flares
k_0	-0.25 ± 0.26	-0.25 ± 0.12
k_1	-10.29 ± 0.58	-8.73 ± 0.34
k_2	-2.53 ± 0.12	-2.02 ± 0.07
k_3	-1.79 ± 0.78	-1.67 ± 0.35
No. obs.	80	127

TABLE 11.5.—Values obtained by least squares of the coefficients of the equation: $M_{DM} = k_0 + k_1 (\log v_\infty - 6.477) + k_2 (\log m_\infty + 0.523) + k_3 (\log \cos Z_R + 0.2)$ for Super-Schmidt meteors minus (A + S + D) and non-flaring small-camera meteors

$k_0 = 0.10 \pm 0.02$
 $k_1 = -8.93 \pm 0.12$
 $k_2 = -2.25 \pm 0.03$
 $k_3 = -1.69 \pm 0.13$
 No. obs. = 494

TABLE 11.6.—Comparison between the values of k_1 , k_2 , k_3 of the general solution (see tables 11.1 and 11.4) and the values of k_1 and k_2 when k_3 is assumed a priori equal to -2.5

SUPER-SCHMIDT METEORS		
ALL METEORS		
	General Solution	Solution with $k_3 = -2.5$
k_1	-8.44 ± 0.16	-8.63 ± 0.17
k_2	-2.19 ± 0.05	-2.21 ± 0.05
k_3	-1.45 ± 0.13	-2.5
No. obs.	411	411

SPORADIC METEORS		
	General Solution	Solution with $k_3 = -2.5$
k_1	-8.57 ± 0.21	-8.83 ± 0.21
k_2	-2.24 ± 0.06	-2.29 ± 0.07
k_3	-1.56 ± 0.17	-2.5
No. obs.	289	289

SMALL-CAMERA METEORS		
ALL METEORS		
	General Solution	Solution with $k_3 = -2.5$
k_1	-10.00 ± 0.37	-10.06 ± 0.36
k_2	-2.46 ± 0.07	-2.47 ± 0.07
k_3	-1.90 ± 0.43	-2.5
No. obs.	207	207

SPORADIC METEORS		
	General Solution	Solution with $k_3 = -2.5$
k_1	-9.37 ± 0.55	-9.50 ± 0.52
k_2	-2.27 ± 0.12	-2.30 ± 0.11
k_3	-2.03 ± 0.63	-2.5
No. obs.	85	85

TABLE 12.—The mass (in g) of a zero visual magnitude meteoroid as a function of velocity v_∞ and zenith angle Z_R

$Z_R \backslash v_\infty$ (km/s)	10	20	30	40	50	60	70
0°	120	8.13	1.66	0.55	0.23	0.11	0.072
30°	132	8.91	1.82	0.63	0.25	0.12	0.068
45°	151	10.2	2.09	0.69	0.29	0.14	0.079
60°	191	12.9	2.63	0.87	0.36	0.18	0.098
75°	269	18.2	3.72	1.23	0.51	0.25	0.14
85°	617	41.7	8.51	2.82	1.17	0.58	0.32

TABLE 13.1.—Photographic magnitude as a function of the velocity for Super-Schmidt meteors ($M_{pm}^{(v)}$ is the maximum photographic magnitude reduced to $v_{\infty}=0.3$ g and $\cos Z_R=10^{-0.2}=0.631$.)

ALL METEORS				SPORADIC METEORS			
Velocity range (km/s)	Mean Z_R	$M_{pm}^{(v)} \pm$ s.d.	No. obs.	Mean v (km/s)	$M_{pm}^{(v)} \pm$ s.d.	$M_{pm}^{(v)}$	No. obs.
10 - 15	13.5	1.2 ± 0.2	9	13.5	1.2 ± 0.2	2.62 ± 0.23	9
15 - 20	17.7	0.7 ± 0.1	2.00 ± 0.09	17.7	0.7 ± 0.1	2.02 ± 0.08	56
20 - 25	22.4	0.6 ± 0.1	1.16 ± 0.07	22.2	0.5 ± 0.1	1.17 ± 0.08	53
25 - 30	27.4	0.4 ± 0.1	0.51 ± 0.07	27.4	0.3 ± 0.2	0.43 ± 0.09	43
30 - 35	31.9	0.0 ± 0.2	0.02 ± 0.06	32.1	0.0 ± 0.2	-0.04 ± 0.06	30
35 - 40	36.7	-0.5 ± 0.2	-0.78 ± 0.06	37.2	-0.2 ± 0.3	-0.88 ± 0.11	15
40 - 45	42.8	0.0 ± 0.2	-1.37 ± 0.07	42.9	0.1 ± 0.3	-1.25 ± 0.12	13
45 - 50	47.3	-0.9 ± 0.3	-1.67 ± 0.08	47.3	-0.9 ± 0.4	-1.66 ± 0.09	12
50 - 55	53.0	-0.7 ± 0.3	-2.11 ± 0.11	53.3	-0.7 ± 0.4	-2.18 ± 0.09	8
55 - 60	58.2	-0.6 ± 0.2	-2.35 ± 0.08	57.9	-0.6 ± 0.3	-2.35 ± 0.10	13
60 - 65	61.8	-0.8 ± 0.2	-2.55 ± 0.05	62.4	-0.5 ± 0.2	-2.62 ± 0.06	17
65 - 70	67.7	-0.9 ± 0.3	-2.92 ± 0.06	67.8	-0.8 ± 0.4	-2.92 ± 0.08	14
70 - 75	71.4	-1.5 ± 1.5	-3.21 ± 0.13	71.5	-1.5 ± 0.5	-3.27 ± 0.17	6
ALL	35.3	0.0 ± 0.1	-0.17 ± 0.08	33.7	0.1 ± 0.1	0.05 ± 0.11	289

TABLE 13.2.—Photographic magnitude as a function of the zenith angle Z_R for Super-Schmidt meteors ($M_{pm}^{(m)}$ is the maximum photographic magnitude reduced to $v_{\infty}=40$ km/s and $\cos Z_R=10^{-0.2}=0.631$.)

ALL METEORS				SPORADIC METEORS				
Range of Z_R	$\cos Z_R$	$M_{pm}^{(m)} \pm$ s.d.	No. obs.	Mean v_{∞} (km/s)	$M_{pm}^{(m)} \pm$ s.d.	$M_{pm}^{(m)}$	No. obs.	
0 - 0.3	0.923	0.2 ± 0.2	-0.30 ± 0.10	21	0.22	0.2 ± 0.2	-0.19 ± 0.10	15
0.3 - 0.4	0.835	0.4 ± 0.2	-0.59 ± 0.09	29	0.36	0.5 ± 0.2	-0.63 ± 0.11	23
0.4 - 0.5	0.741	-0.4 ± 0.2	-0.84 ± 0.06	39	0.46	-0.3 ± 0.2	-0.86 ± 0.07	33
0.5 - 0.6	0.555	0.2 ± 0.2	-0.88 ± 0.10	36	0.54	0.1 ± 0.3	-0.98 ± 0.14	21
0.6 - 0.7	0.455	0.0 ± 0.1	-1.05 ± 0.05	89	0.65	-0.1 ± 0.1	-1.09 ± 0.06	61
0.7 - 0.8	0.375	0.3 ± 0.1	-1.07 ± 0.04	74	0.75	0.4 ± 0.2	-1.05 ± 0.05	50
0.8 - 0.9	0.284	0.2 ± 0.1	-1.14 ± 0.06	77	0.84	0.4 ± 0.1	-1.16 ± 0.07	40
0.9 - 1.0	0.177	-0.7 ± 0.2	-1.31 ± 0.04	46	0.96	-0.4 ± 0.3	-1.36 ± 0.05	26
ALL	0.677	0.0 ± 0.1	-0.99 ± 0.02	411	0.66	0.1 ± 0.1	-1.00 ± 0.03	289

TABLE 13.3.—Photographic magnitude as a function of the observed magnitude reduced to $m_{\infty}=10$ g and $\cos Z_R=10^{-0.2}=0.631$.)

ALL METEORS				SPORADIC METEORS				
Mean range (g)	Mean $m_{pm} \pm$ s.d.	$M_{pm}^{(m)} \pm$ s.d.	No. obs.	Mean v_{∞} (km/s)	$M_{pm}^{(m)} \pm$ s.d.	$M_{pm}^{(m)}$	No. obs.	
0.01 - 0.05	0.031	0.0 ± 0.1	1.26 ± 0.06	66	0.630	0.0 ± 0.1	1.34 ± 0.06	47
0.05 - 0.10	0.072	0.1 ± 0.2	0.39 ± 0.05	53	0.075	-0.0 ± 0.2	0.35 ± 0.05	28
0.10 - 0.20	0.146	0.4 ± 0.1	-0.23 ± 0.05	74	0.147	0.6 ± 0.2	-0.20 ± 0.07	47
0.20 - 0.40	0.290	0.1 ± 0.2	-0.37 ± 0.05	71	0.297	0.3 ± 0.2	-1.02 ± 0.07	47
0.40 - 0.80	0.596	0.1 ± 0.1	-1.72 ± 0.07	61	0.602	0.2 ± 0.2	-1.80 ± 0.08	50
0.8 - 1.6	1.11	0.1 ± 0.2	-2.28 ± 0.10	43	1.10	0.2 ± 0.2	-2.29 ± 0.11	37
1.6 - 5.0	2.51	-0.7 ± 0.2	-2.94 ± 0.11	30	2.51	-0.2 ± 0.2	-3.04 ± 0.14	20
5.0 - 35	10.2	-1.5 ± 0.4	-3.94 ± 0.16	13	10.2	-1.5 ± 0.4	-3.94 ± 0.16	13
ALL	0.80	0.0 ± 0.1	-0.79 ± 0.07	411	0.95	0.1 ± 0.1	-0.94 ± 0.09	289

TABLE 13.4.—The absolute photographic magnitude as a function of velocity for small-camera meteors ($M_{pm}^{(v)}$ is the observed magnitude reduced to $m_{\infty}=10$ g and $\cos Z_R=10^{-0.2}=0.631$.)

ALL METEORS				SPORADIC METEORS			
Velocity range (km/s)	Mean Z_R	$M_{pm}^{(v)} \pm$ s.d.	No. obs.	Mean v_{∞} (km/s)	$M_{pm}^{(v)} \pm$ s.d.	$M_{pm}^{(v)}$	No. obs.
10 - 15	14.2	0.4 ± 0.4	-3.3 ± 0.3	14.2 ± 0.4	-0.10 ± 0.23	7	7
15 - 20	18.2	0.6 ± 0.6	-2.1 ± 0.1	18.2 ± 0.6	-1.24 ± 0.41	9	9
20 - 25	22.0	0.3 ± 0.3	-4.2 ± 0.5	22.0 ± 0.3	-2.77 ± 0.27	21	21
25 - 30	27.5	0.3 ± 0.3	-4.7 ± 0.5	27.5 ± 0.3	-3.63 ± 0.17	24	24
30 - 35	31.7	0.2 ± 0.2	-4.1 ± 0.5	31.7 ± 0.2	-3.46 ± 0.17	24	24
35 - 40	36.7	0.2 ± 0.2	-3.7 ± 0.2	36.7 ± 0.2	-4.34 ± 0.09	51	51
40 - 45	42.7	0.5 ± 0.5	-3.7 ± 0.5	42.7 ± 0.5	-5.21 ± 0.21	10	10
45 - 50	47.8	0.7 ± 0.7	-4.4 ± 1.0	47.8 ± 0.7	-5.28 ± 0.22	4	4
50 - 55	51.3	0.5 ± 0.5	-3.9 ± 0.7	51.3 ± 0.5	-5.86 ± 0.29	4	4
55 - 60	58.2	0.4 ± 0.4	-5.7 ± 1.0	58.2 ± 0.4	-6.51 ± 0.25	7	7
60 - 65	61.8	0.3 ± 0.3	-4.8 ± 0.4	61.8 ± 0.3	-6.97 ± 0.15	25	25
65 - 70	67.1	0.3 ± 0.3	-4.6 ± 0.4	67.1 ± 0.3	-7.33 ± 0.13	15	15
70 - 75	72.4	0.4 ± 0.4	-5.2 ± 0.5	72.4 ± 0.4	-7.39 ± 0.31	7	7
ALL	40.0 ± 1.1	-4.2 ± 0.1	-4.2 ± 0.1	40.0 ± 1.1	-4.59 ± 0.14	207	207

TABLE 13.5.—*The absolute photographic magnitude as a function of mass for small-camera meteors ($M_{pm}^{(m)}$) is the observed magnitude reduced to $v_{\infty}=40$ km/s and $\cos Z_R=10^{-0.3}=0.631$.*

Mass range (g)	Mean $m_n \pm$ s.d. (g)	Mean $M_{pm} \pm$ s.d.	Mean $M_{pm}^{(m)} \pm$ s.d.	No. obs.
0.04 - 1.6	0.78 \pm 0.05	-3.1 \pm 0.2	-2.02 \pm 0.14	65
1.6 - 5.0	3.03 \pm 0.15	-3.5 \pm 0.2	-3.53 \pm 0.12	46
5.0 - 15	9.1 \pm 0.5	-4.3 \pm 0.3	-4.72 \pm 0.13	36
15 - 50	29.0 \pm 2.1	-4.8 \pm 0.3	-5.89 \pm 0.15	23
50 - 150	102 \pm 6	-6.0 \pm 0.5	-7.48 \pm 0.27	20
150 - 3600	811 \pm 232	-6.7 \pm 0.6	-8.48 \pm 0.45	17
All	82 \pm 24	-4.2 \pm 0.1	-4.31 \pm 0.17	207

TABLE 13.6.—*The absolute photographic magnitude as a function of the zenith angle Z_R for small-camera meteors ($M_{pm}^{(Z_R)}$) is the observed magnitude reduced to $m_{\infty}=10$ g and $v_{\infty}=40$ km/s.*

Range of $\cos Z_R$	Mean $\cos Z_R$	Mean $M_{pm} \pm$ s.d.	Mean $M_{pm}^{(Z_R)} \pm$ s.d.	No. obs.
0.0 - 0.3	0.26 \pm 0.02	-6.1 \pm 1.1	-3.87 \pm 0.28	4
0.3 - 0.4	0.33 \pm 0.01	-3.2 \pm 0.4	-4.17 \pm 0.15	8
0.4 - 0.5	0.47 \pm 0.01	-4.5 \pm 0.9	-5.03 \pm 0.52	7
0.5 - 0.6	0.56 \pm 0.01	-4.8 \pm 0.5	-4.86 \pm 0.13	20
0.6 - 0.7	0.66 \pm 0.01	-4.1 \pm 0.5	-4.94 \pm 0.18	20
0.7 - 0.8	0.75 \pm 0.01	-4.2 \pm 0.3	-5.16 \pm 0.12	36
0.8 - 0.9	0.85 \pm 0.01	-4.3 \pm 0.3	-5.19 \pm 0.11	56
0.9 - 1.0	0.95 \pm 0.00	-3.7 \pm 0.2	-5.19 \pm 0.10	56
All	0.76 \pm 0.01	-4.2 \pm 0.1	-5.05 \pm 0.06	207

TABLE 14.1.—*The difference ΔM_{pm} between observed and theoretical absolute magnitudes for Super-Schmidt meteors*

	Mean $\Delta M_{pm} \pm$ s.d.	No. obs.			
All meteors	-0.61 \pm 0.03	395			
Sporadic meteors	-0.66 \pm 0.03	278			
Shower meteors	-0.50 \pm 0.05	117			
Sporadic meteors minus (A + S + D)	-0.58 \pm 0.03	236			
Sporadic meteors with $Q < 0$ a.u.	-0.70 \pm 0.05	159			
Sporadic meteors with $Q > 0$ a.u.	-0.53 \pm 0.03	119			
Sporadic meteors minus (A + S + D) with $\chi \leq 0.2$	-0.47 \pm 0.04	123			
Sporadic meteors minus (A + S + D) with $\chi > 0.2$	-0.71 \pm 0.04	712			
Sporadic meteors minus (A + S + D) with $\log \sigma < -11.4$	-0.37 \pm 0.06	36			
Sporadic meteors minus (A + S + D) with $-11.4 \leq \log \sigma \leq -11.0$	-0.56 \pm 0.03	154			
Sporadic meteors minus (A + S + D) with $\log \sigma > -11.0$	-0.83 \pm 0.07	46			
<u>Individual Showers</u>					
	Mean $\Delta M_{pm} \pm$ s.d.	No. obs.		Mean $\Delta M_{pm} \pm$ s.d.	No. obs.
Quadrantids	-0.59 \pm 0.05	9	κ Cygnids	-0.77 \pm 0.13	4
Virginids	-0.38 \pm 0.28	2	Draconids	-2.17 \pm 0.43	2
Lyrids	-0.19 \pm 0.15	3	Orionids	-0.42 \pm 0.11	6
τ Aquarids	-0.55	1	Southern Taurids	-0.15 \pm 0.05	18
λ Aquarids	-0.91 \pm 0.08	10	Northern Taurids	-0.09 \pm 0.03	5
α Capricornids	-0.45 \pm 0.09	14	Leonids	0.30	1
Southern δ Aquarids	-0.95 \pm 0.28	6	ϵ Hydrids	-0.03 \pm 0.13	3
Northern δ Aquarids	-0.43 \pm 0.14	2	Geminids	-0.33 \pm 0.08	20
Perseids	-0.30 \pm 0.18	9			

TABLE 14.2.—The difference ΔM_{pm} between observed and theoretical absolute magnitudes for small-camera meteors

	Mean $\Delta M_{pm} \pm$ s.d.	No. obs.
All meteors	-0.63 \pm 0.08	90
Sporadic meteors	-0.64 \pm 0.10	42
Shower meteors	-0.63 \pm 0.13	48
Flaring meteors	-1.03 \pm 0.11	41
Nonflaring meteors	-0.30 \pm 0.09	49
Lyrids	-0.04 \pm 0.26	3
Perseids	-0.83 \pm 0.25	6
Southern Taurids	-0.92 \pm 0.31	13
Northern Taurids	-0.65 \pm 0.06	2
χ Orionids	-0.99 \pm 0.28	3
Geminids	-0.30 \pm 0.23	15

TABLE 14.3.—The difference ΔM_{pm} between observed and theoretical absolute magnitudes as a function of χ for sporadic Super-Schmidt meteors

Range of χ	Mean $\chi \pm$ s.d.	Mean $M_{pm} \pm$ s.d.	Mean $\Delta M_{pm} \pm$ s.d.	No. obs.
$\chi < 0$	-0.10 \pm 0.02	-0.1 \pm 0.2	-0.50 \pm 0.06	48
$0 < \chi < 0.1$	0.04 \pm 0.00	0.1 \pm 0.2	-0.46 \pm 0.07	43
$0.1 \leq \chi < 0.2$	0.14 \pm 0.00	0.1 \pm 0.1	-0.62 \pm 0.08	49
$0.2 \leq \chi < 0.3$	0.24 \pm 0.00	-0.1 \pm 0.3	-0.68 \pm 0.08	35
$0.3 \leq \chi < 0.4$	0.34 \pm 0.00	0.4 \pm 0.2	-0.74 \pm 0.07	36
$0.4 \leq \chi < 0.6$	0.48 \pm 0.01	0.2 \pm 0.2	-0.76 \pm 0.07	33
$\chi \geq 0.6$	0.88 \pm 0.07	0.4 \pm 0.4	-0.97 \pm 0.00	37
All	0.27 \pm 0.02	0.1 \pm 0.1	-0.66 \pm 0.03	281

TABLE 15.1.—The color index C.I. as a function of velocity for Super-Schmidt meteors

Velocity range (km/s)	Mean v_{∞} (km/s)	Mean C.I. \pm s.d.	No. obs.
10 - 20	17.2	-1.29 \pm 0.10	62
20 - 30	24.8	-1.39 \pm 0.07	125
30 - 40	34.1	-1.49 \pm 0.07	79
40 - 60	48.4	-1.34 \pm 0.09	71
60 - 73	65.5	-1.30 \pm 0.11	53
All	35.3	-1.37 \pm 0.04	390

The distribution of the color index C.I. for five velocity groups.

Color index	$10 < v_{\infty} \leq 20$	$20 < v_{\infty} \leq 30$	$30 < v_{\infty} \leq 40$	$40 < v_{\infty} \leq 60$	$v_{\infty} > 60$
-4.0 to -3.3	1	2	0	0	2
-3.3 to -3.0	1	3	0	1	0
-3.0 to -2.7	1	3	2	1	1
-2.7 to -2.4	1	4	5	3	1
-2.4 to -2.1	4	11	5	4	1
-2.1 to -1.8	6	10	7	11	6
-1.8 to -1.5	8	11	16	6	7
-1.5 to -1.2	10	16	20	12	6
-1.2 to -0.9	10	21	9	10	13
-0.9 to -0.6	5	23	7	8	5
-0.6 to -0.3	7	15	4	7	7
-0.3 to 0.0	3	5	3	6	2
0.0 to 0.3	5	1	0	1	2
0.3 to 0.6	0	0	1	1	0
All	62	125	79	71	53

TABLE 15.2.—The color index C.I. as a function of the maximum photographic magnitude M_{pm} for Super-Schmidt meteors

Magnitude range (absolute photographic)	Mean M_{pm}	Mean C.I. \pm s.d.	No. obs.
-6.0 to -1.3	-2.18	-1.93 \pm 0.11	48
-1.3 to -0.6	-0.96	-1.77 \pm 0.09	58
-0.6 to -0.1	-0.39	-1.49 \pm 0.10	60
-0.1 to 0.4	0.11	-1.33 \pm 0.09	57
0.4 to 0.9	0.63	-1.16 \pm 0.08	66
0.9 to 1.4	1.18	-0.97 \pm 0.08	63
1.4 to 2.5	1.83	-1.00 \pm 0.10	38
All	0.02	-1.37 \pm 0.04	390

The distribution of the color index C.I. for seven magnitude groups.

Color index	M_{pm}						
	-6.0 to -1.3	-1.3 to -0.6	-0.6 to -0.1	-0.1 to 0.4	0.4 to 0.9	0.9 to 1.4	1.4 to 2.5
-4.0 to -3.3	3	1	0	1	0	0	0
-3.3 to -3.0	1	1	2	1	0	0	0
-3.0 to -2.7	4	1	1	1	1	0	0
-2.7 to -2.4	2	5	5	0	1	0	1
-2.4 to -2.1	2	11	3	2	4	2	1
-2.1 to -1.8	11	8	5	9	5	2	0
-1.8 to -1.5	11	9	12	2	3	7	4
-1.5 to -1.2	5	10	10	9	15	9	6
-1.2 to -0.9	6	5	7	14	12	11	8
-0.9 to -0.6	2	4	3	11	9	12	7
-0.6 to -0.3	0	2	8	6	7	11	6
-0.3 to 0.0	1	0	3	0	7	4	4
0.0 to 0.3	0	1	0	1	2	4	1
0.3 to 0.6	0	0	1	0	0	1	0
All	48	58	60	57	66	63	38

TABLE 16.1.—*The distribution of the ablation coefficient σ for Super-Schmidt meteors*

Range of log σ	Sporadic meteors			Shower meteors	All meteors
	All	Q \leq 6 a.u.	Q > 6 a.u.		
-12.10 — -12.01	1	1	0	0	1
-12.00 — -11.91	1	0	1	0	1
-11.90 — -11.81	2	0	2	2	4
-11.80 — -11.71	0	0	0	4	4
-11.70 — -11.61	6	2	4	1	7
-11.60 — -11.51	8	2	6	6	14
-11.50 — -11.41	18	6	12	12	30
-11.40 — -11.31	30	11	19	25	55
-11.30 — -11.21	50	26	24	16	66
-11.20 — -11.11	43	27	16	16	59
-11.10 — -11.01	39	28	11	12	51
-11.00 — -10.91	21	15	6	3	24
-10.90 — -10.81	15	12	3	5	20
-10.80 — -10.71	4	3	1	3	7
-10.70 — -10.61	3	2	1	0	3
-10.60 — -10.51	1	1	0	0	1
-10.50 — -10.41	0	0	0	1	1
All	242	136	106	106	348

TABLE 16.2.—*The distribution of the ablation coefficient for small-camera meteors*

Range of log σ	Sporadic meteors			Shower meteors	All meteors
	All	Q \leq 6 a.u.	Q > 6 a.u.		
-12.30 to -12.21	0			1	1
-12.20 to -12.11	0			1	1
-12.10 to -12.01	2			2	4
-12.00 to -11.91	2			3	5
-11.90 to -11.81	0			6	6
-11.80 to -11.71	4			9	13
-11.70 to -11.61	1			5	6
-11.60 to -11.51	7			7	14
-11.50 to -11.41	2			3	5
-11.40 to -11.31	4			3	7
-11.30 to -11.21	4			3	7
-11.20 to -11.11	6			2	8
-11.10 to -11.01	4			2	6
-11.00 to -10.91	4			0	4
-10.90 to -10.81	1			0	1
All	41			47	88

TABLE 17.1.1.—*The ablation coefficient σ as a function of the velocity v_∞ for sporadic Super-Schmidt meteors having, respectively, Q \leq 6 a.u. and Q > 6 a.u. (classes A and S excluded)*

Range of v_∞ (km/s)	Q \leq 6 a.u.				Q > 6 a.u.			
	Mean v_∞ (km/s)	Mean log $\sigma \pm$ s.d. (cm^{-2}s^2)	No. obs.		Mean v_∞ (km/s)	Mean log $\sigma \pm$ s.d. (cm^{-2}s^2)	No. obs.	
10 - 20	17.2	-11.05 \pm 0.03	48		18.1	-11.04 \pm 0.08	6	
20 - 25	22.3	-11.12 \pm 0.03	37		22.3	-11.14 \pm 0.06	8	
25 - 30	27.3	-11.17 \pm 0.03	26		27.2	-11.21 \pm 0.07	10	
30 - 35	32.2	-11.22 \pm 0.04	17		31.7	-11.20 \pm 0.05	11	
35 - 40	36.5	-11.33 \pm 0.14	6		37.7	-11.20 \pm 0.08	6	
40 - 50	42.0	-11.46 \pm 0.20	2		45.6	-11.32 \pm 0.06	19	
50 - 60					55.8	-11.32 \pm 0.04	16	
60 - 73					65.6	-11.35 \pm 0.04	30	
All	23.6 \pm 0.6	-11.14 \pm 0.02	136		45.8 \pm 1.6	-11.27 \pm 0.02	106	

TABLE 17.1.2.—The ablation coefficient σ as a function of the velocity for Super-Schmidt meteors (classes A and S excluded)

Velocity range (km/s)	All Meteors					Sporadic Meteors						
	Mean v_{∞} (km/s)	Mean $\log \sigma$ ($\text{cm}^{-2} \text{s}^2$)	S.d. of mean	S.d. of 1 obs.	No. Obs.	Mean $\log \sigma \pm$ s.d. ($m_{\infty} = 0.8 \text{ g}$)	Mean v (km/s)	Mean $\log \sigma$ ($\text{cm}^{-2} \text{s}^2$)	S.d. of mean	S.d. of 1 obs.	Mean $\log \sigma \pm$ s.d. ($m_{\infty} = 0.8 \text{ g}$)	No. Obs.
11 - 20	17.3	-11.05	± 0.03	± 0.19	54	-11.00 ± 0.02	17.3	-11.05	± 0.03	± 0.19	-11.00 ± 0.02	54
20 - 25	22.6	-11.12	0.03	0.20	55	-11.11 ± 0.03	22.3	-11.12	0.03	0.19	-11.11 ± 0.03	45
25 - 30	27.3	-11.19	0.03	0.20	56	-11.18 ± 0.03	27.3	-11.18	0.03	0.19	-11.17 ± 0.03	36
30 - 35	31.7	-11.27	0.03	0.18	44	-11.26 ± 0.03	32.0	-11.21	0.03	0.17	-11.20 ± 0.03	28
35 - 40	36.6	-11.26	0.05	0.28	34	-11.25 ± 0.05	37.1	-11.29	0.08	0.28	-11.28 ± 0.08	12
40 - 50	44.2	-11.35	0.04	0.25	40	-11.35 ± 0.04	45.2	-11.33	0.05	0.25	-11.33 ± 0.05	21
50 - 60	56.2	-11.33	0.03	0.16	21	-11.33 ± 0.03	55.8	-11.32	0.04	0.16	-11.32 ± 0.04	16
60 - 73	65.1	-11.30	0.04	0.24	44	-11.30 ± 0.04	65.6	-11.35	0.04	0.24	-11.35 ± 0.04	30
All	35.0	-11.22	0.01	0.24	348	-11.20 ± 0.01	33.4	-11.19	0.02	0.23	-11.18 ± 0.02	242

TABLE 17.2.—The ablation coefficient σ as a function of the integrated brightness ϵ_{∞} for Super-Schmidt meteors (classes A and S excluded)

Range of ϵ_{∞}	All Meteors						Sporadic Meteors									
	Mean ϵ_{∞}	Mean $\log \sigma$ ($\text{cm}^{-2} \text{s}^2$)	S.d. of mean	S.d. of 1 obs.	No. obs.	No.	Mean $\log \sigma$ ($\text{cm}^{-2} \text{s}^2$)	S.d. of mean	S.d. of 1 obs.	No.	Mean $\log \sigma$ ($\text{cm}^{-2} \text{s}^2$)	S.d.	No.	Mean $\log \sigma$ ($\text{cm}^{-2} \text{s}^2$)	S.d.	No.
-1.40 to -1.00	-1.14	-11.14	± 0.05	± 0.25	23	-1.14	-11.05	± 0.05	± 0.19	16	-11.03	± 0.05	14	-11.15	± 0.22	2
-0.99 to -0.75	-0.85	-11.17	0.03	0.25	65	-0.85	-11.17	0.04	0.26	48	-11.14	0.04	36	-11.24	0.08	12
-0.74 to -0.50	-0.63	-11.21	0.03	0.25	81	-0.64	-11.18	0.03	0.21	57	-11.12	0.03	37	-11.30	0.05	20
-0.49 to -0.25	-0.39	-11.20	0.03	0.22	66	-0.38	-11.18	0.03	0.23	46	-11.10	0.05	19	-11.23	0.04	27
-0.24 to 0.00	-0.14	-11.29	0.02	0.17	53	-0.14	-11.30	0.03	0.18	33	-11.30	0.06	11	-11.31	0.04	22
0.01 to 0.50	0.19	-11.19	0.03	0.20	39	0.18	-11.18	0.04	0.19	29	-11.14	0.05	15	-11.21	0.05	14
0.51 to 1.00	0.67	-11.33	0.06	0.26	18	0.65	-11.31	0.07	0.24	12	-11.32	0.08	4	-11.31	0.10	8
1.01 to 2.00	1.35	-11.67	0.10	0.18	3	1.91	-11.88	—	—	1	—	—	—	-11.88	—	1
All	-0.41	-11.216	0.013	0.235	348	-0.42	-11.194	0.015	0.229	242	-11.135	0.018	136	-11.267	0.024	106

TABLE 17.3.—The ablation coefficient σ as a function of the initial mass m_{∞} for Super-Schmidt meteors (classes A and S excluded)

Range of mass (g)	All Meteors					Sporadic Meteors						
	Mean m_{∞} (g)	Mean $\log \sigma$ ($\text{cm}^{-2} \text{s}^2$)	S.d. of mean	S.d. of 1 obs.	No. obs.	Mean m_{∞} (g)	Mean $\log \sigma$ ($\text{cm}^{-2} \text{s}^2$)	S.d. of mean	S.d. of 1 obs.	No. obs.	Mean $\log \sigma \pm$ s.d. ($v_{\infty} = 30 \text{ km/s}$)	No. obs.
0.01 - 0.05	0.033 \pm 0.002	-11.31	± 0.03	± 0.24	52	0.032 \pm 0.002	-11.30	± 0.04	± 0.24	38	-11.18 \pm 0.04	38
0.05 - 0.1	0.072 \pm 0.002	-11.32	0.04	0.25	47	0.075 \pm 0.003	-11.35	0.05	0.25	24	-11.26 \pm 0.05	24
0.1 - 0.2	0.145 \pm 0.003	-11.23	0.02	0.17	62	0.145 \pm 0.004	-11.21	0.02	0.15	40	-11.20 \pm 0.02	40
0.2 - 0.4	0.294 \pm 0.008	-11.15	0.02	0.18	62	0.306 \pm 0.009	-11.16	0.02	0.14	38	-11.20 \pm 0.02	38
0.4 - 0.8	0.594 \pm 0.016	-11.14	0.04	0.27	53	0.601 \pm 0.017	-11.09	0.04	0.26	42	-11.16 \pm 0.04	42
0.8 - 1.6	1.122 \pm 0.039	-11.15	0.04	0.21	34	1.116 \pm 0.042	-11.12	0.04	0.19	30	-11.22 \pm 0.03	30
1.6 - 5.0	2.59 \pm 0.20	-11.21	0.05	0.24	25	2.56 \pm 0.25	-11.10	0.04	0.16	17	-11.22 \pm 0.03	17
5.0 - 34	10.15 \pm 2.27	-11.26	0.09	0.32	13	10.15 \pm 2.27	-11.26	0.09	0.32	13	-11.37 \pm 0.08	13
All	0.86 \pm 0.13	-11.22	0.01	0.24	348	1.05 \pm 0.19	-11.19	0.01	0.23	242	-11.21 \pm 0.01	242

TABLE 17.4.—The ablation coefficient σ as a function of velocity for small-camera meteors

Range of v_m (km/s)	Mean $v_m \pm$ s.d. (km/s)	Mean $\log \sigma$ (cm^{-2}s^2)	S.d. of mean	S.d. of 1 obs.	Mean $\log \sigma$ (0.8 g)	Mean $\log \sigma$ ($m = 110$ g)	No. obs.
10 - 20	16.2 \pm 0.9	-11.24	\pm 0.07	\pm 0.21	-10.89	-11.34	9
20 - 30	25.9 \pm 0.6	-11.42	0.06	0.29	-11.09	-11.54	27
30 - 40	34.4 \pm 0.5	-11.59	0.06	0.34	-11.36	-11.81	36
40 - 50	45.5 \pm 2.1	-11.53	0.09	0.17	-11.32	-11.77	4
50 - 60	55.5 \pm 1.9	-11.80	0.13	0.29	-11.54	-11.99	5
60 - 70	61.6 \pm 0.9	-11.70	0.06	0.15	-11.59	-12.04	7
All	33.8 \pm 1.3	-11.52	0.03	0.32	-11.26	-11.71	88

TABLE 17.5.—The ablation coefficient σ as a function of the initial mass for small-camera meteors

Range of m_0 (g)	Mean $m_0 \pm$ s.d. (g)	Mean $\log \sigma$ (cm^{-2}s^2)	S.d. of mean	S.d. of 1 obs.	Mean $\log \sigma$ ($v_m = 30$ km/s)	No. obs.
0.1 - 1.6	0.77 \pm 0.13	-11.37	\pm 0.11	\pm 0.34	-11.22	10
1.6 - 5.0	3.23 \pm 0.30	-11.40	0.07	0.28	-11.32	15
5 - 15	9.63 \pm 0.72	-11.46	0.06	0.30	-11.41	22
15 - 50	28.6 \pm 2.6	-11.63	0.07	0.27	-11.63	14
50 - 150	107 \pm 6	-11.68	0.08	0.32	-11.69	16
150 - 2000	664 \pm 18	-11.57	0.12	0.39	-11.67	11
All	110 \pm 31	-11.52	0.03	0.32	-11.49	88

TABLE 17.6.—The ablation coefficient σ for shower meteors; Super-Schmidt (classes A and S excluded) and small-camera meteors

Shower	Super-Schmidt Meteors*						Small-Camera Meteors							
	Mean $\log \sigma$	S.d. of mean	S.d. of 1 obs.	Mean $v_m \pm$ s.d. (km/s)	Mean $m_0 \pm$ s.d. (g)	Mean $\log \sigma$ ($v_m = 30$ km/s) ($m_0 = 0.8$ g)	No. obs.	Mean $\log \sigma$ ($v_m = 30$ km/s) ($m_0 = 0.8$ g)	S.d. of mean	S.d. of 1 obs.	Mean $v_m \pm$ s.d. (km/s)	Mean $m_0 \pm$ s.d. (g)	Mean $\log \sigma$ ($v_m = 30$ km/s) ($m_0 = 11.0$ g)	No. obs.
Quadrantids	-11.48	\pm 0.09	\pm 0.28	43.0 \pm 0.2	0.09 \pm 0.2	-11.35	9	—	—	—	—	—	—	—
Virginids	-11.24	—	—	27.1	1.07	—	1	-11.25	\pm 0.15	\pm 0.21	30.9 \pm 0.1	7 \pm 3	—	2
Lyrids	-11.17	0.17	0.30	48.8 \pm 1.1	0.13 \pm 0.04	-11.0	3	-11.52	0.10	0.17	49.4 \pm 0.7	10 \pm 8	-11.2	3
β Aquarids	-11.01	—	—	66.8	0.04	—	1	—	—	—	—	—	—	—
δ Aquarids	-11.35	0.04	0.10	42.1 \pm 0.3	0.10 \pm 0.04	-11.23	8	—	—	—	—	—	—	—
α Capricornids	-11.09	0.08	0.28	25.6 \pm 0.4	0.53 \pm 0.24	-11.12	14	—	—	—	—	—	—	—
Southern δ Aquarids	-11.35	0.11	0.24	34.2 \pm 1.2	0.10 \pm 0.02	-11.33	5	—	—	—	—	—	—	—
Northern δ Aquarids	-11.48	0.25	0.35	35.9 \pm 1.7	0.11 \pm 0.04	—	2	—	—	—	—	—	—	—
Perseids	-11.26	0.06	0.19	60.3 \pm 0.2	0.30 \pm 0.14	-11.10	9	-11.77	0.10	0.25	60.5 \pm 0.4	29 \pm 20	-11.22	6
α Cygnids	-11.07	0.08	0.16	23.2 \pm 0.4	0.39 \pm 0.06	-11.14	4	—	—	—	—	—	—	—
Draconids	-14.88	0.79	1.12	20.2 \pm 0.1	2.00 \pm 0.13	—	2	—	—	—	—	—	—	—
Orionids	-11.12	0.05	0.10	68.4 \pm 0.8	0.04 \pm 0.01	-10.96	4	—	—	—	—	—	—	—
Southern Taurids	-11.31	0.03	0.11	29.0 \pm 0.4	0.48 \pm 0.13	-11.31	18	-11.70	0.04	0.16	30.3 \pm 0.6	149 \pm 102	-11.38	13
Northern Taurids	-11.41	0.04	0.08	30.9 \pm 0.3	0.85 \pm 0.35	-11.38	5	-11.49	0.23	0.32	28.7 \pm 1.5	99 \pm 65	—	—
Leonids	-10.99	—	—	71.7	0.29	—	1	—	—	—	—	—	—	—
Orionids	—	—	—	—	—	—	—	-11.44	0.20	0.34	30.9 \pm 0.7	156 \pm 117	-11.1	3
Hydrids	-11.46	0.06	0.10	59.2 \pm 0.6	0.05 \pm 0.01	-11.31	3	-11.62	0.03	0.04	55.3 \pm 4.3	46 \pm 38	-11.0	2
eminids	-11.23	0.07	0.29	36.3 \pm 0.1	0.79 \pm 0.29	-11.14	19	-11.69	0.09	0.33	36.4 \pm 0.1	95 \pm 60	-11.34	15
Jrsids	—	—	—	—	—	—	—	-11.19	—	—	35.2	7	—	1

TABLE 17.7.—*The ablation coefficient σ as a function of the initial mass m_0 ; the observed values have been reduced to a velocity of 30 km/s; Super-Schmidt (classes A and S excluded) and small-camera meteors*

Mass range (g)	Mean mass \pm s.d. (g)	Mean $\log \sigma \pm$ s.d. ($\text{cm}^{-2} \text{s}^2$)	No. obs.
0.01 - 0.05	0.03 \pm 0.00	-11.23 \pm 0.03	52
0.05 - 0.10	0.07 \pm 0.00	-11.26 \pm 0.03	47
0.10 - 0.20	0.15 \pm 0.01	-11.23 \pm 0.02	63
0.20 - 0.40	0.29 \pm 0.01	-11.19 \pm 0.02	63
0.40 - 0.80	0.60 \pm 0.02	-11.23 \pm 0.03	58
0.8 - 1.6	1.13 \pm 0.04	-11.30 \pm 0.03	37
1.6 - 5.0	2.83 \pm 0.17	-11.31 \pm 0.04	40
5.0 - 15	8.8 \pm 0.7	-11.41 \pm 0.05	33
15 - 50	28.4 \pm 2.3	-11.62 \pm 0.06	16
50 - 150	107 \pm 6	-11.69 \pm 0.08	16
150 - 2000	664 \pm 180	-11.67 \pm 0.12	11
All	22.9 \pm 6.5	-11.30 \pm 0.01	436

TABLE 17.8.—*The ablation coefficient σ as a function of the integrated brightness ϵ_m for Super-Schmidt (classes A and S excluded) and small-camera meteors*

Range of ϵ_m	Super-Schmidt Meteors				Small-Camera Meteors			All Cameras Meteors				
	Mean ϵ_m	Mean $\log \sigma$ ($\text{cm}^{-2} \text{s}^2$)	No. obs.		Mean ϵ_m	Mean $\log \sigma$ ($\text{cm}^{-2} \text{s}^2$)	No. obs.	Mean ϵ_m	Mean $\log \sigma$ ($\text{cm}^{-2} \text{s}^2$)	S.d. of mean	S.d. of 1 obs.	No. obs.
-1.40	-1.00	-1.14	-11.14	23	—	—	—	-1.14	-11.14	\pm 0.05	\pm 0.25	23
-0.99	-0.75	-0.85	-11.17	65	—	—	—	-0.85	-11.17	0.03	0.25	65
-0.74	-0.50	-0.63	-11.21	81	-0.66	-11.05	1	-0.63	-11.21	0.03	0.25	82
-0.49	-0.25	-0.39	-11.20	66	—	—	—	-0.39	-11.20	0.03	0.22	66
-0.24	0.00	-0.14	-11.29	53	—	—	—	-0.14	-11.29	0.02	0.18	53
0.01	0.50	0.19	-11.19	39	0.31	-11.28	11	0.22	-11.21	0.03	0.23	50
0.51	1.00	0.67	-11.33	18	0.81	-11.34	14	0.73	-11.34	0.04	0.25	32
1.01	1.50	1.08	-11.57	2	1.21	-11.48	24	1.20	-11.49	0.05	0.24	26
1.51	2.00	1.91	-11.88	1	1.76	-11.64	16	1.77	-11.66	0.06	0.23	17
2.01	2.50	—	—	—	2.24	-11.78	10	2.24	-11.78	0.09	0.27	10
2.51	3.40	—	—	—	3.03	-11.76	8	3.03	-11.76	0.15	0.44	8
All		-0.41	-11.22	348	1.43	-11.52	84	-0.05	-11.28	0.01	0.28	432

TABLE 17.9.—The ablation coefficient σ as a function of the zenith angle $\cos Z_R$ for Super-Schmidt meteors (classes A and S excluded)

Range of $\cos Z_R$	All Meteors					Sporadic Meteors				
	Mean $\cos Z_R$	Mean $\log \tau$ (cm^{-2}s^2)	S.d. of mean	S.d. of 1 obs.	No. obs.	Mean $\cos Z_R$	Mean $\log \tau$ (cm^{-2}s^2)	S.d. of mean	S.d. of 1 obs.	No. obs.
0.1 - 0.2	0.140	-11.12	0.10	0.18	3	0.133	-11.08	0.17	0.24	2
0.2 - 0.3	0.253	-11.21	0.06	0.18	9	0.250	-11.21	0.07	0.19	8
0.3 - 0.4	0.351	-11.21	0.05	0.28	28	0.356	-11.19	0.07	0.32	20
0.4 - 0.5	0.461	-11.23	0.04	0.21	32	0.459	-11.23	0.04	0.20	26
0.5 - 0.6	0.555	-11.26	0.04	0.19	29	0.549	-11.23	0.04	0.16	18
0.6 - 0.7	0.648	-11.23	0.03	0.24	76	0.649	-11.19	0.03	0.24	52
0.7 - 0.8	0.751	-11.19	0.03	0.26	70	0.754	-11.18	0.04	0.24	47
0.8 - 0.9	0.843	-11.20	0.03	0.20	61	0.841	-11.18	0.03	0.21	46
0.9 - 1.0	0.969	-11.22	0.04	0.26	40	0.963	-11.19	0.05	0.25	23
All	0.677	-11.216	0.013	0.235	348	0.666	-11.194	0.015	0.229	242

TABLE 17.10.—The ablation coefficient σ as a function of the aphelion distance Q for sporadic Super-Schmidt meteors (classes A and S excluded) (* = harmonic mean)

Range of Q (a.u.)	Mean Q	Mean $\log \tau$ (cm^{-2}s^2)	S.d. of mean	S.d. of 1 obs.	Mean $\log \sigma$ ($v_m = 30 \text{ km/s}$)	No. obs.
0.9 - 3.5	2.65	-11.12	± 0.04	± 0.23	-11.20	32
3.5 - 4.2	3.90	-11.11	0.04	0.23	-11.23	29
4.2 - 4.8	4.56	-11.10	0.04	0.19	-11.22	30
4.8 - 5.4	5.09	-11.18	0.04	0.23	-11.26	30
5.4 - 7.0	6.01	-11.18	0.03	0.15	-11.23	29
7.0 - 20	11.63	-11.27	0.04	0.22	-11.17	35
20 - 70	36.18	-11.31	0.04	0.24	-11.21	32
70 - =	1403*	-11.27	0.05	0.24	-11.17	25
All		-11.19	0.02	0.23	-11.21	242

TABLE 17.11.1.—The ablation coefficient σ as a function of the perihelion distance q for Super-Schmidt meteors (classes A and S excluded)

All Meteors						Sporadic Meteors				
Range of q (a.u.)	Mean q (a.u.)	Mean $\log \sigma$ (cm^{-2}s^2)	S.d. of mean	S.d. of 1 obs.	No. obs.	Mean q (a.u.)	Mean $\log \sigma$ (cm^{-2}s^2)	S.d. of mean	S.d. of 1 obs.	No. obs.
0.0 - 0.1	0.08	-11.41	± 0.04	± 0.13	8	0.08	-11.56	± 0.11	± 0.15	2
0.1 - 0.2	0.14	-11.28	0.06	0.30	30	0.13	-11.39	0.14	0.36	7
0.2 - 0.3	0.25	-11.35	0.04	0.22	28	0.25	-11.33	0.06	0.25	16
0.3 - 0.4	0.35	-11.29	0.03	0.17	30	0.36	-11.26	0.05	0.20	16
0.4 - 0.5	0.46	-11.26	0.03	0.15	20	0.46	-11.25	0.05	0.17	14
0.5 - 0.6	0.55	-11.18	0.04	0.24	30	0.55	-11.25	0.04	0.19	19
0.6 - 0.7	0.66	-11.18	0.04	0.23	35	0.66	-11.18	0.04	0.23	28
0.7 - 0.8	0.74	-11.14	0.04	0.21	28	0.74	-11.14	0.04	0.21	27
0.8 - 0.9	0.85	-11.12	0.04	0.23	33	0.85	-11.10	0.04	0.20	32
0.9 - 1.0	0.96	-11.21	0.02	0.23	91	0.96	-11.19	0.03	0.22	70
1.0 - 1.1	1.01	-11.06	0.06	0.22	15	1.01	-11.05	0.07	0.24	11
All	0.64	-11.22	0.01	0.24	348	0.71	-11.19	0.01	0.23	242

TABLE 17.11.2.—The ablation coefficient σ as a function of the perihelion distance q for short-period and long-period sporadic Super-Schmidt meteors (classes A and S excluded)

Meteors with $q < 6$ a.u.						Meteors with $q > 6$ a.u.				
Range of q (a.u.)	Mean q (a.u.)	Mean $\log \sigma$ (cm^{-2}s^2)	S.d. of mean	S.d. of 1 obs.	No. obs.	Mean q (a.u.)	Mean $\log \sigma$ (cm^{-2}s^2)	S.d. of mean	S.d. of 1 obs.	No. obs.
0.0 - 0.1	0.08	-11.56	± 0.11	± 0.15	2	—	—	—	—	—
0.1 - 0.2	0.11	-11.15	0.05	0.09	3	0.15	-11.57	± 0.19	± 0.39	4
0.2 - 0.3	0.25	-11.38	0.09	0.29	10	0.24	-11.24	0.05	0.13	6
0.3 - 0.4	0.37	-11.16	0.04	0.10	8	0.35	-11.36	0.08	0.23	8
0.4 - 0.5	0.46	-11.19	0.04	0.11	10	0.46	-11.40	0.10	0.21	4
0.5 - 0.6	0.55	-11.23	0.07	0.22	10	0.54	-11.28	0.05	0.16	9
0.6 - 0.7	0.66	-11.10	0.05	0.22	17	0.66	-11.31	0.06	0.19	11
0.7 - 0.8	0.75	-11.05	0.04	0.18	16	0.74	-11.27	0.06	0.18	11
0.8 - 0.9	0.85	-11.07	0.04	0.16	21	0.85	-11.15	0.06	0.27	11
0.9 - 1.0	0.97	-11.10	0.03	0.19	34	0.96	-11.27	0.03	0.21	36
1.0 - 1.1	1.01	-11.11	0.11	0.25	5	1.01	-11.01	0.10	0.24	6
All	0.59	-11.14	0.02	0.21	136	0.72	-11.27	0.02	0.23	106

TABLE 17.12.—Dependence of $\log \sigma$ on χ and vice versa for sporadic Super-Schmidt meteors (classes A and S excluded)

Range of $\log \sigma$	Mean $\log \sigma$	Mean $\chi \pm$ s.d.	No. obs.	Range of χ	Mean χ	Mean $\log \sigma \pm$ s.d.	No. obs.
-12.02 - -11.45	-11.62	0.21 ± 0.05	26	-0.85 - 0.0	-0.10	-11.16 ± 0.03	44
-11.45 - -11.30	-11.37	0.23 ± 0.04	40	0.0 - 0.2	0.09	-11.22 ± 0.02	80
-11.30 - -11.15	-11.23	0.22 ± 0.03	69	0.2 - 0.4	0.29	-11.21 ± 0.03	63
-11.15 - -11.00	-11.09	0.22 ± 0.03	63	0.4 - 0.6	0.47	-11.13 ± 0.04	26
-11.00 - -10.42	-10.87	0.28 ± 0.06	44	0.6 - 1.28	0.78	-11.18 ± 0.05	29

TABLE 18.1.—The distribution of the fragmentation index χ for Super-Schmidt meteors

Table 18.1

Range of χ	Sporadic Meteors			Shower meteors	All meteors
	All				
	Q \leq 6 a.u.	Q > 6 a.u.			
-0.85 -- -0.41	1	0	1	0	1
-0.40 -- -0.31	2	1	1	1	3
-0.30 -- -0.21	3	3	0	2	5
-0.20 -- -0.11	8	3	5	6	14
-0.10 -- -0.01	34	17	17	12	46
0.00 -- 0.09	43	25	18	19	62
0.10 -- 0.19	49	29	20	15	64
0.20 -- 0.29	35	24	11	12	47
0.30 -- 0.39	36	24	12	18	54
0.40 -- 0.49	23	11	12	9	32
0.50 -- 0.59	10	4	6	10	20
0.60 -- 0.69	12	5	7	7	19
0.70 -- 0.79	9	4	5	3	12
0.80 -- 0.89	7	5	2	2	9
0.90 -- 0.99	2	2	0	0	2
1.00 -- 1.09	2	2	0	2	4
1.10 -- 1.19	0	0	0	0	0
1.20 -- 1.29	2	2	0	0	2
1.30 -- 1.39	0	0	0	1	1
1.40 -- 1.49	1	0	1	0	1
1.50 -- 1.99	1	0	1	0	1
2.00 -- 3.00	1	0	1	1	2
All --	281	161	120	120	401

TABLE 18.2.—The distribution of the fragmentation index χ for small-camera meteors

Range of χ	Sporadic meteors	Shower meteors	All meteors
-0.50 -- -0.41	1	0	1
-0.40 -- -0.31	0	3	3
-0.30 -- -0.21	2	3	5
-0.20 -- -0.11	4	5	9
-0.10 -- -0.01	7	5	12
0.00 -- 0.09	3	7	10
0.10 -- 0.19	5	4	9
0.20 -- 0.29	3	0	3
0.30 -- 0.39	3	1	4
0.40 -- 0.49	2	0	2
All	30	28	58

TABLE 19.1.1.—The fragmentation index χ as a function of the velocity for Super-Schmidt meteors (classes A and S excluded)

Velocity range (km/s)	All Meteors						Sporadic Meteors					
	Mean v_m (km/s)	Mean χ	S.d. of mean	S.d. of 1 obs.	Mean χ ($m_m = 0.8$ g)	No. obs.	Mean v_m (km/s)	Mean χ	S.d. of mean	S.d. of 1 obs.	Mean χ ($m_m = 0.8$ g)	No. obs.
11 - 20	17.3	0.25	± 0.04	± 0.29	0.27	56	17.3	0.25	± 0.04	± 0.29	0.27	56
20 - 25	22.5	0.27	0.04	0.33	0.28	57	22.3	0.26	0.05	0.33	0.27	46
25 - 30	27.3	0.22	0.04	0.32	0.22	58	27.3	0.22	0.05	0.32	0.23	38
30 - 35	31.7	0.12	0.04	0.25	0.12	44	32.0	0.15	0.05	0.27	0.15	28
35 - 40	36.6	0.23	0.03	0.20	0.22	35	37.1	0.25	0.05	0.17	0.23	12
40 - 50	44.2	0.37	0.05	0.31	0.33	40	45.3	0.28	0.06	0.28	0.24	20
50 - 60	56.1	0.27	0.05	0.24	0.22	22	55.7	0.29	0.06	0.25	0.24	17
60 - 73	65.1	0.32	0.04	0.26	0.23	47	65.5	0.32	0.05	0.26	0.22	32
All	35.0	0.25	0.02	0.29	0.23	359	33.4	0.25	0.02	0.29	0.23	249

TABLE 19.1.2.—The fragmentation index χ as a function of velocity for sporadic Super-Schmidt meteors in short-period and long-period orbits (classes A and S excluded)

Velocity range (km/s)	Meteors with Q \leq 6 a.u.						Meteors with Q > 6 a.u.					
	Mean v_m (km/s)	Mean χ	S.d. of mean	S.d. of 1 obs.	Mean χ ($m_m = 0.8$ g)	No. obs.	Mean v_m (km/s)	Mean χ	S.d. of mean	S.d. of 1 obs.	Mean χ ($m_m = 0.8$ g)	No. obs.
11 - 20	17.2	0.28	± 0.04	± 0.29	0.30	50	18.1	-0.01	± 0.06	± 0.14	0.01	6
20 - 25	22.3	0.27	0.05	0.33	0.28	38	22.3	0.22	0.11	0.31	0.22	8
25 - 30	27.3	0.22	0.06	0.29	0.22	27	27.2	0.22	0.12	0.41	0.24	11
30 - 35	32.2	0.20	0.07	0.30	0.20	17	31.7	0.07	0.06	0.19	0.07	11
35 - 40	36.5	0.32	0.05	0.12	0.30	6	37.7	0.17	0.08	0.19	0.15	6
40 - 50	42.0	0.28	0.07	0.09	0.20	2	45.7	0.28	0.07	0.29	0.24	18
50 - 60	—	—	—	—	—	—	55.7	0.29	0.06	0.25	0.24	17
60 - 73	—	—	—	—	—	—	65.5	0.32	0.05	0.26	0.21	32
All	23.5	0.26	0.03	0.29	0.27	140	46.1	0.24	0.03	0.28	0.20	109

TABLE 19.2.1.—The fragmentation index χ as a function of the integrated brightness ϵ_m for Super-Schmidt meteors (classes A and S excluded)

All Meteors						Sporadic Meteors				
Range of ϵ_m	Mean ϵ_m	Mean χ	S.d. of mean	S.d. of 1 obs.	No. obs.	Mean ϵ_m	Mean χ	S.d. of mean	S.d. of 1 obs.	No. obs.
-1.40 — -1.00	-1.14	0.32	± 0.06	± 0.28	23	-1.14	0.29	± 0.06	± 0.24	16
-1.00 — -0.75	-0.86	0.24	0.03	0.25	64	-0.86	0.24	0.04	0.26	48
-0.75 — -0.50	-0.64	0.35	0.04	0.33	86	-0.64	0.36	0.05	0.35	60
-0.50 — -0.25	-0.39	0.26	0.04	0.31	69	-0.38	0.23	0.04	0.28	47
-0.25 — 0.00	-0.14	0.17	0.04	0.27	54	-0.14	0.20	0.04	0.24	33
0.00 — 0.50	0.19	0.19	0.04	0.27	41	0.17	0.18	0.05	0.25	31
0.50 — 1.00	0.67	0.10	0.04	0.16	19	0.64	0.05	0.04	0.15	13
1.00 — 1.50	1.08	0.35	0.20	0.28	2	—	—	—	—	0
1.50 — 2.00	1.91	0.23	—	—	1	1.91	0.23	—	—	1
All	-0.41	0.25	0.02	0.29	359	-0.42	0.25	0.02	0.29	249

TABLE 19.2.2.—The fragmentation index χ as a function of the integrated brightness ϵ_m for sporadic Super-Schmidt meteors in short-period and long-period orbits (classes A and S excluded)

Meteors with $Q < 6$ a.u.						Meteors with $Q > 6$ a.u.				
Range of ϵ_m	Mean ϵ_m	Mean χ	S.d. of mean	S.d. of 1 obs.	No. obs.	Mean ϵ_m	Mean χ	S.d. of mean	S.d. of 1 obs.	No. obs.
-1.40, -1.00	-1.13	0.29	± 0.06	± 0.23	14	-1.24	0.32	± 0.28	± 0.39	2
-1.00, -0.75	-0.86	0.22	0.04	0.25	37	-0.86	0.32	0.09	0.31	11
-0.75, -0.50	-0.64	0.36	0.06	0.35	39	-0.63	0.38	0.08	0.35	21
-0.50, -0.25	-0.39	0.21	0.06	0.26	19	-0.37	0.24	0.06	0.30	28
-0.25, 0.00	-0.14	0.25	0.09	0.31	11	-0.14	0.17	0.04	0.21	22
0.00, 0.50	0.17	0.18	0.08	0.32	16	0.17	0.18	0.05	0.18	15
0.50, 1.00	0.60	0.11	0.08	0.15	4	0.66	0.03	0.05	0.16	9
1.00, 1.50	—	—	—	—	—	—	—	—	—	—
1.50, 2.00	—	—	—	—	—	1.91	0.23	—	—	—
All	-0.55	0.26	0.03	0.29	140	-0.26	0.24	0.03	0.28	109

TABLE 19.3.—The fragmentation index χ as a function of mass for Super-Schmidt meteors (classes A and S excluded)

All Meteors						Sporadic Meteors				
Mass range (g)	Mean m_m (g)	Mean χ	S.d. of mean	S.d. of 1 obs.	No. obs.	Mean m_m (g)	Mean χ	S.d. of mean	S.d. of 1 obs.	No. obs.
0.01 - 0.05	0.033	0.40	± 0.04	± 0.27	54	0.032	0.39	± 0.04	± 0.26	38
0.05 - 0.10	0.072	0.26	0.03	0.23	47	0.075	0.23	0.04	0.20	24
0.10 - 0.20	0.146	0.21	0.03	0.24	65	0.146	0.17	0.03	0.21	42
0.20 - 0.40	0.294	0.24	0.04	0.32	64	0.305	0.25	0.05	0.35	40
0.40 - 0.80	0.596	0.20	0.04	0.32	54	0.604	0.24	0.05	0.33	43
0.80 - 1.6	1.12	0.20	0.05	0.29	35	1.11	0.21	0.05	0.29	31
1.6 - 5.0	2.57	0.28	0.07	0.35	27	2.54	0.28	0.08	0.34	18
5.0 - 34	10.2	0.08	0.04	0.14	13	10.2	0.08	0.04	0.14	13
All	0.85	0.25	0.02	0.29	359	1.04	0.25	0.02	0.29	249

TABLE 19.4.—The fragmentation index χ as a function of the velocity for small-camera meteors

Velocity range	Mean velocity	Mean $\chi \pm$ s.d.	Mean χ ($v_m=30$ km/s)	No. obs.
10 - 20	15.4	0.07 \pm 0.04	0.08	7
20 - 30	25.2	-0.01 \pm 0.06	0.00	17
30 - 40	34.0	0.01 \pm 0.04	-0.05	26
40 - 70	57.1	-0.12 \pm 0.04	-0.18	8
All	32.4	-0.01 \pm 0.03	-0.04	58

TABLE 19.6.—The fragmentation index χ as a function of zenith angle Z_R for small-camera meteors

Range of $\cos Z_R$	Mean $\cos Z_R$	Mean $\chi \pm$ s.d.	Mean χ ($v_m=30$ km/s) ($m_m=30$ g)	No. obs.
0.2 - 0.4	0.28	-0.08 \pm 0.17	-0.09	5
0.4 - 0.6	0.52	0.14 \pm 0.06	0.11	8
0.6 - 0.7	0.66	-0.01 \pm 0.06	-0.02	9
0.7 - 0.8	0.75	-0.05 \pm 0.07	-0.10	8
0.8 - 0.9	0.85	-0.07 \pm 0.06	-0.04	14
0.9 - 1.0	0.95	0.04 \pm 0.05	0.01	14
All	0.74	-0.01 \pm 0.03	-0.02	58

TABLE 19.5.—The fragmentation index χ as a function of mass for small-camera meteors

Mass range (g)	Mean mass (g)	Mean $\chi \pm$ s.d.	Mean χ ($v_m=30$ km/s)	No. obs.
0.3 - 5.0	3.1	0.06 \pm 0.06	0.12	12
5.0 - 15	11.1	0.03 \pm 0.06	0.06	12
15 - 50	29.0	-0.02 \pm 0.07	-0.02	9
50 - 150	101	-0.09 \pm 0.06	-0.10	14
150 - 2000	555	0.01 \pm 0.06	-0.03	11
All	137	-0.01 \pm 0.03	0.00	58

TABLE 19.7.—The fragmentation index χ for shower meteors; Super-Schmidt (classes A and S excluded) and small-camera meteors

Shower	Super-Schmidt Meteors ^a					Small-Camera Meteors							
	Mean χ	S. d. of mean	S. d. of 1 obs.	Mean $m_m \pm$ s.d. (g)	(Mean χ) ($m_m = 0.8$ g)	No. obs.	Mean χ	S. d. of mean	S. d. of 1 obs.	Mean $m_m \pm$ s.d. (g)	Mean $v_m \pm$ s.d. (km/s)	(Mean $\chi \pm$ s.d.) ($m_m = 0.8$ g, $v_m = 30$ km/s)	No. obs.
Quadrantids	0.44	\pm 0.11	\pm 0.34	0.08 \pm 0.02	0.41	10	—	—	—	—	—	—	—
Virginids	0.12	—	—	1.07	—	1	-0.08	—	—	3.4	31.1	—	1
Lyrids	0.08	0.09	0.15	0.13 \pm 0.04	0.08	3	-0.11	—	—	26.5	48.8	—	1
η Aquarids	0.09	—	—	0.05	—	1	—	—	—	—	—	—	—
δ Aquarids	0.58	0.09	0.25	0.10 \pm 0.04	0.54	8	—	—	—	—	—	—	—
α Capricornids	0.38	0.07	0.27	0.53 \pm 0.24	0.38	14	—	—	—	—	—	—	—
Southern ϵ Aquarids	0.20	0.11	0.24	0.10 \pm 0.02	0.17	5	—	—	—	—	—	—	—
Northern ϵ Aquarids	0.10	0.26	0.37	0.11 \pm 0.04	—	2	—	—	—	—	—	—	—
Perseids	0.28	0.09	0.28	0.30 \pm 0.14	0.22	9	-0.13	0.10	0.17	46 \pm 41	60.2 \pm 0.8	\sim 0.15	3
κ Cygnids	0.11	0.09	0.19	0.39 \pm 0.06	0.11	4	—	—	—	—	—	—	—
Dracnids	1.89	0.57	0.80	2.00 \pm 0.13	—	2	—	—	—	—	—	—	—
Orionids	0.54	0.06	0.13	0.04 \pm 0.01	0.40	5	—	—	—	—	—	—	—
Southern Taurids	0.04	0.05	0.20	0.48 \pm 0.13	0.04	18	-0.17	0.07	0.17	44 \pm 19	31.3 \pm 0.2	0.02	6
Northern Taurids	0.11	0.15	0.33	0.85 \pm 0.35	0.11	5	-0.13	0.10	0.17	71 \pm 47	29.4 \pm 1.1	\sim 0.10	3
Leonids	0.37	—	—	0.29	—	1	—	—	—	—	—	—	—
χ Orionids	—	—	—	—	—	—	0.06	0.05	0.10	117 \pm 85	30.6 \pm 0.6	\sim 0.25	4
σ Hydrids	0.04	0.04	0.07	0.05 \pm 0.01	-0.01	3	0.00	—	—	84.0	59.6	—	1
Geminids	0.21	0.05	0.20	0.76 \pm 0.28	0.20	20	0.00	0.07	0.21	146 \pm 99	36.2 \pm 0.1	0.15	9

TABLE 19.8.—*The fragmentation index χ as a function of mass for Super-Schmidt (classes A and S excluded) and small-camera meteors. The values for small-camera meteors were reduced to $v_{\infty} = 30$ km/s*

Mass range (g)	Mean m (g)	Mean χ	S.d. of mean	S.d. of 1 obs.	No. obs.
0.01 - 0.05	0.03	0.40	± 0.04	± 0.27	54
0.05 - 0.10	0.07	0.26	0.03	0.23	47
0.1 - 0.2	0.15	0.21	0.03	0.24	65
0.2 - 0.4	0.29	0.24	0.04	0.32	65
0.4 - 0.8	0.60	0.20	0.04	0.32	54
0.8 - 1.6	1.12	0.20	0.05	0.28	37
1.6 - 5.0	2.9	0.24	0.06	0.34	36
5 - 15	9.2	0.07	0.04	0.18	23
15 - 50	28.7	-0.01	0.06	0.20	11
50 - 150	101	-0.10	0.06	0.21	14
150 - 2000	555	-0.03	0.06	0.20	11
All	20	0.22	0.01	0.29	417

TABLE 19.9.—*The fragmentation index χ as a function of the integrated brightness ϵ_{∞} for Super-Schmidt (classes A and S excluded) and small-camera meteors*

Range of ϵ_{∞}	Super-Schmidt Meteors			Small-Camera Meteors			All Meteors				
	Mean ϵ_{∞}	Mean χ	No. obs.	Mean ϵ_{∞}	Mean χ	No. obs.	Mean ϵ_{∞}	Mean χ	S.d. of mean	S.d. of 1 obs.	No. obs.
-1.40 - -1.00	-1.14	0.32	23	—	—	—	-1.14	0.32	± 0.06	± 0.28	23
-0.99 - -0.75	-0.86	0.24	64	—	—	—	-0.86	0.24	0.03	0.25	64
-0.74 - -0.50	-0.64	0.35	86	—	—	—	-0.64	0.35	0.04	0.33	86
-0.49 - -0.25	-0.39	0.26	69	—	—	—	-0.39	0.26	0.04	0.31	69
-0.24 - 0.00	-0.14	0.17	54	—	—	—	-0.14	0.17	0.04	0.27	54
0.01 - 0.50	0.19	0.19	41	0.28	-0.05	2	0.20	0.18	0.04	0.26	43
0.51 - 1.00	0.67	0.10	19	0.81	0.11	11	0.72	0.10	0.03	0.18	30
1.01 - 1.50	1.08	0.35	2	1.21	0.05	14	1.20	0.09	0.05	0.19	16
1.51 - 2.00	1.91	0.23	1	1.76	-0.07	16	1.77	-0.05	0.05	0.19	17
2.01 - 2.50	—	—	—	2.22	-0.15	8	2.22	-0.15	0.05	0.15	8
2.51 - 3.40	—	—	—	3.02	0.00	7	3.02	0.00	0.08	0.22	7
All	-0.41	0.25	359	1.61	-0.01	58	-0.13	0.22	0.01	0.29	417

TABLE 19.10.1.—*The fragmentation index χ as a function of the zenith angle Z_R for Super-Schmidt meteors (classes A and S excluded)*

Range of $\cos Z_R$	All Meteors					Sporadic Meteors						
	Mean $\cos Z_R$	Mean χ	S.d. of mean	S.d. of 1 obs.	Mean χ ($m_{\infty} = 0.8$ g)	No. obs.	Mean $\cos Z_R$	Mean χ	S.d. of mean	S.d. of 1 obs.	Mean χ ($m_{\infty} = 0.8$ g)	No. obs.
0.1 - 0.2	0.15	0.59	± 0.24	± 0.48	0.51	4	0.14	0.64	± 0.33	± 0.57	0.59	3
0.2 - 0.3	0.25	0.36	0.12	0.39	0.33	10	0.25	0.24	0.11	0.31	0.22	8
0.3 - 0.4	0.35	0.39	0.07	0.36	0.36	28	0.36	0.42	0.08	0.37	0.39	20
0.4 - 0.5	0.46	0.38	0.05	0.29	0.35	34	0.46	0.37	0.06	0.30	0.33	28
0.5 - 0.6	0.55	0.26	0.06	0.34	0.24	31	0.55	0.26	0.07	0.31	0.25	19
0.6 - 0.7	0.65	0.27	0.04	0.31	0.25	78	0.65	0.25	0.04	0.31	0.24	53
0.7 - 0.8	0.75	0.22	0.03	0.23	0.21	71	0.75	0.17	0.03	0.19	0.17	48
0.8 - 0.9	0.84	0.17	0.03	0.24	0.16	61	0.84	0.21	0.04	0.25	0.21	46
0.9 - 1.0	0.97	0.14	0.03	0.19	0.13	42	0.96	0.15	0.05	0.22	0.14	24
All	0.67	0.25	0.02	0.29	0.23	359	0.66	0.25	0.02	0.29	0.23	249

TABLE 19.10.2.—The fragmentation index χ as a function of $\cos Z_R$ for sporadic Super-Schmidt meteors (classes A and S excluded)

Meteors with $Q \leq 6$ a.u.						Meteors with $Q > 6$ a.u.				
Range of $\cos Z_R$	Mean $\cos Z_R$	Mean χ	S.d. of mean	S.d. of 1 obs.	No. obs.	Mean $\cos Z_R$	Mean χ	S.d. of mean	S.d. of 1 obs.	No. obs.
0.1 - 0.2	0.16	0.97	± 0.04	± 0.06	2	0.10	-0.01	—	—	1
0.2 - 0.3	0.27	0.16	0.19	0.37	4	0.23	0.32	± 0.13	± 0.25	4
0.3 - 0.4	0.37	0.47	0.13	0.38	9	0.34	0.38	0.12	0.38	11
0.4 - 0.5	0.46	0.44	0.10	0.28	8	0.46	0.33	0.07	0.31	20
0.5 - 0.6	0.55	0.26	0.08	0.32	15	0.53	0.26	0.15	0.29	4
0.6 - 0.7	0.65	0.23	0.05	0.27	34	0.64	0.29	0.08	0.36	19
0.7 - 0.8	0.75	0.17	0.04	0.21	30	0.75	0.17	0.03	0.14	18
0.8 - 0.9	0.84	0.24	0.05	0.27	31	0.83	0.13	0.04	0.17	15
0.9 - 1.0	0.95	0.18	0.09	0.25	7	0.97	0.13	0.05	0.22	17
All	0.67	0.26	0.03	0.29	140	0.65	0.24	0.03	0.28	109

TABLE 19.11.—The fragmentation index χ as a function of the aphelion distance Q for sporadic Super-Schmidt meteors (classes A and S excluded)

Range of Q (a.u.)	Mean χ	S.d. of mean	S.d. of 1 obs.	Mean χ ($m_{\infty} = 0.8 g$)	No. obs.
0 - 3.5	0.29	± 0.07	± 0.40	0.29	36
3.5 - 4.2	0.32	0.04	0.21	0.34	29
4.2 - 4.8	0.26	0.05	0.30	0.26	30
4.8 - 5.4	0.17	0.05	0.27	0.17	30
5.4 - 7.0	0.24	0.07	0.38	0.24	30
7.0 - 20	0.21	0.04	0.22	0.18	36
20 - 70	0.28	0.04	0.22	0.20	32
70 - ∞	0.24	0.05	0.27	0.21	26
All	0.25	0.02	0.29	0.23	249

TABLE 19.12.—Correlation between the fragmentation index χ and the ablation coefficient σ for small-camera meteors

a) χ vs. σ				
Range of $\log \tau$ ($\text{cm}^{-2} \text{s}^{-2}$)	Mean $\log \tau$ ($\text{cm}^{-2} \text{s}^{-2}$)	Mean $\chi \pm$ s.d.	No. obs.	
-12.2 — -11.8	-11.99	-0.11 \pm 0.05	11	
-11.8 — -11.6	-11.72	-0.00 \pm 0.07	13	
-11.6 — -11.3	-11.50	0.04 \pm 0.05	13	
-11.3 — -10.8	-11.15	0.02 \pm 0.04	14	
b) σ vs. χ				
Range of χ	Mean χ	Mean $\log \sigma \pm$ s.d. ($\text{cm}^{-2} \text{s}^{-2}$)	No. obs.	
$\chi < -0.2$	0.28	-11.78 \pm 0.12	9	
$-0.2 < \chi \leq 0$	-0.09	-11.59 \pm 0.06	20	
$0 < \chi \leq 0.2$	0.09	-11.40 \pm 0.10	15	
$\chi > 0.2$	0.34	-11.56 \pm 0.10	7	

TABLE 19.13.1.—The fragmentation index χ as a function of the perihelion distance q for Super-Schmidt meteors (classes A and S excluded)

All Meteors						Sporadic Meteors				
Range of q (a.u.)	Mean q (a.u.)	Mean χ	S.d. of mean	S.d. of 1 obs.	No. obs.	Mean q (a.u.)	Mean χ	S.d. of mean	S.d. of 1 obs.	No. obs.
0.0 - 0.1	0.08	0.44	± 0.07	± 0.19	8	0.08	0.30	± 0.09	± 0.13	2
0.1 - 0.2	0.14	0.32	0.05	0.27	31	0.13	0.43	0.09	0.24	7
0.2 - 0.3	0.25	0.18	0.05	0.24	28	0.25	0.26	0.07	0.27	17
0.3 - 0.4	0.35	0.16	0.05	0.25	30	0.36	0.20	0.06	0.25	16
0.4 - 0.5	0.46	0.21	0.07	0.31	21	0.46	0.26	0.07	0.28	14
0.5 - 0.6	0.55	0.24	0.06	0.33	32	0.55	0.18	0.08	0.34	20
0.6 - 0.7	0.66	0.29	0.05	0.28	36	0.66	0.28	0.05	0.29	29
0.7 - 0.8	0.74	0.28	0.06	0.34	28	0.74	0.27	0.07	0.34	27
0.8 - 0.9	0.85	0.23	0.05	0.32	35	0.85	0.23	0.06	0.32	34
0.9 - 1.0	0.96	0.29	0.03	0.30	95	0.96	0.26	0.03	0.27	72
1.0 - 1.1	1.01	0.12	0.05	0.18	15	1.01	0.14	0.06	0.19	11
All	0.64	0.25	0.02	0.29	359	0.71	0.25	0.02	0.29	249

TABLE 19.13.2.—The fragmentation index χ as a function of the perihelion distance q for sporadic Super-Schmidt meteors (classes A and S excluded)

Range of q (a.u.)	Meteors with $Q \leq 6$ a.u.					Meteors with $Q > 6$ a.u.				
	Mean q (a.u.)	Mean χ	S.d. of mean	S.d. of 1 obs.	No. obs.	Mean q (a.u.)	Mean χ	S.d. of mean	S.d. of 1 obs.	No. obs.
0.0 - 0.1	0.08	0.30	± 0.09	± 0.13	2	—	—	—	—	—
0.1 - 0.2	0.11	0.34	0.07	0.13	3	0.15	0.51	± 0.15	± 0.30	4
0.2 - 0.3	0.25	0.15	0.06	0.21	11	0.24	0.45	0.11	0.27	6
0.3 - 0.4	0.37	0.17	0.06	0.16	8	0.35	0.24	0.11	0.32	8
0.4 - 0.5	0.46	0.22	0.09	0.28	10	0.46	0.35	0.15	0.30	4
0.5 - 0.6	0.55	0.22	0.13	0.40	10	0.55	0.14	0.09	0.28	10
0.6 - 0.7	0.66	0.32	0.07	0.28	18	0.66	0.20	0.09	0.29	11
0.7 - 0.8	0.75	0.34	0.10	0.39	16	0.74	0.17	0.07	0.24	11
0.8 - 0.9	0.85	0.19	0.06	0.27	21	0.85	0.31	0.11	0.38	13
0.9 - 1.0	0.97	0.30	0.05	0.30	36	0.96	0.21	0.04	0.24	36
1.0 - 1.1	1.01	0.20	0.09	0.21	5	1.01	0.10	0.07	0.18	6
All	0.70	0.26	0.03	0.29	140	0.73	0.24	0.03	0.28	109

TABLE 19.13.3.—The fragmentation index χ as a function of the perihelion distance q for Super-Schmidt meteors (classes A and S excluded)

Range of q (a.u.)	Meteors with $Q \leq 6$ a.u.					Meteors with $Q > 6$ a.u.				
	Mean q (a.u.)	Mean χ	S.d. of mean	S.d. of 1 obs.	No. obs.	Mean q	Mean χ	S.d. of mean	S.d. of 1 obs.	No. obs.
0.0 - 0.1	0.08	0.43	± 0.08	± 0.20	7	0.06	0.58	—	—	1
0.1 - 0.2	0.14	0.26	0.04	0.21	26	0.14	0.61	± 0.16	± 0.35	5
0.2 - 0.3	0.25	0.13	0.04	0.18	18	0.24	0.27	0.10	0.31	10
0.3 - 0.4	0.35	0.13	0.05	0.23	22	0.35	0.24	0.11	0.32	8
0.4 - 0.5	0.46	0.19	0.08	0.31	16	0.45	0.26	0.15	0.33	5
0.5 - 0.6	0.55	0.28	0.08	0.35	20	0.55	0.18	0.08	0.29	12
0.6 - 0.7	0.66	0.31	0.06	0.27	21	0.65	0.25	0.08	0.29	15
0.7 - 0.8	0.75	0.34	0.10	0.39	16	0.74	0.20	0.07	0.25	12
0.8 - 0.9	0.85	0.18	0.06	0.27	22	0.85	0.31	0.11	0.38	13
0.9 - 1.0	0.97	0.34	0.05	0.32	46	0.96	0.24	0.04	0.27	49
1.0 - 1.1	1.01	0.13	0.08	0.21	7	1.01	0.12	0.06	0.16	8
All	0.59	0.26	0.02	0.29	221	0.72	0.25	0.03	0.29	138

TABLE 20.1.—The blending and wake indices B and W for Super-Schmidt meteors. Also shown are the percentages of meteors falling within each group of B and W .

	No. obs.	$\bar{B} \pm$ s.d.	$B = 0$	$0 < B < 1$	$1 < B < 2$	$2 < B \leq 3$	$B > 3$	$\bar{W} \pm$ s.d.	$W = 0$	$0 < W \leq 1$	$1 < W \leq 2$	$2 < W \leq 3$	$W > 3$
All meteors	413	0.51 ± 0.05	67.6	15.5	10.2	5.1	1.7	0.74 ± 0.05	46.7	30.3	15.0	5.8	2.2
All meteors minus A and S	375	0.46 ± 0.05	70.9	14.4	8.5	4.8	1.3	0.75 ± 0.05	47.2	29.3	14.9	6.1	2.4
Sporadic meteors	290	0.47 ± 0.05	70.7	13.8	9.3	4.8	1.4	0.77 ± 0.06	45.5	29.7	16.5	6.2	2.1
Sporadic meteors minus A and S	251	0.42 ± 0.06	73.3	13.1	8.0	4.4	1.2	0.71 ± 0.06	47.4	29.1	16.3	5.6	1.6
Sporadic meteors minus A and S, with aphelion distance ≤ 6 a.u.	138	0.46 ± 0.08	71.7	15.2	5.8	5.8	1.4	0.73 ± 0.08	47.1	27.5	19.6	5.1	0.7
Sporadic meteors minus A and S, with aphelion distance > 6 a.u.	113	0.37 ± 0.07	75.2	10.6	10.6	2.7	0.9	0.70 ± 0.09	47.8	31.0	12.4	6.2	2.6
Meteors with abrupt beginning (A)	26	1.35 ± 0.24	23.1	30.8	26.9	11.5	7.7	0.59 ± 0.13	38.5	46.1	15.4	0	0
Short-trail meteors (S)	12	0.57 ± 0.23	58.3	16.7	25.0	0	0	0.83 ± 0.30	50.0	25.0	16.7	8.3	0
Meteors with visible fragments (F)	11	0.27 ± 0.27	90.9	0	0	9.1	0	2.11 ± 0.43	18.2	9.1	27.3	27.3	18.2

TABLE 20.2.—The blending and wake indices B and W for Super-Schmidt shower meteors (arranged in order of time of the year); also shown are the percentages of meteors falling within each group of B and W

Shower	No. obs.	$\bar{B} \pm \text{s.d.}$	$B = 0$	$0 < B \leq 1$	$1 < B \leq 2$	$2 < B \leq 3$	$B > 3$	$\bar{W} \pm \text{s.d.}$	$W = 0$	$0 < W \leq 1$	$1 < W \leq 2$	$2 < W \leq 3$	$W > 3$
Quadrantids	10	0.80 ± 0.11	10.0	90.0	0	0	0	0.40 ± 0.19	60.0	20.0	20.0	0	0
Virginids	2	0.25 ± 0.25	50.0	50.0	0	0	0	1.15 ± 1.15	50.0	0	0	50.0	0
Lyrids	3	0.50 ± 0.50	66.7	0	33.3	0	0	0.43 ± 0.30	33.3	66.7	0	0	0
♄ Aquarids	1	0	100	0	0	0	0	0	100	0	0	0	0
♋ Aquarids	11	1.55 ± 0.27	9.1	27.3	45.5	18.2	0	0.21 ± 0.12	72.7	27.3	0	0	0
♏ Capricornids	14	1.00 ± 0.34	57.1	0	21.4	21.4	0	0.74 ± 0.27	42.9	35.7	7.1	14.3	0
Southern ♋ Aquarids	6	0.83 ± 0.54	66.7	0	16.7	16.7	0	0.33 ± 0.21	66.7	33.3	0	0	0
Northern ♋ Aquarids	2	0.50 ± 0.50	50.0	50.0	0	0	0	0.50 ± 0.50	50.0	50.0	0	0	0
Perseids	11	0.03 ± 0.03	90.9	9.1	0	0	0	0.96 ± 0.35	36.4	36.4	9.1	18.2	0
♌ Cygnids	4	0.50 ± 0.50	75.0	0	25.0	0	0	1.00 ± 0.20	0	75.0	25.0	0	0
Draconids	3	4.00 ± 0.00	0	0	0	0	100	0.33 ± 0.33	66.7	33.3	0	0	0
Orionids	8	0.41 ± 0.19	50.0	37.5	12.5	0	0	0.34 ± 0.25	75.0	12.5	12.5	0	0
Southern Taurids	18	0.00 ± 0.00	100	0	0	0	0	0.14 ± 0.08	83.3	16.7	0	0	0
Northern Taurids	5	0.06 ± 0.06	80.0	20.0	0	0	0	0.72 ± 0.43	40.0	20.0	40.0	0	0
Leonids	1	0	100	0	0	0	0	4	0	0	0	0	100
♊ Hydrids	3	0.00 ± 0.00	100	0	0	0	0	0.33 ± 0.33	66.7	33.3	0	0	0
Geminids	20	0.47 ± 0.17	60.0	25.0	10.0	5.0	0	1.48 ± 0.26	10.0	45.0	30.0	5.0	10.0

TABLE 20.3.—The blending and wake indices B and W as functions of velocity v_{∞} for (1) all Super-Schmidt meteors, (2) sporadic meteors only; also shown are the percentages of meteors falling within each group of B and W

1) Range of velocity v_{∞} , km/s	\bar{v}_{∞}	No. obs.	$\bar{B} \pm \text{s.d.}$	$B = 0$	$0 < B \leq 1$	$1 < B \leq 2$	$2 < B \leq 3$	$B > 3$	$\bar{W} \pm \text{s.d.}$	$W = 0$	$0 < W \leq 1$	$1 < W \leq 2$	$2 < W \leq 3$	$W > 3$
10 - 20	17.1	67	0.70 ± 0.15	65.7	11.9	9.0	9.0	4.5	1.02 ± 0.13	34.3	31.3	23.9	6.0	4.5
20 - 30	24.9	128	0.51 ± 0.09	71.1	12.5	7.8	5.5	3.1	0.74 ± 0.08	45.3	31.3	14.8	8.6	0
30 - 40	34.0	87	0.41 ± 0.08	70.1	16.1	9.2	4.6	0	0.85 ± 0.11	42.5	31.0	17.2	5.8	3.5
40 - 50	44.1	48	0.92 ± 0.12	33.3	33.3	27.1	6.3	0	0.56 ± 0.11	50.0	35.4	10.4	2.1	2.1
50 - 60	56.5	27	0.23 ± 0.12	85.2	3.7	11.1	0	0	0.47 ± 0.13	59.3	25.9	14.8	0	0
> 60	65.4	56	0.20 ± 0.06	78.6	16.1	3.6	1.8	0	0.52 ± 0.14	62.5	23.2	5.4	5.4	3.6
2) 10 - 20	17.1	66	0.65 ± 0.14	66.7	12.1	9.1	9.1	3.0	1.02 ± 0.14	34.8	30.3	24.2	6.1	4.6
20 - 30	24.5	96	0.43 ± 0.09	70.8	16.7	6.2	4.2	2.1	0.81 ± 0.09	40.6	33.3	17.7	8.3	0
30 - 40	33.8	45	0.38 ± 0.12	73.3	13.3	8.9	4.4	0	0.75 ± 0.15	51.1	22.2	15.6	8.9	2.2
40 - 50	45.0	25	0.70 ± 0.17	52.0	16.0	26.0	4.0	0	0.76 ± 0.19	40.0	40.0	12.0	4.0	4.0
50 - 60	56.1	21	0.30 ± 0.15	80.9	4.8	14.3	0	0	0.53 ± 0.16	57.1	23.8	19.1	0	0
> 60	65.9	37	0.20 ± 0.08	81.1	13.5	2.7	2.7	0	0.34 ± 0.13	67.6	24.3	2.7	2.7	2.7

TABLE 20.4.—The blending and wake indices B and W as functions of m_m for (1) all Super-Schmidt meteors, (2) sporadic meteors only; also shown are the percentages of meteors falling within each group of B and W

Range of m_m	\bar{m}_m	No. obs.	$\bar{B} \pm$ s.d.	$B = 0$	$0 < B \leq 1$	$1 < B \leq 2$	$2 < B \leq 3$	$B > 3$	$\bar{W} \pm$ s.d.	$W = 0$	$0 < W \leq 1$	$1 < W \leq 2$	$2 < W \leq 3$	$W > 3$
1) $m_m < 0.10$	0.05	119	0.45 ± 0.07	63.0	22.7	10.1	4.2	0	0.19 ± 0.04	75.6	21.0	3.4	0	0
$0.10 \leq m_m < 0.5$	0.24	159	0.44 ± 0.06	68.6	15.1	13.2	2.5	0.6	0.60 ± 0.06	47.2	37.1	12.0	3.1	0.6
$0.5 \leq m_m < 1.0$	0.71	64	0.41 ± 0.11	78.1	7.8	7.8	6.3	0	1.06 ± 0.12	26.6	35.9	28.1	6.3	3.1
$1.0 \leq m_m < 5$	1.93	56	0.92 ± 0.19	57.1	14.3	7.1	12.5	8.9	1.54 ± 0.16	16.1	30.4	28.6	19.6	5.4
$m_m > 5$	10.15	13	0.19 ± 0.19	92.3	0	0	7.7	0	2.48 ± 0.33	7.7	0	38.4	30.8	23.1
2) $m_m < 0.10$	0.05	75	0.34 ± 0.08	72.0	16.0	9.3	2.7	0	0.20 ± 0.05	73.3	22.7	4.0	0	0
$0.10 \leq m_m < 0.5$	0.24	103	0.36 ± 0.07	71.8	15.5	10.7	1.0	1.0	0.52 ± 0.07	52.4	34.0	10.7	2.9	0
$0.5 \leq m_m < 1.0$	0.71	57	0.41 ± 0.11	77.2	8.8	8.8	5.3	0	1.09 ± 0.12	24.6	36.8	28.1	7.0	3.5
$1.0 \leq m_m < 5$	1.86	41	0.96 ± 0.20	51.2	17.1	9.8	17.1	4.9	1.44 ± 0.17	17.1	31.7	31.7	17.1	2.4
$m_m > 5$	10.15	13	0.19 ± 0.19	92.3	0	0	7.7	0	2.48 ± 0.33	7.7	0	38.4	30.8	23.1

TABLE 20.5.—The blending and wake indices B and W as functions of ΔM , the difference between the plate limit and the maximum absolute magnitude, for (1) all Super-Schmidt meteors, (2) sporadic meteors only; also shown are the percentages of meteors falling within each group of B and W

Range of ΔM	$\bar{\Delta M}$	No. obs.	$\bar{B} \pm$ s.d.	$B = 0$	$0 < B \leq 1$	$1 < B \leq 2$	$2 < B \leq 3$	$B > 3$	$\bar{W} \pm$ s.d.	$W = 0$	$0 < W \leq 1$	$1 < W \leq 2$	$2 < W \leq 3$	$W > 3$
1) $\Delta M \leq 1.5$	1.29	38	0.32 ± 0.05	86.8	0	7.9	2.6	2.6	0.18 ± 0.03	84.2	13.2	0	2.6	0
$1.5 < \Delta M \leq 2.5$	2.10	153	0.43 ± 0.05	69.3	18.9	7.2	2.6	2.0	0.33 ± 0.03	67.3	23.5	8.5	0.7	0
$2.5 < \Delta M \leq 3.5$	3.02	111	0.69 ± 0.08	55.9	19.8	14.4	7.2	2.7	0.63 ± 0.06	41.4	42.3	13.5	2.7	0
$3.5 < \Delta M \leq 5$	4.18	92	0.52 ± 0.11	66.3	14.1	13.0	6.5	0	1.35 ± 0.11	13.0	38.0	32.6	13.0	3.3
$\Delta M > 5$	5.69	18	0.31 ± 0.24	88.9	0	0	11.1	0	2.86 ± 0.48	0	5.6	22.2	38.9	33.3
2) $\Delta M \leq 1.5$	1.30	31	0.33 ± 0.06	87.1	0	6.5	3.2	3.2	0.19 ± 0.04	83.9	12.9	0	3.2	0
$1.5 < \Delta M \leq 2.5$	2.09	106	0.32 ± 0.06	75.5	15.1	7.6	0.9	0.9	0.40 ± 0.05	63.2	25.5	10.4	0.9	0
$2.5 < \Delta M \leq 3.5$	3.00	77	0.69 ± 0.09	55.8	20.8	13.0	7.8	2.6	0.67 ± 0.08	41.6	39.0	16.9	2.6	0
$3.5 < \Delta M \leq 5$	4.21	64	0.48 ± 0.14	70.3	12.5	10.9	6.3	0	1.42 ± 0.14	10.9	37.5	32.8	14.1	4.7
$\Delta M > 5$	5.71	12	0.46 ± 0.26	83.3	0	0	16.7	0	2.63 ± 0.48	0	8.3	25.0	41.7	25.0

TABLE 20.6.—The blending and wake indices B and W as functions of the integrated brightness ϵ for (1) all Super-Schmidt meteors, (2) sporadic meteors only; also shown are the percentages of meteors falling within each group of B and W

Range of ϵ_m	$\bar{\epsilon}_m$	No. obs.	$\bar{B} \pm$ s.d.	$B = 0$	$0 < B \leq 1$	$1 < B \leq 2$	$2 < B \leq 3$	$B > 3$	$\bar{W} \pm$ s.d.	$W = 0$	$0 < W \leq 1$	$1 < W \leq 2$	$2 < W \leq 3$	$W > 3$
1) $\epsilon_m \leq -0.75$	-0.92	98	0.36 ± 0.07	71.4	15.3	11.2	2.1	0	0.27 ± 0.05	70.4	25.5	4.1	0	0
$-0.75 < \epsilon_m \leq -0.50$	-0.64	100	0.64 ± 0.10	57.0	25.0	9.0	7.0	2.0	0.44 ± 0.07	58.0	28.0	12.0	2.0	0
$-0.50 < \epsilon_m \leq -0.25$	-0.39	77	0.62 ± 0.12	62.3	16.9	13.0	3.9	3.9	0.70 ± 0.09	41.6	40.3	14.3	3.9	0
$-0.25 < \epsilon_m \leq 0.00$	-0.14	60	0.55 ± 0.13	70.0	8.3	13.3	6.7	1.7	0.79 ± 0.10	33.3	40.0	23.3	3.3	0
$\epsilon_m > 0$	0.37	67	0.29 ± 0.09	82.1	7.5	4.5	6.0	0	1.97 ± 0.14	7.5	22.4	31.3	25.4	13.4
2) $\epsilon_m \leq -0.75$	-0.92	75	0.32 ± 0.07	73.3	14.7	10.7	1.3	0	0.31 ± 0.06	66.7	28.0	5.3	0	0
$-0.75 < \epsilon_m \leq -0.50$	-0.64	70	0.52 ± 0.11	62.9	22.9	7.1	4.3	2.9	0.46 ± 0.08	57.1	27.1	14.3	1.4	0
$-0.50 < \epsilon_m \leq -0.25$	-0.39	52	0.39 ± 0.11	73.1	13.5	9.6	3.8	0	0.78 ± 0.12	40.4	36.5	17.3	5.8	0
$-0.25 < \epsilon_m \leq 0.00$	-0.14	40	0.70 ± 0.17	65.0	5.0	20.0	7.5	2.5	0.92 ± 0.13	22.5	47.5	25.0	5.0	0
$\epsilon_m > 0$	0.34	45	0.34 ± 0.13	82.2	6.7	2.2	8.9	0	1.98 ± 0.17	8.9	17.8	33.3	26.7	13.3

TABLE 20.7.—The blending and wake indices B and W as functions of the mass-loss coefficient σ for (1) all Super-Schmidt meteors, (2) sporadic meteors only; also shown are the percentages of meteors falling within each group of B and W

	Range of $\log \sigma$ ($\text{cm}^{-2} \text{s}^{-2}$)	$\overline{\log \sigma}$ ($\text{cm}^{-2} \text{s}^{-2}$)	No. Obs.	$\bar{B} \pm \text{s.d.}$	$B=0$	$0 < B \leq 1$	$1 < B \leq 2$	$2 < B \leq 3$	$B > 3$	$\bar{W} \pm \text{s.d.}$	$W=0$	$0 < W \leq 1$	$1 < W \leq 2$	$2 < W \leq 3$	$W > 3$
1)	$\log \sigma < -11.45$	-11.66	51	0.61 ± 0.15	64.7	17.7	7.8	3.9	5.9	0.78 ± 0.16	51.0	23.5	15.7	3.9	5.9
	$-11.45 \leq \log \sigma < -11.3$	-11.37	63	0.22 ± 0.07	84.1	7.9	6.4	1.6	0	0.54 ± 0.12	63.5	20.6	9.5	3.2	3.2
	$-11.30 \leq \log \sigma < -11.15$	-11.23	102	0.36 ± 0.08	76.5	13.7	4.9	2.9	2.0	0.66 ± 0.09	49.0	32.3	10.8	6.9	1.0
	$-11.15 \leq \log \sigma < -11.0$	-11.09	92	0.52 ± 0.09	65.2	14.1	16.3	3.3	1.1	0.78 ± 0.09	39.1	37.0	17.4	6.5	0
	$\log \sigma \geq -11.0$	-10.83	88	0.74 ± 0.11	53.4	21.6	13.6	11.4	0	1.02 ± 0.11	29.5	35.2	23.9	8.0	3.4
2)	$\log \sigma < -11.45$	-11.62	28	0.35 ± 0.14	71.4	17.9	7.1	0	3.6	0.75 ± 0.21	50.0	25.0	17.9	0	7.1
	$-11.45 \leq \log \sigma < -11.3$	-11.37	37	0.25 ± 0.11	83.8	5.4	8.1	2.7	0	0.51 ± 0.14	62.2	21.6	10.8	2.7	2.7
	$-11.3 \leq \log \sigma < -11.15$	-11.23	78	0.35 ± 0.10	78.2	11.5	5.1	2.6	2.6	0.68 ± 0.10	46.1	35.9	10.3	6.4	1.3
	$-11.15 \leq \log \sigma < -11.0$	-11.09	68	0.42 ± 0.09	70.6	11.8	16.2	1.5	0	0.85 ± 0.11	38.2	33.8	19.1	8.8	0
	$\log \sigma > -11.0$	-10.82	68	0.69 ± 0.12	57.3	20.6	10.3	11.8	0	1.04 ± 0.13	32.4	29.4	26.5	8.8	2.9

TABLE 20.8.—The blending and wake indices B and W as functions of the fragmentation index χ for (1) all Super-Schmidt meteors, (2) sporadic meteors only; also shown are the percentages of meteors falling within each group of B and W

	Range of χ	$\bar{\chi}$	No. Obs.	$\bar{B} \pm \text{s.d.}$	$B=0$	$0 < B \leq 1$	$1 < B \leq 2$	$2 < B \leq 3$	$B > 3$	$\bar{W} \pm \text{s.d.}$	$W=0$	$0 < W \leq 1$	$1 < W \leq 2$	$2 < W \leq 3$	$W > 3$
1)	$\chi < 0$	-0.11	69	0.29 ± 0.09	84.1	5.8	4.3	5.8	0	0.76 ± 0.11	44.9	31.9	13.0	8.7	1.5
	$0 \leq \chi < 0.2$	0.09	137	0.32 ± 0.06	79.2	9.6	8.9	2.3	0	0.72 ± 0.08	50.7	26.1	15.2	5.8	2.2
	$0.2 \leq \chi < 0.4$	0.30	101	0.49 ± 0.09	61.4	25.7	6.9	4.0	2.0	0.77 ± 0.10	39.6	37.6	16.8	3.0	3.0
	$0.4 \leq \chi < 0.6$	0.48	52	0.59 ± 0.11	57.7	17.3	21.2	3.8	0	0.64 ± 0.12	53.8	25.0	15.4	3.9	1.9
	$\chi > 0.6$	0.89	53	1.20 ± 0.18	37.7	22.6	17.0	15.1	7.6	0.79 ± 0.14	45.3	30.2	13.2	9.4	1.9
2)	$\chi < 0$	-0.11	48	0.31 ± 0.11	83.3	6.3	4.2	6.2	0	0.81 ± 0.14	43.7	29.2	14.6	10.4	2.1
	$0 \leq \chi < 0.2$	0.09	100	0.38 ± 0.08	77.5	8.2	11.1	3.2	0	0.70 ± 0.09	49.5	27.7	15.8	6.0	1.0
	$0.2 \leq \chi < 0.4$	0.29	71	0.35 ± 0.08	67.6	23.9	5.6	1.4	1.4	0.77 ± 0.11	39.4	38.0	16.9	2.8	2.8
	$0.4 \leq \chi < 0.6$	0.48	33	0.40 ± 0.12	69.7	15.2	12.1	3.0	0	0.70 ± 0.16	54.6	18.2	21.2	3.0	3.0
	$\chi > 0.6$	0.89	37	1.11 ± 0.21	43.3	18.9	16.2	16.2	5.4	0.94 ± 0.19	40.6	29.7	16.2	10.8	2.7

TABLE 20.9.—The blending and wake indices B and W as functions of the zenith angle Z_R for (1) all Super-Schmidt meteors, (2) sporadic meteors only; also shown are the percentages of meteors falling within each group of B and W

	Range of $\cos Z_R$	$\overline{\cos Z_R}$	No. Obs.	$\bar{B} \pm \text{s.d.}$	$B=0$	$0 < B \leq 1$	$1 < B \leq 2$	$2 < B \leq 3$	$B > 3$	$\bar{W} \pm \text{s.d.}$	$W=0$	$0 < W \leq 1$	$1 < W \leq 2$	$2 < W \leq 3$	$W > 3$
1)	$\cos Z_R < 0.4$	0.30	51	0.79 ± 0.17	56.9	21.6	5.9	9.8	5.9	0.79 ± 0.13	45.1	25.5	21.6	7.8	0
	$0.4 < \cos Z_R \leq 0.6$	0.50	76	0.64 ± 0.12	65.8	11.8	13.2	6.6	2.6	0.73 ± 0.12	53.9	25.0	11.8	5.3	4.0
	$0.6 < \cos Z_R \leq 0.7$	0.65	88	0.56 ± 0.10	65.9	15.9	10.2	5.7	2.3	0.67 ± 0.10	47.7	33.0	12.5	4.5	2.3
	$0.7 < \cos Z_R \leq 0.8$	0.75	75	0.44 ± 0.09	68.0	16.0	10.7	5.3	0	0.62 ± 0.10	50.7	28.0	14.7	6.7	0
	$0.8 < \cos Z_R \leq 0.9$	0.84	77	0.30 ± 0.07	72.7	15.6	11.7	0	0	0.67 ± 0.11	46.7	36.4	10.4	2.6	3.9
	$\cos Z_R > 0.9$	0.97	46	0.32 ± 0.10	76.1	13.0	6.5	4.4	0	1.12 ± 0.16	28.3	32.6	26.1	10.9	2.2
2)	$\cos Z_R < 0.4$	0.30	38	0.75 ± 0.20	63.2	15.8	5.3	10.5	5.3	0.83 ± 0.17	47.4	18.4	23.7	10.5	0
	$0.4 < \cos Z_R \leq 0.6$	0.49	55	0.62 ± 0.15	69.1	9.1	10.9	9.1	1.8	0.90 ± 0.15	45.4	27.3	16.4	5.5	5.5
	$0.6 < \cos Z_R \leq 0.7$	0.65	60	0.41 ± 0.11	71.7	15.0	8.3	3.3	1.7	0.78 ± 0.12	38.3	38.3	16.7	5.0	1.7
	$0.7 < \cos Z_R \leq 0.8$	0.75	51	0.29 ± 0.09	76.5	11.8	9.8	2.0	0	0.59 ± 0.12	54.9	23.5	15.7	5.9	0
	$0.8 < \cos Z_R \leq 0.9$	0.84	60	0.37 ± 0.08	66.7	20.0	13.3	0	0	0.65 ± 0.11	46.7	35.0	13.3	1.7	3.3
	$\cos Z_R > 0.9$	0.96	26	0.37 ± 0.17	80.8	7.7	3.9	7.7	0	0.95 ± 0.21	38.5	30.8	15.4	15.4	0

TABLE 20.10.—The blending and wake indices as functions of the aphelion distance Q for (1) all Super-Schmidt meteors, (2) sporadic meteors only; also shown are the percentages of meteors falling within each group of B and W

Range of Q (a.u.)	\bar{Q}	No. obs.	$\bar{B} \pm \text{s.d.}$	B=0	0<B≤1	1<B≤2	2<B≤3	B>3	$\bar{W} \pm \text{s.d.}$	W=0	0<W≤1	1<W≤2	2<W≤3	W>3
1) $Q \leq 3.5$	2.6	75	0.70 ± 0.13	57.3	22.7	6.7	10.7	2.7	0.81 ± 0.11	40.0	34.7	21.3	1.3	2.7
$3.5 < Q \leq 5$	4.3	122	0.55 ± 0.09	66.4	15.6	12.3	4.1	1.6	0.71 ± 0.08	46.7	30.3	16.4	4.9	1.6
$5 < Q \leq 7$	5.7	78	0.66 ± 0.12	64.1	14.1	10.3	7.7	3.8	0.80 ± 0.11	43.6	32.0	12.8	10.3	1.3
$7 < Q \leq 20$	12.1	42	0.27 ± 0.10	81.0	7.1	11.9	0	0	0.64 ± 0.15	52.4	28.6	11.9	4.8	2.4
$Q > 20$	60	94	0.32 ± 0.07	73.4	14.9	9.6	2.1	0	0.72 ± 0.11	52.1	25.5	11.7	7.5	3.2
2) $Q \leq 3.5$	2.6	44	0.97 ± 0.19	47.7	25.0	6.8	15.9	4.6	0.68 ± 0.11	43.2	34.1	22.7	0	0
$3.5 < Q \leq 5$	4.3	84	0.42 ± 0.10	71.4	16.7	8.3	2.4	1.2	0.79 ± 0.11	44.0	28.6	20.2	4.8	2.4
$5 < Q \leq 7$	5.7	54	0.43 ± 0.13	77.8	5.6	9.3	5.6	1.8	0.93 ± 0.15	38.9	33.3	13.0	13.0	1.8
$7 < Q \leq 20$	11.6	37	0.31 ± 0.11	78.4	8.1	13.5	0	0	0.68 ± 0.16	51.4	27.0	13.5	5.4	2.7
$Q > 20$	63	70	0.34 ± 0.08	74.3	12.9	10.0	2.9	0	0.72 ± 0.12	50.0	27.1	12.9	7.1	2.9

TABLE 21.—Physical characteristics of individual meteor showers

	v_m (km/s)	$\cos Z_R$	M_{pm}	H_B (km)	$H_{2.5}$ (km)	H_{ML} (km)	H_E (km)	D (s)	ϵ_m	m_m (g)
All meteors	35.3 ± 0.8	0.67 ± 0.01	+0.0 ± 0.1	100.0 ± 0.4	99.6 ± 0.5	89.8 ± 0.4	85.1 ± 0.4	0.76 ± 0.02	-0.42 ± 0.02	0.80 ± 0.11
Sporadic meteors	33.7 ± 1.0	0.66 ± 0.01	+0.1 ± 0.1	98.8 ± 0.6	98.2 ± 0.6	89.1 ± 0.5	84.5 ± 0.5	0.80 ± 0.03	-0.44 ± 0.03	0.96 ± 0.16
Shower meteors	39.3 ± 1.2	0.69 ± 0.02	-0.2 ± 0.1	102.9 ± 0.6	103.0 ± 0.7	91.5 ± 0.7	86.5 ± 0.7	0.67 ± 0.03	-0.36 ± 0.05	0.42 ± 0.07
Abrupt-beginning meteors	28.8 ± 3.1	0.67 ± 0.04	-0.1 ± 0.2	92.5 ± 2.1	92.4 ± 2.3	87.6 ± 1.7	81.5 ± 1.4	0.62 ± 0.04	-0.50 ± 0.07	0.65 ± 0.12
Short, flare-like meteors	36.8 ± 4.2	0.78 ± 0.04	-0.8 ± 0.2	94.3 ± 2.7	94.4 ± 2.8	89.7 ± 2.0	85.2 ± 1.9	0.32 ± 0.02	-0.52 ± 0.10	0.32 ± 0.09
Individual Showers:										
Quadrantids	43.1 ± 0.2	0.61 ± 0.05	+0.2 ± 0.3	102.8 ± 0.7	103.1 ± 0.7	95.7 ± 1.5	90.6 ± 1.6	0.48 ± 0.03	-0.58 ± 0.09	0.08 ± 0.02
Virginids	30.8 ± 3.7	0.73 ± 0.02	-0.2 ± 0.3	96.0 ± 5.4	96.0 ± 3.4	83.7 ± 0.8	77.7 ± 1.1	0.89 ± 0.42	-0.31 ± 0.31	0.59 ± 0.47
Lyrids	48.8 ± 1.1	0.93 ± 0.05	-1.0 ± 0.3	107.1 ± 0.9	107.9 ± 0.7	97.3 ± 2.6	87.6 ± 2.5	0.43 ± 0.07	-0.18 ± 0.14	0.13 ± 0.04
η Aquarids	66.8	0.42	-0.7	115.6	119.6	102.1	99.7	0.58	-0.20	0.04
δ Aquarids	42.5 ± 0.3	0.58 ± 0.03	-0.1 ± 0.3	99.8 ± 1.1	99.8 ± 1.2	93.0 ± 0.7	88.4 ± 0.8	0.49 ± 0.06	-0.59 ± 0.11	0.09 ± 0.03
α Capricornids	25.6 ± 0.4	0.69 ± 0.03	+0.7 ± 0.2	97.8 ± 0.8	96.9 ± 0.8	89.6 ± 1.1	86.0 ± 1.3	0.70 ± 0.08	-0.67 ± 0.12	0.53 ± 0.24
Southern α Aquarids	34.4 ± 1.0	0.54 ± 0.04	+0.5 ± 0.4	96.3 ± 1.9	95.7 ± 1.7	90.2 ± 1.1	86.5 ± 1.1	0.58 ± 0.12	-0.73 ± 0.12	0.11 ± 0.02
Northern α Aquarids	35.9 ± 1.7	0.70 ± 0.08	+0.6 ± 0.9	99.1 ± 1.5	98.8 ± 1.4	89.9 ± 3.9	84.7 ± 4.1	0.57 ± 0.02	-0.63 ± 0.24	0.11 ± 0.04
Perseids	60.2 ± 0.2	0.52 ± 0.08	-1.4 ± 0.4	114.1 ± 1.1	114.8 ± 1.1	99.0 ± 1.5	94.3 ± 1.8	0.67 ± 0.10	+0.16 ± 0.20	0.27 ± 0.13
α Cygnids	23.2 ± 0.4	0.68 ± 0.13	+0.8 ± 0.3	99.2 ± 0.8	97.1 ± 1.1	88.9 ± 2.3	85.5 ± 2.0	0.94 ± 0.08	-0.65 ± 0.05	0.39 ± 0.06
Draconids	20.2 ± 0.1	0.61 ± 0.06	+0.1 ± 0.0	103.6 ± 0.2	102.6 ± 0.2	96.7 ± 0.4	91.0 ± 0.4	1.22 ± 0.12	-0.29 ± 0.03	2.00 ± 0.13
Orionids	68.0 ± 0.4	0.60 ± 0.08	-1.1 ± 0.3	117.0 ± 0.5	119.6 ± 1.0	105.9 ± 1.7	99.3 ± 1.7	0.47 ± 0.05	-0.14 ± 0.10	0.06 ± 0.02
Southern Taurids	29.0 ± 0.4	0.73 ± 0.03	+0.5 ± 0.3	100.8 ± 0.5	99.6 ± 0.6	87.9 ± 0.9	82.2 ± 0.9	0.91 ± 0.05	-0.45 ± 0.10	0.48 ± 0.13
Northern Taurids	31.1 ± 0.5	0.84 ± 0.07	-0.8 ± 0.5	103.3 ± 1.0	103.0 ± 1.2	83.2 ± 1.3	79.5 ± 1.4	0.97 ± 0.16	+0.00 ± 0.22	1.01 ± 0.32
Leonids	71.7	0.89	-3.3	127.8	125.9	89.1	87.2	0.64	+0.72	0.29
σ Hydrids	59.2 ± 0.6	0.84 ± 0.02	-0.7 ± 0.1	111.7 ± 0.3	113.6 ± 1.6	92.9 ± 0.4	88.8 ± 1.8	0.46 ± 0.02	-0.29 ± 0.08	0.05 ± 0.01
Geminids	36.2 ± 0.1	0.86 ± 0.04	-0.8 ± 0.3	100.4 ± 0.3	101.3 ± 0.5	85.6 ± 1.5	80.0 ± 1.8	0.64 ± 0.04	-0.18 ± 0.13	0.76 ± 0.28

TABLE 21.—Physical characteristics of individual meteor showers.—Continued

	$\log \sigma$ ($\text{cm}^{-2} \text{s}^{-2}$)	x	$\overline{\Lambda \log \sigma}_{\text{corr}}$ (g/cm^3)	W	B	D/D_{th}	$N H_{2.5}$ (km)	No. obs.
All meteors	-11.19 ± 0.01	0.27 ± 0.01	0.00 ± 0.01	0.74 ± 0.05	0.51 ± 0.05	0.61 ± 0.01	$+0.3 \pm 0.5$	413
Sporadic meteors	-11.16 ± 0.01	0.27 ± 0.02	0.00 ± 0.02	0.77 ± 0.06	0.47 ± 0.05	0.60 ± 0.01	0.0 ± 0.6	290
Shower meteors	-11.25 ± 0.02	0.27 ± 0.03	0.00 ± 0.02	0.67 ± 0.08	0.63 ± 0.08	0.65 ± 0.02	$+1.0 \pm 0.7$	123
Abrupt-beginning meteors	-11.04 ± 0.06	0.25 ± 0.05	-0.18 ± 0.08	0.59 ± 0.13	1.35 ± 0.24	0.45 ± 0.03	-5.1 ± 2.3	26
Short, flare-like meteors	-11.18 ± 0.12	0.27 ± 0.06	0.15 ± 0.12	0.83 ± 0.30	0.57 ± 0.23	0.35 ± 0.04	-7.0 ± 2.8	12
Individual Showers:								
Quadrantids	-11.46 ± 0.09	0.44 ± 0.11	0.03 ± 0.08	0.40 ± 0.19	0.80 ± 0.11	0.61 ± 0.03	$+0.3 \pm 0.7$	10
Virginids	-11.19 ± 0.06	0.15 ± 0.03	-0.36 ± 0.12	1.15 ± 1.15	0.25 ± 0.25	0.67 ± 0.17	-3.0 ± 3.4	2
Lyrids	-11.17 ± 0.17	0.08 ± 0.09	-0.10 ± 0.09	0.43 ± 0.30	0.50 ± 0.50	0.64 ± 0.11	-0.7 ± 0.7	3
η Aquarids	-11.01	0.09	-0.21	0.0	0.0	0.63	$+5.3$	1
δ Aquarids	-11.40 ± 0.05	0.52 ± 0.08	0.03 ± 0.04	0.21 ± 0.12	1.55 ± 0.27	0.50 ± 0.05	-3.1 ± 1.2	11
α Capricornids	-11.09 ± 0.08	0.38 ± 0.07	0.15 ± 0.03	0.74 ± 0.27	1.00 ± 0.34	0.58 ± 0.04	$+2.4 \pm 0.8$	14
Southern δ Aquarids	-11.27 ± 0.12	0.18 ± 0.09	-0.05 ± 0.06	0.33 ± 0.21	0.83 ± 0.54	0.53 ± 0.10	-3.2 ± 1.7	6
Northern δ Aquarids	-11.48 ± 0.25	0.10 ± 0.26	-0.24 ± 0.28	0.50 ± 0.50	0.50 ± 0.50	0.63 ± 0.04	-1.2 ± 1.4	2
Perseids	-11.26 ± 0.06	0.28 ± 0.10	-0.03 ± 0.05	0.96 ± 0.35	0.03 ± 0.03	0.56 ± 0.04	$+0.8 \pm 1.1$	11
κ Cygnids	-11.07 ± 0.08	0.11 ± 0.09	0.15 ± 0.06	1.00 ± 0.20	0.50 ± 0.50	0.69 ± 0.03	$+4.1 \pm 1.1$	4
Draconids	$[-14.88 \pm 0.79]$	1.89 ± 0.57	4.61 ± 0.85	0.00 ± 0.00	4.00 ± 0.00	0.50 ± 0.02	$+9.5 \pm 0.2$	2
Orionids	-11.20 ± 0.11	0.46 ± 0.06	0.14 ± 0.08	0.34 ± 0.25	0.41 ± 0.19	0.55 ± 0.04	$+4.8 \pm 1.0$	8
Southern Taurids	-11.31 ± 0.03	0.04 ± 0.05	-0.00 ± 0.03	0.14 ± 0.08	0.00 ± 0.00	0.84 ± 0.02	$+2.2 \pm 0.6$	18
Northern Taurids	-11.36 ± 0.06	0.03 ± 0.07	-0.06 ± 0.07	0.72 ± 0.43	0.06 ± 0.06	0.77 ± 0.05	$+2.7 \pm 1.2$	5
Leonids	-10.99	0.37	-0.23	4.0	0.0	0.44	$+5.7$	1
σ Hydrids	-11.46 ± 0.06	0.04 ± 0.04	-0.10 ± 0.12	0.33 ± 0.33	0.00 ± 0.00	0.87 ± 0.10	$+2.1 \pm 1.6$	3
Geminids	-11.23 ± 0.07	0.21 ± 0.05	-0.39 ± 0.06	1.48 ± 0.26	0.47 ± 0.17	0.69 ± 0.03	-0.5 ± 0.5	20

